Florida State University Libraries

Electronic Theses, Treatises and Dissertations | The Graduate School

2013

Isotopic Characterization of Methane Obtained from Hypersaline Environments

Amanda Maaza Tazaz

Follow this and additional works at the FSU Digital Library. For more information, please contact lib-ir@fsu.edu

FLORIDA STATE UNIVERSITY

COLLEGE OF ARTS AND SCIENCES

ISOTOPIC CHARACTERIZATION OF METHANE OBTAINED FROM HYPERSALINE ENVIRONMENTS

By

AMANDA MAAZA TAZAZ

A Dissertation submitted to the
Department of Earth, Ocean and Atmospheric Science
in partial fulfillment of the
requirements for the degree of
Doctor of Philosophy

Degree Awarded:
Fall Semester, 2013

Amanda M. Tazaz defended this dissertation on October 15, 2013.

The members of the supervisory committee were:

Jeffery Chanton
Professor Directing *Dissertation*

Patrick Mason
University Representative

Marcus Huettel
Committee Member

Yang Wang
Committee Member

Laura Lapham
Committee Member

The Graduate School has verified and approved the above-named committee members, and certifies that the dissertation has been approved in accordance with university requirements.

To My Family

ACKNOWLEDGEMENTS

I would like to thank my mentors, family, and friends for all of their support and encouragement over the last five years. I would especially like to thank Dr. Jeffrey Chanton for his guidance over those years as I have greatly enjoyed working in your lab and learning only a small fraction of the wealth of knowledge you possess. I would like to thank all of the other research members in this project: Dr. Brad Bebout, Dr. Cheryl Kelley, Jennifer Poole, Angela Detweiler, Erich Fleming, Adrienne Frisbee, and Brooke Nicholson as this project would not have been possible without your efforts. I would also like to thank my Dissertation Committee and to The Florida Education Fund and my McKnight Fellowship family for all of their efforts and support along my journey in graduate school.

Over the course of my life I have had the opportunity to have the support from the following people and I just want to thank you all from the bottom of my heart. First and foremost, I am forever grateful for my amazing family. Mom and Dad you have always been an inspiration to me. You both did everything that you could to ensure that we all had a wonderful life and for that words cannot express how much I am grateful. You both gave me the confidence to go after any dream that I wanted. Mike and Senai, although we have our ups and downs, I am truly grateful to have you guys as my brothers, as you have taught me a lot of things along the way. To my sister from another mister (and misses), Hirut what more can I say than you are awesome. I know over the last 5 years you did not want to hear anything else about a conference talk, my dissertation chapters, or about methane or Mars, but you did and I guess you can share my diploma (only temporarily, so get your own…lol). I would be remiss for not mentioning my three beautiful nieces and my handsome nephew, Kaitlyn, Kayleigh, Lia and Mattie, you all are wonderful and I wish the world for you all.

To my Granny (aka. Auntie Ethel) and Adey (aka Lemlem) I love you soooo much. Guess what I'm a Doctor now. Well not that kind of Doctor but close enough, right. To Zaida thanks for coming to all of my graduations over the years, even when they always seem to fall on your birthday. I hope that I will be able to come to all of your graduations in the coming years as you are one smart cookie. To my other sisters from another mister (and misses), Hana and Eden, thanks for all of your support over the years. Thanks for giving me support when I needed it and even when I did not need it. To all of my numerous family members, Cheryl, Lydia, Yordanos, Kidane, Ann, Francis, Merril, John, Negasi, Harague, Almaz, Auntie Nelis, Kevin and everyone else (sorry guys I did not forget you, I can write a dissertation alone based on how big my family is) who have supported me along the way I am truly grateful for all that you have done for me.

To my OSB family, thank you for all of your support over these last few years. I would especially like to thank Claire for all of her help with the mass spec and with understanding what is going on in my samples. Thanks for tolerating all the smells that came out of the machine when I ran samples and for having patience with me and my gazillion questions about running hydrogen samples. To Michaela, thank you for all of your support. I remember the day that I brought my application for the department into your office and you have always been so supportive and nice to me over the years. To Mr. Ray, thanks for making me feel at home in OSB I am going to miss talking sports with you. To everyone who has ever come out to run in the Salmonole Run, thanks so much for all of your support, we raised a lot of money for the Thalassic society and graduate student research in the department, and for that I am forever grateful. To all of my lab mates over the years, Liz, Jiyoung, Kirstin, Jimmy, Rachel, Beth, Tyler, and Kelsey thanks for answering all of my questions and helping me with my research. To Laura, what can I say, thanks for taking me under your wing when you where at FSU and even

after you left. You made me feel so at home, you are such a good mentor and role model and I am forever grateful.

To my new family at LSI, thank you guys for all of your encouraging words over the last year. I would especially like to thank Rob for giving me a shot in the education world. I am truly learning a lot about myself and the world as a whole.

To my SGA family, thank you for everything. Student government has been an integral part of my life and I am glad to say that my experience in COGS and SGA was truly worth giving up my Monday nights. To Vicki and Danielle, although we sometimes have our differences in opinions you both always take the time to listen and for that I am truly grateful. To Mrs. Kim, Mrs. Barb, Mrs. Shenika, Mrs. Mattie, Mrs. Carolyn, and Miss. Whitney, thank you for making my long stay in SGA/COGS a smooth and pleasant one. I will miss you guys and SGA so much.

To my wonderful and furry dog, Cherie, woof, woof, woof. but really you have been there when I prepped for conferences, you sat quietly in my office while I tried to wrap up data analysis, and occasionally you ran down the hallway in OSB to hint that its time to go home. You are my road warrior and companion and my life has forever been changed since you entered it. Although you cant read, I do think you can understand me when I talk, so once this is all said and done I will read this to you, and give you lots of doggie treats, because you deserve it.

And last, but definitely not least, Corry, we have had our ups and downs but you have always been a loving and supportive partner over the last 6 years. Who would have thought when we met 11 years ago that we would have taken this path, the path less traveled, but we did and for that I am grateful. I am not going to sit here and say that it was always easy but you always seem to keep mind in the game, for example when it has been a long day and when I get home

from school or work and all I want to do is just unplug my brain, but noooo you want to watch Science channel or NASA channel and so I should too, lol, don't change because that's what makes you, you, and I love you for that.

Wait….one more. I forgot the most important person of all _____ (Insert your name there) thanks for reading my dissertation, the very first dissertation I read from front to back was Dr. Oremlands dissertation, and I hope if I ever meet you, you will be as excited to meet me as I was to meet him. I leave you with two of my favorite quotes.

I am not going to question your opinions. I am not going to meddle with your belief. I am not going to dictate to you mine. All that I say is, examine, inquire. Look into the nature of things. Search out the grounds of your opinions, the for and against. Know why you believe, understand what you believe, and possess a reason for the faith that is in you.

– Frances Wright, "Divisions of Knowledge" (1828)

My life amounts to no more than one drop in a limitless ocean. Yet what is any ocean, but a multitude of drops?

–David Mitchell, "Cloud Atlas"

TABLE OF CONTENTS

List of Tables xiii

List of Figures xv

List of Abreviations xvii

Abstract xviii

CHAPTER ONE 1

INTRODUCTION 1

1.1 Dissertation Objectives and Overview 1

1.2 Chapter Outline 1

1.2.1 Chapter 2: Sample Sites 1

1.2.2 Chapter 3: Experimental Procedure 2

1.2.3 Chapter 4: Isotopic Characterization and Classification of Methane Bubbles 2

1.2.4 Chapter 5: Analysis of Methane Production from Hypersaline Sediment Samples 2

1.2.5 Chapter 6: Methane Production and Isotopic Analysis from Hypersaline Microbial Mat Incubations when Sulfate Reduction is Inhibited 3

1.2.6 Chapter 7: Fractionation Factors in Hypersaline Ponds 3

1.2.7 Chapter 8: Conclusions 3

1.3 Background to the Study and Key Terms 3

1.3.1 Hypersaline Environments 3

1.3.2 Hypersaline Microbial Community Habitats 6

1.3.3 Methane 8

1.3.4 Methanogens 8

1.3.5 Isotopes 12

1.3.6 Astrobiological Significance of Project 15

CHAPTER TWO 22

DESCRIPTION OF SITES SAMPLED FOR THE STUDY 22

2.1 Geographic Overview 22
2.2 Northern California, USA Sampling Sites 23
2.2.1 Don Edwards National Wildlife Refuge 23
2.3 Baja California, Mexico Sampling Sites 24
2.3.1 Guerrero Negro 24
2.3.2 Laguna Figueroa 27
2.3.3 Laguna San Ignacio 28
CHAPTER THREE 34
EXPERIMENTAL PROCEDURES 34
3.1 Sample Collection 34
3.1.1 Microbial Mat, Sediment and Evaporite Mineral Collection 34
3.1.2 Overlying Water 35
3.1.3 Gas Samples 35
3.2 Analytical Methods 36
3.2.1 Dissolved Inorganic Carbon 36
3.2.2 Sulfate Concentrations 36
3.2.3 $\delta^{18}O$ and δD of Water 37
3.2.4 Gas Bubble Hydrocarbon Concentrations 37
3.2.5 Methane Production in Incubation Samples 38
3.2.6 Stable Isotopes 40
3.2.7 Radiocarbon Analyses 42
CHAPTER FOUR 46
ISOTOPIC CHARACTERIZATION AND CLASSIFICATION OF METHANE BUBBLES 46
4.1 Introduction 46
4.2 Material and Methods 49

4.3 Results 53
4.4 Discussion 55
4.5 Conclusions 60
CHAPTER FIVE 68
INCUBATIONS 68
5.1 Introduction 68
5.2 Methods 72
5.2.1 Site Description 72
5.2.2 Incubations 72
5.2.3 Methane Production and Isotope Analysis 75
5.3 Results 76
5.3.1 Methane Production from $\delta^{13}C$ Substrate Additions 76
5.3.2 $\delta^{13}C$ Isotopic Analysis from Sediments Receiving ^{13}C-labeled Substrates 77
5.3.3 Methane Production from $\delta^{2}H$ Substrate Addition 85
5.3.4 $\delta^{13}C$ and $\delta^{2}H$ Isotope Analysis from ^{2}H-labeled Incubations 86
5.4 Discussion 88
5.4.1 Evidence of Current Biologic Methane Production 88
5.4.2 Evidence of Methane Production in the Sediments of Endoevaporite Sites 91
5.4.3 Methane Production as a Function of Salinity 92
5.4.4 Evidence of Methane Production Occurring Primarily from Non-Competitive Substrates 95
5.5 Conclusion 99
CHAPTER SIX 113
METHANE PRODUCTION AND ISOTOPIC ANALYSIS FROM HYPERSALINE MICROBIAL MAT INCUBATIONS WHEN SULFATE REDUCTION IS INHIBITED 113
6.1 Introduction 113

6.2 Methods 117
6.2.1 Site Description 117
6.2.2 Incubations 117
6.2.3 Methane Production and Isotope Analysis 119
6.3 Results 120
6.3.1 Methane Production Rates When Sulfate Reducing Bacteria Are Inhibited 120
6.3.2 Isotopic Analysis of Methane Produced Under SRB Inhibition 122
6.3.3 Competitive Substrates Utilization in Sediments Experiencing SRB Inhibition 123
6.4 Discussion 126
6.4.1 Increased Methane Production When Sulfate Reducing Bacteria Are Inhibited 127
6.4.2 Isotopic Analysis of Methane Produced Under SRB Inhibition 128
6.4.3 Competitive Substrates Utilization In Sediments Experiencing SRB Inhibition 130
6.5 Conclusion 134
CHAPTER SEVEN 143
FRACTIONATION FACTORS IN HYPERSALINE PONDS 143
7.1 Introduction 143
7.2 Methods 146
7.2.1 Site Description 146
7.2.2 Sampling Methods 146
7.2.3 Analytical Methods 147
7.2.4 Data Analysis and Calculations 148
7.3 Results and Discussion 149
7.3.1 δD and $\delta^{18}O$ Water Analysis 149
7.3.2 Porewater Analysis 151
7.3.2 α_C and α_D Analysis 151

7.4 Conclusion 152
CHAPTER EIGHT 158
CONCLUSIONS 158
APPENDICES 161
A. BUBBLE SAMPLE DATA 161
B. METHANE RATE PRODUCTION DATA 168
C. INCUBATION ISOTOPE DATA 179
REFERENCES 187
BIOGRAPHICAL SKETCH 198

LIST OF TABLES

1.1 Reactions and standard changes in free energies for sulfate reduction and methanogenesis. Reactions producing more negative numbers are thermodynamically favorable. 19

1.2 Isotopic abundances and relative atomic masses of the pertinent elements in stable isotope geochemistry. 21

3.1 Substrates used for each incubation experiment for each separate incubation trial. 45

4.1 Temperature, salinity, methane concentrations in bubble samples, ethane concentrations in bubble samples, methane isotopic carbon values from both bubbles collected at the site and methane produced within incubation vials, and δ^2H methane values for bubble samples. 64

5.1 Temperature, salinity, methane production rates in incubation samples, methane isotopic carbon values methane produced within incubation vials, and δ^{13}C-CO2 values for production within incubation vials. 102

5.2 Salinity, methane production rate, methane isotopic carbon values, carbon dioxide isotopic values, deuterium isotopic values for incubations receiving deuterium labeled DMS. 112

6.1 Temperature, salinity, methane production rates in incubation samples, methane isotopic carbon values methane produced within incubation vials, and $\delta^{13}C\text{-}CO_2$ values for production within incubation vials. 136

7.1 Salinity, methane isotopic carbon values, carbon dioxide isotopic values, deuterium isotopic values oxygen isotopic values, and fractionation factors.....154

7.2 Salinity, methane isotopic carbon values, carbon dioxide isotopic values, deuterium isotopic values, and oxygen isotopic values. 155

A.1 Methane bubble concentration, ethane concentration, methane isotopic carbon values, carbon dioxide isotopic values, deuterium isotopic values from California pond samples collected in December 2008.....161

A.2 Methane bubble concentration, ethane concentration, methane isotopic carbon values, carbon dioxide isotopic values, deuterium isotopic values from Baja pond samples collected in March 2009.. 162

A.3 Methane bubble concentration, ethane concentration, methane isotopic carbon values, carbon dioxide isotopic values, deuterium isotopic values from Baja pond samples collected in October 2009......164

A.4 Methane bubble concentration, ethane concentration, methane isotopic carbon values, carbon dioxide isotopic values, deuterium isotopic values from California pond samples collected in January 2010.....166

A.5 Methane bubble concentration, ethane concentration, methane isotopic carbon values, carbon dioxide isotopic values, deuterium isotopic values from Baja pond samples collected in September 2010.. 167

B.1 Methane incubation rate production data from Baja pond incubation samples collected in March 2009.. 168

B.2 Methane incubation rate production data from Baja pond incubation samples collected in October 2009..... 175

B.3 Methane incubation rate production data from California pond incubation samples collected in January 2010. 177

B.4 Methane incubation rate production data from California pond incubation samples collected in August 2010. 178

C.1 Methane incubation rate production data, methane isotopic data from Baja pond incubation samples collected in March 2009..... 179

C.2 Methane incubation rate production data, methane isotopic data from Baja pond incubation samples collected in October 2009. 182

C.3 Methane incubation rate production data, methane isotopic data from California pond incubation samples collected in January 2010.. 185

C.4 Methane incubation rate production data, methane isotopic data from California pond incubation samples collected in August 2010..... 186

LIST OF FIGURES

1.1 Approximate upper salt concentration limits for microbial processes. 17

1.2 Schematic of a cyanobacterial microbial mat with associated depth-related light and chemical gradients. 18

1.3 Substrates which lead to methanogenesis in hypersaline environments. 20

2.1 Map of field sampling site. 30

2.2 Map of South San Francisco Bay field sampling site.....31

2.3 Map of Guerrero Negro field site 32

2.4 Sketch of Laguna Figueroa field site (modified after Horodyski 1977). 33

3.1 Picture of Microbial Mat subsection from GN Pond 4 and CAL Pond 15.....43

3.2 Picture of small cores from GN Pond 9 and CAL Pond 23.....44

4.1 Map of field sampling sites 62

4.2 Percentage of methane in bubbles plotted against the $\delta^{13}C_{CH4}$ values (‰). 63

4.3 The salinity of ponds sampled plotted against the $\delta^{13}C_{CH4}$ values (‰) obtained from bubble samples.....65

4.4 Cross plot of $\delta^{13}C_{CH4}$ against $\delta^{2}H_{CH4}$ values of methane-rich bubbles.....66

4.5 Measurements of the ratio of methane to ethane concentrations (C_1/C_2) plotted against the $\delta^{13}C_{CH4}$ values of the methane-rich bubbles. 67

5.1 Picture (**A**) CAL pond 23, picture (**B**) GN Area 4, picture (**C**) GN Area 9 gypsum crust, picture (**D**) GN Area 9 core with all layers.....101

5.2 Methane production rates from sites in Don Edwards National Wildlife Refuge and Guerrero Negro. 103

5.3 Methane production measurements from the gypsum crust of CAL Pond 23, sampled in January 2010 104

5.4 Isotopic composition of methane produced from incubation samples from CAL Pond 15 collected in January 2010. 105

5.5 Isotopic composition of methane produced from incubation samples from CAL Pond 23 collected in January 2010 (**A**) and August 2010 (**B**). 106

5.6 Isotopic composition of methane produced from incubation samples from GN Area 1 site 1 (**A**) and GN Area 1 site 2 (**B**) collected in March 2009. 107

5.7 Isotopic composition of methane produced from incubation samples from GN Area 1 collected in October 2009. 108

5.8 Isotopic composition of methane produced from incubation samples from GN Area 4 collected in March 2009 (**A**) and October 2009 (**B**). 109

5.9 Isotopic composition of methane produced from incubation samples from GN Area 9 top mud (**A**) and bottom mud (**B**) collected in March 2009. 110

5.10 Isotopic composition of methane produced from incubation samples from GN Area 9 crust (**A**) and rubble (**B**) collected in October 2009. 111

6.1 Methane production rates from GN Area 1, GN Area 4, GN Area 9 rubble, and GN Area 9 crust sampled in October 2009 (**A**) and CAL Pond 15 and CAL Pond A23 sampled in January and August 2010 (**B**). 137

6.2 Isotopic composition from GN Area 1, GN Area 4, GN Area 9 rubble, and GN Area 9 crust sampled in October 2009 (**A**) and CAL Pond 15 and CAL Pond A23 sampled in January and August 2010 (**B**). 138

6.3 Methane production rates from GN Area 1 collected in March 2012. 139

6.4 Methane isotopic composition from GN Area 1 collected in March 2012 140

6.5 Methane production rates from GN Area 1 collected in October 2012. 141

6.6 Methane isotopic composition from GN Area 1 collected in October 2012. 142

7.1 δD and $\delta^{18}O$ analysis of overlying water from GN Ponds 1-9.. 156

7.2 δD versus the $\delta^{18}O$ of the overlying water in the pond systems sampled in comparison to the global meteoric water line $\delta D = 8(\delta^{18}O) + 10$.. 157

B.1 Methane rate production values for Guerrero Negro Area 1 sampled in October 2009.. ...171

LIST OF ABREVIATIONS

California ..... CAL
Dimethylsulfide ..... DMS
Dissolved Inorganic Carbon ..... DIC
Gas Chromatograph ..... GC
Guerrero Negro ..... GN
Isotope Ratio Mass Spectrometer ..... IRMS
Laguna San Ignacio ..... LSI
Mars Atmosphere and Volatile EvolutioN ..... MAVEN
Methanol ..... MeOH
Monomethylamine ..... MMA
Particulate Organic Carbon ..... POC
Parts Per Thousand ..... PPT
Sample Analysis at Mars ..... SAM
Sodium Bicarbonate ..... Bicarb
Sodium Hydroxide ..... NaOH
Sulfate Reducing Bacteria ..... SRB
Trimethylamine ..... TMA

ABSTRACT

The recent reports of methane in the atmosphere of Mars, as well as the findings of hypersaline paleoenvironments on that planet, have underscored the need to evaluate the importance of biological (as opposed to geological) trace gas production and consumption, particularly in hypersaline environments. Methane in the atmosphere of Mars may be an indication of extant life, but it may also be a consequence of geologic activity and/or the thermal alteration of ancient organic matter. On Earth these methane sources can be distinguished using stable isotopic analyses and the ratio of methane (C_1) to C_2 and C_3 alkanes present in the gas source (C_1/(C2+C3)). We report here that methane produced in hypersaline environments on Earth has an isotopic composition and alkane content outside the values presently considered to indicate a biogenic origin. Higher salinity endoevaporites yielded what would be considered nonbiogenic methane based upon stable isotopic and alkane content, however incubation of crustal and algal mat samples resulted in methane production with similar isotopic values. Radiocarbon analysis indicated that the production of the methane was from recently fixed carbon. An extension of the isotopic boundaries of biogenic methane is necessary in order to avoid the possibility of false negatives returned from measurements of methane on Mars and other planetary bodies.

CHAPTER ONE

INTRODUCTION

This chapter introduces the study objectives and provides a brief overview of each chapter. The chapter also provides an introduction to methane and its role in hypersaline environments, and includes an explanation of the importance of understanding methane in hypersaline environments in terms of its impact on the study of life outside of our planet.

1.1 Dissertation Objectives and Overview

The objective of this dissertation was to provide an in-depth analysis of methane production in hypersaline environments. This was accomplished through the analysis of sediment and gaseous samples collected in diverse hypersaline environments. Methane production rates and isotopic signatures were analyzed to reveal a complete picture of the hypersaline methane production. The analysis of substrate utilization in the various hypersaline environments studied provided information on methanogenic pathways and community preferences.

1.2 Chapter Outline

1.2.1 Chapter 2: Sample Sites

Chapter 2 introduces the sampling locations used for this study and describes them based on location, salinity, and quality of microbial mats and/or endoevaporites. Historical information about the ponds as well as current usage purposes also are provided.

1.2.2 Chapter 3: Experimental Procedure

Chapter 3 provides a detailed description of all methods used for sample collection, which varied based on differences in sediment type at each of the different salinity levels. The methods used for the analytical analysis of gas samples, sediment samples, and water samples also are explained.

1.2.3 Chapter 4: Isotopic Characterization and Classification of Methane Bubbles

Methane sources can be distinguished using stable isotopic analysis and the ratio of methane (C_1) to C_2 and C_3 alkanes present in the gas source ($C_1/(C_2+C_3)$. Chapter 4 characterizes the stable isotopic composition of methane produced in hypersaline environments, an unexamined ecosystem. This chapter is published in ICARUS (2013).

1.2.4 Chapter 5: Analysis of Methane Production from Hypersaline Sediment Samples

Chapter 5 provides an in-depth analysis of the utilization of carbon substrates for methane production in sediment samples obtained in hypersaline environments. The goals of this chapter were to provide evidence of overall biogenic methane production, provide evidence of the source of methane production within endoevaporite sites, perform a comparative analysis of methane production in various high salinity ranges, and to provide isotopic evidence of methane production from non-competitive substrates.

1.2.5 Chapter 6: Methane Production and Isotopic Analysis from Hypersaline Microbial Mat Incubations when Sulfate Reduction is Inhibited

Chapter 6 provides an analysis of the isotopic and production rates of methane produced in sediment and gypsum crustal samples when sulfate reducing bacteria are chemically inhibited. The goals were to provide evidence of lower methane production in our hypersaline environments due to active sulfate reducing bacteria, and to provide evidence of methane production through the use of competitive substrates, when sulfate reducing bacteria are not active.

1.2.6 Chapter 7: Fractionation Factors in Hypersaline Ponds

Chapter 7 provides an isotopic analysis of the dissolved inorganic carbon and the formation water found in our hypersaline ponds. The goal of this chapter were to determine if apparent fractionation factors could be used to determine substrate utilization by methanogens.

1.2.7 Chapter 8: Conclusions

Chapter 8 contains a discussion of the conclusions of this study, as well as areas needing further research.

1.3 Background to the Study and Key Terms

1.3.1 Hypersaline Environments

Hypersaline environments are those environments that contain a greater concentration of salts than seawater and can be found in coastal, inland, and deep sea areas. Both man-made and

natural coastal environments may be subject to desiccation which results in a wide variety of habitats – from small, ephemeral salt pans within temperate salt marshes to large, permanently hypersaline sabkhas, also called salt flats (McGenity, 2010). Similarly, inland salt lakes can be as large as the Great Salt Lake or as tiny as a spring. Hypersaline environments are widespread and were even more prevalent in former geologic times (Zharkov and Yanshin, 1981). Deep-sea, anoxic, hypersaline brines, derived from the dissolution of such ancient evaporates, form large lakes on the floor of the Gulf of Mexico, the Mediterranean, and the Red Sea (McGenity, 2010). This study focuses on coastal environments that contain saltern systems in three different stages of commercial salt production: natural non-commercial salt flats, commercial salt flats, and post-commercial salt flats.

Natural salt flats are areas where salt water forms a small pool on land and gets trapped. Evaporative processes eventually will cause the precipitation of brine material. Commercial salt flats are typically flow-through systems where seawater is pumped into a series of shallow evaporative ponds. The high surface-to-volume ratio promotes evaporation as the brines slowly flow to each succeeding, more saline pond in the series (Javor, 2002; Oren et al., 2009). Such systems are designed to manage the precipitation of the less soluble marine minerals, calcium carbonate and gypsum, so that only sodium chloride precipitates in the crystallizer ponds (Javor, 2002; Oren et al., 2009). Once the sodium chlorides have precipitated in these crystallizer ponds, the brines continue to evaporate and the more soluble minerals that contain high concentrations of magnesium, potassium, chloride, and sulfate begin to precipitate(Javor, 2002; Oren et al., 2009). Finally, depending on the intentions of the salt company the minerals either are harvested or they are returned to the sea.

Hypersaline environments contain rich and varied communities of microorganisms (Foster and Green, 2011; Foster and Mobberley, 2010; Green et al., 2008; Horodyski, 1977; Ley et al., 2006; Margulis et al., 1980; Orphan et al., 2008; Smith et al., 2008). Characteristic salt-adapted microbial communities are found along the salinity gradient (Oren, 2001; Smith et al., 2008). In ponds with salinities up to ~150 ppt microbial mats are present while in ponds with salinities greater than ~150 ppt endoevaporitic microbial communities develop on the bottom of the ponds. In either case, only halophilic and halotolerant microbes can survive the harsh environment found in hypersaline ponds (Madigan and Martinko, 2006; Oren, 1999b; Oren, 2001).

Within the microbial world, two fundamentally different strategies enable microorganisms to cope with the stresses of high salt concentrations. In the first, the salt-in strategy, cells maintain high intracellular salt concentrations and all intracellular systems are adapted to the presence of high salt concentrations (Oren, 1999b). In the second, the compatible-solute strategy, cells maintain low salt concentrations within their cytoplasm while the osmotic pressure is balanced by organic-compatible solutes and osmotic pump (Oren, 1999b). Although the salt-in strategy has been shown to be energetically more favorable (Oren, 1999b) than the maintenance of a low salt cytoplasm with organic osmotic solutes, in nature generally, and in our hypersaline sites in particular, the salt-in method is not widely found (Kunin et al., 2008). Most microbes inhabiting hypersaline environments employ the compatible-solute strategy since it does not involve the need for specially adapted proteins to tolerate the higher internal salinity (Oren, 1999b). A survey of halophilic microorganisms indicates that not all microbes can function in the presence of high salt concentrations (Oren, 1999b). Figure 1.1, modified from Oren (1999), illustrates the approximate upper limits of salt tolerance for microorganisms based

on laboratory studies of pure cultures (solid bars) and activity measurements of microbial communities in hypersaline environments in nature (open bars).

1.3.2 Hypersaline Microbial Community Habitats

Microbial mats. Microbial mats are self-sustaining, complex aquatic ecosystems that occur on surface sediments of hot springs, deep sea vents, polar lakes, hypersaline lagoons, coral reefs, sewage treatment plants, and estuaries (Des Marais, 1990). They are composed of microbial cells (which are often driven by oxygenic and anoxygenic photosynthesis) that facilitates the cycling of chemical elements (Dupraz and Visscher, 2005; Foster and Mobberley, 2010). Radiant energy from the sun sustains photosynthesis, which in turn provides chemical energy to the rest of the community (Bebout et al., 2002).

Typical of most microbial mats, light penetration is only a few millimeters into the mat during the day, and oxygen produced by photosynthesis rapidly diminishes with depth (Jorgensen and Des Marais, 1986). At night, the mat, and in some cases, the overlying water become anoxic and concentrations of hydrogen sulfide can become high due to ongoing sulfate reduction in the absence of photosynthesis (Bebout et al., 2002; Jorgensen et al., 1979; Kirk Harris et al., 2013). Microbial mats are not all phototrophic; active chemotropic communities have been found in remote settings like deep-sea hydrothermal vent areas and sediments underlying oxygen-minimum zones (Canfield et al., 2005). For the purposes of this study, however, we will only consider photosynthetic microbial mats located in hypersaline lagoons.

Microbial mats typically are known to be vertically stratified (Figure 1.2). These stratifications are dictated by the microbial community within the mat, with dominant populations positioned relative to their requirements for light and chemical interfaces (Canfield

et al., 2005; Dupraz and Visscher, 2005) .Within a mat system various types of diverse bacteria and *Archaea* have been found to function as a consortium that together performs the chemical cycling necessary to thrive in waters that are typically depleted in basic nutrient elements (Javor, 1983; Smith et al., 2008).

During initial microbial mat formation, primary producers must adhere at the sediment/water interface and form an initial establishment (Franks and Stolz, 2009; Stal, 1995; Stal et al., 1985). Once the initial establishment has occurred, these photoautotroph's (including cyanobacteria) photosynthesize and produce carbohydrates by fixing inorganic carbon, which in turn serves as a source of energy (Bebout et al., 2002; Des Marais, 2003) (Figure 1.2a). In this way, the mat becomes a self-sustaining ecosystem. The oxygen-rich phototrophic layer is typically followed by a layer of phototrophic or chemotropic sulfide-oxidizing organisms (Figure 1.2b). Below this, a zone of heterotrophic organisms provide a region of sulfate reduction and methanogenesis (Figure 1.2c).

Endoevaporites. In some hypersaline environments, seawater salinity is high enough (usually >~150 ppt) to prevent the formation of soft microbial mats. In these instances microbial communities form within evaporative rocks. These endoevaporitve rocks are often characterized by the development of multicolored stratified microbial communities. The various microbes in these communities, including different types of cyanobacteria, purple sulfur bacteria, and other pigmented microorganisms, arrange themselves according to the gradient of light energy (Oren et al., 2009). Because of the light channeled by gypsum crystals, light penetration is relatively deep into the crust, allowing for a much deeper photic zone (Canfield et al., 2005).

1.3.3 Methane

Methane is the most abundant hydrocarbon in the atmosphere, where it plays an important role in atmospheric chemistry. An important greenhouse gas, methane absorbs infrared radiation more effectively than carbon dioxide and is 21 times more potent greenhouse gas than CO_2 (Petit et al., 1999). Ice core records over the last 470,000 years have revealed that atmospheric methane concentrations have varied between about 350 and 700 ppbv, a range similar to changes observed in atmospheric CO_2 (Lelieveld et al., 1998; Petit et al., 1999). Because the concentration of methane in our atmosphere has increased from around 700 ppbv to the present values of about 1760 ppbv over the last 300 years, however, both the public and the scientific community have focused more on the causes and climate consequences of increased methane.

The primary sources of atmospheric methane are wetlands, biomass burning, landfills, rice paddies, ruminant animals, and marine environments. Although marine environments are a minor source of atmospheric methane, our interest in methane production in hypersaline environments stems from a need for greater knowledge about methane production and microbial evolution here on Earth.

1.3.4 Methanogens

Methanogens are *Archaea* that produce methane as the end-product of their anaerobic respiration. They differ from other archeabacteria because they contain large amounts of coenzymes essential for methane synthesis (Madigan and Martinko, 2006). Methanogens are typically abundant in habitats where electron acceptors such as O_2, NO_3^-, Fe^{3+}, and SO_4^{2-} are limiting. A distinctive feature of methanogens is their extreme sensitivity to oxygen, which

forces methanogens to be very strict anaerobes. For this reason, they are generally present only in anoxic environments in nature. Methanogens have been cultivated from a variety of anaerobic environments, including those with extreme temperatures, salinity, and pH.

Methanogens are related to each other primarily by their mode of energy metabolism, but they are very diverse with respect to other properties. Most methanogens form methane by pathways that are commonly classified according to the type of carbon precursor they utilize (Thauer et al., 2008; Whiticar, 1999). Methanogens utilize few and simple compounds to obtain energy and they can be separated into competitive and non-competitive substrates. Methanogens obtain their energy for growth from the conversion of a limited number of substrates to methane gas.

Growth substrates for methanogenic *Archaea* include a variety of compounds including carbon dioxide and hydrogen, formate, acetate, methanol, ethanol, ethylated sulfur compounds and methylated amines (Canfield et al., 2005; King et al., 1983; Madigan and Martinko, 2006; Oremland et al., 1987). While a variety of compounds may be utilized as substrates during methanogenesis, most natural environments do not contain sufficient concentrations of these compounds to maintain methanogenesis. The dominant substrates fueling methanogenesis globally are acetate (Equation 1, acetototrophic methanogenesis) and the reduction of CO_2 by hydrogen gas (Equation 2, hydrogenotrophic methanogenesis):

$$CH_3COO^- + H_2O \rightarrow CH_4 + HCO_3^- \quad (1)$$

$$CO_2 + 4H_2 \rightarrow CH_4 + 2H_2O \quad (2)$$

Though both pathways can occur in marine and freshwater systems, CO_2-reduction dominates in marine sediments while acetotrophic methanogenesis dominates in freshwater sediments (Whiticar et al., 1986). In acetotrophic methanogenesis, acetate is the major source of methane

with the methyl carbon being oxidized to CO_2. In hydrogenotrophic methanogenesis, the electron donor is H_2, formate or certain alcohols and the electron acceptor is CO_2, which is further reduced to methane.

The active pathway for methanogenesis is controlled by the presence or absence of sulfate. In marine environments, in the presence of excess sulfate, sulfate reducing bacteria (SRB) outcompete methanogens for the common substrates hydrogen and acetate since they have a lower affinity and higher threshold (Burdige, 2006; Kristjansson and Schönheit, 1983; Muyzer and Stams, 2008). This can be expressed by comparing the ΔG of both methanogens and sulfate reducers utilizing both substrates(Muyzer and Stams, 2008; Whitman et al., 2006) (Table 1.1). The reaction producing the more negative value would be more favorable thermodynamically and would, therefore, proceed. Hydrogen-utilizing methanogens are easily and rapidly outcompeted by hydrogen-utilizing sulfate reducing bacteria, and the same can be said for acetoclastic methanogens and acetate-utilizing sulfate reducers because they have a lower affinity and higher threshold value for hydrogen (Muyzer and Stams, 2008) (Table 1.1). The utilization of competitive substrates for the process of methanogenesis is severely limited in the water column or sediment pore fluid because of an abundance of dissolved sulfate.

While the presence of sulfate and SRB inhibits methanogenic activity, the products of sulfate reduction can lead to ideal chemical conditions for methanogens. The continued remineralization of organic matter from sulfate reduction eventually leads to an increase in dissolved inorganic carbon. Once sulfate reducing bacteria utilize all available sulfate and acetate, the now elevated bicarbonate concentrations provide the substrate for methane production to occur via CO_2-reduction (Whiticar, 1999; Whiticar et al., 1986). When in low

sulfate concentrations typical of freshwater environments, acetate fermentation is the dominant pathway of methane production due to the absence of competitive communities.

In environments where sulfate concentrations never become depleted methanogens have evolved a third pathway for methane production. The third pathway, methylatrophic methanogenesis, is a non-competitive pathway that includes the use of methylated substrates such as methanol (Equation 3 and 4), methylated amines (Equations 5, 6 and 7), and dimethylsulfide (Equation 8) for the production of methane. This group, methylotrophic methanogenesis, involves methanogens that utilize methyl-containing C_1 compounds as both electron donor and acceptor. When this dual usage of methyl compound occurs some molecules of the methylated substrates are oxidized to CO_2 while the remaining methyl group becomes the electron acceptors and are reduced directly to methane.

$$CH_3OH + H_2 \rightarrow CH_4 + H_2O \quad (3)$$

$$4CH_3OH \rightarrow 3CH_4 + CO_2 + 2H_2O \quad (4)$$

$$4CH_3NH_2 + 2H_2O \rightarrow 3CH_4 + CO_2 + 4NH_4^+ \quad (5)$$

$$2(CH_3)_2NH + 2H_2O \rightarrow 3CH_4 + CO_2 + 2NH_4^+ \quad (6)$$

$$4(CH_3)_3N + 6H_2O \rightarrow 9CH_4 + 3CO_2 + 4NH_4^+ \quad (7)$$

$$2(CH_3)_2S + 2H_2O \rightarrow 3CH_4 + CO_2 + H_2S \quad (8)$$

The use of these non-competitive substrates is thought to be of great importance in hypersaline environments (Oremland et al., 1982), due to the high concentration of sulfate present in these environments as well as the abundance of noncompetitive substrate precursors (Figure 1.3). In marine sediments, trimethylamine may be formed from choline, glycine betaine, or trimethylamine oxide (TMAO) (Oremland and King, 1989; Whitman et al., 2006) (Figure 1.3). Dimethylsulfide is derived primarily from hydrolysis of its precursor molecule

dimethylsulfoniopropionate (DMSP), which, like glycine betaine, is a compatible solute aiding in the osmotic balance of microbes in hypersaline environments and, as such, is common in those environments (Jonkers et al., 1998; Kiene et al., 1986; Oremland and King, 1989; Visscher and Van Gemerden, 1991) (Figure 1.3). Similarly, methanol may be formed from the anaerobic transformation of the methoxy groups of pectin (Ollivier et al., 1994; Oremland and King, 1989; Whitman et al., 2006) (Figure 1.3).

1.3.5 Isotopes

The use of isotopes in geochemistry has become important in understanding geochemical processes. Isotopes are atoms of the same element with the same atomic number but different atomic masses. They have the same number of protons in the nucleus, which defines their atomic number and chemical behavior; however, they have a different number of neutrons which provides the difference in their atomic mass (Burdige, 2006). Isotopes can be classified into two main categories: unstable isotopes and stable isotopes.

Unstable Isotopes. Unstable isotopes, otherwise known as radioactive isotopes, are those isotopes whose nuclei are unstable and undergo radioactive decay over time. Radioactive decay of an element has a characteristic decay constant, the amount of time it takes for half of the available material to decay away. Because of this characteristic, radioisotopes have been used to date sediment material for geologic purposes. In this paper we will focus on the radioisotope of carbon ^{14}C and its usefulness for dating sediment samples and helping to determine methane sources.

All living biomass is imprinted with a $\Delta^{14}C$ signature set by carbon fixation from atmospheric CO_2, which is naturally enriched with ^{14}C. Because of nuclear-weapons testing in

the 1950s and 1960s, contemporary atmospheric CO_2, and the biomass fixed from it, has a $\Delta^{14}C$ value of +55 ± 5‰ (=106% modern) relative to pre-bomb atmospheric CO_2 (100% modern) (Turnbull et al., 2007). Similarly, biogenic methane, which is derived from recently fixed organic matter, also should be relatively enriched in ^{14}C. On the other hand, thermogenic methane, which can be millions of years old, generally contains no ^{14}C because of the relatively short half-life of ^{14}C (~5730 years) (Brady et al., 2009). Even petroleum being formed near the spreading center of Guaymas Basin, a geologically very young location approximately 5000 years old (Didyk and Simoneit, 1989), is readily distinguishable from modern organic matter with ^{14}C analyses. Therefore, ^{14}C analyses can assist in providing an estimated time frame for methane gas formation and aid in the identification of the substrates supporting methane production (Chanton et al., 2008).

Stable Isotopes. Stable isotopes are those isotopes that do not undergo radioactive decay. The slight differences in the number of neutrons present in these atoms affect the way they respond in either chemical reactions or physical processes that are mass dependent (Burdige, 2006). These differences also lead to isotope fractionation from which researchers studying stable isotopes can extract information about biogeochemical processes in nature.

The delta (δ) notation was introduced in the 1950's to report stable isotope data because relative differences in isotopic ratios can be determined far more precisely than absolute isotopic ratios (Sharp, 2007) Isotope compositions are generally expressed as the isotope ratio of the sample (R_{sample}) relative to that in a common standard ($R_{standard}$),

$$\delta = 1000 \left[\left(\frac{R_{sample}}{R_{standard}}\right) - 1\right]$$

where R is the ratio of the heavy isotope to the light isotope, and δ is reported as parts per thousand, or per mil (‰). If δ is greater than zero, then the ratio of the heavy to the light isotope

is higher in the sample than in the standard (Sharp, 2007). Conversely, if δ is less than zero than the sample is depleted in the heavy isotope. Our focus in this study is on the stable isotopes of carbon and hydrogen.

Carbon has two main stable isotopes ^{12}C and ^{13}C (Table 1.2). In nature ^{12}C is 98.9% more abundant than ^{13}C. The analysis of carbon isotopes can help to distinguish between methane pathways. Naturally occurring biogenic methane is characterized by a low $^{13}C/^{12}C$ ratio, with $\delta^{13}C_{CH4}$ values ranging from –110‰ to –50‰, whereas thermogenic methane generally has $\delta^{13}C$ values > –50 ‰ and is characterized by progressive enrichment in ^{13}C content with increasing maturity, eventually approaching the $^{13}C/^{12}C$ of the original organic matter (Kotelnikova, 2002; Whiticar, 1999). Isotope analysis of carbon also allows for distinction between the two main biogenic pathways, acetate fermentation with values ranging from –70‰ to –50‰ for $\delta^{13}C_{CH4}$ and CO_2 reduction with values ranging from –100‰ to –60‰ for $\delta^{13}C_{CH4}$, making isotopic analysis particularly valuable with respect to those pathways (Whiticar, 1999). Work with cultured methanogens suggests that methane produced from noncompetitive substrates, such as methanol, methylamines, and dimethyl sulfide, should be more depleted in ^{13}C than methane produced from either CO_2 reduction or acetate fermentation(Conrad, 2005; Potter et al., 2009).

Hydrogen has two main stable isotope forms, ^{1}H and ^{2}H (Table 1.2). In nature ^{1}H is approximately 99.98% more abundant than ^{2}H, also referred to as deuterium (D). The use of stable hydrogen isotopes to help distinguish between methane pathways is not as definitive as the use of carbon isotopes because of overlapping isotopic ranges. Biogenic methane has a wide range in $\delta^{2}H_{CH4}$ values, varying from –400‰ to –150‰, whereas thermogenic methane has a smaller $\delta^{2}H_{CH4}$ range, from –275‰ to –100‰ (Whiticar, 1999). This overlap does not allow for much interpretation of hydrogen isopes alone in regards to methane production pathways,

however when combined with carbon isotope data, a clearer separation between the biogenic methane production pathways exists. Isotopic analysis of methane from acetate fermentation reveals an isotopic signature of –70‰ to –50‰ and –375‰ to –300‰ for $\delta^{13}C_{CH4}$ and $\delta^{2}H_{CH4}$ values, respectively (Whiticar, 1999). The analysis of methane produced from CO_2 reduction reveals an isotopic signature of –100‰ to –60‰ and –250‰ to –150‰ for $\delta^{13}C_{CH4}$ and $\delta^{2}H_{CH4}$ values, respectively (Whiticar, 1999).

1.3.6 Astrobiological Significance of Project

The search for life on planets both within and outside our solar system has rapidly increased over the last 75 years. One planet that has received a great deal of attention is Mars, particularly as a potential location of life. The multiple spacecrafts currently operating on or around Mars have provided us with valuable but limited information. One way to better understand the data obtained from Mars is to study and analyze information from Mars-like analogue sites. These analogue sites are terrestrial locations that resemble Mars in certain ways and exhibit compositional traits as similar as possible to Martian soils or environments (Marlow et al., 2011).

Hypersaline environments have been considered analogue sites due to recent discoveries of past liquid brines, as well as the present-day frozen water on the surface of Mars (McEwen et al., 2011; Rennó et al., 2010; Smith et al., 2009) and the widespread occurrence of chloride-containing deposits also on the surface of Mars (Osterloo et al., 2008). The use of methane as a biosignature gas in these environments is extremely relevant as methane concentrations have been detected in the Martian atmosphere (Formisano et al., 2004; Krasnopolsky et al., 2004; McEwen et al., 2011; Mumma et al., 2009). The presence of methane has been challenged (Zahnle et al., 2011) and is being searched for by the Mars Science Laboratory, which landed on

Mars in August 2012. The detection of any methane on Mars would lead to questions about its origin, as Mars has an extremely oxidizing atmosphere and methane has been estimated to have an approximate residence time of around 300 years on Mars (Mischna et al., 2011; Nair et al., 2005). Obtaining a better understanding of biogenic methane production in a Mars analogue site can only enhance our understandings of information retrieved from the Mars Rovers and Orbital spacecrafts.

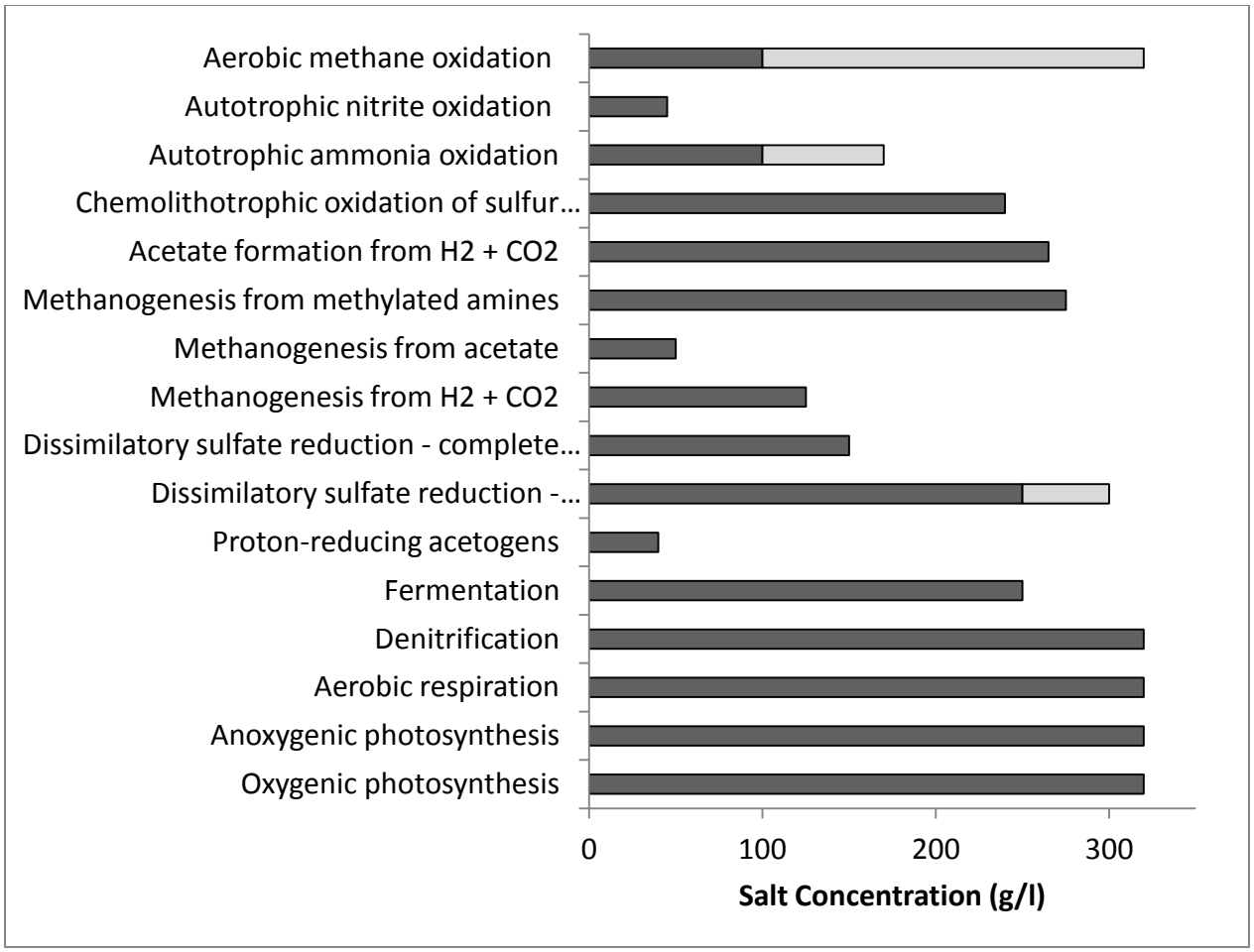

Figure 1.1 Approximate upper salt concentration limits for microbial processes. Values presented in solid bars are based on laboratory studies of pure cultures. Values presented in light shade bars are based on activity measurements of microbial communities in hypersaline environments in nature. Modified after Oren (1999).

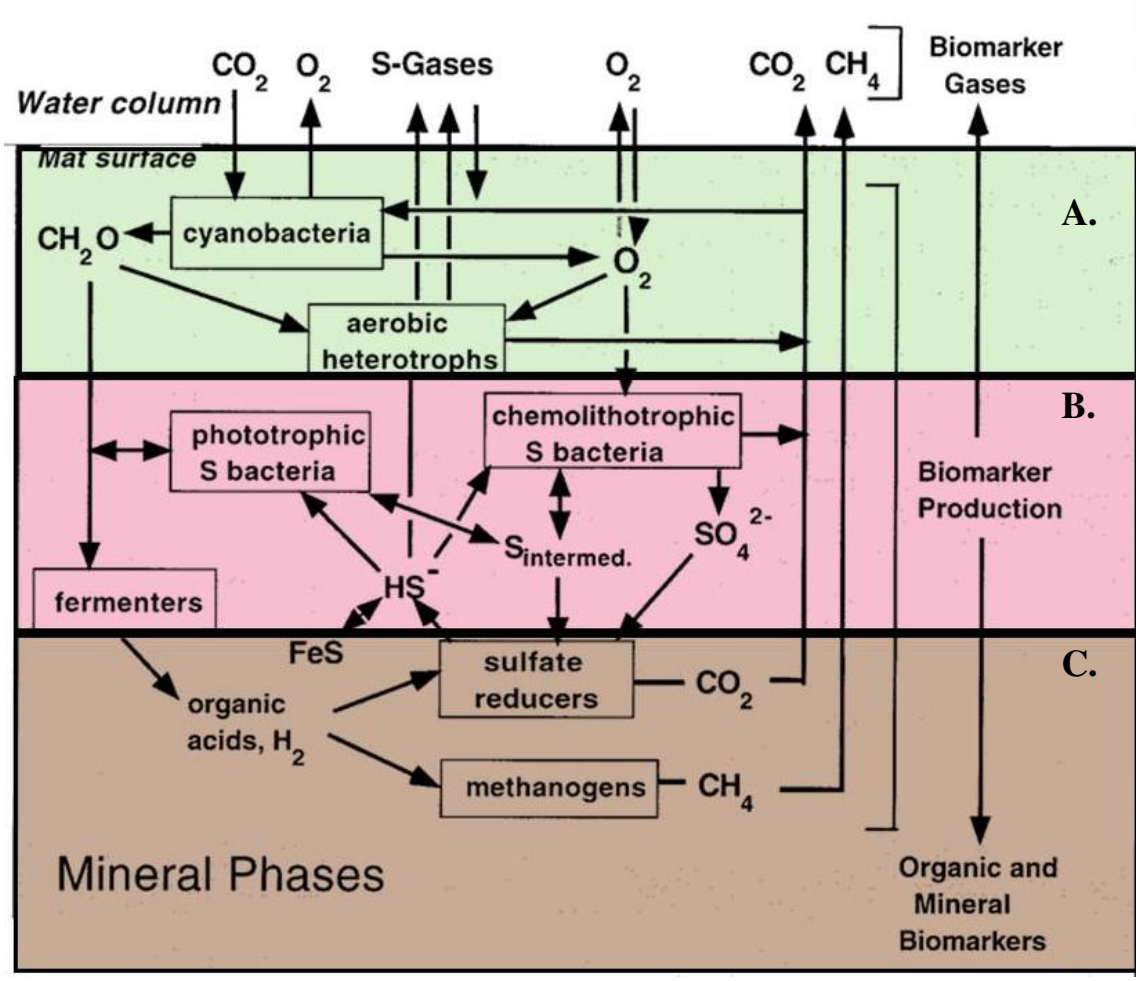

Figure 1.2. Schematic of a cyanobacterial microbial mat with associated depth-related light and chemical gradients. Boxes denote functional groups of microorganisms, and arrows denote flows of chemical species into or out of microorganisms. ***A.*** *This layer indicates the oxygen rich phototrophic layer.* ***B****. This layer indicates the phototropic or chemotrophic sulfide-oxidizing layer.* ***C.*** *This layer indicates the heterotrophic layer. Modeled after Des Marias (2003).*

Table 1.1 Reactions and standard changes in free energies for sulfate reduction and methanogenesis. Reactions producing more negative numbers are thermodynamically favorable. Data obtained from (Whitman et al., 2006) and (Muyzer and Stams, 2008).

Sulfate Reducing reactions	**ΔG°' (kJ/reaction)**
$4H_2 + SO_4^{2-} + H^+ \rightarrow HS^- + 4H_2O$	-151.9
$CH_3COO^- + SO_4^{2-} \rightarrow 2HCO_3^- + HS^-$	-47.6
Methanogenic reactions	**ΔG°' (kJ/mol of CH4)**
$CH_3COO^- + H_2O \rightarrow CH_4 + HCO_3^-$	-31.0
$CO_2 + 4H_2 \rightarrow CH_4 + 2H_2O$	-135.6
$CH_3OH + H_2 \rightarrow CH_4 + H_2O$	-112.5
$4CH_3OH \rightarrow 3CH_4 + CO_2 + 2H_2O$	-104.9
$4CH_3NH_2 + 2H_2O \rightarrow 3CH_4 + CO_2 + 4NH_4^+$	-75.0
$2(CH_3)_2NH + 2H_2O \rightarrow 3CH_4 + CO_2 + 2NH_4^+$	-73.2
$4(CH_3)_3N + 6H_2O \rightarrow 9CH_4 + 3CO_2 + 4NH_4^+$	-74.3
$2(CH_3)_2S + 2H_2O \rightarrow 3CH_4 + CO_2 + H_2S$	-73.8

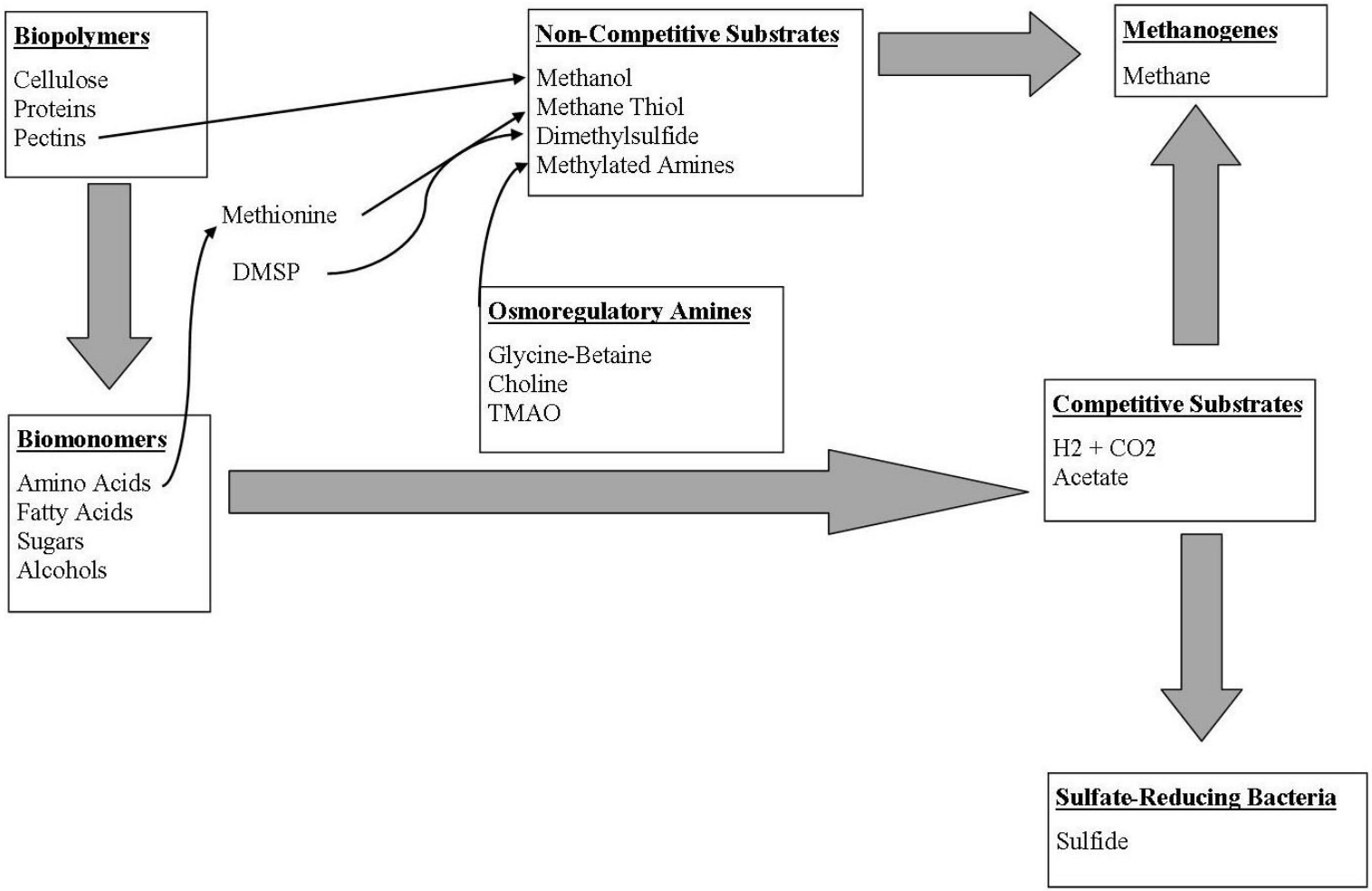

Figure 1.3 Substrates which lead to methanogenesis in hypersaline environments. Biopolymers, biomonomers, and osmoregulatory amines are readily available precursors available for conversion to be utilized as substrates by methanogens. Modified after (Oremland and King, 1989).

Table 1.2 Isotopic abundances and relative atomic masses of the pertinent elements in stable isotope geochemistry. Modified from Sharp (2007).

Symbol	Atomic Number	Mass Number	Abundance (percent)	Atomic Weight (^{12}C=12)
H	1	1	99.985	1.007825
D	1	2	0.015	2.0140
C	6	12	98.89	12
C	6	13	1.11	13.00335
O	8	16	99.759	15.99491
O	8	17	0.037	16.99914
O	8	18	0.204	17.99916

CHAPTER TWO

DESCRIPTION OF SITES SAMPLED FOR THE STUDY

2.1 Geographic Overview

Between 2008 and 2012, samples were taken for this study from two regions, Northern California, USA and Baja California, Mexico. Ponds A15 and A23 represent the two Northern California sampling sites, located within the Don Edwards National Wildlife Refuge in south San Francisco Bay. The numbers of these ponds were assigned by their previous owner, Cargill Inc., and are referenced throughout the research literature over the last 50 years. For the purposes of this study Pond A15 and A23 will be referred to as CAL Pond 15 and CAL Pond A23, respectively.

Samples were also taken for this study from Baja California, Mexico from three different areas, Guerrero Negro, Laguna Figueroa, and Laguna San Ignacio, within the Baja region (Figure 2.1). Guerrero Negro samples were from Ponds 1, 4, 6, 9, 10, 11, and 13 all located within the Exportadora de Sal salt production area. The numbers of the ponds in this area were assigned by the current owners of the salt company, Mitsubishi and the Mexican Government, and are similarly referenced throughout the literature during the last 30 years. The sampling sites in Laguna Figueroa and Laguna San Ignacio were ponds with no previously-assigned number structure, so for the purposes of this study these ponds were assigned numbers in ascending order with a prefix to differentiate Laguna Figueroa from Laguna San Ignacio.

2.2 Northern California, USA Sampling Sites

2.2.1 Don Edwards National Wildlife Refuge

In December 2008, January 2010, and August 2010, CAL Pond 15 and CAL Pond 23, were sampled at Don Edwards San Francisco Bay National Wildlife Refuge (Fig 2.2). These commercially-operated salt ponds were acquired by the U.S. Fish and Wildlife Service from Cargill, Inc. in March 2003. At the time of the study they were part of a long-term restoration project aimed at returning these artificially-enhanced salt ponds natural wetland habitats.

CAL Pond 15. Located within the Alviso slough unit, CAL Pond 15 spanned 249 acres and had an approximate salinity of 120 parts per thousand (ppt). This pond was bordered by the Alviso slough trail, a pedestrian path open for public use. The north side of the pond was bordered by tidal marsh land adjacent to Coyote Creek, which fed into South San Francisco Bay. The east end of the pond was bordered by Union Pacific Railroad tracks while the south and the west are bordered by ponds A13 and A14, respectively.

CAL Pond A23. Also located within the Alviso slough unit, CAL Pond A23 had an approximate salinity of 300 ppt. This pond was not visible to the public except by passing trains using the Union Pacific tracks. Unlike other ponds in the Alviso slough system, at the time of the study CAL Pond A23 was not permitted for waterfowl hunting due to historically high salinity and low water levels limiting waterfowl habitat. The south side of the pond was bordered by minimal tidal-marsh land and was adjacent to Mud Slough, which feeds into Coyote Creek. The north side was bordered by pond A22, while the west side was bordered by pond M4 which was an active commercial salt pond owned by Cargill Inc.

2.3 Baja California, Mexico Sampling Sites

2.3.1 Guerrero Negro

Guerrero Negro (GN) samples were obtained from salterns managed for the production of salt by the company Exportadora de Sal S.A. de C.V in Guerrero Negro, Baja California Sur, Mexico (Fig. 2.3). The salt works, located about 700 km south of the Mexico–USA border along the Pacific coast of the Baja California Peninsula at the edge of the Vizcaino Desert, covered an area greater than 300 km^2(Des Marais, 2010; Shumilin et al., 2002). The climate in this area is typically hot and dry, precipitation averaging less than 120 mm/year and exceeding 300 mm/year less than once per decade (Des Marais, 2010). The area also is characterized by year-round prevailing northwestern winds (Shumilin et al., 2002).

In the inter-linked system of salt producing ponds in Guerrero Negro region, seawater with a salinity of approximately 40 ppt (sampled in March 2009) is pumped in from the adjacent Ojo de Liebre lagoon through the pumping station into GN Pond 1. The ponds in this region did receive any groundwater influence because they lay above the local hydrologic gradient (Des Marais, 2010). Once in GN Pond 1, the system became density-driven. The seawater flowed through a series of 13 connected concentrating ponds in which salinity increased due to solar- and wind-induced evaporation. At the end of the concentration areas, the brine was pumped into a 32-pond crystallization system where salt was then harvested for shipment to commercial vendors across the globe. These ponds have been studied extensively over the last 20 years (Bebout et al., 2004; Des Marais, 2010; Green et al., 2008; Kelley et al., 2006; Ley et al., 2006; Orphan et al., 2008; Potter et al., 2009; Smith et al., 2008).

The salinity gradients of the ponds throughout the system were sampled in order to properly asses the system and collect a wide range of mat types. Ponds with salinity ranging from 40–65 ppt have been known to be dominated by the seagrass, *Ruppia* sp. and the green alga, *Enteromorpha* (Des Marais, 2010; Javor, 1983). Well-developed, laminated microbial mats are known to occur at salinities ranging from 60–125 ppt (Bebout et al., 2004; Des Marais, 2010), just as ponds with salinity over 130 ppt contain evaporite deposits consisting primarily of halite (NaCl) and gypsum ($CaSO_4 \bullet 2H_2O$) crusts with a wide variety of microbial communities present(Sahl et al., 2008).

In March 2009, Ponds 1, 4, 6, 9, 10, 11, and 13 were sampled. In October 2009, all ponds except Ponds 6 and 13 were sampled. In September 2010, Pond 9 was sampled only for bubble content.

GN Pond 1. GN Pond 1 was sampled in March 2009 and October 2009 and on both dates had a salinity of 55 ppt. In March 2012 and October 2012 samples had salinity levels of 62 ppt and 60 ppt, respectively. In March 2009, samples were obtained from two locations in GN Pond 1 with visibly different mat morphology, referred to from here on as GN Pond 1 site 1 and GN Pond 1 site 2. GN Pond 1 site 1 contained mat that was fully submerged, green in surface color and relatively thick with embedded seagrass blades throughout. Approximately 100 meters west of the original collection site but in similar water depth, GN Pond 1 site 2 contained microbial mats that were not as thick as those collected from GN Pond 1site 1, but in which seagrass blades were still visible.

On the October 2009 trip, samples were collected from approximately these same two locations in GN Pond 1, however, the visible appearance of the mats were different. The water level was significantly lower in the pond, with most of the mat in the outer rim of the pond

partially exposed to air. The mat was no longer solid and continuous throughout but was broken and cracked in the upper surface layer. To avoid the selection of an unhealthy microbial mat community, samples were taken from an area that was submerged in water and still maintained a semi-green surficial color. On the March and October 2012 trips, samples were collected from approximately the same locations in the pond where October 2009 samples were collected.

GN Pond 4. GN Pond 4 was sampled in March 2009 and October 2009. On the March 2009 trip the salinity was measured at 92 ppt. The mat sampled was fully submerged and similar to previously published descriptions of typical mat from this pond; it had a cohesive, rubbery texture mat 10 cm thick, with a smooth olive-tan surface color (Bebout et al., 2004; Des Marais, 2010). On the October 2009 trip the measured salinity was slightly lower at 84 ppt and the mats sampled were very similar in appearance to those sampled in March 2009, although the water level was slightly lower.

GN Pond 6. GN Pond 6 was sampled in March 2009 from the dyke near GN Pond 5. The salinity was measured at 136 ppt. Mat collected from this pond was obtained from an area that was fully submerged. The texture of the mat was not laminated as in the previous ponds sampled. Though this pond contained more gelatinous material, visible layering of microbial communities was still present.

GN Pond 9. GN Pond 9 was sampled in March 2009, October 2009, and September 2010. On the March 2009 trip, salinity was measured at 184 ppt a level that was no longer favorable for soft laminated microbial mat production but was favorable for the production of microbial communities within evaporites (endoevaporites). On the October 2009 trip, salinity was measured at 192 ppt. In September 2010 bubble samples were collected from this site though no salinity information was collected.

GN Pond 10. GN Pond 10 was sampled in March 2009 and October 2009. On the March 2009 trip GN Pond 10 was sampled in two locations, one area (ESSA C) fully connected to the entire pond with a salinity of 258 ppt, and the other (ESSA D) from an area partially cut off from the entire pond with a salinity of 306 ppt. This pond contained a smooth gypsum surface that resembled CAL Pond A23 from our Northern California Site. On the October 2009 trip, salinity was measured at three locations in GN Pond 10; GN Pond 10A, 10B, and 10C. GN Pond 10A and 10B contained seawater with salinity of 270 ppt while GN Pond 10C had a salinity of 298 ppt.

GN Pond 11. GN Pond 11 was sampled in March 2009 and October 2009. During both sampling trips salinity was measured at 300 ppt. This pond contained a fully submerged solid halite crust. Samples from this pond were obtained from within and underneath the halite crust.

GN Pond 13. GN Pond 13 only was sampled in March 2009. This pond contained a fully submerged solid halite crust. Samples also were obtained from within and underneath the solid halite crust.

2.3.2 Laguna Figueroa

Laguna Figueroa samples were obtained from a natural salt flat located in the Baja California del Norte region, approximately 400 km north of Guerrero Negro, Mexico, 15 km north of the Mexican city of San Quintin, and 300 km south of San Diego, California. This site, referred to in previous studies as Laguna Mormona, has been extensively studied over the last 40 years; it has been described as a closed hypersaline lagoonal complex consisting of an extensive evaporite flat and a narrow salt marsh (Fig. 2.4) (Franks and Stolz, 2009; Giovannoni et al., 1988; Horodyski, 1977; Horodyski and Bloeser, 1977; Horodyski and Vonder Haar, 1975;

Margulis et al., 1980). The area extends some 16 X 2 ½ km during wet periods with the main influx of seawater coming through the barrier dune ridge separating the lagoon from the sea and from runoff during rainy periods (Horodyski, 1977; Margulis et al., 1980).

In October 2009 samples were collected from multiple locations spanning both the evaporite flat and the narrow salt marsh. At the time of sampling, salinity in the region ranged from 54 to 200 ppt. Areas sampled were not fully submerged in water; however marsh-like conditions were present throughout and small sections of thin evaporite formations were observed. At the time of sampling, no qualitative determination was made about the state of the evaporites, and no compositional analysis was performed to determine the stage of the evaporite formations. Nor was it determined if seawater intrusion through the barrier dunes was occurring or had recently occurred at our site. We did, however, note that the locations sampled represented a mixture of both soft microbial mats and endoevapoirte formation, thus serving as an intermediate (or pre-endoevaporite) site.

2.3.3 Laguna San Ignacio

Laguna San Ignacio samples were obtained in March 2009 from three small ponds in a natural salt flat region located approximately 150 km south of Guerrero Negro and 950 km south of the U.S.–Mexico border. At Laguna San Ignaico (LSI) Pond-1 the salinity was found to be 360 ppt, at LSI Pond-2 it was 300 ppt, and at LSI Pond-3 it was 342 ppt. This region is part of the 2.5 million hectare (ha.) area known as El Vizcaino Biosphere reserve, which lies between 26°58'N and 113°16'W. These salt flats are adjacent to the actual San Ignacio lagoon, which has an extension of approximately 17,500 ha. Strong tidal currents that commonly exceed 2 m at spring tides (Senko et al., 2010a; Senko et al., 2010b) supply the region with a constant supply of

water. The mean annual temperature ranges between 18 and 26°C (Lopez-Castro et al., 2010). At the time of our sampling, this area produced salt through natural evaporation processes, but the area has been under review for some time as a possible location for a second salt-harvesting factory by Exportadora de Sal S.A. de C.V (Ortega-Rubio et al., 2001).

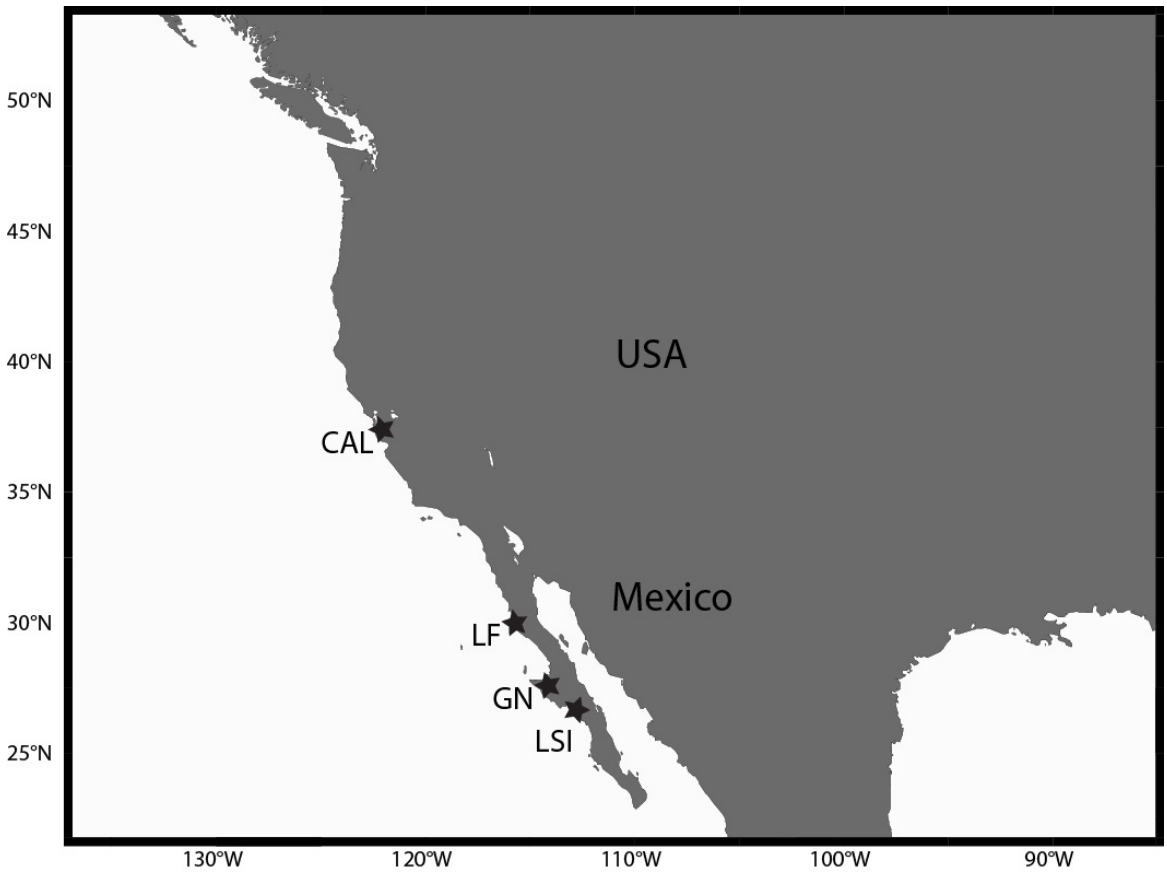

Figure 2.1. Map of field sampling site. Northern California sites are shown as CAL. Laguna Figueroa sites are shown as LF. Guerrero Negro sites are shown as GN. Laguna San Ignacio sites are shown as LSI.

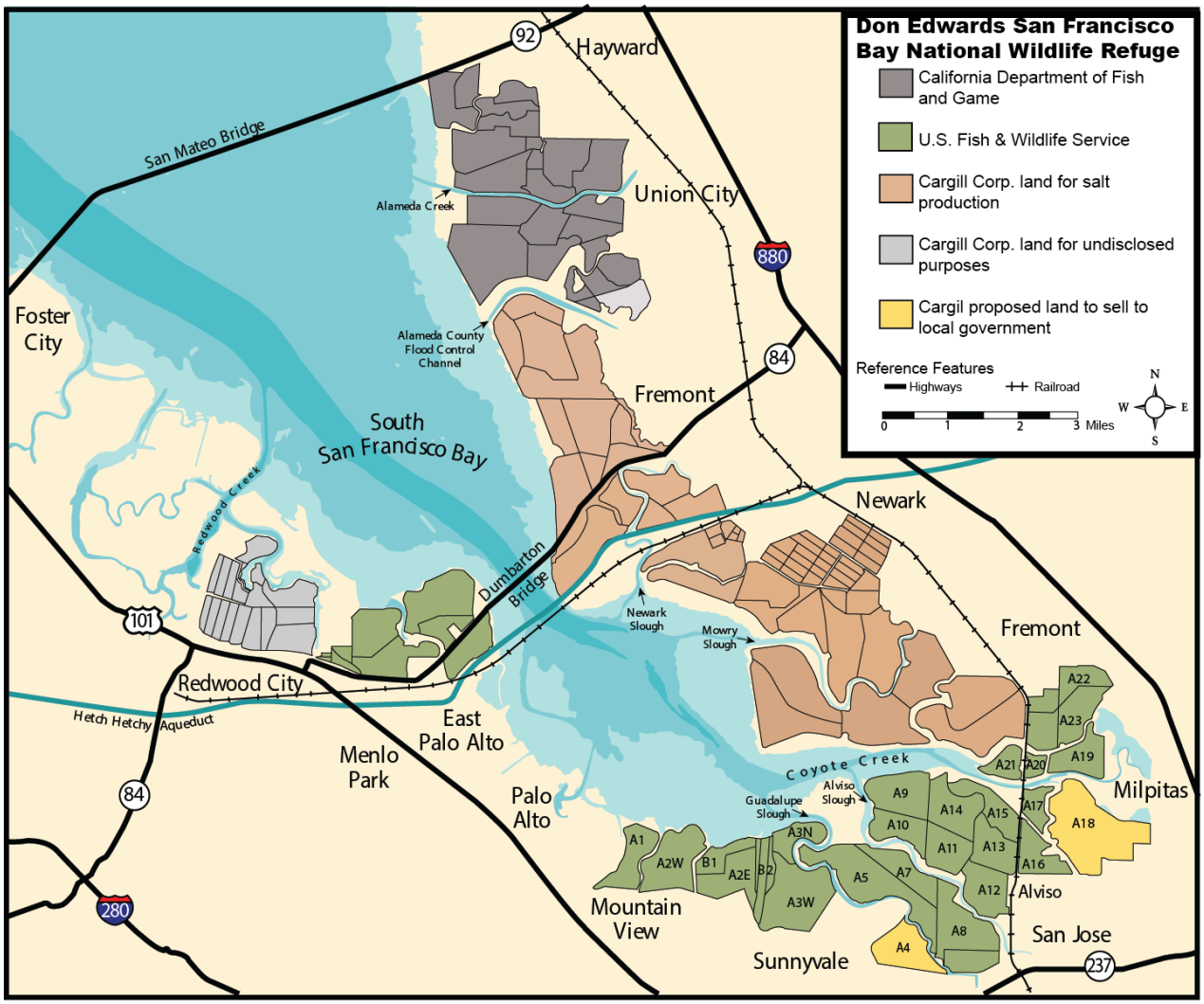

Figure 2.2. Map of South San Francisco Bay field sampling site. Areas shaded in green are owned and managed by U.S. Fish and Wildlife Services, areas shaded in dark gray are owned and managed by California Department of Fish and Game, areas shaded in orange, light grey and yellow are currently owned and managed by Cargill Corporation.

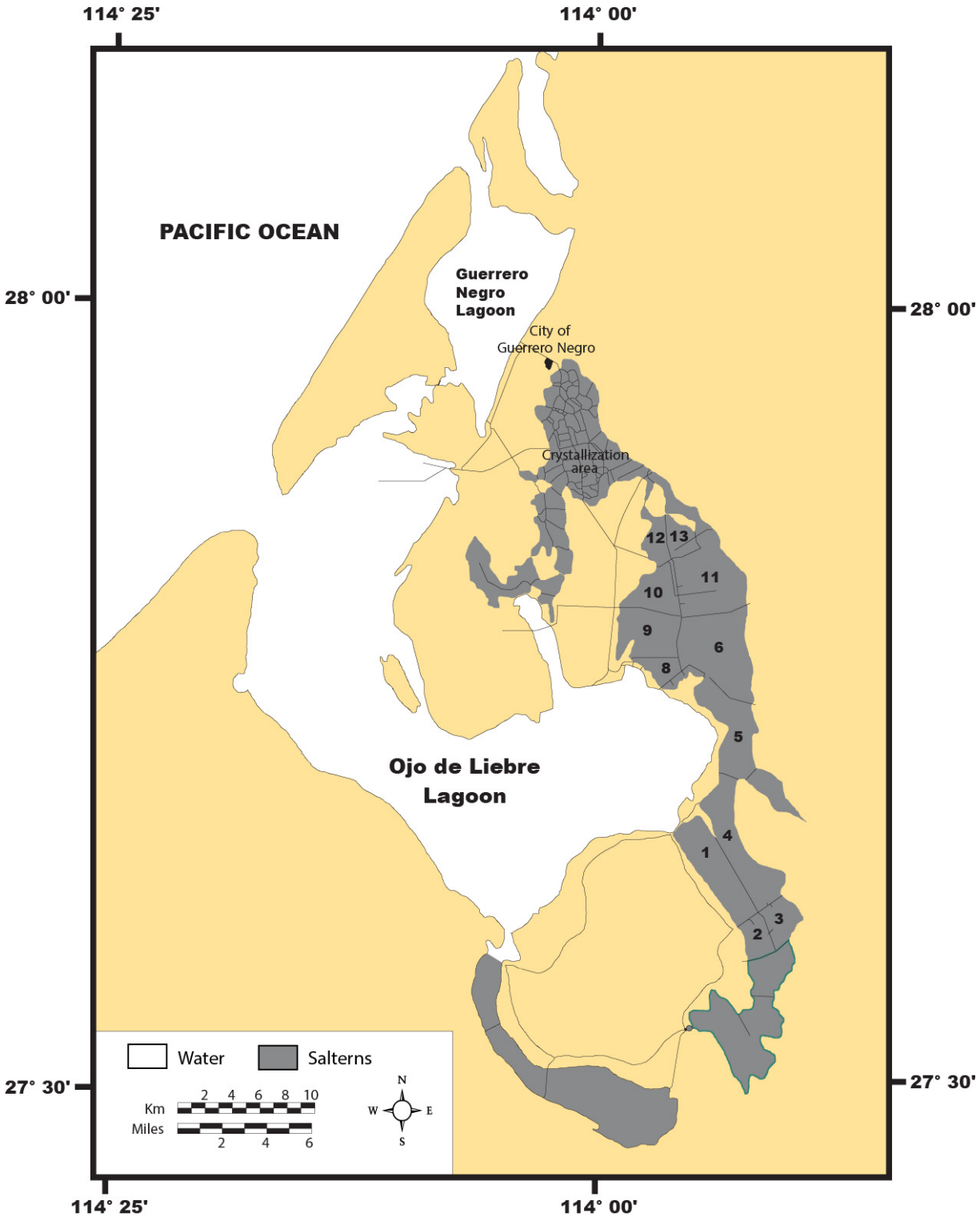

Figure 2.3. Map of Guerrero Negro field site. Salterns are shown in dark gray. Salt production concentration ponds are represented with corresponding pond number.

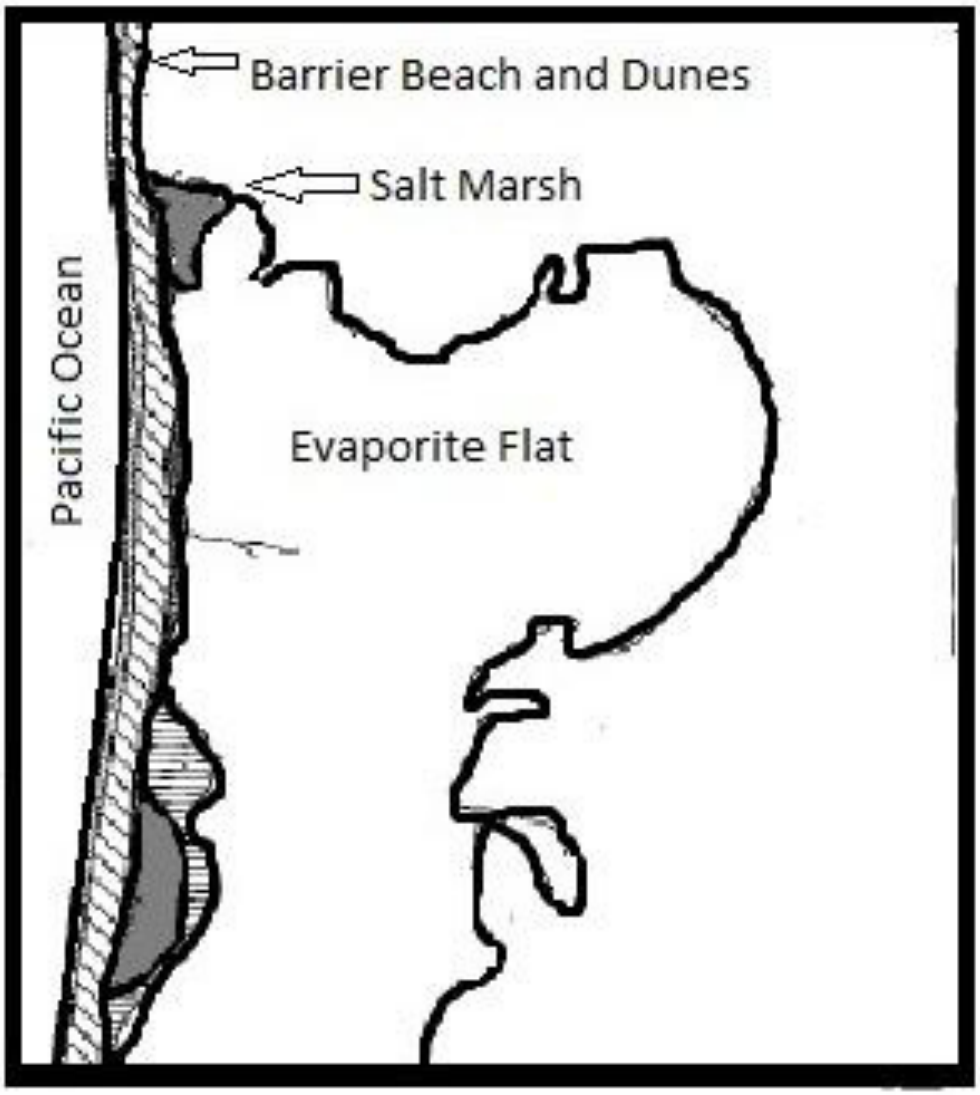

Figure 2.4 Sketch of Laguna Figueroa field site (modified after Horodyski 1977).

CHAPTER THREE

EXPERIMENTAL PROCEDURES

3.1 Sample Collection

Each of the sites sampled provided a variety of materials for collection. At the majority of the sites, microbial mats, sediment, or evaporite minerals (when present), overlying water, and gas bubbles were collected. CAL Ponds were those in the Don Edwards San Francisco Bay National Wildlife Refuge, GN Ponds were those in the Guerrero Negro Salterns and LSI Ponds were those in the Laguna San Ignacio area.

3.1.1 Microbial Mat, Sediment and Evaporite Mineral Collection

The soft microbial mats collected for this study were obtained from CAL Pond 15 and from GN Ponds 1 and 4. Mats were collected from CAL Pond 15 by traditional coring methods using short cores (Figure 3.1). This method was chosen due to the increased depth at this location and to preserve sediment layering during transport to surface. GN Ponds 1 and 4 were sampled via a different method due to the greater cohesiveness of the mats. Mat sections were cut and removed in 10-inch by 13-inch sections from the bottom of the ponds and placed immediately into tight fitting plastic trays. Mats were covered with water collected from the respective ponds and taken to shore for immediate processing (Figure 3.1).

Evaporites were collected from CAL Pond A23 and from GN Pond 9. Gypsum crust and black sulfur-rich sediment were collected from CAL Pond A23 by scooping them into a short core tube and filling the tube with site water prior to sealing. Evaporites and sediments were

collected from GN Pond 9 by breaking through the top crustal layer and then using short cores to core further down to collect the remaining crust, crustal rubble, and underlying sediment.

3.1.2 Overlying Water

Overlying water was collected from each site in different quantities for multiple purposes. Salinity of the overlying water was determined with a hand-held refractometer. In each location 60 mls of site water was collected in two 30 ml nalgene bottles for analysis of ^{18}O and ^{2}H. An additional 250 ml of site water was collected from GN Ponds 1, 4, and 9, and CAL Ponds 15 and A23 in two 125 ml nalgene bottles for use during incubation preparation.

3.1.3 Gas Samples

Gas bubbles from GN Ponds 1, 9, 10, 11, and 13, CAL Ponds 15 and A23, LSI Ponds 1, 2, and 3, and from multiple locations in Laguna Figueroa, consisted of bubbles emitted during the perturbation of sediment and crustal material. In instances where evaporite crusts were thick, manual breaking of the crust was necessary to gain access to trapped gas. These samples were collected under water by means of an inverted capped funnel. Gas collected in the funnel was removed with a 10-ml syringe and then transferred to a previously evacuated 10-mL glass vial capped with a butyl rubber stopper. Bubbles collected from one area were pooled to obtain a total volume of 20-ml in each vial. At least triplicate, and in some cases up to ten vials of gas samples, were collected from each site. Samples were then transported on ice to the laboratory, where subsamples were taken and analyzed for methane and other hydrocarbons.

3.2 Analytical Methods

3.2.1 Dissolved Inorganic Carbon

Dissolved inorganic carbon (DIC) samples were obtained by taking a small section of microbial mat and/or sediment and centrifuging to separate pore water DIC from sediment particulate organic carbon (POC). All available pore water was injected into previously evacuated 2 mL glass serum vials and stored frozen upside down. Prior to analysis, 200 µL of 70% H_3PO_4 was injected into each vial along with enough helium to bring the vial pressure back to atmospheric pressure. Subsamples of headspace containing the evolved CO_2, was injected onto the gas chromatograph (GC) connected to a continuous flow isotope ratio mass spectrometer (IRMS) for isotopic determination. DIC methods followed those described by Kelley et al. (2006). POC methods and analyses followed those described by Poole 2010.

3.2.2 Sulfate Concentrations

Samples were collected from all sites for sulfate concentrations. In locations where soft microbial mats/sediment were present, pore water sulfate samples were obtained by taking a small section of microbial mat/sediment and centrifuging to provide separation of organic matter from pore water. In locations where evaporites were present pore water samples could not be obtained, so samples collected for sulfate analysis were obtained from overlying water. In both cases, samples were taken back to the laboratory where sulfate concentrations were determined using a Dionex Ion Chromatograph (Sunnyvale, CA).

3.2.3 $\delta^{18}O$ and δD of Water

In the laboratory, $\delta^{18}O$ and δD values were determined by sampling the headspace of a 500µL water sample in a borosilicate sample bottle. Samples for $\delta^{18}O$ were prepared by using a 1 ml disposable pipette to place 500 µl of the overlying sample water into an acid washed and dried Borosilicate sample bottle. The vials were then flushed with a mixture of 0.3% to 0.5% CO_2 in He using a Finnigan GasBench II as described by Hilkert and Avak (T.E. Corporation). After flushing, samples were equilibrated for 24 hours in a temperature-stabilized autosampler tray at 24°C. Once equilibrated, sampling proceeded. Samples for δD were prepared in a similar manner except for the addition of a platinum catalyst to each sample. The samples were then flushed with a mixture of 2% H_2 in He using a Finningan GasBench II as described by Duhr and Hilkert (T.E. Corporation). After flushing, samples were equilibrated for approximately 40 minutes prior to the start of sequence acquisition.

3.2.4 Gas Bubble Hydrocarbon Concentrations

Upon arrival to the lab, gaseous bubble samples were processed for methane and hydrocarbon concentrations. Adequate detection and separation of hydrocarbons present in the sample was provided by a Shimadzu Mini-2 gas chromatograph (GC) with flame-ionization detector (FID) fitted with a 1.83-m, 1/8 inch (3.1mm) stainless steel tubing packed with HayeSep Q 80/100 mesh (Valco Instruments Co. Inc). All samples were handled by directly injecting the gas (~250ul) into the GC set at 40°C, where the sample was carried by UHP helium for analysis. Multiple methane concentration standards (Scott Gas, PA, USA) and a 10 ppm ethane standard (Scott Gas, PA, USA) were run along with the samples. The analytical errors for methane and

ethane concentration analysis were ±0.5 ppm. Sample areas were converted to concentrations (in parts per million, ppm) by:

$$CH_4 \text{ (ppm)} = (\text{standard ppm x sample area})/\text{standard area}$$

where standard ppm is the known concentration of the gas standards, sample area is the integrated area of the sample, and standard area is the integrated area of the gas standard.

3.2.5 Methane Production in Incubation Samples

Sediment samples upon arrival to the lab were prepared for incubation experiments. The amount of sediment used for each incubation vial varied slightly with most containing between 10-20 g of sediment. The difference in sediment texture and quality in the different sampling locations made it difficult to divide the sediment and crustal material in the same manner. GN Ponds 1 and 4 contained more cohesive mat allowing for multiple sub-coring with a cut off 5 mL plastic syringe. The individual sub cores then were processed for each vial, with only the upper 1 to 3 cm of the mat being used. At CAL Pond 15, the relatively thin microbial mat was homogenized with the upper 8-10 cm of black sediment collected in the short core below the mat. The crustal material and underlying sediment collected from CAL Pond A23 were homogenized together. GN Pond 9 was divided into different sub-samples, top gypsum crust, underlying gypsum rubble, surface tan sediment (~ upper 8cm) and deep black sandy sediment (~8 to ~20 cm) below. The crust and rubble sections were broken into small pieces prior to incubations, while the sediment sections were homogenized prior to incubations. Vials were prepared by placing samples from the various sites in 38 mL glass serum vials with 10 mL of corresponding deoxygenated (N_2-purged) site water.

To determine the substrate(s) used by the methanogens in these environments during the March 2009, October 2009, January 2010 and August 2010 sampling trips, 99% ^{13}C-labeled substrates (trimethylamine (TMA), monomethylamine (MMA), methanol, acetate, and bicarbonate) were added to incubations of mats/sediments and the evolved methane was monitored for ^{13}C content. Because of the ease of procurement, MMA was used for the March 2009 sampling trips; TMA was used for all the later trips. The ^{13}C-labeled bicarbonate was added to a final concentration of 10 µM in the slurry. However, *in situ* concentrations of TMA, MMA, methanol and acetate at these sites are unknown, so a range of substrate concentrations (0.1 µM, 1 µM and 10 µM final concentration) was used. Individual incubation vials received one substrate at one concentration (in quadruplicates during March 2009 and triplicates during October 2009, January 2010 and August 2010) and so at a minimum a suite of 33 vials, excluding the controls with no added substrate, was used at each site. In some Ponds, not all substrates were used while in others additional substrates were added (Table 3.1).

During the 2009-2012 sampling trips, molybdate was added at a final concentration of 50mM to incubations of microbial mats and endoevaporite crust to inhibit sulfate reducing bacteria and enable us to determine the effects of sulfate reducing bacteria on methane production in these environments. In March 2012, to determine the effects of competitive substrate utilization when sulfate reducing bacteria were inhibited, 99% ^{13}C-labeled acetate and bicarbonate were added to sediment vials treated with molybdate, and the evolved methane was monitored for ^{13}C content. ^{13}C-labeled acetate and bicarbonate were added to a final concentration of 10 µM in the slurry. In October 2012, in order to determine the extent to which bicarbonate is used as a substrate in sediment vials treated with molybdate to inhibit sulfate

reducing bacteria, a range of ^{13}C-labeled bicarbonate concentrations (10 µM, 100 µM and 1,000 µM final concentration) were used.

After filling the vials with sediment they were capped with blue butyl rubber stoppers (Bellco Glass, NJ, USA) and the headspace was flushed for 5 minutes with N_2 to remove any O_2 and return sediment to an anoxic state. The vials were allowed to equilibrate for 24 hours prior to the first extraction of headspace in a dark area with temperature similar to *in situ* temperature. Methane concentration in the headspace was monitored through time to obtain the production rate.

3.2.6 Stable Isotopes

Methane Carbon Stable Isotope Analysis. Isotope samples were analyzed for carbon isotope ratios using a Thermo Scientific Delta V advantage IRMS coupled via a combustion interface to a Hewlett Packard 5890 Series II GC. The GC was equipped with a 52.5m x 0.32mm PoraPlot Q column set at 45°C. Depending on the methane concentration, gas subsamples were injected in the GC-IRMS using one of two methods. High concentration samples (>1000 ppm) were handled by directly injecting no more than 250µl of the gas into a GC connected to a Finnagan Delta Plus continuous-flow IRMS. Low concentration samples (<1000 ppm) were handled using a modified cryofocusing method to amplify the methane peak (Rice et al., 2001). The gas sample (~5 mL) was introduced from the sample vial to the gas transfer line where it was swept by UHP helium through the first of two traps. The first trap, a 35.6-cm long, 1/8 inch (3.1 mm) stainless steel tubing packed with PoraPak Q (Agilent Technologies, USA), was placed in a liquid nitrogen/ethanol slush designed to separate N_2 and O_2 from the sample allowing absorption of CH_4 onto the pre-column. To cryofocus, the pre-column was warmed with warm

water and the CH_4 sample was transferred by UHP He carrier to the second trap, the first 23.5-cm of a 52.5-m PoraPLOT Q capillary chromatographic column, which was maintained in liquid nitrogen bath providing a second concentration step, freezing the gas onto the capillary tubing. This second trap furthered the removal of N_2 and O_2 from the sample, focusing the methane thus lowering the IRMS signal background, and improving the overall precision of the measurement. To release the methane, the cryofocusing loop was brought out of the liquid nitrogen bath and warmed to room temperature, thereby transferring the sample CH4 for analysis. Duplicate analyses were performed on all gas samples. Isotope data are reported in the "del" notation (e.g., $\delta^{13}C$, $\delta^{2}H$) :

$$\delta = 1000[(R_{sample}/R_{standard}) - 1]$$

where R_{sample} is the isotopic ratio (e.g., $^{13}C/^{12}C$) of the sample and $R_{standard}$ is the isotopic ratio of the referenced standard (Pee Dee belemnite (PDB), a fossil-containing limestone from the Pee Dee Belemnite Formation in South Carolina) (Canfield et al., 2005). The units of δ are per mil (‰). The analytical error for carbon stable isotopic analyses is ±0.4‰.

Methane Hydrogen Stable Isotope Analysis. Isotope samples were analyzed for hydrogen isotope ratios using a Thermo Finnigan Delta Plus XP IRMS coupled via a combustion interface to a Finnigan Trace GC ultra gas chromatograph. The GC was equipped with a 30 m x 0.32 mm Poropac Q column set at 100°C. Depending on the methane concentrations, gas subsamples were injected in the GC-IRMS in one of two methods. High concentration samples (>4000 ppm) were handled by injecting no more than 250 µl directly onto the GC column via injector. Low concentration samples (<4000 ppm) were handled using the same modified cryofocusing method described for methane carbon stable isotope analysis. Isotope data are reported in the "del" notation as previously described where R_{sample} is the isotopic ratio (e.g.,

$^{2}H/^{1}H$) of the sample and $R_{standard}$ is the isotopic ratio of the referenced standard (standard mean ocean water (SMOW)). The analytical error for hydrogen stable isotopic analyses is ± 5‰. Duplicate analyses were performed on all samples.

3.2.7 Radiocarbon Analyses

The gas was collected and stored in evacuated vials as previously described in section 3.1.3. In the laboratory at Florida State University, the methane was removed from the gas sample with a helium stream and combusted over copper oxide at 800°C. The resulting CO_2 was cryogenically trapped, purified, and sealed into a break seal vial. The vials were then sent to the National Ocean Sciences Accelerator Mass Spectrometry at the Woods Hole Oceanographic Institution where they were further converted to graphite for ^{14}C analysis.

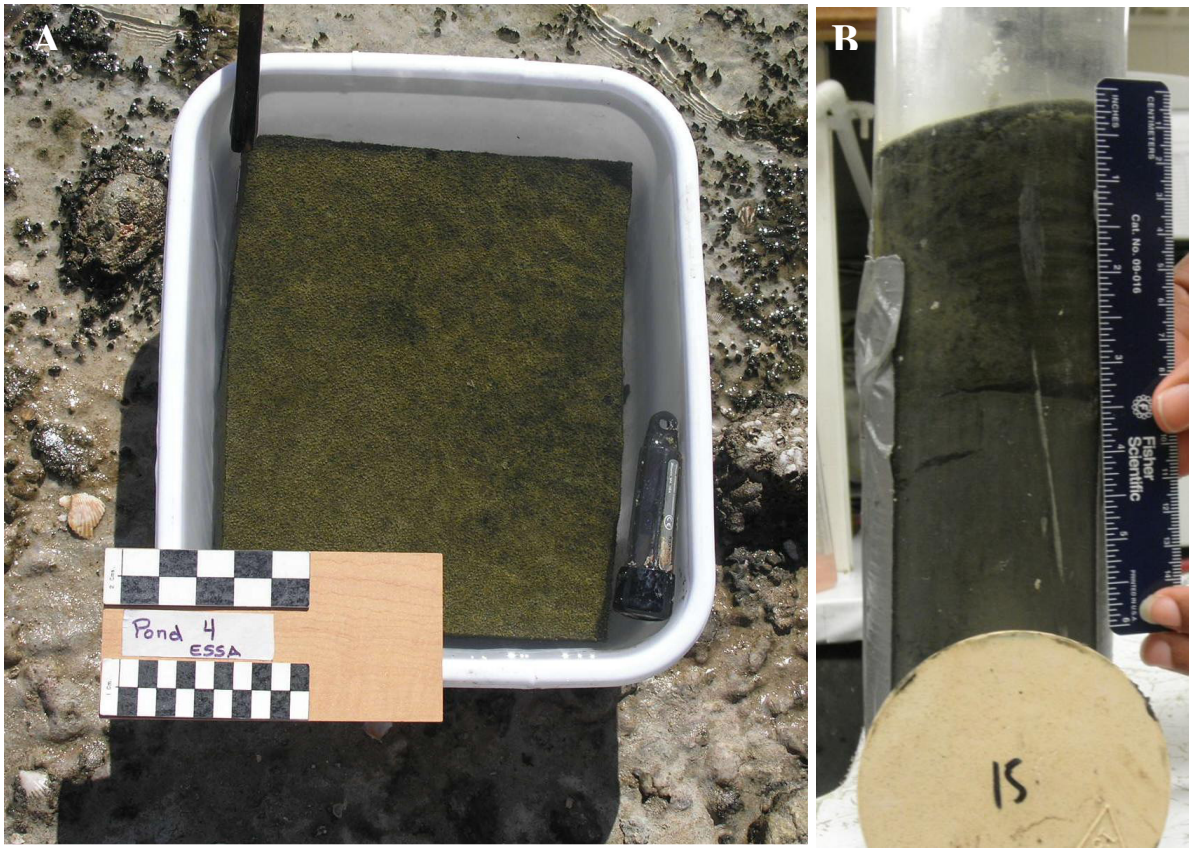

Figure 3.1. Picture of Microbial Mat subsection from GN Pond 4 and CAL Pond 15. ***A.*** *Large checkered boxes on top of scale represent 2cm intervals, smaller checkered boxes on bottom of scale represents 1cm intervals. Microbial mat is submerged under site water and a temperature logger is placed with each section for transport to our field laboratory.* ***B.*** *Microbial mat section was obtained by small core and is submerged under site water for transport to laboratory at NASA Ames Center.*

*Figure 3.2.Picture of small cores from GN Pond 9 and CAL Pond 23.**A.** GN Pond 9.Samples were broken down into three sections to represent the visible differences in the sediment, top crustal material, middle rubble material, bottom black sediment. **B.** Small core from CAL Pond 23 shows the black sediment and gypsum crust that was hand-placed into the small cores; site water also was collected and placed in the small cores for transport back to NASA Ames Center.*

Table 3.1. Substrates used for each incubation experiment for each separate incubation trial.

	Guerrero Negro Sites												Don Edwards Sites			
Final Concentration of Substrates in Incubation Vials	**GN Area 1 Site 1**	**GN Area 1 Site 2**	**GN Area 4**	**GN Area 9 Black Sediment**	**GN Area 9 Top Mud**	**GN Area 9 Crust**	**GN Area 1**	**GN Area 4**	**GN Area 9 Rubble**	**GN Area 9 Crust**	**GN Area 1**	**GN Area 1**	**CAL Pond 15**	**CAL Pond 23**	**CAL Pond 15**	**CAL Pond 23**
	Mar-09	**Mar-09**	**Mar-09**	**Mar-09**	**Mar-09**	**Mar-09**	**Oct-09**	**Oct-09**	**Oct-09**	**Oct-09**	**Mar-12**	**Oct-12**	**Jan-10**	**Jan-10**	**Aug-10**	**Aug-10**
No Substrate addition	X	X	X	X	X	X	X	X	X	X	X	X	X	X	X	X
500µM Unlabled TMA	X	X	X	X	X	X										
500µM Unlabled DMS	X	X	X	X	X	X										
0.1µM 13C-MMA		X	X	X	X											
1µM 13C-MMA		X	X	X	X	X										
10µM 13C-MMA	X	X	X	X	X											
0.1µM 13C-TMA							X	X	X	X			X	X	X	X
1µM 13C-TMA							X	X	X	X			X	X	X	X
10µM 13C-TMA							X	X	X	X			X	X	X	X
0.1µM 13C-MeOH		X	X	X	X		X	X	X	X			X	X	X	X
1µM 13C-MeOH		X	X	X	X	X	X	X	X	X			X	X	X	X
10µM 13C-MeOH	X	X	X	X	X		X	X	X	X			X	X	X	X
0.1µM 13C-Acetate		X	X	X	X			X	X	X			X	X	X	X
1µM 13C-Acetate		X	X	X	X	X		X	X	X			X	X	X	X
10µM 13C-Acetate	X	X	X	X	X			X	X	X			X	X	X	X
10µM 13C-Bicarbonate	X	X	X	X	X	X		X	X	X			X	X	X	X
0.1µM 2H-DMS							X	X	X	X						
1µM 2H-DMS							X	X	X	X						
10µM 2H-DMS							X	X	X	X						
10µM Unlabled TMA													X	X	X	X
100µM Unlabled TMA													X	X	X	X
1,000µM Unlabled TMA													X	X	X	X
10µM Unlabled DMS													X	X	X	X
100µM Unlabled DMS													X	X	X	X
1,000µM Unlabled DMS													X	X	X	X
Molybdate							X	X	X	X	X	X	X	X	X	X
5% paraformaldehyde													X	X		X
NaOH									X	X						
Molybdate + 10µM 13C-Acetate											X					
Molybdate + 10µM 13C-Bicarbonate											X	X				
Molybdate + 100µM 13C-Bicarbonate												X				
Molybdate + 1,000µM 13C-Bicarbonate												X				

CHAPTER FOUR

ISOTOPIC CHARACTERIZATION AND CLASSIFICATION OF METHANE BUBBLES

4.1 Introduction

The search for life beyond Earth remains one of the main goals for planetary exploration worldwide. Identifying biogenic gases, such as methane, in the atmospheres of planets and icy moons both within and outside of our solar system are at the core of life detection strategies. Seasonal methane releases (Mumma et al., 2009), as well as planetary atmospheric methane concentrations of approximately 10 ppb (Formisano et al., 2004; McEwen et al., 2011; Mumma et al., 2009), have been reported on Mars. The interpretation of recent detections of methane has been challenged (Zahnle et al., 2011), but any methane present on Mars or any potentially habitable world would immediately raise the question of its origin. Biogenic, thermogenic, and geologic sources, all possibilities on Earth, are potential contributors to the presence of any methane on Mars.

On Earth 80-90% of the methane in the atmosphere is of biogenic origin (Whiticar, 1999); thermogenic and geologic sources make up the remainder. Biogenic methane results from the activity of microbes that use carbon dioxide, acetate, or a limited number of methylated substrates to produce methane. Thermogenic production occurs at elevated temperatures in deeply buried insoluble organic material, whereas methane and higher hydrocarbons (ethane, propane, etc.) are formed by thermal decomposition of organic compounds. Geologic methane, the product of water-rock reactions in zones near mantle-derived magma and crustal material,

currently contributes very little to the atmospheric methane budget (~0.4%), although it may have been more important in Earth's geologic past (Emmanuel and Ague, 2007).

The use of carbon and hydrogen stable isotope ratios can distinguish between biogenic, thermogenic and geologic methane-production pathways (Allen et al., 2006; Whiticar, 1999). These measurements, a capability of both current and planned planetary missions, will be key for determining whether any methane present on Mars is biologically produced. Naturally occurring biogenic methane is characterized by a low $^{13}C/^{12}C$ ratio, with $\delta^{13}C_{CH4}$ values ranging from –110‰ to –50‰, whereas thermogenic methane generally has $\delta^{13}C$ values > –50 ‰ and is characterized by progressive enrichment in ^{13}C content with increasing maturity, eventually approaching the $^{13}C/^{12}C$ of the original organic matter (Kotelnikova, 2002; Whiticar, 1999). Biogenic methane has a wide range in $\delta^{2}H_{CH4}$ values, varying from –400‰ to –150‰, whereas thermogenic methane has a smaller $\delta^{2}H_{CH4}$ range, from –275‰ to –100‰ (Whiticar, 1999). There is a considerable overlap in the general fields for $\delta^{2}H_{CH4}$ values for biogenic and thermogenic methane, as well as a smaller overlap in the general fields for $\delta^{13}C_{CH4}$ values. Geologic methane production from low-temperature water-rock reactions varies between $\delta^{13}C_{CH4}$ values of –40‰ to –10‰ and $\delta^{2}H_{CH4}$ values of –100‰ to –400‰ although it is less well characterized (Allen et al., 2006; Horita, 2005; Horita and Berndt, 1999; Sherwood Lollar et al., 2008; Sherwood Lollar et al., 2002; Whiticar, 1999). Although it is common to measure only the carbon isotopes of CH_4 to differentiate biogenic from thermogenic methane, the use of both $\delta^{13}C_{CH4}$ and $\delta^{2}H_{CH4}$ in combination allows for useful separation between the general fields of biogenic, thermogenic, and geologic methane. Isotope analysis also allows for distinction between the two main biogenic pathways, acetate fermentation (–70‰ to –50‰ and –375‰ to –300‰ for $\delta^{13}C_{CH4}$ and $\delta^{2}H_{CH4}$ values, respectively) and CO_2 reduction (–100‰ to –60‰ and –

250‰ to −150‰ for $\delta^{13}C_{CH4}$ and $\delta^{2}H_{CH4}$ values, respectively) making this tool particularly valuable (Whiticar, 1999) with respects to those pathways. Previous work with cultured methanogens suggest that methane produced from noncompetitive substrates, such as methanol, methylamines, and dimethyl sulfide, should be more depleted in ^{13}C than methane produced from either CO_2 reduction or acetate fermentation (Conrad, 2005; Horodyski and Vonder Haar, 1975; Potter et al., 2009; Whiticar et al., 1986).

In addition to the isotopic composition of the methane, the presence of higher n-alkane hydrocarbon gases, such as ethane, can be used to distinguish between methane sources. Biogenic methane production is usually not accompanied by significant ethane production (Bernard et al., 1978; Oremland et al., 1988; Vogel et al., 1982), whereas the processes that form thermogenic and geologic methane also produce ethane (Bernard et al., 1978; Horita and Berndt, 1999; Oremland et al., 1988; Sherwood Lollar et al., 2002). It has been proposed that a methane/ethane ratio of over 1,000 is indicative of a biogenic source, while a ratio of less than 50 suggests a thermogenic source (Bernard et al., 1976; Vogel et al., 1982).

Radiocarbon (^{14}C) dating is also useful for the determination of methane sources. All living biomass is imprinted with a $\Delta^{14}C$ signature set by carbon fixation from atmospheric CO_2, which is naturally enriched with ^{14}C. Because of nuclear-weapons testing in the 1950's and 1960's, contemporary atmospheric CO_2, and the biomass fixed from it, has a $\Delta^{14}C$ value of +55 ± 5‰ (=106% modern) relative to pre-bomb atmospheric CO_2 (100% modern) (Turnbull et al., 2007). Similarly, biogenic methane, which is derived from recently fixed organic matter, should also be relatively enriched in ^{14}C. On the other hand, thermogenic methane, which can be millions of years old, generally contains no ^{14}C because of the relatively short half-life of ^{14}C (~5730 years (Brady et al., 2009)). Even petroleum being formed near the spreading center in

Guaymas Basin, which is geologically very young (about 5000 years old (Didyk and Simoneit, 1989)), is readily distinguishable from modern organic matter with ^{14}C analyses. Therefore, ^{14}C analyses can assist in providing an estimated time frame for methane gas formation or aid in the identification of the substrates supporting methane production (Chanton et al., 2008).

Methane can have different origins: hydrogeochemical activity, external supply by meteorites and comets, volcanism, and biologic activity. Owing primarily to their relevance to planetary environments which might support life outside of Earth (e.g., Mars and Europa), much focus has been directed at methane formation in hydrothermal systems through the process of serpentinization (Atreya et al., 2007; Chassefière and Leblanc, 2011a; Chassefière and Leblanc, 2011b; Lyons et al., 2005). Methane production has also been reported, however, in hypersaline environments (Bebout et al., 2004; Oremland, 1981; Oremland and King, 1989; Oremland et al., 1987; Oremland et al., 1988). Given the importance of methane as an indicator of biological activity, the widespread occurrence of chloride containing deposits (Osterloo et al., 2008) and possibility of liquid brines on the surface of Mars (McEwen et al., 2011), the objective of this study was to characterize the stable isotopic composition of methane produced in diverse Mars analogue hypersaline environments on Earth.

4.2 Material and Methods

Sampling for this work was performed in two regions, Northern California, USA and Baja California, Mexico, from 2008 through 2010 (Figure. 4.1). Northern California sampling sites (CAL) were within the Don Edwards National Wildlife Refuge, located in southern San Francisco Bay. CAL Pond 15 (~120 parts per thousand (ppt) salinity) and CAL Pond A23 (~300 ppt) from the refuge were sampled in December 2008, January 2010, and August 2010. Baja

California sampling sites were in three different areas, Guerrero Negro (GN), Laguna Figueroa, and Laguna San Ignacio. Guerrero Negro samples were obtained from salterns located in Exportadora de Sal, one of the world's largest solar salt production site located midway along the Pacific coast of the Baja California Peninsula. These salterns, GN Area 1 (~55 ppt), GN Area 9 (~190 ppt), GN Area 10 (~280 ppt), and GN Area 11 (~300 ppt) were sampled in March and October 2009. GN Area 9 was sampled again in September 2010. The surface sediments found in these ponds change in sediment composition, from black silty fine sands with a brownish surface layer in the lower salinity ponds, to microbial mats containing grains of precipitated carbonates and gypsum in subsequent ponds, to ponds with crusts of gypsum and halite which have been described elsewhere (Huerta-Diaz et al., 2011; Phleger and Ewing, 1962; Shumilin et al., 2002). Laguna San Ignacio samples were obtained in March 2009 from three small ponds having salinities ranging from 300-360 ppt, located in a natural salt flat ca. 150 km south of Guerrero Negro. Laguna Figueroa samples were obtained in October 2009 in a location ca. 400 km north of Guerrero Negro having salinities ranging from 54 ppt to 200 ppt. This site, also referred to in the literature as Laguna Mormona, had been extensively studied over the last 40 years and has been described as a closed hypersaline lagoon consisting of an extensive evaporite flat and a narrow salt marsh (Giovannoni et al., 1988; Horodyski, 1977; Horodyski and Bloeser, 1977; Horodyski and Vonder Haar, 1975; Margulis et al., 1980).

Across all of our four study sites, microbial communities at the lower salinities (55 ppt to 130 ppt) were usually soft microbial mats growing on top of highly sulfidic sediments, whereas at higher salinities (190 ppt to 360 ppt), the microbial communities were generally encrusted within evaporitic minerals. These endolithic microbial communities have been called endoevaporites (Rothschild et al., 1994; Sahl et al., 2008; Spear et al., 2003). Samples from all

sites consisted of bubbles released during the perturbation of sediment and crustal material. These samples were collected under water by means of an inverted, septum-capped funnel. Gas collected in the funnel was removed with a 10-ml syringe and then transferred to a previously evacuated 10-ml glass vial capped with a blue butyl rubber stopper (Bellco Glass, NJ, USA). Blue butyl rubber stoppers were chosen for this study because of the known durability in sample storage (Fulghum and Worthington, 1977) and the numerous reports of gaseous organic contaminate release from other butyl rubber stoppers requiring them to be boiled prior to use (Ettwig et al., 2009; Oremland et al., 1987; Zinder and Anguish, 1992). Bubbles collected from an area were pooled to obtain a total volume of 20-ml in each vial, overpressurizing the vial to about two atmospheres, eliminating the potential for fractionation during sampling. At least triplicate, and in some cases up to 10 vials of gas samples, were collected from each site during each sampling trip. Samples were then transported to the laboratory, where subsamples were taken and analyzed for methane and ethane concentrations. A Shimadzu Mini-2 gas chromatograph (GC) with a flame-ionization detector, fitted with a 1.83-m, 1/8 inch (3.1mm) stainless steel tubing packed with HayeSep Q 80/100 mesh (Valco Instruments Co. Inc) was used to provide adequate detection and separation of hydrocarbons present in the sample. All samples were handled by directly injecting the gas (~250 µl) into the GC, where the sample was carried by UHP helium for analysis. Multiple methane and ethane standards (Scott Gas, PA, USA) were run along with samples. The analytical errors for methane and ethane concentration analyses are ± 0.5 ppm.

Stable isotope values were obtained by one of two methods depending upon methane concentrations. High methane concentration samples (>1000 ppmv and >4000 ppmv for $\delta^{13}C_{CH4}$ and for $\delta^{2}H_{CH4}$ values, respectively) were handled by directly injecting the gas into a GC

connected to a Finnigan Delta Plus continuous-flow isotopic ratio mass spectrometer (IRMS). Low methane concentration samples (<1000 ppmv and <4000 ppmv for $\delta^{13}C_{CH4}$ and for $\delta^{2}H_{CH4}$ values, respectively) were handled using a modified cryofocusing method to amplify the methane peak (Rice et al., 2001). In the cryofocusing method, the gas sample (~ 5 ml) is introduced from the sample vial to the gas transfer line where it is swept by UHP helium through the first of two traps. The first trap, a 35.6-cm, 1/8 inch (3.1 mm) stainless steel tubing packed with PoraPak Q (Agilent Technologies, USA) placed in a liquid nitrogen/ethanol slush is designed to separate N_2 and O_2 from the sample allowing absorption of CH_4 onto this pre-column. To cryofocus, the pre-column is warmed and CH_4 is transferred by He carrier to the second trap, the first 23.5-cm of a 52.5-m PoraPLOT Q capillary chromatographic column, which is maintained in a liquid nitrogen bath. This second trap furthers the removal of N_2 and O_2 from the sample, focuses the methane thus lowering the IRMS signal background and improves the overall precision of the measurement. To release the CH_4, the cryofocusing loop is brought out of the low-temperature bath and warmed to room temperature, transferring the sample CH_4 for analysis. Duplicate analyses were performed on all gas samples. Isotope data are reported in the "del" notation (e.g., $\delta^{13}C$, $\delta^{2}H$):

$$\delta = 1000[(R_{sam}/R_{std}) - 1],$$

where R_{sam} is the isotopic ratio (e.g., $^{13}C/^{12}C$ and $^{2}H/^{1}H$) of the sample and R_{std} is the isotopic ratio of the referenced standard (Pee Dee belemnite (PDB) and standard mean ocean water (SMOW) for carbon and hydrogen, respectively). The units of δ are permil (‰). The analytical errors for stable isotopic analyses are ± 0.4‰ for $\delta^{13}C_{CH4}$ and ± 5‰ for $\delta^{2}H_{CH4}$.

In addition to the concentration and stable isotopic work, radiocarbon analyses were completed on select methane gas samples from GN Area 9. The gas was collected and stored in previously evacuated vials as described above. In our laboratory, the methane was removed from the gas sample with a helium stream and combusted over copper oxide at 800°C. The resulting CO_2 was cryogenically trapped, purified, and sealed into a break seal vial. The vials were then sent to the National Ocean Sciences Accelerator Mass Spectrometry at the Woods Hole Oceanographic Institution where they were further converted to graphite for ^{14}C analysis.

4.3 Results

Gas bubbles present within these microbial communities were readily liberated upon disturbance. Gas trapped under mineralized deposits (gypsum and/or halite) was often under pressure, and would effervesce for some time when the mineral layer was broken. In many cases, some effort (hammer and chisel) was required to break the mineral layers. Most bubble samples contained elevated concentrations of methane, ranging upwards to over 30% by volume (Figure 4.2 and Table 4.1), with some of the most methane-rich bubbles released from endoevaporites.

A distinct carbon isotopic separation between the lower-salinity soft microbial mats and the higher-salinity endoevaporites was observed with the methane from the endoevaporites being significantly enriched in ^{13}C relative to the methane from the soft mats (Figure 4.2); the difference is statistically significant at the 99% confidence level ($p < 0.01$, Student T-Test, n=135). This carbon isotopic difference between the soft microbial mats and endoevaporites is also observed when examining the isotopic composition of bubble methane as a function of salinity (Figure 4.3, n=135). There were two exceptions to this grouping. Samples from GN

Area 1 (Area 1 site 2, n=5, closed diamond) collected in March 2009 appeared isotopically distinct (enriched in $\delta^{13}C_{CH4}$) from other soft microbial mats (closed symbols) despite the fact that the mat did not appear visibly different from other soft mats, one of which (GN Area 1, site 1, closed triangle) was collected within 20 meters of site 2. Another location, Laguna Figueroa (n=8, closed circle) plots between the two distinct groupings; this location contained a combination of soft microbial mat and regions that resemble pre-endoevaporites (areas just forming crusts), providing a possible explanation for the wide range in $\delta^{13}C_{CH4}$ values from that site (Figure 4.2 and 4.3).

A plot of both the carbon and hydrogen isotopic compositions of methane bubbles within these samples support a distinct isotopic separation between the lower-salinity soft microbial mats and the higher-salinity endoevaporites (Figure 4.4, n=123). Bubbles collected from soft microbial mats have methane isotope values ranging from –65 to –50‰ for $\delta^{13}C_{CH4}$ and –350 to –110‰ for $\delta^{2}H_{CH4}$ (n = 37), whereas bubbles collected from areas dominated by endoevaporites have isotopic values ranging from –45 to –35‰ for $\delta^{13}C_{CH4}$ and –350 to –250‰ for $\delta^{2}H_{CH4}$ (n= 86). Most bubbles collected from the soft microbial mats exhibit values that are within the biogenic methane ranges (CO_2 reduction and acetate fermentation) with the exception of two locations. GN Area 1 site 2 (n=5, closed diamond) displayed a previously described enrichment in $\delta^{13}C_{CH4}$, while CAL Pond 15 (n=9, closed square) displayed an enrichment in $\delta^{2}H_{CH4}$ placing it somewhat outside of the range generally used for biogenic methane production. The methane released from the endoevaporites are clearly outside of the range of previously defined biogenic methane.

The difference between soft microbial mats and endoevaporites is also reflected in the alkane content of the gases present in the bubbles. The methane/ethane (C_1/C_2) ratios measured

in bubbles from lower-salinity soft microbial mats range from 1,000 to 15,000 (n=15), clearly within the biogenic range (Figure 4.5, n=86). The C_1/C_2 ratios from the higher-salinity endoevaporites range from 40 to 15,000 (n = 63), while the C_1/C_2 ratios from the pre-endoevaporite sites found in Laguna Figueroa range from 300 to 1,000 (n=8). The wide range in values from endoevaporites, combined with the $\delta^{13}C_{CH4}$ values obtained from the same sites would traditionally suggest a non-biogenic origin. However, the radiocarbon analysis of gas samples collected from endoevaporites in GN Area 9 reveal that the methane within the bubbles collected has a percent modern value of +107 ± 0.2% with a $\Delta^{14}C$ value of +63 ± 2‰ (n=3) indicating that the methane was produced from recently photosynthesized carbon and not from ancient geologic or thermogenic sources.

4.4 Discussion

Finding elevated methane concentrations in bubbles (over 30% by volume at some sites) at hypersaline sites was unexpected. Methanogens form methane by pathways that are commonly classified with respect to the type of carbon substrate utilized (Thauer et al., 2008; Whiticar, 1999). They utilize relatively few and simple compounds to obtain carbon and energy via competitive and noncompetitive substrates. The utilization of competitive substrates for the process of methanogenesis is limited in most marine environments because of the abundance of dissolved sulfate. Generally, at the high sulfate concentrations characteristic of marine and hypersaline environments, sulfate reducing microorganisms outcompete methanogens for the substrates acetate and H_2 (used by methanogens to reduce CO_2) (Burdige, 2006; Kristjansson and Schönheit, 1983; Muyzer and Stams, 2008). However, methane production can also be achieved through the demethylation of noncompetitive substrates, such as methylamines, which, at the

salinity levels found in our sites, are not biologically available for use by sulfate reducing microorganisms (King, 1988a; Oren, 1999b; Thauer et al., 2008). Incubation experiments performed using the mats, sediments, and crustal materials from many of the sites revealed that methane is indeed being produced from the noncompetitive substrates at these locations (Kelley et al., 2012; Poole, 2010), indicating a biogenic origin to the methane-rich bubbles (Table 4.1).

There have been some published reports that, at salinity levels lower than those found in our study, sulfate reducing bacteria can in fact utilize some noncompetitive substrates, notably methanol and methylamine (King et al., 1983). At our study sites, however, we conclude that sulfate reducing bacteria are not utilizing these noncompetitive substrates. We base this on the fact that when incubation vials containing sediments and crustal materials were amended with ^{13}C-labeled methanol and methylamines, the production of ^{13}C labeled carbon dioxide from sulfate reduction was not observed. The $\delta^{13}C_{CO2}$ values were similar between our non-amended control incubations and those that received ^{13}C labeled substrate additions (Chapter 5 and Appendix C).

The carbon isotopic composition of methane has been previously shown to vary widely (Whiticar, 1999) and this is true for the samples reported here. In general, the isotopic values reported here for methane within soft microbial mats are within the traditional boundaries (Whiticar, 1999; Whiticar and Faber, 1986) for biogenic methane production, with three exceptions (Figure 4.4) described below.

One of the soft mats sampled (CAL Pond 15, n=9, closed square), plots slightly above the range for CO_2 reduction because of a substantial difference in the δ^2H_{CH4} value. Methanogens derive a specific proportion of their hydrogen, for methane formation, from the water in which they live. Methanogens utilizing the CO_2 reduction pathway alone would have hydrogen isotopic

values similar to but offset from the formation water since it is the only hydrogen source for that pathway (Chanton et al., 2006; Whiticar, 1999). However, analysis of the overlying water at that sampling site reveals no substantial enrichment in ^{2}H values when compared to the other ponds sampled (Chapter 7) and a complete understanding of the hydrogen isotope effects associated with formation waters and the methanogens in this location is limited. The only visible difference noted in CAL Pond 15 was the significantly thinner mats present at that site, so the production of methane may have occurred in the sediment below the mat. The second outlier (GN Area 1 site 2, n=5, closed diamond), previously described to have an enriched $\delta^{13}C_{CH4}$ value, is isotopically different from similar soft microbial mats collected in the same area, falling outside the biogenic range and resembling the methane released from the endoevaporites. The third outlier is seen from the samples collected from the pre-endoevaporites found at the Laguna Figueroa site (n=8). The area is prone to seawater intrusion through the barrier dunes separating the lagoon from the sea, allowing for dissolution of evaporites and subsequent reformation of evaporites in the region when the seawater intrusion ceases (Horodyski, 1977; Margulis et al., 1980). At the time of our sampling, there was no qualitative determination made about the state of the evaporites. No compositional analysis was performed to determine the stage of evaporite formation or if seawater intrusion through the barrier dunes was occurring or had recently occurred at our site. It was, however, noted that the locations sampled represented a mixture of both soft microbial mats and endoevaporite formation, thus serving as an intermediate (or pre-endoevaporite) site. The eight bubble samples collected were from multiple locations across this natural transition between the soft microbial mat phase and the evaporite phase in this location, and may provide an explanation for the wide range in $\delta^{13}C_{CH4}$ observed within the bubble samples.

In contrast to most of the bubbles contained within soft mats (n=24) and a small portion of samples collected from the pre-endoevaporite site (n=3), the bubbles from endoevaporites (n=86) and some locations within the pre-endoevaporite site (n=5) and soft microbial mats (n=5) displayed carbon and hydrogen isotopic values that are outside the range considered to indicate biogenic origin (Figure 4.4). This discovery was particularly significant because incubation experiments in our soft microbial mats, as well as the endoevaporites of GN Area 9 and CAL Pond A23, clearly demonstrated biological methane production, with the methane produced having similar isotopic values as those measured for the bubbles (Kelley et al., 2012; Poole, 2010). Across all sites there was no difference in the $\delta^{13}C_{CH4}$ from the bubbles obtained *in situ* and the bubbles produced during incubation experiments (Table 4.1). In methanogenic culture experiments, the carbon fractionation associated with noncompetitive substrates is greater than with acetate fermentation or CO_2 reduction, while the hydrogen fractionation associated with noncompetitive substrates is similar with that of acetate fermentation (Horodyski and Vonder Haar, 1975) this however was not observed in our study. It has been noted that in cases of substrate limitation, the carbon isotope values of bacterial methane can approach very enriched levels while the hydrogen isotope values remain unchanged (Whiticar, 1999). This phenomenon has been hypothesized to explain the carbon isotopic values from the endoevaporite sites (Kelley et al., 2012). To ensure that this observation was not a product of our closed culture experiments but was indeed occurring in-situ and to gain information with regard to other classification models used for methane production pathways, we performed additional analyses on the bubble samples collected.

The use of methane/ethane ratios, in conjunction with the $\delta^{13}C_{CH4}$ values, has been used in the past to provide an assessment of methane production pathway (Bernard et al., 1978;

Martens et al., 1991). Previous studies have demonstrated difficulties in using C_1/C_2 ratios alone to determine biogenicity, since methanogens have been shown to produce small amounts of ethane and other light hydrocarbon gases as a result of their metabolism (Davis and Squires, 1954; Oremland, 1981; Oremland et al., 1988; Vogel et al., 1982). Indeed, our measurements support the conclusion that methane/ethane ratios may not be used as a conclusive indicator of biogencity; the C_1/C_2 ratios measured from lower-salinity soft microbial mats (n=15) are within the range considered to be from biogenic origin while our higher-salinity endoevaporite samples (n=63) and samples collected from pre-endoevaporite sites (n=8) are outside of this range.

The C_1/C_2 ratio of the collected gases from these hypersaline environments, together with the ^{13}C-enriched $\delta^{13}C_{CH4}$ values would, using conventional criteria, place the methane from endoevaporites outside the range for biogenic methane production (Figure 4.5), suggesting either thermogenic methane, geologic methane or biogenic methane that has been oxidized (Bernard et al., 1978; Martens et al., 1991; Whiticar, 1999). Microbial methane oxidation in our samples must, therefore, be considered. Microbial oxidation of methane lowers the C_1/C_2 ratio by the selective removal of methane over ethane and preferentially removes methane containing the lighter isotopes (^{12}C and ^{1}H), resulting in an enrichment of both ^{13}C and ^{2}H in the remaining methane (Whiticar, 1999; Whiticar and Faber, 1986). Our work shows that enrichment in ^{13}C is present in our higher-salinity samples and the C_1/C_2 ratio is lower, but a simultaneous progressive enrichment in the $\delta^{2}H_{CH4}$ values was not observed (Figure 4.4), effectively ruling out methane oxidation in our samples.

The use of radiocarbon dating has become a useful tool in recent years for separation between biogenic and thermogenic methane. Since all living biomass is imprinted with a ^{14}C signature, obtained from atmospheric CO_2, methane produced biogenically would result in $\Delta^{14}C$

value similar to atmospheric CO_2, while older thermogenic methane would result in relatively no ^{14}C because of the short half life of ^{14}C (~5730 years). Although we have conclusively shown from incubation experiments that methane produced at these sites are, in fact, biologically produced (Chapter 5), we wanted to further exclude the possibility that the methane we measured in the salt ponds was of thermogenic origin (as may be concluded on the basis of its stable isotopic composition and C_1/C_2 ratio). Samples of the methane from one of the endoevaporites from GN Area 9, was analyzed for its ^{14}C (radiocarbon) content. Methane within bubbles collected from the endoevaporites of GN Area 9 has a percent modern value of +107 ± 0.2% with a $\Delta^{14}C$ value of +63 ± 2‰ (n = 3). These values reveal that bubbles produced in this endoevaporite has values consistent with carbon produced after the nuclear weapons moratorium on atmospheric testing in the 1960's and is of modern age and is not consistent with geologic or thermogenic sources.

4.5 Conclusions

Previously, methane sources have been characterized using a combination of $\delta^{13}C_{CH4}$, $\delta^{2}H_{CH4}$ and C_1/C_2 data from various environments, including marine, marsh, wetland, and lake settings. Therefore, the conventional isotopic boundaries for biogenic methane were delineated from sites where methanogens used the two main methane-production pathways, CO_2 reduction and acetate fermentation, presumably under conditions where these substrates were abundant (Whiticar, 1999; Whiticar et al., 1986). Biogenic methane produced in cyanobacterially-dominated hypersaline environments was not included in these previous studies. The isotopic values for methane produced from noncompetitive substrates (Chapter 5) in endoevaporites where the microbial community is physically isolated from the environment, allowing for

substrate limitation to occur (Kelley et al., 2012), could be misinterpreted under the traditional boundaries (Whiticar, 1999; Whiticar et al., 1986) currently available for defining methane production pathways.

Biological methane production has been previously reported from hypersaline environments on Earth (King, 1988b; Oremland and King, 1989; Oremland et al., 1987; Oremland et al., 1988; Oren et al., 2009), including the Baja California field sites (Bebout et al., 2004; Potter et al., 2009; Smith et al., 2008), but to our knowledge, few measurements of the stable isotopic composition of the methane have been made. Our measurements confirm hypersaline environments are places in which methane is produced biologically and extend the traditional boundaries for the characteristics of methane produced biologically. These new observations (Figure 4.4) delineate a region in $\delta^{13}C_{CH4}$ - $\delta^{2}H_{CH4}$ space for biogenic methane production from endoevaporite environments, apparently under substrate-limited conditions (Kelley et al., 2012). These revised boundaries will lessen the possibility that samples obtained from regions similar to those described being misinterpreted as having thermogenic, geologic or a mixed origin. In addition, given the relatively high concentrations of ethane measured in some of the endoevaporite mat samples, future expansion of the C_1/C_2 limits for biogenic methane production should also be considered. Additionally, more work should be done to establish if there are any isotopic carbon and hydrogen effects from the use of methylated sulfur substrates, preliminary work shows some isotopic effects however more work needs to be performed. This is of critical importance to properly determine the source of any methane measured by the NASA Mars Science Laboratory and the proposed ESA ExoMars Trace Gas Orbiter. As a result of this work, we have an improved the delineation of the biogenic methane signal.

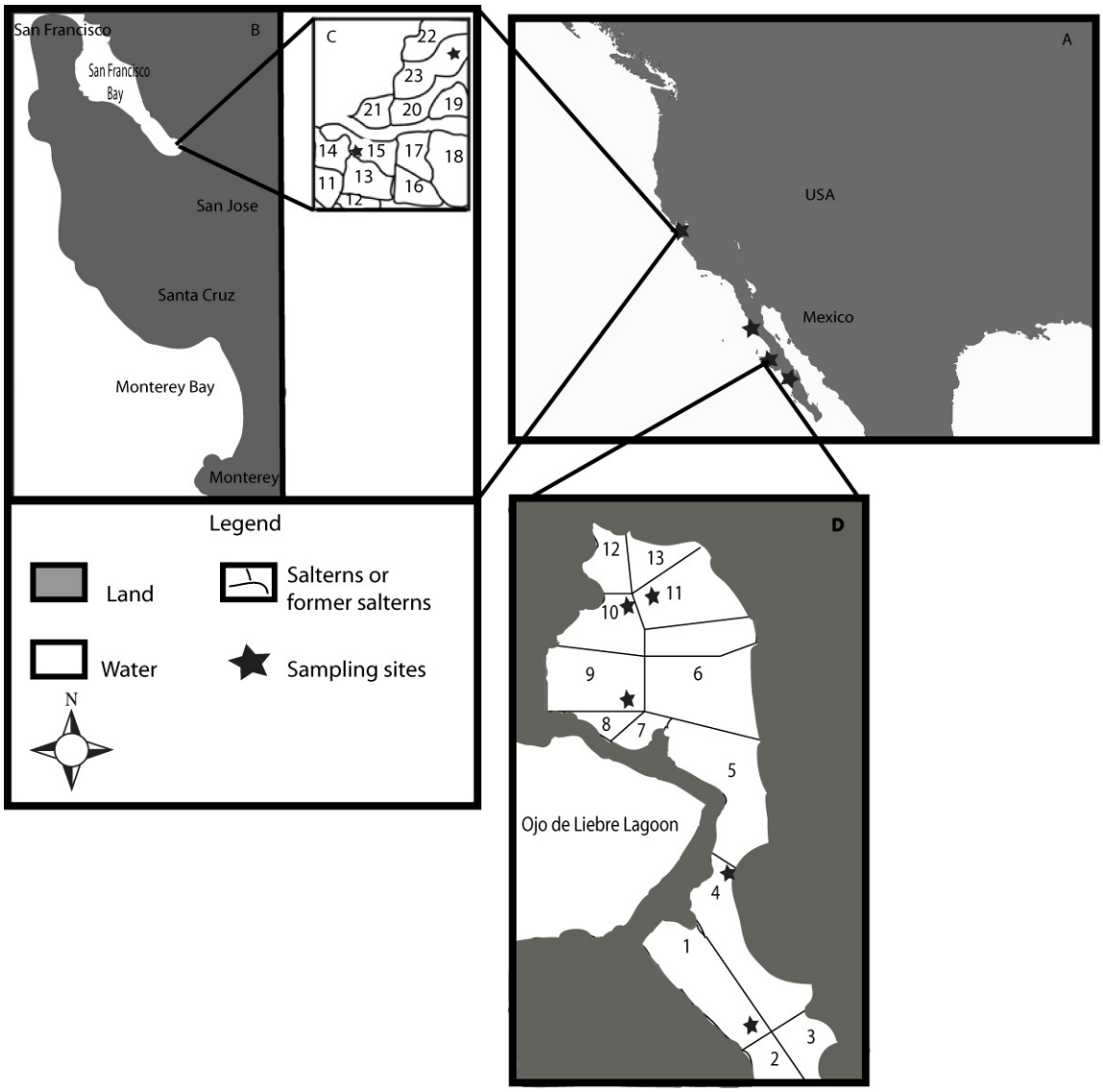

Figure 4.1. Map of field sampling sites. Inset A shows the location of all 4 sampling sites, depicted with stars. Inset B shows the location of the Northern California sites in the Don Edwards National Wildlife Refuge relative to San Francisco Bay. Inset C shows the locations of the sampling sites, depicted with stars, within the Don Edwards National Refuge. Inset D represents the location of the Guerrero Negro sampling sites, depicted with stars. Maps of the sites were modified from Kelley et al. (2012).

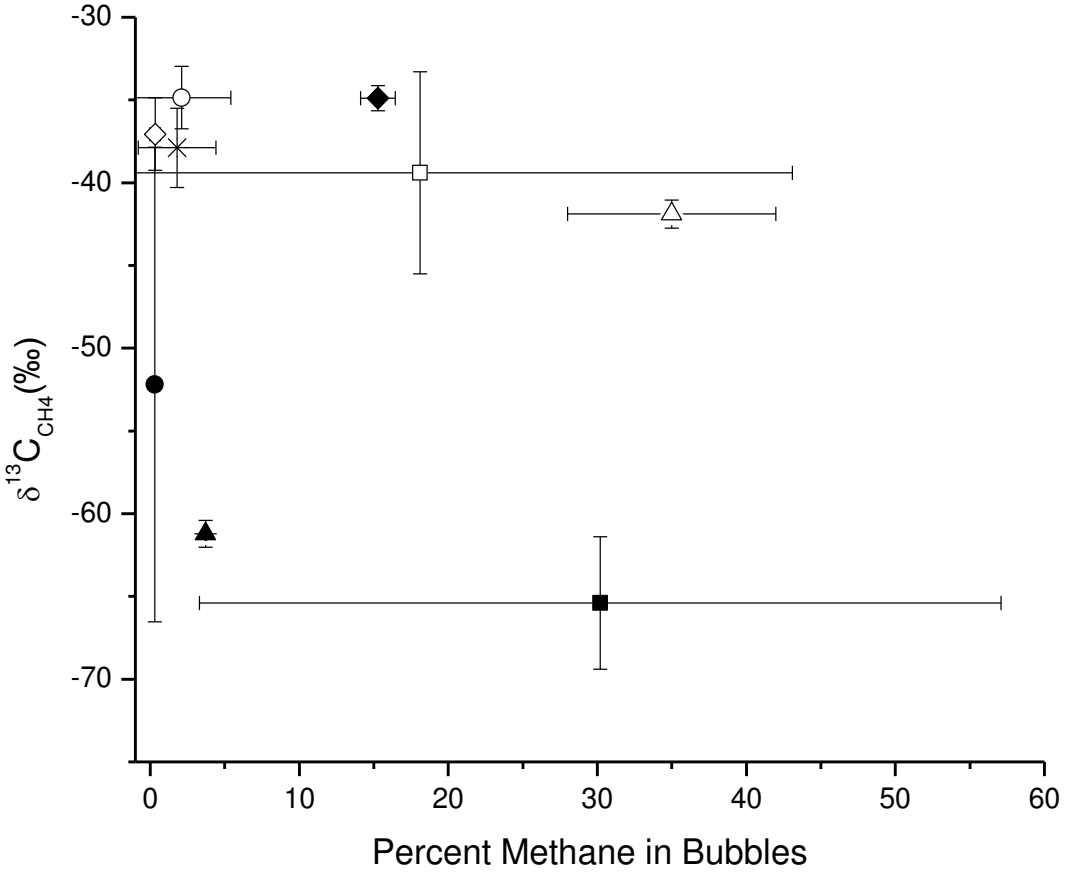

Figure 4.2. Percentage of methane in bubbles plotted against the $\delta^{13}C_{CH4}$ values (‰). Data were averaged across sampling times for all sites (n=135). Closed symbols indicate soft microbial mats, open symbols indicate endoevaporite mats. Area 1 site 1 (GN, ~55 ppt salinity, closed triangle, n = 15), Area 1 site 2 (GN, ~55 ppt, closed diamond, n = 5), Pond 15 (CAL, ~120 ppt, closed square, n = 12), and Laguna Figueroa (~90 ppt, closed circle, n = 8), contained soft microbial mat. Area 9 (GN, ~190 ppt, open triangle, n = 35), Area 10 (GN, ~280 ppt, open circle, n = 21), Area 11 (GN, ~300 ppt, open diamond, n = 12), Laguna San Ignacio (~330 ppt, star, n = 9), and Pond 23 (CAL, ~300 ppt, open square, n = 18) contained endoevaporite mat. A clear isotopic distinction between the soft microbial mat and the endoevaporite mat in the $\delta^{13}C_{CH4}$ values is visible despite the wide range of methane present in the bubble samples. Methane from endoevaporite mats was significantly ^{13}C enriched ($p < 0.01$; Student's T test) relative to methane from soft mats.

Table 4.1. Temperature, salinity, methane concentrations in bubble samples, ethane concentrations in bubble samples, methane isotopic carbon values from both bubbles collected at the site and methane produced within incubation vials, and δ^2H methane values for bubble samples. Error estimates (standard deviations) presented in parentheses. Values that were unable to be determined are depicted in the table as n.d. Methane production values for incubation samples (*) can be found in Kelley et al 2012.

Site	Date	Methane Bubble Sample number (n)	Temp (°C)	Salinity (ppt)	Methane Bubble Concentration (%)	Ethane Bubble Concentration (ppm)	Methane Bubble δ13C (‰)	Methane Incubations δ13C (‰)*	Methane Bubble δ2H (‰)
Don Edwards									
Pond 15	December 2008	4	n.d.	105	11.2 (15.9)	9.2 (6.6)	–62.6 (5.7)	n.d.	–100.8 (39.2)
	January 2010	5	12	126	63.3 (11.3)	41.5 (12.4)	–65.1 (1.2)	–62.9 (0.2)	–108.0 (14.9)
	August 2010	3	14	115	47.5	n.d.	–66.0 (7.4)	–64.3 (0.3)	n.d.
Pond 23	December 2008	7	n.d.	290	0.3 (0.2)	1.7 (1.0)	–35.1 (0.7)	n.d.	–283.7 (41.8)
	January 2010	5	24	320	46.3 (0.5)	103.6 (1.3)	–40.4 (0.1)	–41.5 (0.7)	–302.7 (2.9)
	August 2010	6	40	275	33.4 (4.4)	n.d.	–46.3 (1.3)	–44.5 (1.1)	n.d
Guerrero Negro									
Area 1 site 1	March 2009	9	23	55	3.7 (0.3)	n.d.	–61.8 (0.9)	–51.9 (1.6)	–352.2 (2.9)
Area 1 site 2	March 2009	5	23	55	15.3 (1.2)	n.d.	–34.9 (0.8)	–45.6 (0.5)	–341.6 (0.9)
Area 1	October 2009	6	31	55	3.8 (0.4)	34.8 (2.5)	–60.6 (0.2)	–48.1 (3.4)	–335.6 (6.2)
Area 9 crust	October 2009	8	25	192	28.2 (8.7)	17.6 (7.2)	–41.5 (1.4)	–36.2 (2.8)	–327.1 (7.9)
Area 9 rubble	March 2009	8	22	184	31.9 (1.9)	n.d.	–41.8 (0.3)	–33.5	–317.8 (4.3)
	October 2009	10	25	192	44.5 (6.8)	17.6 (7.2)	–41.5 (1.4)	–33.1 (0.6)	–332.7 (5.2)
Area 9	September 2010	9	n.d.	190	35.3 (15.9)	26.9 (4.7)	–43.0 (0.5)	n.d.	–344.0 (2.1)
Area 9 surface	March 2009	n.d.	22	184	no bubbles	no bubbles	no bubbles	–40.9 (1.1)	no bubbles
Area 9 deep sediment	March 2009	n.d.	22	184	no bubbles	no bubbles	no bubbles	n.d.	no bubbles
Area 10-A	March 2009	3	n.d.	258	0.7 (0.2)	n.d.	–37.0 (0.4)	n.d.	–311.2 (1.0)
Area 10-B	March 2009	3	n.d.	306	0.4 (0.3)	n.d.	–34.3 (1.5)	n.d.	–253.8 (7.2)
Area 10-A	October 2009	5	28	270	1.4 (0.7)	117.3 (63.8)	–32.6 (0.9)	n.d.	–298.4 (25.8)
Area 10-B	October 2009	4	33	270	7.9 (0.3)	660.1 (80.3)	–33.8 (0.2)	n.d.	–265.8 (8.7)
Area 10-C	October 2009	6	33	298	0.1 (0.0)	3.4 (1.7)	–36.6 (1.7)	n.d.	–266.3 (38.5)
Area 11	March 2009	3	n.d.	300	0.1 (0.0)	n.d.	–35.5 (0.8)	n.d.	n.d.
Area 11	October 2009	9	n.d.	300	0.6 (0.4)	148.1 (140.4)	–38.6 (2.8)	n.d.	–316.1 (1.7)
Laguna Figueroa									
	October 2009	8	n.d.	54-200	0.3 (0.3)	5.4 (4.2)	–52.2 (14.3)	n.d.	–369.0 (8.6)
Laguna San Ignicio									
Pond 1	March 2009	3	n.d.	360	0.5 (0.2)	n.d.	–38.5 (1.0)	n.d.	–343.5 (21.1)
Pond 2	March 2009	3	n.d.	300	4.8 (0.7)	n.d.	–35.3 (0.4)	n.d.	–345.7 (7.4)
Pond 3	March 2009	3	n.d.	342	0.1 (0.0)	n.d.	–39.9 (2.6)	n.d.	–327.8 (2.4)

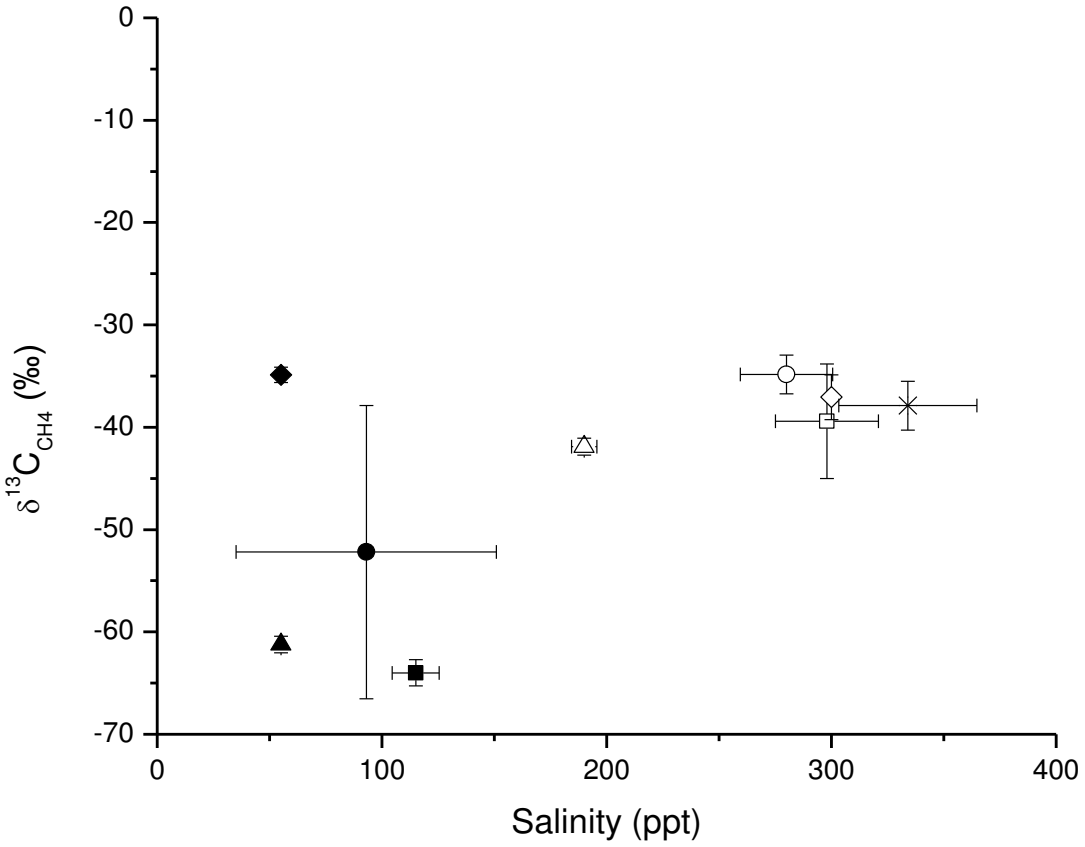

Figure 4.3. The salinity of ponds sampled plotted against the $\delta^{13}C_{CH4}$ values (‰) obtained from bubble samples. Data were averaged across sampling times for all sites (n=135). The symbols are the same as in Figure 4.2

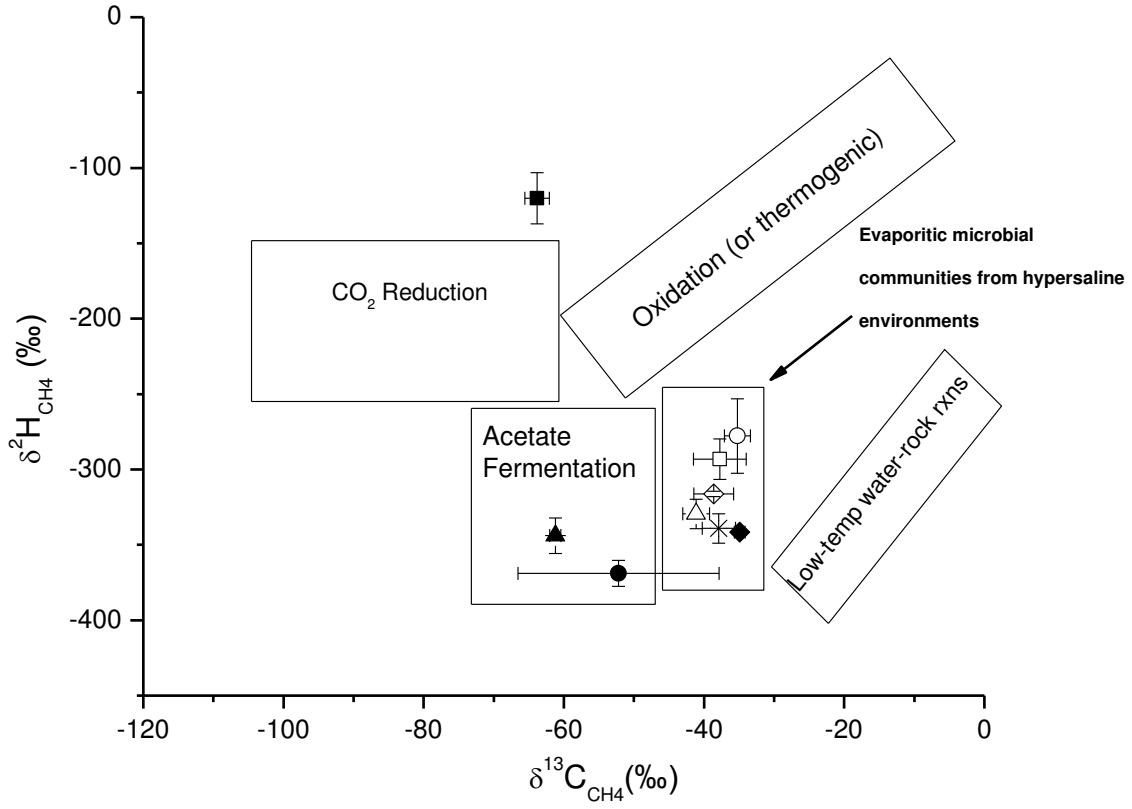

Figure 4.4. Cross plot of $\delta^{13}C_{CH4}$ against δ^2H_{CH4} values of methane-rich bubbles. Data were averaged across sampling times for all sites (n=123). General fields for CO_2 reduction and acetate fermentation, the two main biogenic methane production pathways, are shown, as are the fields for low-temperature water-rock reactions and the general direction for methane oxidation and thermogenic methane production pathway (Allen et al., 2006; Whiticar, 1999). The symbols are the same as in Figure 4.2. Although the majority of the data from GN Area 1 (closed triangle, n=15), the lowest-salinity site, and some samples obtained from Laguna Figueroa (n=3) fall within the acetate fermentation field, the sample obtained from GN Area 1 site 2 (closed diamond, n=5) and the samples obtained from endoevaporite mats (open symbols, n=86) and the remaining samples from Laguna Figueroa (n=5) group together outside the fields for biogenic methane production. The isotopic composition of methane at CAL Pond 15 (closed square, n=9) has substantially different δ^2H_{CH4} values and falls nearest the CO_2-reduction field. Proposed extension of biogenic methane production, to include production of methane from endoevaporite in hypersaline environments, is shown.

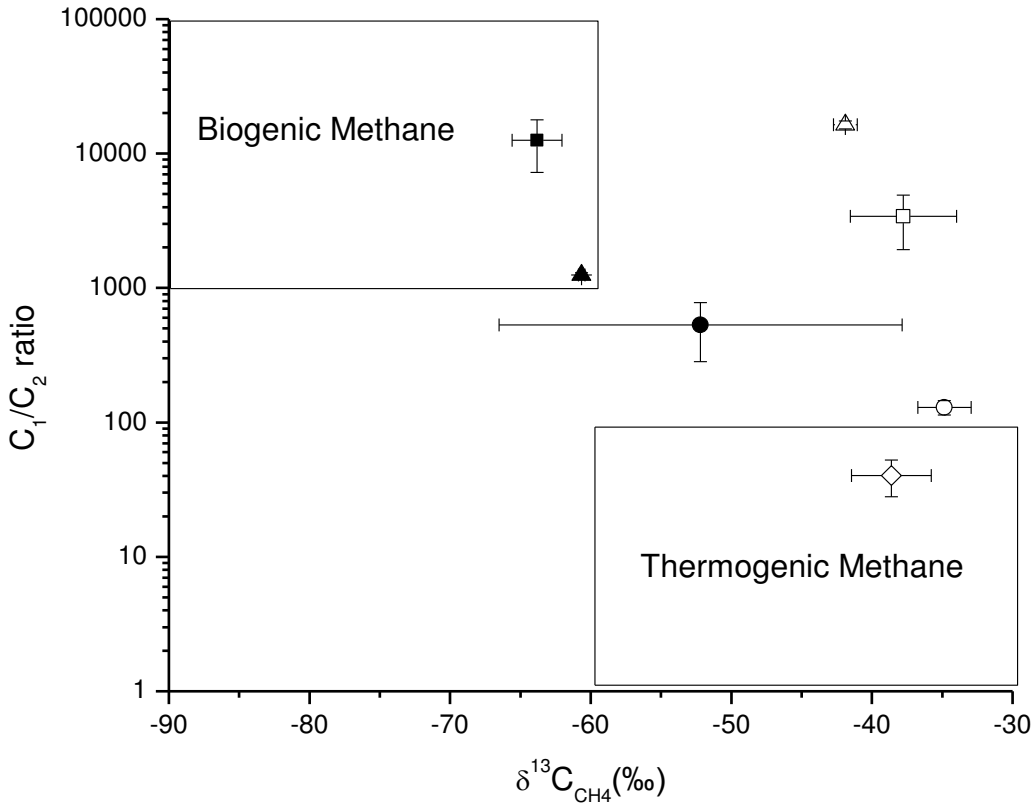

Figure 4.5. Measurements of the ratio of methane to ethane concentrations (C_1/C_2) plotted against the $\delta^{13}C_{CH4}$ values of the methane-rich bubbles. Data were averaged across sampling times for all sites (n=86). General fields for biogenic and thermogenic methane are shown (Bernard et al., 1978; Martens et al., 1991). The symbols are the same as in Figure 4.2. Methane from lower-salinity soft microbial mats (closed square and triangle, n=15) are within the classification for biogenic production. Methane in bubbles obtained from higher-salinity endoevaporite mats (open symbols, n=63) and the intermediate site (closed circle, n=8) would not be classified as biogenic according to current criteria.

CHAPTER FIVE

INCUBATIONS

5.1 Introduction

The search for life on planets both within and outside of our solar systems has led to research aimed at better understanding analogue sites for those planets here on Earth. One type of analogue site in particular, the hypersaline environment, has become very relevant in understanding biological and chemical processes thought to be occurring on Mars. With recent discoveries of past liquid brine, as well as present-day frozen water on the surface of Mars (McEwen et al., 2011; Smith et al., 2009) and the widespread occurrence of chloride containing deposits (Osterloo et al., 2008) the in depth analysis of hypersaline environments has become important to the future of space exploration.

With the findings of water on Mars, there is an increased probability of finding life on that planet as well. Through remote sensing with telescopes scientists have been able to search the atmospheric spectra of planets and moons for biosignature gases. An atmospheric biosignature gas are gases produced by life, on Earth the most important biosignature gases are O_2, CH_4 and N_2O (Seager, 2010). Methane recently has been found in the atmosphere of our neighboring planet Mars at concentrations of approximately 10 ppb (Formisano et al., 2004; Krasnopolsky et al., 2004; McEwen et al., 2011; Mumma et al., 2009). Although the interpretation of these findings has been challenged (Zahnle et al., 2011), the presence even small amounts of methane on Mars would immediately raise the question of its origin. In an oxidizing atmosphere like that on Mars, a reduced gas like methane would not be present for long. In fact, because the lifetime of methane in the Martian atmosphere is estimated to be only

around 300 years (Mischna et al., 2011; Nair et al., 2005), the presence of methane would require an active or recent emission source.

On Mars, the presence of methane can be attributed to one of the three sources of methane found here on Earth, biogenic, thermogenic, or geologic sources. Given that 80-90% of methane in the Earth's atmosphere is thought to derive from microbial sources (Whiticar, 1999), the analysis of methanogens, the anaerobic *Archaea* that produce methane, is important for understanding biologic production in these environments. Methanogens form methane by pathways that are commonly classified according to the type of carbon substrate they utilize (Formolo, 2010; Whiticar, 1999; Whitman et al., 2006). They utilize relatively few and simple carbon compounds to obtain energy.

Methanogens obtain their energy for growth from the conversion of a limited number of substrates to methane gas (Whitman et al., 2006). The substrates required for growth can be divided into three groups, hydrogenotrophic methanogenesis, acetotrophic methanogenesis, methylatrophic methanogenesis (Madigan and Martinko, 2006; Whiticar, 1999; Whitman et al., 2006). Hydrogenotrophic methanogenesis, the reduction of CO_2 by hydrogen gas and acetotrophic methanogenesis, the assimilation of acetate, are the two main methane production pathways and are also known as competitive pathways (Formolo, 2010; Whitman et al., 2006). Competitive pathways are pathways for methane production in which methanogens have to compete with other microorganisms for the use of substrates. The third type, methylatrophic methanogenesis, is a non-competitive pathway that includes the use of methylated substrates such as mono, di and tri-methylamine and methanol in the production of methane. Non-competitive pathways are pathways that utilize substrates in which methanogens do not have to compete with other microorganisms for use of the substrate. In marine environments the use of

competitive substrates for the process of methanogenesis is severely limited in the water column or sediment pore fluid because of the abundance of dissolved sulfate. In the presence of excess sulfate, sulfate reducing bacteria (SRB) outcompete methanogens for the common substrates hydrogen and acetate since they have a higher affinity for those substrates (Muyzer and Stams, 2008). In the presence of high sulfate concentrations, through the use of non-competitive pathways, methanogens no longer have to compete with sulfate reducing bacteria as they are unable to utilize non-competitive substrates such as methylamines, methanol, and dimethylsulfide. Non-competitive pathways, although not well understood, are thought to be of great importance in hypersaline environments because of the high concentrations of sulfate found in these environments and the abundance of non-competitive substrate precursors (Chapter 1). Because sulfate concentration levels never become exhausted in hypersaline environments and sulfate reducing bacteria remain active, theory would suggest that in such circumstances methane production would not occur or methanogenesis would commence using non-competitive substrates (McGenity, 2010).

Carbon and hydrogen stable isotope ratios have been used to distinguish methane production pathways, which will be key in the determination of biogenic methane on Mars and/or other planets. Methane produced through biogenic processes is characterized by a $\delta^{13}C_{CH4}$ value < –50 ‰ and a $\delta^{2}H_{CH4}$ range from –275‰ to –100‰ (Whiticar, 1999). Through the use of stable isotopes we can further distinguish the substrate used for methane production. The reduction of CO_2 produces methane in the range of –100‰ to –55‰ and –250‰ to –150‰ for $\delta^{13}C_{CH4}$ and $\delta^{2}H_{CH4}$ values, respectively, and acetate assimilation produces methane in the range of –70‰ to –45‰ and –375‰ to –300‰ for $\delta^{13}C_{CH4}$ and $\delta^{2}H_{CH4}$ values, respectively (Whiticar, 1999). Less is known about the isotopic composition of methane produced from non-

competitive substrates. Culture work has suggested that there is a depletion in ^{13}C values for methane produced from both methylamines and methanol (Margulis et al., 1980; Summons et al., 1998; Zahnle et al., 2011). Thermogenic methane generally has $\delta^{13}C$ values > –50‰ and is characterized by a progressive enrichment in ^{13}C content with increasing maturity, eventually approaching the $^{13}C/^{12}C$ of the original organic matter with the $\delta^{2}H$ range between –275‰ to –100‰ (Kotelnikova, 2002; Whiticar, 1999). Geologic methane production from low-temperature water-rock reactions ranges between $\delta^{13}C$ of –40‰ to –10‰ to $\delta^{2}H$ values of –100‰ to –400‰ although it is less well characterized (Allen et al., 2006; Whiticar, 1999).

This research entails an in-depth analysis of the utilization of carbon substrates for methane production in hypersaline environments in order to develop a better understanding of the processes that may be occurring in these environments and on other planets. This shall be achieved through the analysis of the following goals and objectives:

1. Provide evidence of current biogenic methane production in these hypersaline environments.
2. Provide evidence that methane production is occurring in sediments of endoevaporite sites.
3. Conduct a comparative analysis of methane production in brine and extremely brine sites.
4. Provide evidence that methane production in our sites derives primarily from non-competitive substrates as opposed to competitive substrates.

5.2 Methods

5.2.1 Site Description

Sampling for this work was performed in two locations, the Don Edwards National Wildlife Refuge in southern San Francisco Bay (CAL) and Exportadora de Sal in Guerrero Negro (GN) (see more detailed site description in Chapter 2). CAL Pond 15 and CAL Pond 23 from the refuge were sampled in January 2010 and August 2010. At CAL Pond 15 (~120 parts per thousand [ppt] salinity), a very thin, soft microbial mat was present on top of black mud that extended to a depth of approximately 8-10 cm. Below this, grey mud became the dominant sediment. CAL Pond 23 (~300 ppt) was capped by a thin gypsum and halite crust. This crust had endolithic microbial communities (endoevaporitic mat) present, as indicated by the green and pink coloring within the crust (Figure 5.1a), and overlaid black, sulfur-rich mud. GN Areas 1, 4, and 9 from the salterns in Guerrero Negro were sampled in March 2009 and October 2009. GN Area 1 (~55 ppt) and Area 4 (~92 and 84 ppt) contained thick, soft, well-laminated microbial mats (Figure5.1b). GN Area 9 (~190 ppt) was capped by a thick gypsum crust that was also populated with an endoevaporitic mat; this crust overlaid a gypsum rubble, surface tan mud, and deeper black sand sediment layer (Figure 5.1c and 5.1d).

5.2.2 Incubations

Methane production rates from soft mat and crust sediment samples were determined based on incubations of slurries in serum vials. Soft microbial mats were collected from CAL Pond 15 and from GN Areas 1 and 4, our lower salinity ponds referred as brine ponds from henceforth. Mat samples from CAL Pond 15 were collected by traditional coring methods using

short cores, capturing the thin microbial mat as well as the upper 8-10 cm of black mud, which was later homogenized prior to use in incubations. Mat samples from GN Areas 1 and 4 were sampled differently from CAL Pond 15 due to the greater cohesiveness of the mats. In these areas mat sections were cut and removed from the bottom of the ponds and placed into tight-fitting plastic trays. At the time of incubation preparation, only the upper 1 to 3 cm of the soft microbial mat from GN Areas 1 and 4 was used. Endoevaporitic crust and sediment were collected from CAL Pond A23 and GN Area 9, higher salinity ponds that are henceforth referred as extreme brine ponds. Endoevaporitic crust and sediment from CAL Pond A23 was collected by short cores of crust and sediments which were later homogenized. GN Area 9 was subsampled into the top gypsum crust, underlying gypsum rubble, surface tan mud, and deep black sandy sediment below. The crust and rubble were broken into small pieces before incubating, while the sediment intervals were homogenized. The rubble area of GN Area 9 was sampled in both March 2009 and October 2009, while the crust was sampled only in October 2009 and the sediments only in March 2009. In addition, overlying water used for our incubations was obtained from each site. The salinity of the overlying water was determined with a hand-held refractometer (Table 5.1).

The amount of sediment used for each incubation vial varied slightly, with most samples containing between 10-20 g of sediment. Vials were prepared by placing samples from the various sites in 38 mL glass serum vials with 10 mL of corresponding deoxygenated (N_2-purged) site water to make the slurries.

To determine the substrate(s) used by the methanogens in these hypersaline environments, 99% ^{13}C-labeled substrates (trimethylamine (TMA), monomethylamine (MMA), methanol (MeOH), acetate, and bicarbonate) as well as ^{2}H-labeled DMS were added to

incubations of mats/sediments and the evolved methane was monitored for ^{13}C and ^{2}H content. The ^{13}C-labeled bicarbonate was added to a final concentration of 10 µM in the slurry. Previous analyses of dissolved inorganic carbon (DIC) concentrations within the soft microbial mats of Guerrero Negro were approximately 2 to 8 mM (Potter et al., 2009), and so we determined that this small addition of ^{13}C-labeled bicarbonate would not substantially change the total concentration of DIC. However, the *in situ* concentrations of TMA, MMA, MeOH, DMS and acetate at these sites are unknown, so a range of substrate concentrations (0.1 µM, 1 µM, and 10 µM final concentration) was used. Individual incubation vials received one substrate at one concentration, resulting in a suite of vials, including the controls with no added substrate, being used at each site (Chapter 3, Table 3.1).

Because of concerns that methane could increase in the headspaces of the incubation vial due to physical de-gassing from the endoevaporitic crusts, killed controls were used during all sampling trips after March 2009. For GN Area 9, a high concentration of sodium hydroxide made with site water to yield 0.1 M NaOH final concentration was used to kill the microbes in the crust and rubble incubations. For CAL Ponds A15 and A23, 5% paraformaldehyde was diluted down in site water from 20% stock solution to serve as a more efficient inhibitor of microbial activity.

Once the vials were filled with sediment, site water, and respective substrate (or no substrate for control) they were capped with blue butyl rubber stoppers (Bellco Glass Co.), and the headspace was flushed for 5 minutes with nitrogen gas to remove any oxygen gas, returning the sediment to an anoxic state. The vials were allowed to equilibrate for 24 hours prior to the first extraction of headspace.

5.2.3 Methane Production and Isotope Analysis

Methane concentration in the headspace was monitored on a Shimadzu Mini-II Gas Chromatograph (GC) through time to obtain the production rate. Approximately 250µl of headspace from all samples was injected directly into the GC (more detail available in Chapter 3.2.4). Sample areas were converted to concentrations (in parts per million, ppm) by:

$$CH_4\ (ppm) = \frac{(Standard\ ppm\ \times Sample\ area)}{Standard\ area}$$

where standard ppm is the known concentration of the gas standard, sample area is the integrated area of the sample, and standard area is the integrated area of the standard. Samples were then charted over time to calculate methane production rates (Appendix B).

The isotopic composition of the evolved methane was measured after incubating. The stable isotopic composition of the evolved methane from the incubations was determined using a GC interfaced with a Finnegan Delta Plus Isotope Ratio Mass Spectrometer. When methane concentrations were not high enough for direct injection (~1,000 ppm for ^{13}C and ~5,000 ppm for ^{2}H), cryofocusing was used to amplify the signal (more detail available in Chapter 3.2.6). Isotope data are reported in the "del" notation ($\delta^{13}C$, $\delta^{2}H$):

$$\delta\ = 1{,}000\ \left[\left(\frac{R_{sample}}{R_{standard}}\right) - 1\right]$$

where R_{sample} is the isotopic ratio of the sample and $R_{standard}$ is the isotopic ratio of the referenced standard (PDB or SMOW).

5.3 Results

5.3.1 Methane Production from $\delta^{13}C$ Substrate Additions

Methane production across the salinity gradients at these sites revealed relatively high methane production rates at ponds with both the lowest salinity (GN Area 1, ~55 ppt) and the highest salinity (GN Area 9, ~190 ppt) (Figure 5.2). Methane production rates ranged from 0.06 to 15.36 nmol g^{-1} d^{-1} for the brine ponds with salinities ranging from 55 ppt to 130 ppt and 0.02 to 18.80 nmol g^{-1} d^{-1} for the extreme brine ponds with salinities ranging from 180 ppt to 320 ppt (Table 5.1). The highest methane production rates occurred within the gypsum crust of GN Area 9 while the lowest rates, interestingly enough, were observed in the same pond in the deep sediments of GN Area 9 (Table 5.1).

To ensure that production in the evaporitic sites were from biologic activity and not degassing, killed controls were performed after the March 2009 trip. At the Guerrero Negro site we presumed that the use of high pH would be effective at stopping the growth of many microorganisms. The use of a strong NaOH solution for the killed control at this site was not entirely successful, however, although production was significantly reduced (Table 5.1). We believe that this reduction but not elimination of microbial production may be due to a greater tolerance to high pH levels in microbes that can live under hypersaline conditions (Jones et al., 1998). Switching to a 5% paraformaldehyde solution at the Don Edwards site proved successful at stopping methanogenesis (Table 5.1).

Production rates were monitored throughout the entire length of the incubations to ensure that the addition of ^{13}C-labeled substrate did not stimulate additional methane production. Throughout all sites, production rates were similar to the controls (Figure 5.3), therefore it is

presumed that the total concentration of each of the substrate was not substantially increased by the relatively low concentration of ^{13}C addition and that the ^{13}C-labeled uptake and use was indicative of what occurs *in situ* (Figure 5.3).

5.3.2 $\delta^{13}C$ Isotopic Analysis from Sediments Receiving ^{13}C-labeled Substrates

Isotopic analysis of incubations receiving substrate addition provided insight on substrate utilization by methanogens in our hypersaline sites. All sites sampled displayed similar trends in $\delta^{13}C$-CH_4 from the various substrate additions. When ^{13}C-labeled methylamines and methanol were added to incubation vials we observed a significant increase in $\delta^{13}C$-CH_4 in comparison to control samples. This increase was substantially more significant in the vials that received ^{13}C-labeled methyalmines. Though the vials that received ^{13}C-labeled acetate and bicarbonate did produce methane, however this methane was either not enriched in ^{13}C (indicating that the labeled substrate was not used as a carbon source for methane production) or was slightly enriched in ^{13}C. The sample sites displayed a slight variation in the amount of ^{13}C-enrichment from the overall trend and so we will examine each individually.

CAL Pond 15. Isotopic analysis of the samples obtained from CAL Pond 15 in January 2010 revealed significant isotopic enrichment in samples receiving ^{13}C-labeled trimethylamine and methanol (Figure 5.4). Incubated sediments receiving no substrate addition produced methane with an average $\delta^{13}C$ of –62.85‰. Samples incubated with 0.1μM, 1μM, and 10μM TMA produced methane with an average isotopic signature of +375.86‰, +5,532.63‰, and +55,760.01‰, respectively. Samples receiving ^{13}C-labeled methanol also produced methane that was more enriched in comparison to the control groups, but not as enriched in comparison to the TMA group. Vials receiving ^{13}C-labeled 0.1μM MeOH had an average isotopic $\delta^{13}C$ of

+57.86‰, while vials which received ^{13}C-labeled 1µM and 10µM MeOH had on average an isotopic δ^{13}C of +694.17‰ and +13,000.03‰, respectively. CAL Pond 15 samples, receiving ^{13}C-labeled competitive substrates, revealed no isotopic enrichment in methane production (Figure 5.4). Samples receiving ^{13}C-labeled 0.1µM and 1µM acetate produced methane with an average isotopic value of –61.49‰ and –60.99‰, respectively. Samples receiving10µM acetate and bicarbonate produced methane that was slightly enriched in ^{13}C-CH_4 with an average δ^{13}C of –54.14‰ and –56.68‰, respectively.

CAL Pond A23. Isotopic data for CAL Pond A23 from the January 2010 (Figure 5.5a) and August 2010 (Figure 5.5b) sampling trips was analyzed. Because the isotopic results from the two separate trips varied slightly, the results will be presented separately. In January 2010, samples receiving no additional substrate produced methane with an average δ^{13}C of –41.51‰. This value, although slightly outside of the traditional range for biogenic methane production was produced from the microbial community within the vial and was not a product of degassing from the gypsum rubble, as shown in our killed control experiments. All of the vials receiving ^{13}C-labeled TMA and MeOH, produced methane that was significantly enriched in ^{13}C in comparison to the controls (Figure 5.5a). The samples that showed the most enrichment were those receiving 0.1µM, 1µM, and 10µM TMA. The samples produced methane with an average δ^{13}C of +506.20‰, +6,384.25‰, and +61,115.43‰, respectively. The next most enriched group of samples was the group receiving ^{13}C-labeled MeOH. These 3 concentrations (0.1µM, 1µM, and 10µM) although identical in concentration amount added to the incubation vials in the TMA group produced significantly less enriched methane. Samples receiving 0.1µM ^{13}C-labeled MeOH produced methane with an average δ^{13}C of +139.38‰ while those receiving 1µM or 10µM ^{13}C-labeled MeOH produced methane with an average δ^{13}C of +1,849.32‰ and

+17,047‰, respectively. Samples receiving 0.1µM and 1µM ^{13}C-labeled acetate produced methane that was not significantly different from the controls, and had an average δ^{13}C values of –38.83‰ and –37.02‰, respectively. Samples receiving 10µM ^{13}C-labeled acetate and bicarbonate were slightly enriched in ^{13}C, with average δ^{13}C values of –35.76‰ and –37.87‰, respectively.

In August 2010, incubation samples that had received no substrate addition produced methane with an average δ^{13}C of –44.52‰, similar to isotopic values from control samples obtained in January 2010 (Figure 5.5b). During this sampling trip, vials with the addition of ^{13}C-labeled TMA were the most enriched in ^{13}C-CH_4 content, though not as enriched as in our previous sampling trip. During the August 2010 trip, samples amended with 0.1µM, 1µM, and 10µM ^{13}C-labeled TMA produced methane with δ^{13}C average value of +38.77‰, +1,176.0‰, and +9,772.26‰, respectively. These enrichment values were about six times lower than what was observed eight months earlier in our January 2010 trip. The next most enriched samples were from the 0.1µM, 1µM, and 10µM ^{13}C-labeled MeOH. The samples were in some cases three times less enriched than what was observed in January 2010 and had δ^{13}C values of –1.35‰, +452.7‰, and +3,086.0‰, respectively. Vials receiving ^{13}C-labeled acetate and bicarbonate did not produce methane enriched with ^{13}C in respect to the controls, these samples were slightly depleted in ^{13}C. Isotopic values obtained for 0.1µM and 1µM acetate were –45.65‰ and –47.54‰, respectively, while isotopic values for 10µM acetate and bicarbonate were –50.22‰ and –48.48‰, respectively.

GN Area 1. Isotopic data was collected from GN Area 1 during two sampling trips. Because of some differences in substrates used during sampling trips we will address the results from each trip separately. In March 2009, sediments were collected from two locations

approximately 100 meters apart. GN Area 1 site 1 received an abbreviated list of substrate additions while GN Area 1 site 2, located 100 meters west of site 1, received the full suite of substrate additions. Since the two sites were visibly different and contained methane bubbles that were significantly different from each other (Chapter 4) we will discuss the results from the two March 2009 Area 1 sites separately.

Isotopic analysis of samples obtained from GN Area 1 site 1 in March 2009 revealed that samples receiving no addition of ^{13}C-labeled substrate had an average δ^{13}C value of –51.8‰ (Figure 5.6a). This site was treated with the abbreviated list of substrates only and received the largest concentrations of ^{13}C-labeled substrates. The substrate additions that displayed the most enrichment from ^{13}C-labeled substrates were from the 10µM MMA and 10µM MeOH additions. Those additions produced methane with average δ^{13}C values of +3,983.03‰ and +3,355.79‰, respectively. The samples receiving ^{13}C-labeled 10µM acetate and 10µM bicarbonate produced methane that was not enriched in ^{13}C with isotopic values of –46.76‰ and –48.07‰, respectively.

Isotopic analysis of samples obtained from GN Area 1 site 2 in March 2009 revealed that samples receiving no ^{13}C-labeled addition produced methane with an average δ^{13}C value of –45.55‰ (Figure 5.6b). The only samples that produced methane enriched in ^{13}C were those that had received ^{13}C-labeled MMA and MeOH. Vials that received 0.1µM, 1µM, and 10µM ^{13}C-labeled MMA produced methane with average δ^{13}C values of –19.44‰, +381.1‰, and +5,319.2‰, respectively. Samples receiving 0.1µM, 1µM, and 10µM ^{13}C-labeled MeOH produced methane with δ^{13}C values of –24.41‰, +254.11‰, and +2,783.68‰, respectively. Samples that were treated with ^{13}C-labeled acetate and bicarbonate did not produce methane that was enriched in ^{13}C. The 0.1µM, 1µM, and 10µM ^{13}C-labeled acetate samples produced

methane with average $\delta^{13}C$ values of –44.68‰, –44.16‰, and –44.70‰ respectively. The samples that received 10µM ^{13}C-labeled bicarbonate produced methane with an isotopic carbon signature similar to the control, –44.53‰.

Isotopic analysis of samples obtained from Area 1 in October 2009 revealed that sediment unamended with ^{13}C-labeled substrates produced methane with an average $\delta^{13}C$ value of –48.06‰ (Figure 5.7). In October 2009, samples from this site were treated only with ^{13}C-labeled non-competitive substrates because our previous experiments had revealed no incorporation of competitive substrates in this location. Of the samples receiving non-competitive substrates, the ones that received ^{13}C-labeled TMA showed the most enrichment in ^{13}C-CH_4. The three concentrations of ^{13}C-labeled TMA that were used, 0.1µM, 1µM, and 10µM TMA, produced methane with average $\delta^{13}C$ values of +8.89‰, +671.05‰, and +5,595.44‰, respectively. The samples receiving 0.1µM, 1µM, and 10µM ^{13}C-labeled MeOH produced methane with average $\delta^{13}C$ values of –38.86‰, +86.47‰, and +1,707.56‰, respectively.

GN Area 4. Isotopic data from GN Area 4 was analyzed for the March 2009 (Figure 5.8a) and October 2009 (Figure 5.8b) sampling trips. Because of some differences in the ^{13}C-labeled substrates used during the different dates as well as differences in the isotopic methane composition of the unamended sediment, we will examine the results from both trips separately.

In March 2009, sediments with no additional ^{13}C-labeled substrate produced methane with an average δ^{13} value of –77.12‰ (Figure 5.8a). This value was the most negative $\delta^{13}C$ value from all sites sampled (Table 5.1). Incubations from GN Area 4 sampled in March 2009 did not become as enriched in ^{13}C-CH_4 in comparison to all other locations sampled. The only substrate that showed any enrichment in ^{13}C-CH_4 was that to which ^{13}C-labeled MMA had been added. Incubations receiving ^{13}C-labeled 0.1µM, 1µM, and 10µM MMA produced methane with

average $\delta^{13}C$ values of –71.97‰, –68.24‰, and –46.33‰, respectively. This enrichment was significantly less than at any other location treated with ^{13}C-labeled methylated substrate. The sediments receiving 0.1µM, 1µM, and 10µM MeOH produced methane with average $\delta^{13}C$ values of –67.82‰, –70.20‰, and –62.37‰, respectively. Samples receiving 0.1µM, 1µM, and 10µM acetate produced methane with average $\delta^{13}C$ values of –70.84‰, –70.83‰, and –67.65‰, respectively. Samples receiving 10µM ^{13}C-labeled bicarbonate produced methane with an average $\delta^{13}C$ value of –69.06‰.

The incubation samples from GN Area 4 that were sampled in October 2009 displayed very different isotopic results than those collected in March 2009. Sediments incubated with no additional substrates produced methane with an average $\delta^{13}C$ value of –36.87‰, significantly more enriched in ^{13}C than in our previous trip (Figure 5.8b). Incubation samples receiving ^{13}C-labeled TMA showed the most enrichment in ^{13}C-CH_4. The three concentration of TMA 0.1µM, 1µM, and 10µM, produced methane with average $\delta^{13}C$ values of –25.79‰, +393.51‰, and +6,004.61‰, respectively. The next most enriched samples were those from 0.1µM, 1µM, and 10µM MeOH substrates. The samples produced methane with average $\delta^{13}C$ values of –58.50‰, +34.79‰, and +815.96‰, respectively. Samples receiving ^{13}C-labeled acetate and bicarbonate did not produce methane enriched in ^{13}C, however, these vials were slightly depleted in ^{13}C. Vials receiving 0.1µM, 1µM, and 10µM ^{13}C-labeled acetate produced methane with average $\delta^{13}C$ values of –52.97‰, –57.0‰, and –52.46‰, respectively. Samples treated with 10µM bicarbonate produced methane with an average $\delta^{13}C$ value of –58.04‰.

GN Area 9. Isotopic analysis of sediments from GN Area 9 was sampled in March 2009 (Figure 5.9) and October 2009 (Figure 5.10). During each sampling trip, sediments were

separated into the different layers of gypsum crust, rubble or sediment. We will present data from each sampling date and each sediment layer separately.

In March 2009, sediment from GN Area 9 top mud was analyzed for $\delta^{13}C\text{-}CH_4$ content (Figure 5.9a). Sediments not treated with ^{13}C-labeled substrate produced methane with an average $\delta^{13}C$ value of –40.88‰. Of the sediments treated with ^{13}C-labeled substrates, those to which ^{13}C-labeled MMA had been added provided the most enriched $\delta^{13}C\text{-}CH_4$. Samples treated with 0.1µM, 1µM, and 10µM ^{13}C-labeled MMA produced methane with average $\delta^{13}C$ values of +103.4‰, +2,825.50‰, and +34,563.3‰, respectively. The next most enriched incubations were from the vials receiving ^{13}C-labled MeOH. Sediments enriched with 0.1µM, 1µM, and 10µM ^{13}C-labeled MeOH produced methane with average $\delta^{13}C$ values of +238.28‰, +2,397‰, +27,171.88‰, respectively. Sediments amended with ^{13}C-labeled competitive substrates did not produce methane enriched in ^{13}C. Sediments amended with 0.1µM, 1µM, and 10µM ^{13}C-labeled acetate produced methane with average $\delta^{13}C$ values of –33.37‰, –39.35‰, and –33.53‰, respectively, while sediments amended with 10µM bicarbonate produced methane with an average $\delta^{13}C$ value of –37.84‰.

In March 2009, sediment from GN Area 9 bottom mud, which was not treated with any addition of ^{13}C-labeled substrates, produced methane with an average $\delta^{13}C$ value of –49.44‰ (Figure 5.9b). GN Area 9 bottom mud sediment only displayed an enrichment in $\delta^{13}C$ content from the addition of ^{13}C-labeled MMA and MeOH. The addition of 0.1µM and 1µM ^{13}C-labeled MMA produced methane with average $\delta^{13}C$ value of –28.33‰ and +2,136.05‰, respectively. Sediments treated with 0.1µM, 1µM, and 10µM ^{13}C-labeled MeOH produced methane with average $\delta^{13}C$ values of +243.59, +2,282.24‰, and +23,829.3‰ respectively. Samples treated with 0.1µM, 1µM, and 10µM ^{13}C-labeled acetate did not produce methane enriched in ^{13}C

content; rather, these samples produced methane with average $\delta^{13}C$ values of –52.47‰, –52.84‰, and –47.31‰, respectively. Similar results were observed for sediments amended with 10µM ^{13}C-labeled bicarbonate. These sediments produced methane with an average $\delta^{13}C$ value of –41.42‰.

In October 2009, crustal material was collected and incubated from the gypsum crust of GN Area 9 (Figure 5.10a). Crustal material not incubated with any addition of ^{13}C-labeled substrate produced methane with an average $\delta^{13}C$ value of –36.18‰. This isotopic value, although outside the range typically associated with biogenic processes, was produced within our incubation vials and not from the degassing of the gypsum crust. Crustal material incubated with ^{13}C-labeled TMA and MeOH produced the most enriched methane from our site. Samples receiving 0.1µM, 1µM, and 10µM ^{13}C-labeled TMA produced methane with an average $\delta^{13}C$ value of +15.06‰, +526.28‰, and +6,201.87‰, respectively. Crustal material incubated with ^{13}C-labeled MeOH produced methane enriched in ^{13}C content in comparison to the controls, although not as enriched as ^{13}C as that observed from the addition of TMA. The vials receiving 0.1µM, 1µM, and 10µM ^{13}C-labeled MeOH produced methane with average $\delta^{13}C$ values of –18.02‰, +99.43‰, and +1,411.71‰, respectively. Crustal material incubated with the addition of 0.1µM, 1µM, and 10µM ^{13}C-labeled acetate produced methane that was slightly enriched in ^{13}C content with average $\delta^{13}C$ values of –30.39‰, –32.64‰, and –36.54‰, respectively. Samples incubated with 10µM ^{13}C-labeled bicarbonate also displayed a slight enrichment in ^{13}C content with average $\delta^{13}C$ value of –29.93‰.

In October 2009, rubble material was collected from the layer just below the crustal layer in GN Area 9 (Figure 5.10b). When incubated with no addition of ^{13}C-labeled substrates, this rubble material produced methane with an average $\delta^{13}C$ value of –33.07‰. Samples incubated

with ^{13}C-labeled TMA produced ^{13}C-methane that was more enriched than any other substrate used with this rubble material. From the addition of 0.1µM, 1µM, and 10µM ^{13}C-labeled TMA, average δ^{13}C methane values were +90.21‰, +1,285.4‰, and +14,760.52‰, respectively. The addition of 0.1µM, 1µM, and 10µM ^{13}C-labeled MeOH produced methane with average δ^{13}C values of –8.94‰, +269.11‰, and +3,585.16‰, respectively. Samples incubated with ^{13}C-labled competitive substrates produced methane; however, it was not enriched in ^{13}C content. Average δ^{13}C values for methane produced from the incubation of rubble material and 0.1µM, 1µM, and 10µM ^{13}C-labeled acetate were –33.67‰, –33.23‰, and –31.85‰, respectively. Samples incubated with 10µM ^{13}C-labeled bicarbonate produced methane with an average δ^{13}C value of –31.77‰.

5.3.3 Methane Production from δ^2H Substrate Addition

In October 2009 a set of incubations from the Guerrero Negro, Mexico site received the addition of a δ^2H-labeled non-competitive substrate DMS. This addition was performed in order to analyze if methane could be produced in this environment through the use of this substrate. Methane production rates observed for GN Areas 1 and 4 sediments incubated with 0.1µM, 1µM, and 10µM ^{2}H-labeled DMS were statistically similar to that of their respective controls (Table 5.2), indicating that the addition did not stimulate additional methane production and were similar to what is available *in situ* (Table 5.2). GN Area 9 rubble and crustal sediment incubated with 0.1µM, 1µM, and 10µM ^{2}H-labeled DMS displayed a decrease in methane production rates that were statistically different from their respective controls (Table 5.2).

5.3.4 $\delta^{13}C$ and $\delta^{2}H$ Isotope Analysis from ^{2}H-labeled Incubations

Isotopic analysis of the $\delta^{13}C$-CH_4 produced from the incubations receiving ^{2}H-labeled DMS and from control samples revealed no statistically significant $\delta^{13}C$ values for all concentration additions from GN Area 1 and GN Area 4, as well as for the 0.1µM addition from GN Area 9 crust. There was, however, a significant difference between $\delta^{13}C$-CH_4 from the controls and the remaining concentrations of DMS from GN Area 9 crust and all concentrations from GN Area 9 rubble (Table 5.2). Isotopic analysis of the $\delta^{13}C$-CH_4 and $\delta^{2}H$-CH_4 produced from incubations receiving $\delta^{2}H$-labeled DMS revealed an enrichment in $\delta^{2}H$ for all locations (Table 5.2). This enrichment varied in the different locations; for this reason the results from each location will be presented separately (Table 5.2).

GN Area 9 rubble. The samples with the most deuterium enrichment from the addition of ^{2}H-labeled DMS (although with the lowest methane production rate) were those obtained from GN Area 9 rubble (Table 5.2). Samples not receiving any ^{2}H-labeled DMS produced methane with a $\delta^{13}C$ value of –33.08‰ and $\delta^{2}H$ value of –345.88‰. Samples receiving the addition of 0.1µM ^{2}H-labeled DMS produced methane with average $\delta^{13}C$ and $\delta^{2}H$ value of –37.76‰ and +147.03‰ respectively. Samples receiving the addition of 1µM ^{2}H-labeled DMS produced methane with an average $\delta^{13}C$ and $\delta^{2}H$ value of –39.17‰ and +3,176.71‰ respectively. Samples receiving the addition of 10µM ^{2}H-labeled DMS produced methane with average $\delta^{13}C$ and $\delta^{2}H$ values of –39.91‰ and +30,271.63‰, respectively.

GN Area 9 crust. The samples with the second overall most deuterium enriched methane from the addition of ^{2}H-labeled DMS were those obtained from GN Area 9 crust. Samples not receiving any ^{2}H-labeled DMS produced methane with average $\delta^{13}C$ and $\delta^{2}H$ values of –36.18‰ and –336.75‰, respectively. Samples receiving the addition of 0.1µM ^{2}H-labeled DMS

produced methane with average $\delta^{13}C$ and $\delta^{2}H$ value of –42.23‰ and –218.81‰, respectively. Samples receiving the addition of 1µM ^{2}H-labeled DMS produced methane with average $\delta^{13}C$ and $\delta^{2}H$ values of –44.77‰ and –151.24‰, respectively. Samples receiving the addition of 10µM ^{2}H-labeled DMS produced methane with average $\delta^{13}C$ and $\delta^{2}H$ values of –42.40‰ and +483.11‰, respectively.

GN Area 1. The samples with the third overall most deuterium enriched methane from the addition of ^{2}H-labeled DMS were those collected from GN Area 1. Samples not receiving any ^{2}H-labeled DMS produced methane with average $\delta^{13}C$ and $\delta^{2}H$ values of –48.07‰ and –323.34‰, respectively. Samples receiving the addition of 0.1µM ^{2}H-labeled DMS produced methane with average $\delta^{13}C$ and $\delta^{2}H$ values of –52.05‰ and –269.58‰, respectively. Samples receiving the addition of 1µM ^{2}H-labeled DMS produced methane with average $\delta^{13}C$ and $\delta^{2}H$ values of –52.86‰ and –269.56‰, respectively. Samples receiving the addition of 10µM ^{2}H-labeled DMS produced methane with average $\delta^{13}C$ and $\delta^{2}H$ values of –50.36‰ and +1,010.04‰, respectively.

GN Area 4. The samples with the smallest amount of deuterium enriched methane from the addition of ^{2}H-labeled DMS were those collected from GN Area 4. Samples not receiving ^{2}H-labeld DMS, produced methane with average $\delta^{13}C$ and $\delta^{2}H$ values of –47.61‰ and –388.62‰, respectively. Samples receiving the addition of 0.1µM ^{2}H-labeled DMS produced methane with average $\delta^{13}C$ and $\delta^{2}H$ values of –53.47‰ and –391.11‰, respectively. Samples receiving the addition of 1µM ^{2}H-labeled DMS produced methane with average $\delta^{13}C$ and $\delta^{2}H$ values of –59.13‰ and –384.32‰, respectively. Samples receiving the addition of 10µM ^{2}H-labeled DMS produced methane with average $\delta^{13}C$ and $\delta^{2}H$ values of –55.80‰ and +117.06‰, respectively.

5.4 Discussion

Methane production has been observed in a wide variety of hypersaline environments ranging from laminated hypersaline microbial mats to areas with endolithic microbial mats (Bebout et al., 2004; Conrad et al., 1995; Hoehler et al., 2001; Kelley et al., 2012; King, 1988a; Oremland and King, 1989; Oremland et al., 1982; Potter et al., 2009; Sorensen et al., 2005). In this study, the discovery of bubbles with elevated methane concentrations of up to 30% in some locations was unexpected (Chapter 4). With the recent findings of methane and chloride deposits on Mars, hypersaline environments here on Earth provide an analogue experimental environment that can provide insight into the processes occurring on other planets. Because research on methane in hypersaline environments is limited, we set out to conduct an in-depth analysis of the utilization of carbon substrates for methane production. Our first goal was to provide evidence of current biologic methane production despite high sulfate concentrations. Second, we sought evidence of methane production in the sediments of endoevaporite sites. Third, we wanted to compare methane production in brine and extreme brine sites. Last, we wanted to provide evidence of methane production derived primarily from non-competitive substrates as opposed to acetate fermentation and CO_2 reduction.

5.4.1 Evidence of Current Biologic Methane Production

We found that methane production rates were relatively high over a range of salinities (from 55 ppt to 320 ppt) (Table 5.1; Table 5.2). In most environments, methanogens compete with sulfate reducing bacteria (SRB) for substrates, particularly hydrogen and acetate (Whitman et al., 2006). It is well documented that where sulfate concentrations are sufficiently high, as in our study sites, sulfate reduction will be a dominant process due to the higher affinity of sulfate

reducing bacteria with those competitive substrates acetate and hydrogen (Madigan and Martinko, 2006; McGenity, 2010). For our experiment, we used two methods to help provide evidence to confirm biogenicty of methane at our site. The first method was a comparison of methane production rates between unamended sediments collected from our sampling sites and sediments receiving a biocide to cease biologic activity. The second method was the isotopic analysis of methane produced from sediments enriched with 99% ^{13}C-labeled substrates (trimethylamine (TMA), monomethylamine (MMA), methanol (MeOH), acetate, and bicarbonate).

Methane Production Rates vs. Killed Control Rates. Methane production rates from unamended sediments ranged from 0.06 to 15.36 nmol g^{-1} d^{-1} for brine ponds with salinities ranging from 55 ppt to 130 ppt and 0.02 to 18.80 nmol g^{-1} d^{-1} for extreme brine ponds with salinities ranging from 180 ppt to 320 ppt (Table 5.1). In October 2009, sediments from GN Area 9 were incubated with 0.1 M NaOH in an effort to cease biologic production and to ensure that the rates and isotopic data obtained in our study were from present-day biogenic activity. Because methane isotope values obtained from the gypsum crusts were outside of the traditional biogenic range (Chapter 4) we wanted to insure that this methane was in fact being produced within the gypsum and not just degassing from the sediment below. To accomplish this we incubated crustal material with NaOH as we presumed that the use of such a high pH would be effective at stopping the growth of many microorganisms. This procedure was not entirely successful, however, although production rates were significantly reduced (Table 5.1). We presume that the reduction but not elimination of microbial methane production may be due to a higher tolerance of these halophilic microbes to high pH levels (Jones et al., 1998). In later experiments performed in January 2010 and August 2010 we switched to the use of a 5%

paraformaldehyde as an inhibitor and were more successful in ceasing biologic activity (Table 5.1). In comparing the lack of methane production from sediments amended with paraformaldehyde as an inhibitor of biologic activity to those incubated without an inhibitor it is reasonable to conclude that the production of methane observed in our sample site was from biologic activity (Table 5.1).

Production of ^{13}C-labeled Methane as an Indicator of Biogenicity. Isotopic analysis of methane produced from labeled incubation experiments is a second way to determine if production is occurring during an incubation experiment. Through the addition of labeled substrates one can determine if specific substrates are converted to methane gas via methanogenesis. During our incubation experiments, both labeled competitive and non-competitive substrates were used to monitor methane production. Figure 5.3 displays the comparison of methane production rates between the control samples that received no labeled substrate addition and those that did, in sediments from CAL Pond A23 sampled in January 2010. This figure is representative of what was observed at all sites sampled. The similarity in production rates between the control sediment and those amended with substrate provide evidence that the substrate additions were at tracer levels and did not stimulate methane production. Figures 5.4 to 5.10 display the isotopic comparison between sediments that were incubated with isotopically labeled competitive and non-competitive substrates. The incubations with labeled competitive substrates in these experiments resulted in methane isotopic signatures similar to the unamended control samples. As we previously showed in the killed control comparisons, methane produced in the control vials derived from current methanogenic activity. We can conclude that the methane produced in the incubation vials receiving competitive substrates was not from the labeled competitive pathways but was instead from current

methanogenic activity, since they have similar $\delta^{13}C\text{-}CH_4$ values to control samples. In the incubations receiving ^{13}C labeled non-competitive substrate there was a significant enrichment in $\delta^{13}C\text{-}CH_4$ in those samples, providing evidence that methane was produced and that this methane production was supported exclusively by those substrates.

5.4.2 Evidence of Methane Production in the Sediments of Endoevaporite Sites

One site in particular, GN Area 9, an extreme brine gypsum pond with salinities ranging from 180 ppt to 195 ppt, was the location where both the highest and lowest methane production rates were observed (Table 5.1; Figure 5.2). Due to significantly higher methane production in the gypsum crustal material (Table 5.1) we will discuss this site's methane production separate from the remaining sites. When comparing methane production within GN Area 9, we sought to determine if the methane observed was produced within the crustal material or if the methane production occurred within the sediment below the gypsum crust, with the subsequent gas then traveling upward, becoming trapped below/in the gypsum crust, where bubbles with upwards of 30% methane were observed (Chapter 4). In fact, our results indicated that methane production was higher in the crust relative to the sediments below the crust. We observed in the gypsum crust of GN Area 9 methane production rates of 18.80 nmol g^{-1} d^{-1} and only 0.02 nmol g^{-1} d^{-1} within the sediment underlying the gypsum crust and rubble (Table 5.1; Figure 5.2). One explanation for the greater production of methane in the gypsum crust as opposed to in the underlying sediment is the capping of the sediment from direct exposure to the overlying water by the gypsum crust. Such capping prevents the input of substrates and/or organic material. Within the gypsum crust there is apparent production of organic substrates from the production of organic matter by the photosynthetic communities. This relationship may seem contradictory

because methanogens have an extreme sensitivity to oxygen (Madigan and Martinko, 2006; Whitman et al., 2006), forcing them to be obligate anaerobes that are generally present only in anoxic environments (Madigan and Martinko, 2006; Whitman et al., 2006). However, rapid mineralization rates can lead to more favorable oxygen levels and high turnover of dead cells with the subsequent release of osmoregulatory solutes that are readily converted to methanogenic precursors (King, 1984; King, 1988a; King et al., 1983; Ollivier et al., 1994; Oremland and King, 1989; Oren, 1999b; Smith et al., 2008).

5.4.3 Methane Production as a Function of Salinity

Previous work on microbial mats obtained from our Area 4 brine pond revealed that methane production increased when the mat was subjected to lower salinity levels (Kelley et al., 2006; Smith et al., 2008). Our review of this work led us to hypothesize that the mats found in brine ponds with salinity ranging from 55 ppt to 130 ppt would have greater rates of methane production than endolithic algae mats found in extreme brine ponds with salinity ranging from 180 ppt to 320 ppt. In hypersaline environments, salinity levels play a key role in limiting the microbial community composition by affecting the osmotic pressure necessary for cell growth, the utilization of substrates due to high salinity, the limitations of photosynthesis, and decreases in cellular water activity (Lozupone and Knight, 2007; Madigan and Martinko, 2006; Oren, 2001).

To test this hypothesis, we analyzed methane production data in microbial-mat dominated brine ponds and endoevaporite-dominated extreme brine ponds. In our sites we observed the highest methane production rates (18.80 nmol g^{-1} d^{-1}) in crustal samples obtained from October 2009 samples from GN Area 9, one of our extreme brine ponds with salinity ranging from 180

ppt to 195 ppt (Table 5.1). The second- to fourth- highest methane production rates, however, were obtained from GN Area 1 (a soft mat located in a brine pond with salinity of 55 ppt) during both the March 2009 and October 2009 sampling trips (Table 5.1; Figure 5.2). We were unable to find a statistical difference in the overall methane production rates ($p > 0.3$, Student T-Test) of samples collected from our microbial-mat dominated brine sites (55 ppt to 130 ppt) and our endoevaporite-dominated extreme brine sites (180 ppt to 320 ppt).

One possible explanation for the insignificant difference in the methane production rates of our brine ponds and our extreme brine ponds was the methanogenic pathway utilized. As mentioned earlier, the very few substrates methanogens use for methane production can be divided into three groups: hydrogenotrophic methanogenesis, acetotrophic methanogenesis, methylatrophic methanogenesis (Madigan and Martinko, 2006; Whiticar, 1999; Whitman et al., 2006). At higher salinities, methanogens utilizing hydrogen and/or CO_2 become limited because of salinity-level tolerance, only allowing for methanogenesis to occur from methylated substrates (Oren, 1999b; Oren, 2001). In theory, higher methane production should have occurred in our lower-salinity brine sites because methanogens in lower-salinities can utilize more pathways for methane production (McGenity, 2010; Ollivier et al., 1994; Oren, 2001). However, we observed no significant difference in methane production between our brine and extreme brine sites.

Since the increase in salinity did not cause a decrease in methane production rates, we presumed that another factor must have been contributing to the similar methane production rates. One possible explanation was differences in the availability of substrates between the brine and extreme brine sites. The percent of particulate organic carbon was measured at all sites and was higher at the brine sites in comparison to the extreme brine sites, meaning that more substrates were available for methane production at the brine sites (Kelley et al., 2012). In

theory, in lower-salinity brine ponds methanogens should be capable of utilizing all competitive and non-competitive substrates because maximum salinity tolerance levels have not been met, however, the substrates may become more limited in the lower-salinity brine ponds due to the active presence of sulfate reducing bacteria.

Just as with methanogens, the energetic cost associated with SRB living in hypersaline environments is high. Sulfate reducing bacteria have been shown to grow at salinities of up to 250 ppt in the lab and 300 ppt in nature (Oren, 1999b). Growth at such high salinities requires adaptive measures to ensure osmotic balance, which in some cases costs energetically more than the energy received from the utilization of a substrate like acetate (Oren, 1999b). However, as salinity levels get lower the energetic costs associated with the environment decrease because osmotic balance is no longer needed and SRB and methanogens are more likely to compete for acetate and hydrogen as substrates because salinity levels are no longer a limiting factor for SRB (McGenity, 2010; Oren, 1999b; Oren, 2001).

Although POC was found to be higher in the brine ponds, in both sites there was presumably an abundant supply of non-competitive substrate precursors, which methanogens can utilize without competition from SRB. For example, one precursor, glycine betaine, an osmolyte used by organisms in hypersaline environments can be rapidly transformed to trimethylamine which provides a ready supply of non-competitive substrate for methanogens (King, 1984; King, 1988a; King et al., 1983; McGenity, 2010; Mitterer, 2010; Summons et al., 1998). Alternately, the bacterial-mediated breakdown of pectin in hypersaline environments that leads to the production of methanol (Ollivier et al., 1994) may provide an additional non-competitive substrate for utilization.

While the concentration of methylated substrates at our sites has not been quantified, Figures 5.4 to 5.10 show that the methanogens in our sites were capable of using those compounds, so we can conclude that these reactions are occurring *in situ* allowing for sufficient amount of non-competitive methylated substrate production. Some reports suggest that at salinity levels lower than those found in our study, sulfate reducing bacteria can in fact utilize some non-competitive substrates, notably methanol and methylamine (King et al., 1983). At our study sites, however, we did not see evidence for this is occurring because the analysis of $\delta^{13}C\text{-}CO_2$ from incubation vials receiving ^{13}C-labeled substrates did not reveal any enrichment (Appendix).

5.4.4 Evidence of Methane Production Occurring Primarily from Non-Competitive Substrates

We hypothesized that methane production in our sampling sites was derived primarily from non-competitive substrates as opposed to competitive substrates. To test this hypothesis we conducted labeled incubation studies. Isotopic analysis of methane produced from ^{13}C- or ^{2}H-labeled substrates during our incubations allowed us to determine which substrates were utilized by the microbes present in our samples. Typically, methane produced from CO_2 reduction ranges from ~ –110‰ to –60‰ and methane produced from acetate fermentation ranges from ~ –70‰ to –50‰ (Whiticar, 1999). While less is known about the isotopic composition of methane from non-competitive substrates, studies of methanogenic cultures suggest that methane produced from the use of methanol and methylamines would result in a more depleted $^{13}C\text{-}CH_4$ than from acetate or CO_2 (Krzycki et al., 1987; Londry et al., 2008; Summons et al., 1998).

^{13}C-labeled Incubations. Figure 5.3 refers to data from samples collected in CAL Pond A23 in January 2010. It displays the comparison of methane production rates in the control

samples that received no ^{13}C-labeled substrate addition and the treatment samples that did receive ^{13}C-labeled substrate additions. The similarity in production rates between the control site and the site that received labeled additions revealed that we were successful in not stimulating additional methane production from the tracer amounts of labeled substrates in our experiment. This is important because it allowed us to conclude that any incorporation of the substrate into methane production is directly related with the methanogenic community preference for that substrate rather than just because it is more readily available.

At most study sites, we found that the treatment samples receiving ^{13}C-labeled bicarbonate or ^{13}C-labeled acetate produced methane that did not exhibit a significant isotopic enrichment relative to controls. In fact, CAL Pond 15 (Figure 5.4) and CAL Pond A23 (Figure 5.5a), both sampled in January 2010, as well as GN Area 9 top mud (Figure 5.9a), sampled in March 2009, and GN Area 9 crust (Figure 5.10a), sampled in October 2009, were the only sites that displayed isotopic enrichment from ^{13}C-labeled bicarbonate or ^{13}C-labeled acetate. This enrichment on average was no greater than 8‰ from the control samples and was far less significant than the enrichment amount that were observed from similar concentration additions of ^{13}C-labeled methylamines and methanol, which averaged an increase of between +60‰ to +60,000‰ . In two other instances, CAL Pond A23 (Figure 5.5b), sampled in August 2010, and GN Area 4 (Figure5.8b), sampled in October 2009, methane produced from treatments receiving ^{13}C-labeled bicarbonate or acetate was slightly depleted in ^{13}C relative to unamended control samples.

Traditionally, the presence of high sulfate concentrations, as found in our sites, limits the use of competitive substrates (like acetate and hydrogen) by methanogens due to competition with SRB. An added limitation to the use of these competitive substrates by methanogens is

related to the salinity tolerance levels for methanogens capable of utilizing hydrogen and acetate and the low energy gained from the use of acetate for methanogenesis (McGenity, 2010; Oren, 2001). Either of these reasons could account for the limited to complete lack of incorporation of competitive substrates at our site.

One example of this phenomenon is illustrated in Figure 5.6b, which shows the isotopic analysis of GN Area 1 site 2 from March 2009. The isotopic ^{13}C methane signature for the control samples was –45.5‰ and the isotopic signature from those vials that received the competitive substrates ^{13}C-acetate and ^{13}C-bicarbonate were –44.5‰ and –44.5‰ respectively. This isotopic change was not statistically significant. We did reveal an enrichment in the ^{13}C-CO_2 isotopic values from these competitive substrate additions (Appendix), however, and this enrichment indicates that the ^{13}C-labeled substrate was utilized by sulfate reducers in our ponds and that methanogens were, in fact, being outcompeted for those substrates.

In the incubations that received ^{13}C-labeled methylamines and ^{13}C-labeled methanol, the methane produced was enriched in ^{13}C. Figure 5.6b represents data from all sites, except GN Area 4 (Figure 5.8a), regarding the isotopic composition of methane produced from ^{13}C-methanol and ^{13}C-methylamines. The ^{13}C-CH_4 isotopic signature for the control samples from GN Area 1 site 2 was -45.5‰. The isotopic signature from the vials receiving ^{13}C-methylamines and ^{13}C-methanol became more enriched in ^{13}C as the concentration of ^{13}C in the addition increased. These subsequent production of ^{13}C-CH_4 indicated that the methanogens at our sites were utilizing methylamines and methanol for the production of methane. This occurrence, which was observed in the majority of the sites, was not surprising because methanogensis that utilizes methylated amines or methanol as an energy source can function up to much higher salt

concentrations (McGenity, 2010; Oren, 1999b; Oren, 2001) without competition from SRB for substrates.

Figure 5.8a displays $\delta^{13}C\text{-}CH_4$ values from GN Area 4, which were collected in March 2009. During this sampling trip there was a marked difference in $\delta^{13}C$ values isotopic values observed (–75.4‰) in comparison to our October 2009 sampling trip illustrated in Figure 5.8b (–47.61‰). During the March 2009 visit to GN Area 4, there did not seem to be any significant incorporation of ^{13}C in the labeled substrate additions with the exception of 10µM MMA, which shifted to –46.3‰. We remain unsure of why there was such a significant shift in substrate utilization in that site during the different sampling trips.

^{2}H-labeled incubations. In the incubations that received ^{2}H-labeled DMS, the methane produced was enriched in ^{2}H, indicating utilization of that substrate, although the overall methane production rates with added DMS in most sites were lower than unamended control sediments rates (Table 5.2). Importantly, the addition of three concentrations of ^{2}H-labeled DMS to our samples did not stimulate additional methane production when compared to control samples. This result showed that the utilization of DMS in our incubations was similar to what occurs *in situ*. We did notice, however, a decrease in methane production from samples from GN Area 9 (Table 5.2). Although the decrease in production rates is perplexing because of the relatively low concentrations added, it is possible that the concentration of DMS added could have been too high and proved toxic to the methanogens present (Oremland personal communication).

We did observe some isotopic differences between ^{2}H-labeled DMS treatment groups and unamended control samples. We were able to show that methanogens in all locations sampled had the capacity to utilize DMS in the production of methane, as depicted in the $\delta^{2}H\text{-}CH_4$ data

presented in Table 5.2. Of all the sites that displayed ^{2}H-enrichment, GN Area 9 rubble contained the samples with the most enriched ^{2}H-methane from all concentrations of ^{2}H-labeled DMS added. This ^{2}H-enrichment was perplexing because samples from GN Area 9 rubble (which had received ^{2}H-labeled DMS), all represented the same site and showed the greatest reduction in methane production from the addition of the^{2}H-labeled DMS substrates. Production rates fell from 3.53 nmol g^{-1} d^{-1} for unamended control samples to 0.65 nmol g^{-1} d^{-1} on average for samples receiving ^{2}H-labeled substrate, although the methane subsequently produced was significantly more enriched than at any other site receiving the same concentration amounts. A possible explanation for our findings is that although all locations contained methanogens capable of utilizing DMS as a substrate for methane production, the enrichment in ^{2}H at all sites, suggests a difference in the methanogenic community in GN Area 9.

Another salient observation was a significant difference in the isotopic shift in δ^{13}C-CH_4 in the controls and all concentrations of the treatment groups from GN Area 9 rubble and between the controls and only the 1μM, and 10μM ^{2}H-labeled DMS additions from GN Area 9 crust (Table 5.2). This shift was unexpected, especially since methane production in these treatment samples was significantly lower than what was observed in the controls. One possible explanation for this shift is that the slower rates of methane production have caused more fractionation of the methane produced. Finally, although an isotopic shift was observed in the ^{13}C from GN Areas 1 and 4, however it was not statistically significant.

5.5 Conclusion

Our goal was to provide an in-depth analysis of the utilization of carbon substrates for methane production in hypersaline environments. From the analysis of sediment samples and

gypsum crust we have shown that biogenic methane production occurred in our hypersaline locations. A comparative analysis of methane production in the endoevaporite site of GN Area 9 provided evidence of methane production within the gypsum crust and not within the sediments underlying the crust. The statistical analysis of the pond system as a whole based on salinity, revealed no significant difference in the production of methane from brine and extreme brine locations. Isotopic analysis of the methane produced indicated that non-competitive substrates like methanol, methylamine, and dimethylsulfide were preferred by methanogens over the competitive substrates acetate and bicarbonate. We concluded that the competition between methanogens and sulfate reducing bacteria as well as environmental conditions experienced in hypersaline environments has lead to the utilization of alternative substrates for methane production by methanogens.

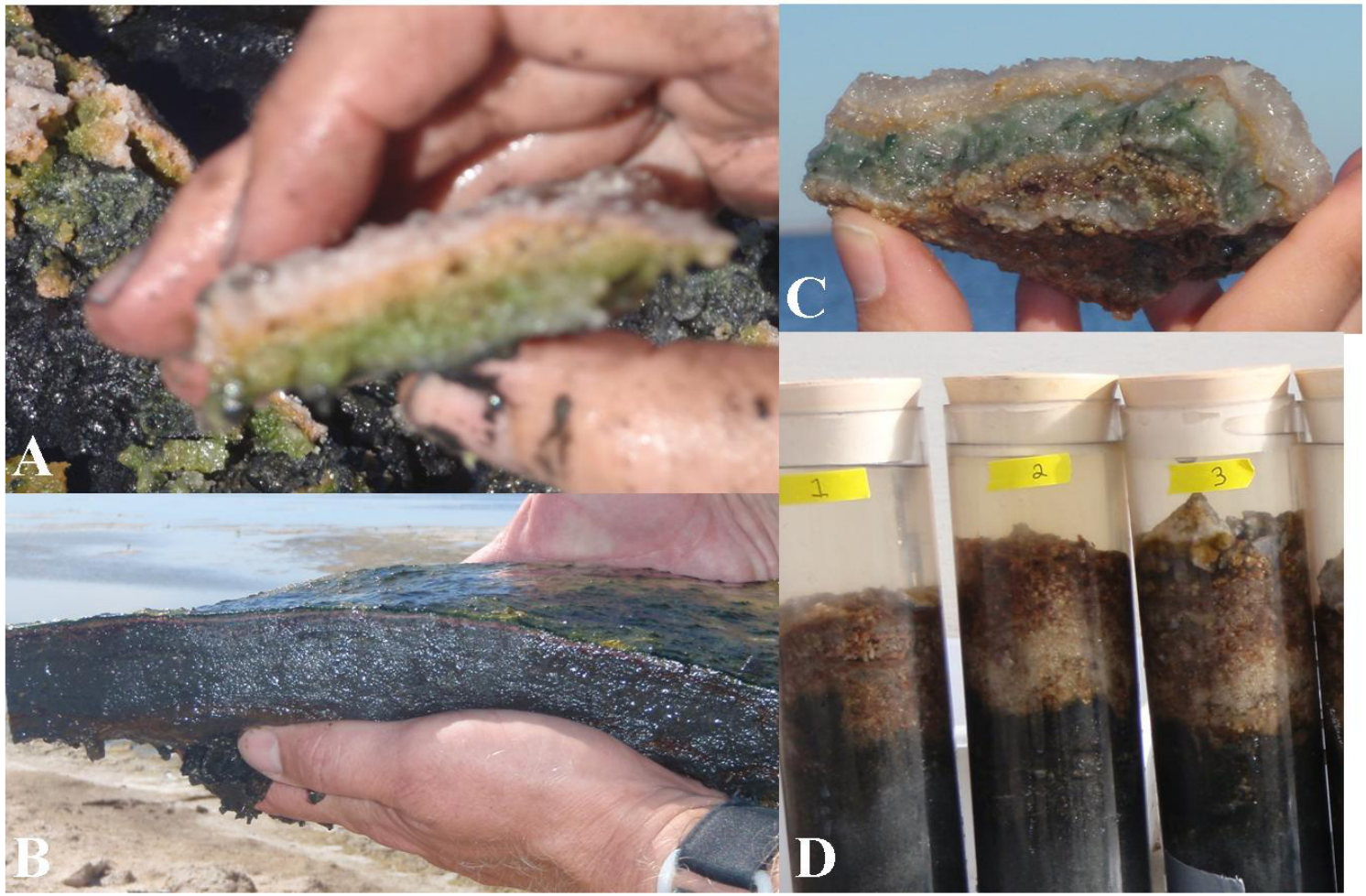

*Figure 5.1. Picture (**A**) CAL pond 23, picture (**B**) GN Area 4, picture (**C**) GN Area 9 gypsum crust, picture (**D**) GN Area 9 core with all layers.*

Table 5.1. Temperature, salinity, methane production rates in incubation samples, methane isotopic carbon values methane produced within incubation vials, and $\delta^{13}C$-CO_2 values for production within incubation vials. Error estimates (standard deviations) presented in parentheses. Values that were not determined are depicted in the table as n.d.

Site	Date	Temp (°C)	Salinity (ppt)	Incubation days	Methane production in control (nmol g-1 d-1)	Methane production in killed control (nmol g-1 d-1)	Incubation δ13C-CH4 (‰)	Incubations δ13C-CO2 (‰)	Incubation δ2H (‰)
Don Edwards									
Pond 15	January 2010	12	126	6	0.71 (0.04)	0.00 (0.01)	-62.85 (0.28)	n.d.	n.d.
	August 2010	14	115	36	0.06 (0.01)	n.d.	-64.30	n.d.	n.d.
Pond 23	January 2010	24	320	7	0.20 (0.06)	0.05 (0.03)	-41.51 (0.95)	n.d.	n.d.
	August 2010	40	275	34	1.53 (0.07)	0.00 (0.00)	-44.50 (1.10)	n.d.	n.d.
Guerrero Negro									
Area 1 site 1	March 2009	23	55	7	13.50 (2.14)	n.d.	-51.89 (1.57)	-15.31 (1.08)	-307.63 (1.29)
Area 1 site 2	March 2009	23	55	7	15.36 (3.5)	n.d.	-45.56 (0.48)	-16.50 (2.61)	-291.59 (13.65)
Area 1	October 2009	31	55	8	14.52 (5.30)	n.d.	-48.07 (3.41)	-14.54 (1.00)	-344.06
Area 4	March 2009	19	93	17	3.40 (0.37)	n.d.	-75.37 (7.45)	cryo?	-397.20 (24.31)
Area 4	October 2009	25	84	25	2.96 (1.41)	n.d.	-47.61 (2.82)	-17.89 (0.55)	-388.62 (12.18)
Area 9 crust	October 2009	25	192	8	18.80 (1.13)	1.07 (1.07)	-36.18 (2.82)	-18.08 (0.18)	-336.75
Area 9 rubble	March 2009	22	184	20-30	3.91 (0.40)	n.d.	-33.50	n.d.	-342.37 (10.93)
Area 9 rubble	October 2009	25	192	26	3.53 (1.11)	0.08 (0.02)	-33.08 (0.58)	-19.28 (0.34)	-345.88
Area 9 top mud	March 2009	22	184	30	0.194 (0.05)	n.d.	-40.88 (1.58)	n.d.	-239.91 (51.78)
Area 9 deep sediment	March 2009	22	184	30	0.02 (0.01)	n.d.	-49.95 (1.64)	n.d.	n.d.

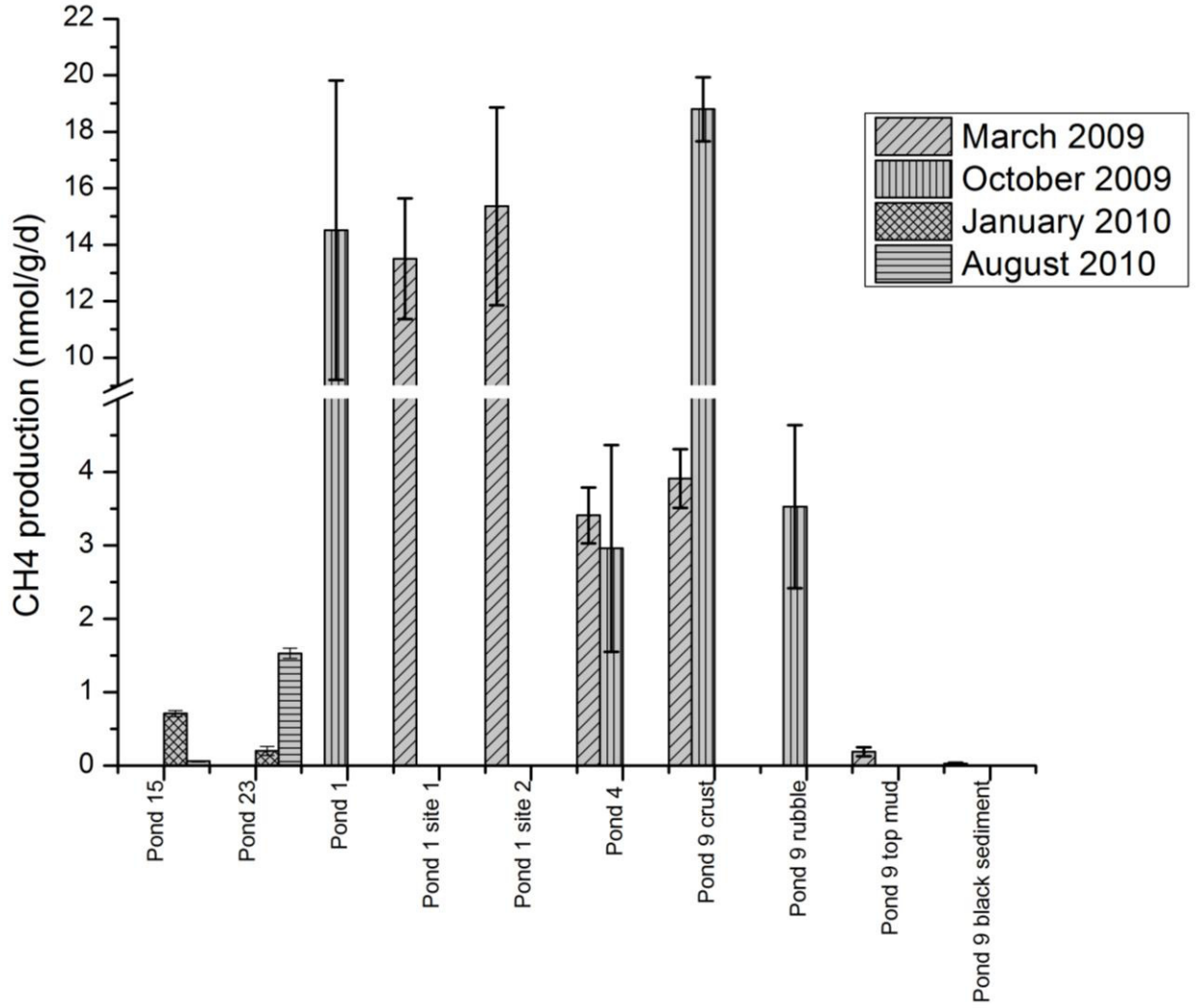

Figure 5.2. Methane production rates from sites in Don Edwards National Wildlife Refuge and Guerrero Negro.

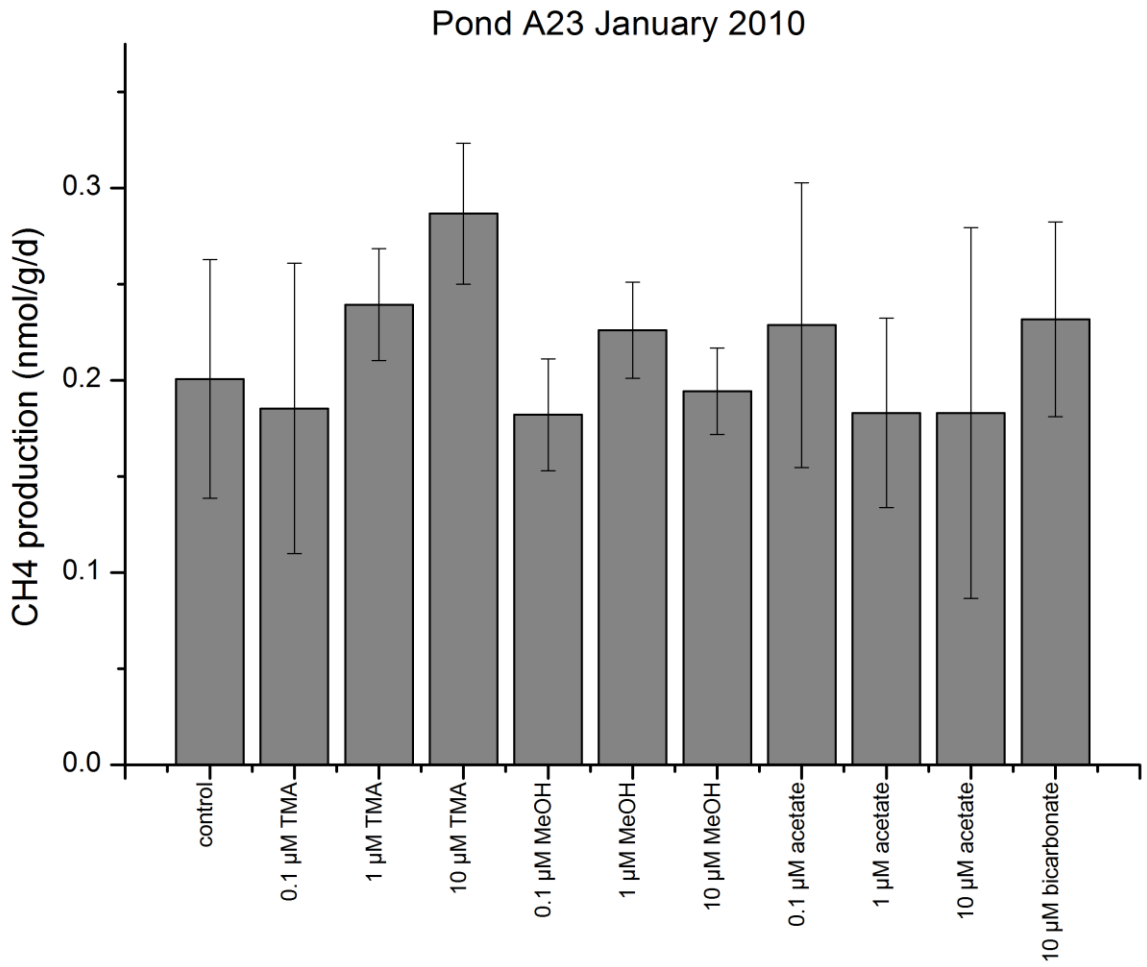

Figure 5.3. Methane production measurements from the gypsum crust of CAL Pond 23, sampled in January 2010. Other incubations produced similar results with added substrates having similar production rates as the controls (Appendix).

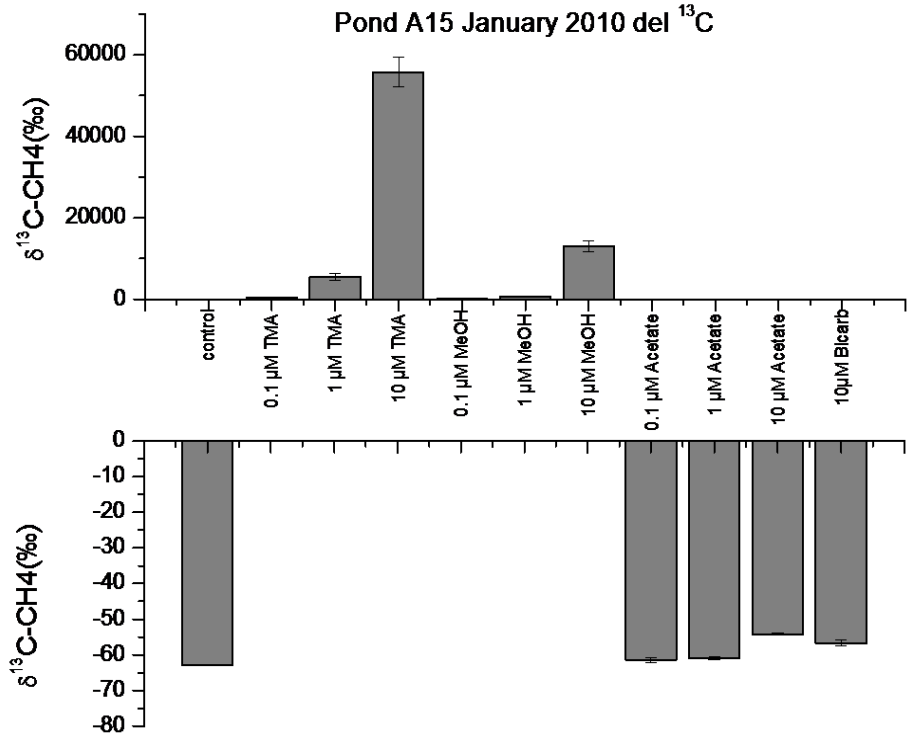

Figure 5.4. Isotopic composition of methane produced from incubation samples from CAL Pond 15 collected in January 2010. Addition of ^{13}C-labeled noncompetitive substrates resulted in the production of ^{13}C-labeled methane, while ^{13}C-labeled competitive substrates did not result in the production of ^{13}C-labeled methane.

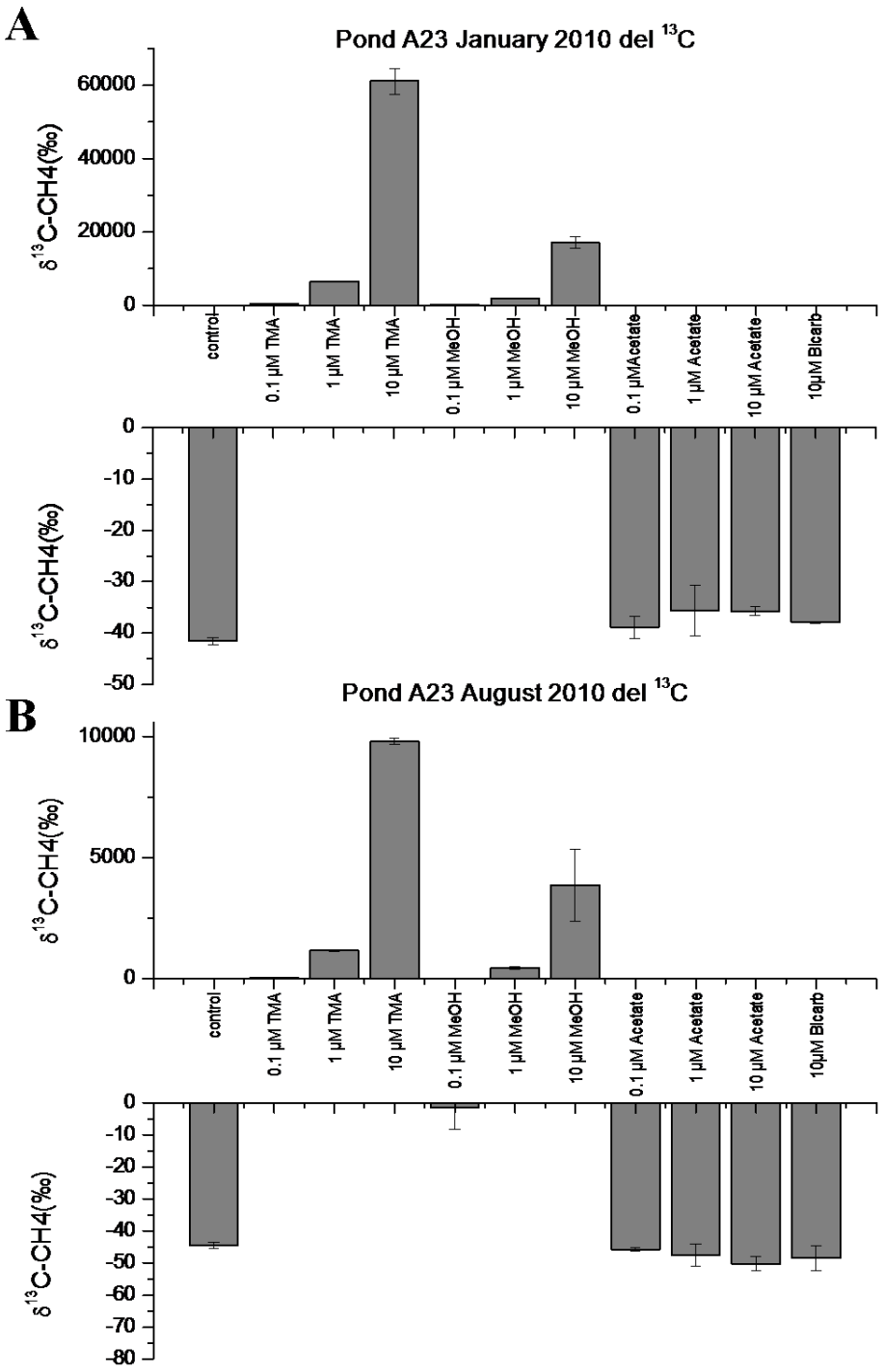

Figure 5.5. Isotopic composition of methane produced from incubation samples from CAL Pond 23 collected in January 2010 (A) and August 2010 (B). Addition of ^{13}C-labeled noncompetitive substrates resulted in the production of ^{13}C-labeled methane, while addition of ^{13}C-labeled competitive substrates did not result in production of ^{13}C-labeled methane.

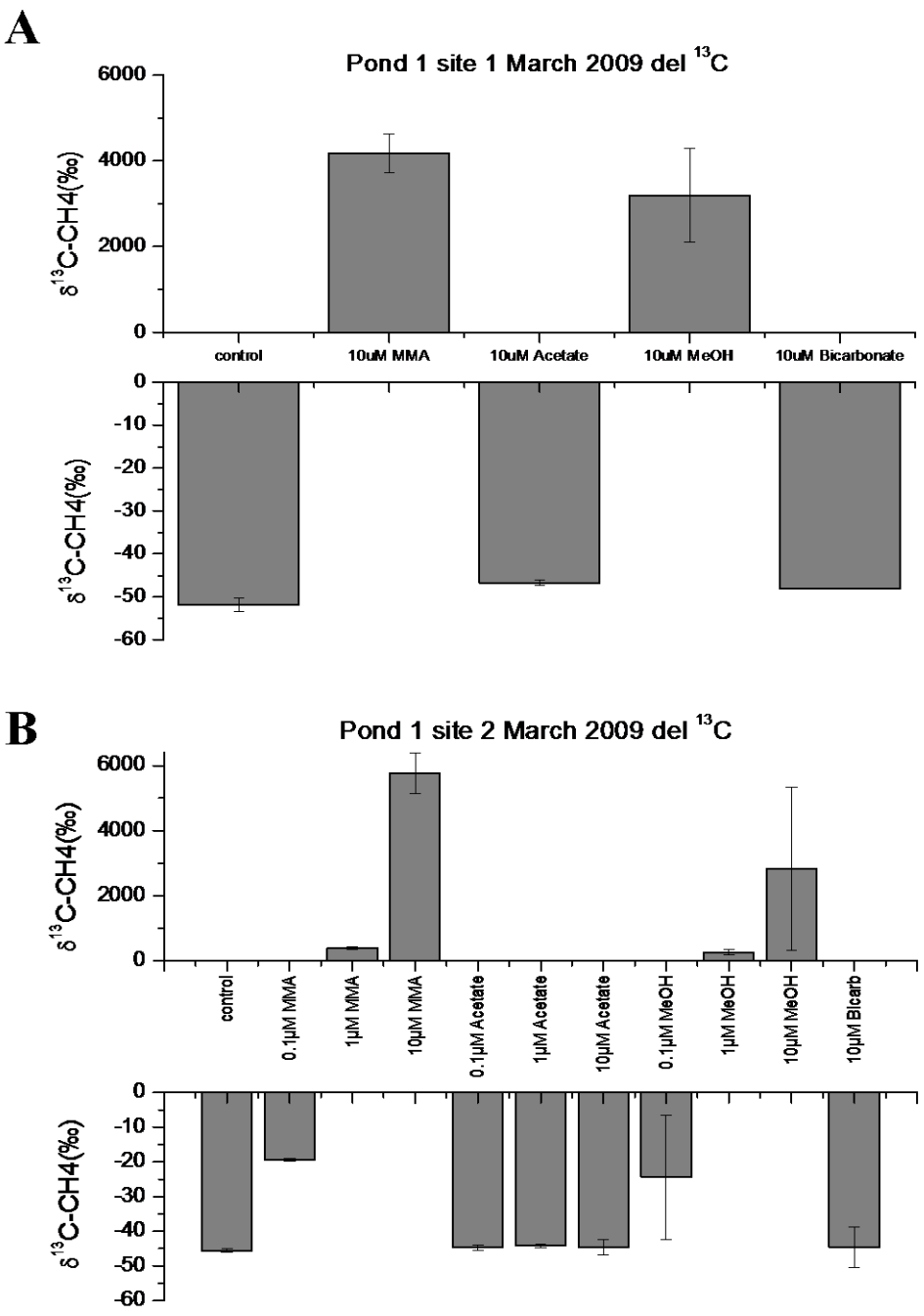

Figure 5.6. Isotopic composition of methane produced from incubation samples from GN Area 1 site 1 (A) and GN Area 1 site 2 (B) collected in March 2009. Addition of ^{13}C-labeled competitive substrates did not result in the production of ^{13}C-labeled methane, while the addition of ^{13}C-labeled noncompetitive substrates resulted in the production of ^{13}C-labeled methane.

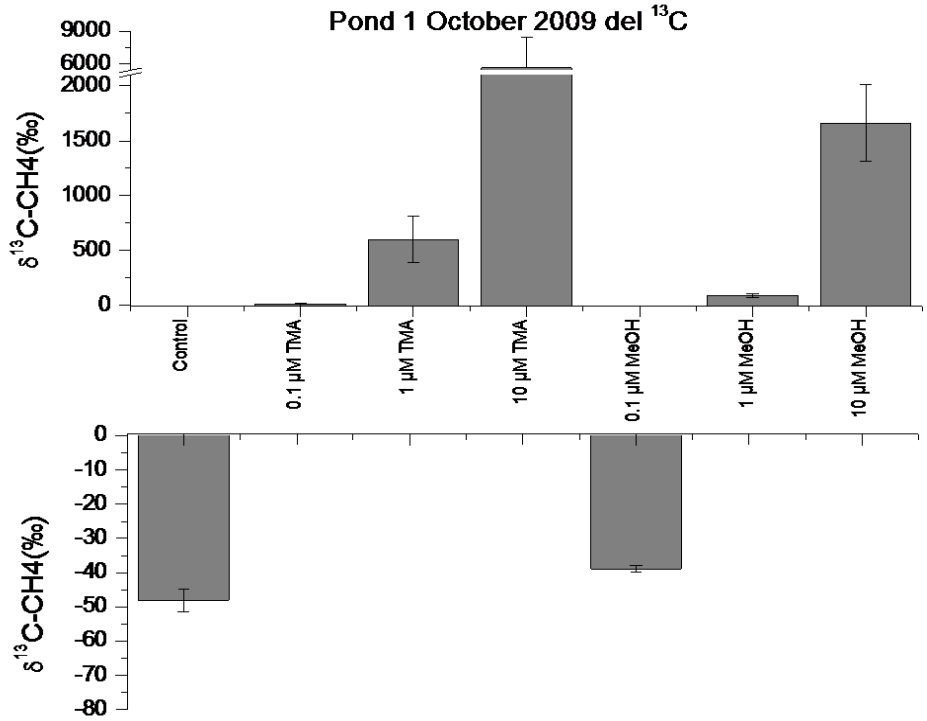

Figure 5.7. Isotopic composition of methane produced from incubation samples from GN Pond 1 collected in October 2009. Addition of ^{13}C-labeled noncompetitive substrates did result in the production of ^{13}C-labeled methane

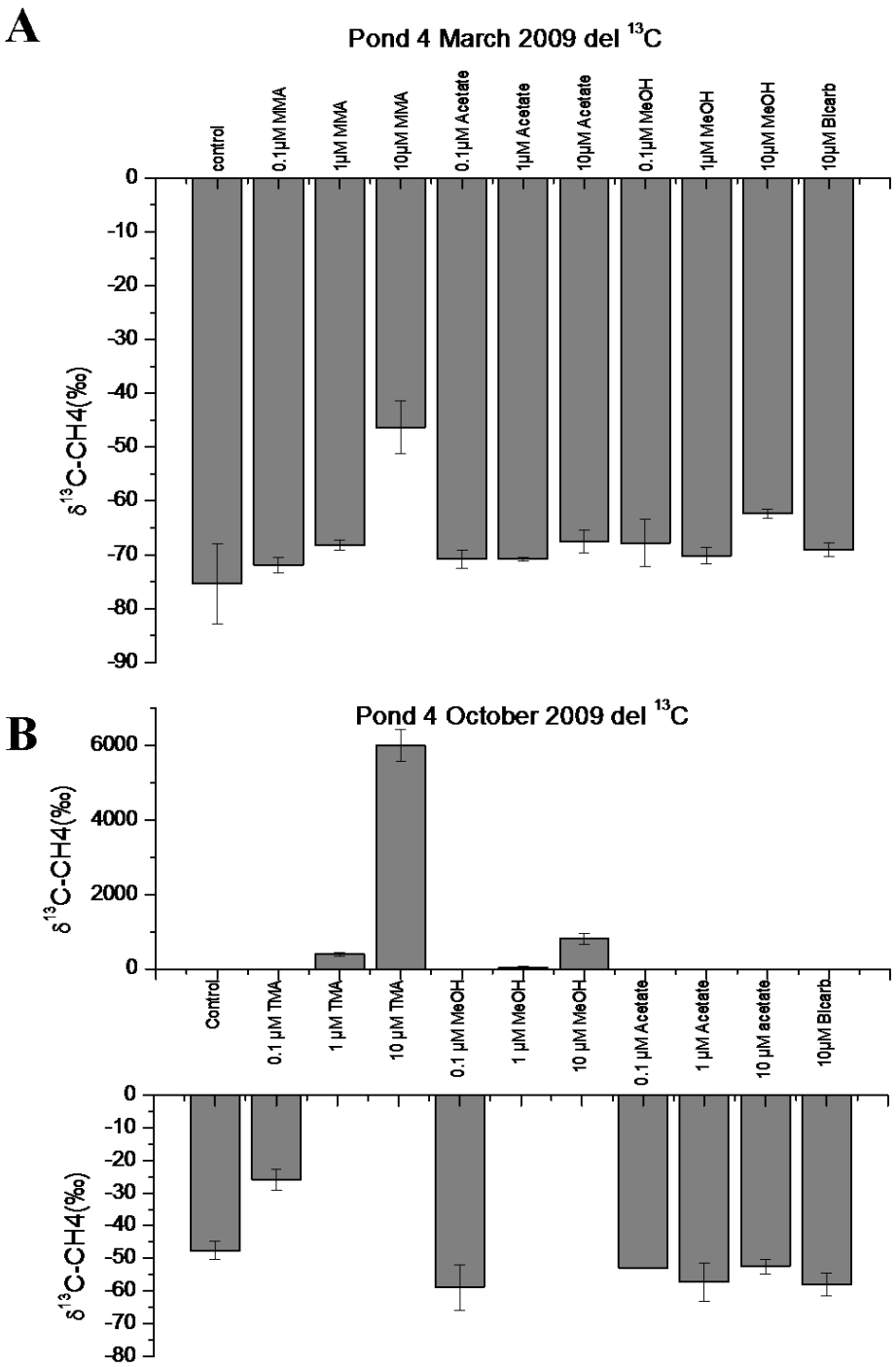

Figure 5.8. Isotopic composition of methane produced from incubation samples from GN Area 4 collected in March 2009 (A) and October 2009 (B). ***A****. Addition of ^{13}C-labeled competitive or noncompetitive substrates did not result in the production of ^{13}C-labeled methane.* ***B****. Addition of ^{13}C-labeled noncompetitive substrates resulted in the production of ^{13}C-labeled methane, while the addition of ^{13}C-labeled competitive substrates did not result in ^{13}C-labeled methane.*

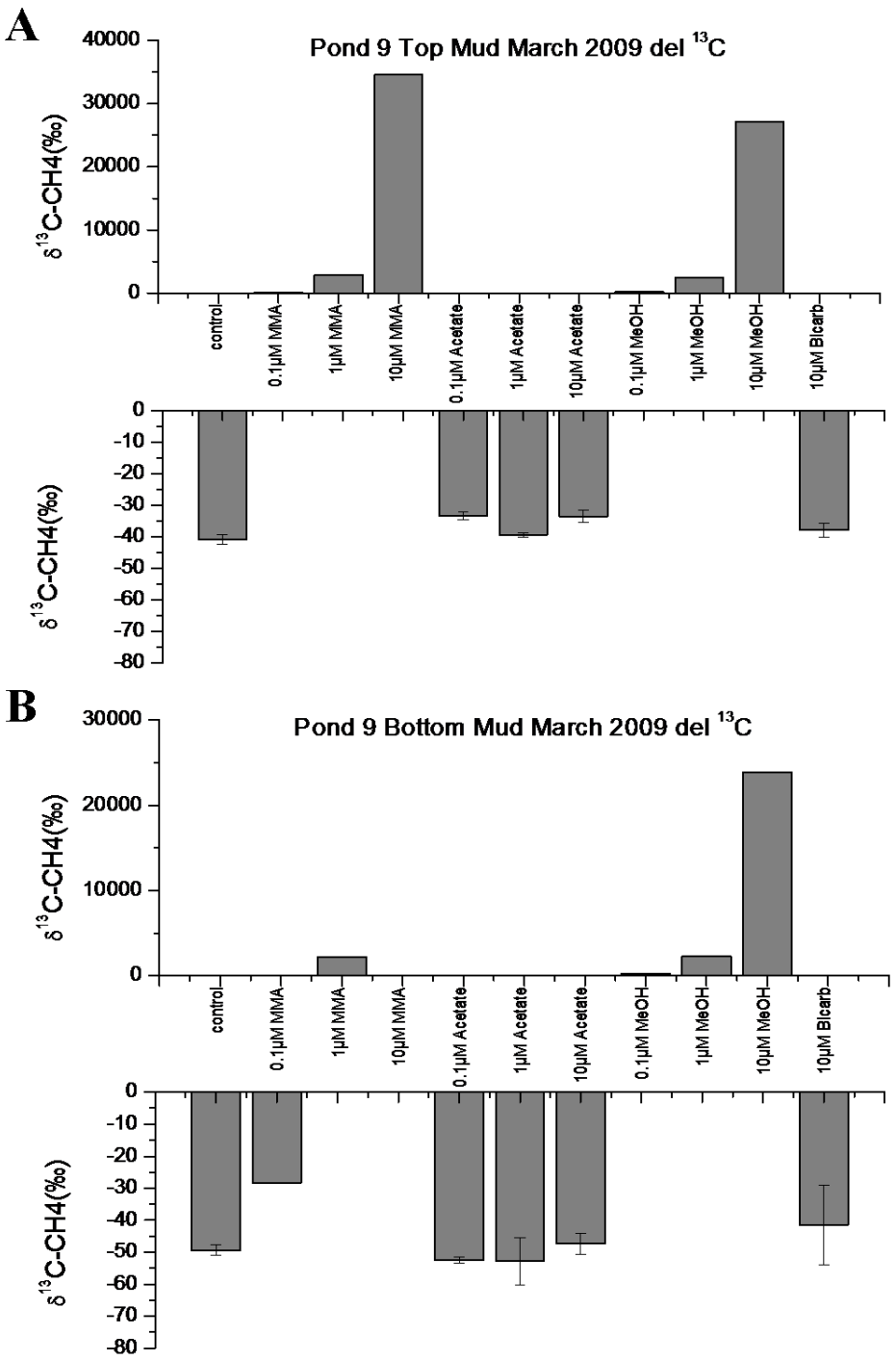

Figure 5.9. Isotopic composition of methane produced from incubation samples from GN Area 9 top mud ***(A)*** *and bottom mud* ***(B)*** *collected in March 2009. Addition of ^{13}C-labeled noncompetitive substrates resulted in the production of ^{13}C-labeled methane, while ^{13}C-labeled competitive substrates did not result in the production of ^{13}C-labeled methane.*

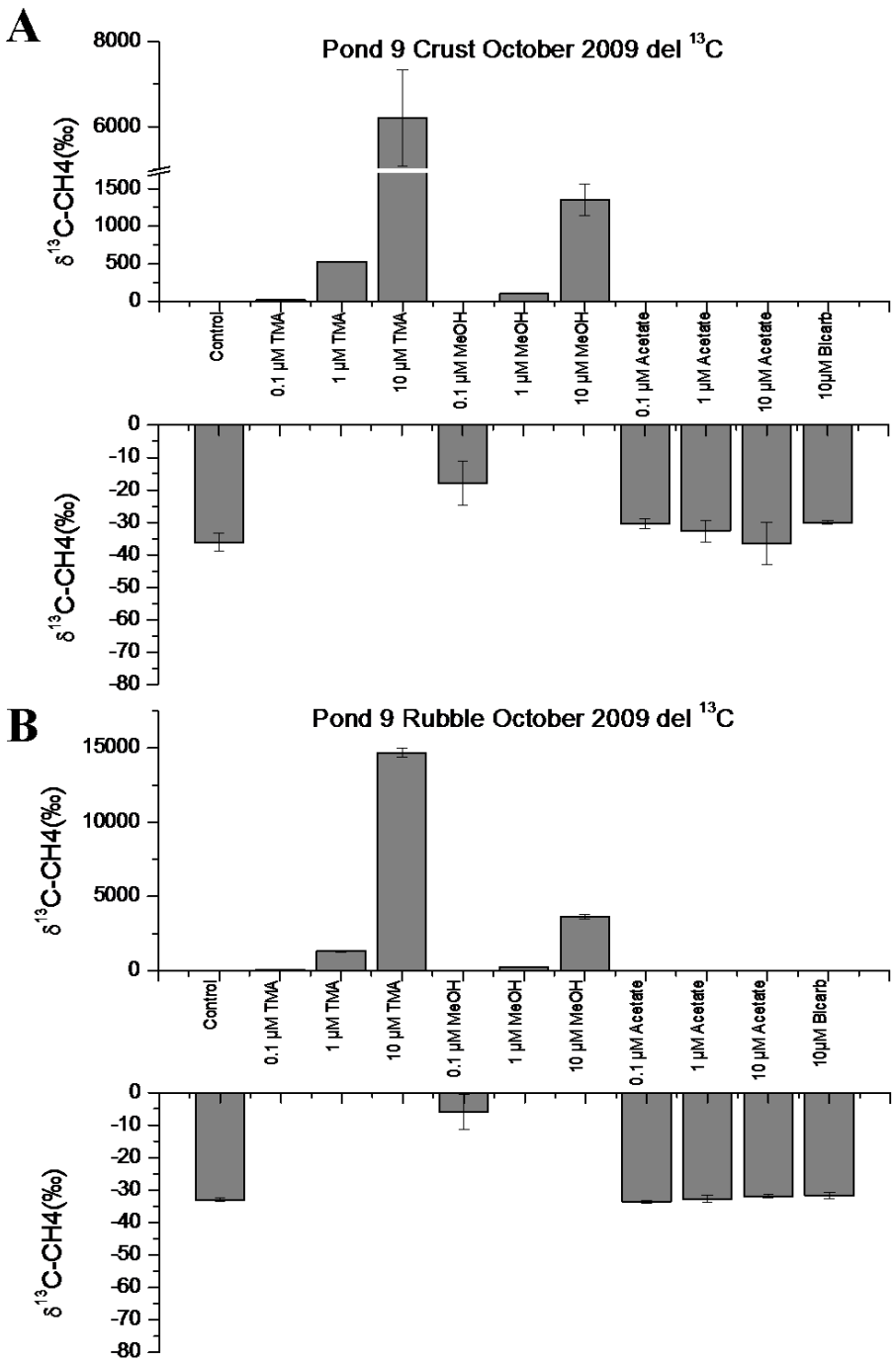

Figure 5.10. Isotopic composition of methane produced from incubation samples from GN Area 9 crust ***(A)*** *and rubble* ***(B)*** *collected in October 2009. Addition of ^{13}C-labeled noncompetitive substrates resulted in the production of ^{13}C-labeled methane, while ^{13}C-labeled competitive substrates did not result in the production of ^{13}C-labeled methane.*

Table 5.2. Salinity, methane production rate, methane isotopic carbon values, carbon dioxide isotopic values, deuterium isotopic values for incubations receiving deuterium labeled DMS. Error estimates (standard deviations) presented in parentheses. Values that were unable to be determined are depicted in the table as n.d.

Site	Date	Substrate	Salinity (ppt)	Incubation days	Methane production (nmol g-1 d-1)	Incubations δ13C-CH4 (‰)	Incubations δ13C-CO2 (‰)	Incubations δ2H (‰)
Guerrero Negro								
Area 1	October 2009	control	55	8	14.52 (5.30)	-48.07 (3.41)	-14.54 (1.00)	-323.34
		0.1µM DMS	55	8	27.59 (10.86)	-52.05 (5.15)	-17.86 (5.89)	-269.58
		1µM DMS	55	8	16.31 (0.74)	-52.86 (1.34)	-25.02 (14.80)	-269.56
		10µM DMS	55	8	23.51 (11.97)	-50.36 (6.94)	-24.01 (17.13)	1010.04
Area 4	October 2009	control	84	25	2.96 (1.41)	-47.61 (2.82)	-17.89 (0.55)	-388.62 (12.18)
		0.1µM DMS	84	25	1.68 (0.08)	-53.47 (1.37)	n.d.	-391.11
		1µM DMS	84	25	1.25 (0.09)	-59.13 (6.81)	n.d.	-384.32
		10µM DMS	84	25	1.51 (0.31)	-55.80 (4.95)	n.d.	117.06
Area 9 crust	October 2009	control	192	8	18.80 (1.13)	-36.18 (2.82)	-18.08 (0.18)	-336.75
		0.1µM DMS	192	8	4.90 (0.51)	-42.23 (1.06)	-19.21 (0.59)	-218.81
		1µM DMS	192	8	4.72 (0.70)	-44.77 (4.20)	-18.98 (1.02)	-151.24
		10µM DMS	192	8	5.84 (0.74)	-42.40 (0.66)	-19.08 (0.79)	483.11
Area 9 rubble	October 2009	control	192	26	3.53 (1.11)	-33.08 (0.58)	-19.28 (0.34)	-345.88
		0.1µM DMS	192	26	0.67 (0.29)	-37.76 (2.70)	n.d.	147.03
		1µM DMS	192	26	0.67 (0.11)	-39.17 (1.81)	n.d.	3176.71
		10µM DMS	192	26	0.65 (0.03)	-39.91 (0.31)	n.d.	30271.63

CHAPTER SIX

METHANE PRODUCTION AND ISOTOPIC ANALYSIS FROM HYPERSALINE MICROBIAL MAT INCUBATIONS WHEN SULFATE REDUCTION IS INHIBITED

6.1 Introduction

The formation of methane is often the direct result of the biodegradation of organic matter and can occur in terrestrial, lacustrine, and marine environments. Methanogenesis is the last step in the remineralization of complex organic matter in anaerobic systems (Kiene, 1991; Oremland and King, 1989; Reeburgh, 2007). This organic matter degradation involves a sequence of reactions in which complex organic matter is hydrolyzed to monomers and these are fermented to H_2, low-molecular weight fatty acids, alcohols, and methylated compounds (Formolo, 2010).

Methanogens require simple molecules as substrates and are dependent on the activities of other microorganisms to provide these substrates. Growth substrates for methanogens include a variety of compounds including carbon dioxide and hydrogen, formate, acetate, methanol, ethanol, ethylated sulfur compounds, and methylated amines (Canfield et al., 2005; King et al., 1983; Madigan and Martinko, 2006; Oremland and King, 1989; Oremland et al., 1987). While a variety of compounds may be utilized as substrates during methanogenesis, the majority of natural environments do not contain sufficient concentrations of these compounds to maintain methanogenesis. Globally, the most important substrates are $CO_2 + H_2$ and acetate. The principal biologically mediated reactions for methanogens are as follows:

$$CH_3COO^- + H_2O \rightarrow CH_4 + HCO_3^- \quad (1)$$

$$CO_2 + 4H_2 \rightarrow CH_4 + 2H_2O \quad (2)$$

Both pathways can occur in marine and freshwater systems however acetate fermentation (Equation 1) dominates in freshwater sediments while CO_2-reduction (Equation 2) dominates in marine sediments (Burdige, 2006; Reeburgh, 2007; Whiticar, 1999; Whiticar et al., 1986).

The active pathway for methanogenesis is controlled by the presence or absence of sulfate. In marine environments, in the presence of excess sulfate, sulfate reducing bacteria (SRB) outcompete methanogens for the common substrates hydrogen and acetate, since they have a lower affinity and higher threshold (Burdige, 2006; Kristjansson and Schönheit, 1983; Muyzer and Stams, 2008). This can be expressed by comparing the ΔG of both methanogens and sulfate reducers utilizing both substrates (Muyzer and Stams, 2008; Whitman et al., 2006) (Chapter 1 Table 1.1). Thermodynamic energy yield from the oxidation of organic matter coupled to various electron acceptors decreases in the order of $O_2 > NO_3^- > Mn(IV) > Fe(III) > SO_4^{2-} > CO_2$ and these electrons are utilized in the above sequence (Reeburgh, 2007). Results from anoxic sediments indicate that methanogenesis does not occur until sulfate is nearly exhausted and sulfate reduction rates decrease (Burdige, 2006; Reeburgh, 2007). This is not only due to the energy yield constraints presented above but also because SRB are very effective in their uptake of H_2 and acetate and are capable of maintaining H_2 and acetate at concentrations too low for methanogens to function (Reeburgh, 2007).

Despite the thermodynamics and kinetic arguments presented, methane production can occur in systems involving sulfate reduction (Kiene, 1991; Oremland and King, 1989; Reeburgh, 2007; Whiticar, 1999). This methane production occurs through the use of non-competitive substrates like methanol, methylated amines, and dimethylsulfide. The use of these non-

competitive substrates is thought to be of great importance in all hypersaline environments (Oremland et al., 1982) and have been measured in the locations sampled for this research (more details in Chapter 5).

In an effort to better understand the methanogen community in hypersaline environments, we have conducted a series of systematic substrate additions. We previously conducted incubation experiments where sediments and crustal material were amended with competitive and non-competitive substrates and evolved methane was monitored and analyzed isotopically (more detail in Chapter 5). Methane production rates in our microbial mats and gypsum crusts were higher in vials amended with non-competitive substrates, while in vials amended with competitive substrates methane production rates did not increase in comparison to the unamended controls (Chapter 5). Although methanogens at our sampling site are capable of utilizing non-competitive substrates for the production of methane (Kelley et al., 2012), we were still interested in methanogen use of traditional competitive substrates. Previous work performed at one of our sampling sites noted an increase in methane production when sulfate reducing bacteria were inhibited (Smith et al., 2008). In the Smith et al. 2008 study, the researchers conducted a small incubation analysis with molybdate, a specific inhibitor of SRB and determined that methane production increased in their samples. They concluded that the low methane production in the unamended samples could be due to competition between methanogens and SRB. We concluded from our previous experiments that methanogens in our hypersaline sites are utilizing non-competitive substrates for methane production and we hypothesized that the same competition seen in the Smith et al study is occurring at our site causing competition for substrates between methanogens and sulfate reducing bacteria.

The goal of this research is to analyze the effects sulfate reducing bacteria have on methane production in hypersaline environments. We hypothesize that methane production rates will be lower in sediments with active sulfate reducing bacteria communities. We also hypothesize that in sediments where sulfate reducing bacteria are not active, methane production will proceed through the use of competitive substrates, acetate and bicarbonate, because competition is no longer a factor.

To test these hypotheses we needed to create *in situ* like conditions while inhibiting sulfate reduction. We chose to inhibit sulfate reduction by amending the sediments with molybdate. Molybdate as an inhibitor of sulfate metabolism is well established (Banat et al., 1983; Biswas et al., 2009; Fukui et al., 1997; Lovley et al., 1982; Lovley and Goodwin, 1988; Oremland and Taylor, 1978; Oren et al., 2009; Peck, 1959; Smith and Klug, 1981; Sørensen et al., 1981). Molybdate is said to uncouple the energy metabolism of sulfate reducing bacteria at the level of ATP sulfurylase, the first enzyme in sulfate activation (Biswas et al., 2009; Peck, 1959), allowing for the production of hydrogen but preventing the coupling of hydrogen to sulfur. Previous studies have shown that when sediments with active sulfate reducing bacteria populations are amended with molybdate, sulfate reduction rates cease (Banat et al., 1983; Lovley et al., 1982; Lovley and Goodwin, 1988; Oremland and Taylor, 1978; Oren et al., 2009; Peck, 1959; Smith and Klug, 1981; Sørensen et al., 1981). In sediments where active competition between sulfate reducing bacteria and methanogens are occurring, the addition of molybdate causes a cease in sulfate reduction allowing for an increase in methane production, because of two reasons. First, because of the inhibition of sulfate reducing bacteria, methanogens are now free to utilize H_2 and acetate for methane production; and second, in instances where anaerobic methane oxidation is occurring, methane is no longer being oxidized in sediments because

sulfate reducing bacteria are inhibited. In our site, we have concluded that methane oxidation is not occurring (Chapter 4) and so this research will focus on molybdate inhibition allowing for more substrate utilization.

6.2 Methods

6.2.1 Site Description

Sampling for this work was performed in two regions Northern California, USA and Baja California, Mexico, from 2009-2012. Northern California sampling sites (CAL) were within the Don Edwards National Wildlife Refuge, located in southern San Francisco Bay. CAL Pond 15 (~120 ppt) and CAL Pond A23 (~300 ppt) from the refuge were sampled in January 2010 and August 2010. CAL Pond 15 consisted of soft microbial mat while CAL Pond A23 consisted of gypsum encrusted microbial mat (more details in Chapter 2). Baja California sampling was conducted in Exportadora de Sal, one of the world's largest solar salt production sites located in the city of Guerrero Negro (GN), Mexico. These salterns GN Area 1 (~55 ppt), GN Area 4 (~84 ppt) and GN Area 9 (~190 ppt) were sampled in October 2009. GN Area 1 was sampled again in March and October 2012. GN Area 1 and 4 consist of soft microbial mat while GN Area 9 consists of gypsum encrusted microbial mat (more details in Chapter 2).

6.2.2 Incubations

Methane production rates from soft mat and crust sediment samples were determined from incubations of slurries in serum vials. Soft microbial mats were collected from CAL Pond 15 and from GN Area 1 and 4. Mat samples from CAL Pond 15 were collected by traditional

short coring methods while samples from GN Area 1 and 4 were cut and removed from the bottom of the ponds and placed into tight fitting plastic trays (detailed description in Chapter 3). Endoevaporitic crust and sediment were collected from CAL Pond A23 and GN Area 9. Endoevaporitic crust and sediment from CAL Pond A23 was collected by short cores of crust and sediments while GN Area 9 was subsampled into the top gypsum crust and underlying gypsum rubble (detailed description in Chapter 3). The crust and rubble were broken into small pieces before incubating. In addition, overlying water used for our incubations was also obtained from each site. Salinity of the overlying water was determined with a hand-held refractometer (Table 6.1).

The amount of sediment used for each incubation vial varied slightly with most samples containing between 10-20 g of sediment. Vials were prepared by placing samples from the various sites in 38 mL glass serum vials with 10 mL of corresponding deoxygenated (N_2-purged) site water to make the slurries. To determine the effects sulfate reducing bacteria have on methane production, molybdate was added to incubations of soft microbial mats and endoevaporite crust and the evolved methane was monitored. The molybdate was added as a final concentration of 50 mM in the slurry. To determine the effects of competitive substrate utilization when sulfate reducing bacteria were inhibited, additional competitive substrates, acetate and bicarbonate, were added to sediment vials treated with molybdate and the evolved methane was monitored.

Once the vials were filled with sediment, site water, and respective substrate (or no substrate for control), they were capped with blue butyl rubber stoppers (Bellco Glass Co.), and the headspace was flushed for 5 minutes with nitrogen gas to remove any oxygen gas returning

the sediment to an anoxic state. The vials were allowed to equilibrate for 24 hours prior to the first extraction of headspace.

6.2.3 Methane Production and Isotope Analysis

Methane concentration in the headspace was monitored on a Shimadzu Mini-II Gas Chromatograph (GC) through time to obtain the production rate. Approximately 250µl of headspace from all samples were injected directly into the GC (more detail available in Chapter 3.2.4). Sample areas were converted to concentrations (in parts per million, ppm) by:

$$CH_4\ (ppm) = \frac{(Standard\ ppm\ \times Sample\ area)}{Standard\ area}$$

where standard ppm is the know concentration of the gas standard, sample area is the integrated area of the sample, and standard area is the integrated area of the standard.

The isotopic composition of the evolved methane was measured after incubating. The stable isotopic composition of the evolved methane from the incubations was determined by using a GC interfaced with a Finnegan Delta Plus Isotope Ratio Mass Spectrometer. When methane concentrations were not high enough for direct injection (~1000 ppm for ^{13}C), cryofocusing was used to amplify the signal (more detail available in Chapter 3.2.6). Isotope data are reported in the "del" notation ($\delta^{13}C$) :

$$\delta\ = 1000\ \left[\left(\frac{R_{sample}}{R_{standard}}\right) -\ 1\right]$$

where R_{sample} is the isotopic ratio of the sample and $R_{standard}$ is the isotopic ratio of the referenced standard (PDB).

6.3 Results

6.3.1 Methane Production Rates When Sulfate Reducing Bacteria Are Inhibited

Comparison of methane production rates for sediments with and without sulfate reducing bacteria inhibition were taken in October 2009, January 2010, August 2010, March 2012, and October 2012. We classify the sites into brine sites and extreme brine sites as the response of the microbes to the molybdate addition varied markedly between across these sites. Our lower-salinity brine sites (55 ppt to 126 ppt), consisted of CAL Pond 15, GN Area 1, and GN Area 4 and our higher-salinity extreme brine sites (with salinities from 180 ppt to 320 ppt) consisted of CAL Pond A23 and GN Area 9. The differences observed in methane production between the brine sites and the extreme brine sites were significantly different and so they will be discussed separately.

Production in Brine Sites. Methane production rates in unamended sediment obtained from the brine sites with salinities ranging from 55 ppt to 126 ppt ranged from 0.06 nmol/gram/day to 14.52 nmol/gram/day (Table 6.1). The highest methane production rates within our brine sites were observed in the microbial mats from GN Area 1 (14.52 nmol/g/d), our lowest salinity site (Table 6.1). Our second and third highest methane production rates were observed in GN Area 4 (2.96 nmol/g/d) and CAL Pond 15 (0.7 and 0.06 nmol/g/d), our second and third lowest salinity sites (Table 6.1).

When sediment from our brine sites were incubated with molybdate, the production of methane was significantly higher than what was observed in the unamended control samples (Table 6.1 and Figure 6.1). Our highest methane production shifts were observed in GN Area 1 (Table 6.1). Methane production increased from about 14.52 nmol/g/d to 279.83 nmol/g/d in

2009 when molybdate was added (Figure 6.1). Another example, one of our lower shifts, CAL Pond 15 sampled in August 2010, saw a production shift from 0.06 nmol/g/d to 2.68 nmol/g/d with the addition of molybdate (Table 6.1; Figure 6.1). CAL Pond 15 was sampled on two different occasions January and August 2010. While the rates of methane production were higher in the January samples, in August we still observed the same trend of increased methane production when molybdate was added to sediments (Table 6.1; Figure 6.1).

Production in Extreme Brine Sites. Methane production rates in the extreme brine sites, with salinities from 180 ppt to 320 ppt, ranged from 0.20 nmol/g/d to 18.80 nmol/g/d (Table 6.1). The highest methane production rates observed (18.80 nmol/g/d) were from the gypsum crust of GN Area 9, our lower-salinity extreme brine site (~190 ppt). Our next highest methane production rates were observed within the rubble of the same area, GN Area 9, measured at 3.53 nmol/g/d (Table 6.1). While our lowest methane production rates observed in the extreme brine sites were 0.02 nmol/g/d and 1.53 nmol/g/d which were from CAL Pond A23 sampled in both January 2010 and August 2010 respectively (Table 6.1; Figure 6.1).

When sediments from our extreme brine sites were treated with molybdate, the addition of molybdate produced no statistical difference in methane production rates between vials amended with molybdate and those that were not (Table 6.1 and Figure 6.1). One example, GN Area 9 crust, saw a slight production decrease in methane production from 18.80 nmol/g/d to 17.40 nmol/g/d when molybdate was added (Table 6.1; Figure 6.1), however this decrease was not statistically significant (Student T-test). Another example, CAL Pond A23, stayed the same with respect to methane production with rates of 0.2 nmol/g/d and 1.5 nmol/g/d for the January and August 2010 sampling trips regardless of the addition of molybdate (Table 6.1; Figure 6.1).

6.3.2 Isotopic Analysis of Methane Produced Under SRB Inhibition

Isotopic analysis of methane produced from sediments incubated with molybdate as an inhibitor of sulfate reducing bacteria provided insight on *in situ* substrate utilization by methanogens in hypersaline sites. Differences observed in isotopic composition between brine sites and extreme brine sites were again significant, as such they will be discussed separately.

Brine Sites. Isotopic analysis of unamended sediments incubated from GN Area 1, in October 2009, produced methane with an average $\delta^{13}C$ value of –48.07‰ (Table 6.1; Figure 6.2). When sediments from GN Area 1 were amended with molybdate we observed a statistically significant enrichment in the $\delta^{13}C$ value to –34.95‰ (Mann-Whitney Rank Sum; P-value = 0.002) (Table 6.1; Figure 6.2). Sediments from GN Area 4 collected in October 2009, provided similar isotopic effects between unamended sediments, which had a $\delta^{13}C$ value of –47.61‰ and those sediments which received molybdate, with a $\delta^{13}C$ value of –36.98‰. This enrichment in $\delta^{13}C$ was statistically significant (Mann-Whitney Rank Sum) with a P-value = 0.029. Sediments collected from CAL Pond 15 in 2010 displayed similar enrichment in $\delta^{13}C$ when sediments were incubated with molybdate. In January 2010, unamended sediments produced methane with an average $\delta^{13}C$ value of –62.85‰, while sediments incubated with molybdate had a $\delta^{13}C$ value of –39.91‰ which was statistically significant (Student T-test; $P \leq 0.001$) (Table 6.1; Figure 6.2). In August 2010, a similar statistically significant shift was observed in CAL Pond 15 between unamened sediments which had a $\delta^{13}C$ value of –64.3‰ and molybdate amended sediment which had a $\delta^{13}C$ value of –43.4‰ (Table 6.1; Figure 6.2).

Extreme Brine Sites. Isotopic analysis of methane produced from extreme brine sites provided a different isotopic shift than what was observed in brine sites. In fact, the evolved methane did not produce a similar isotopic trend across all extreme brine sites. Unamended

sediments incubated from GN Area 9 crust produced methane with a $\delta^{13}C$ value of –36.18‰. A statistically significant isotopic shift (P-value ≤ 0.001) was observed, in evolved methane from sediments incubated with molybdate producing a $\delta^{13}C$ values of –54.4‰ which is depleted in ^{13}C in comparison to unamended control samples. Samples collected from GN Area 9 rubble produced a similar isotopic trend with $\delta^{13}C$ values of –33.08‰ for unamended sediments and a $\delta^{13}C$ value of –51.17‰ for sediments amended with molybdate.

Sediments incubated from CAL Pond A23 however did not produce methane with a similar isotopic shift to what was observed from the other extreme brine sites. Unamended sediments sampled from CAL Pond A23 in January 2010 produced methane with a $\delta^{13}C$ value of –41.5‰ while sediments incubated with molybdate produced methane with an average $\delta^{13}C$ value of –42.33‰, which is not statistically different. Similarly, samples obtained from the same location in August 2010 produced methane with a $\delta^{13}C$ value of –44.5‰ and –45.7‰ for unamended and amended sediments respectively.

6.3.3 Competitive Substrates Utilization in Sediments Experiencing SRB Inhibition

Sediments from Baja California were analyzed to understand competitive substrate utilization by methanogens when sulfate reducing bacteria were inhibited. This was performed during two separate experiments, during different sampling periods as such they will be discussed separately.

March 2012. Sediments from GN Area 1 were collected and sampled in March 2012 for competitive substrate utilization by methanogens when sulfate reducing bacteria were inhibited. This was accomplished by incubating microbial mat samples with molybdate to inhibit SRB and

then amending with 10µM ^{13}C-labeled acetate or bicarbonate and monitoring the evolved methane production rates and isotopic signatures.

Methane production rates observed from GN Area 1 in March 2012 were lower than previous sampling trips (Table 6.1; Chapter 5 Table 5.1). Unamended sediments had methane production rates of 4.31 nmol/g/day while sediments amended with molybdate displayed a significant increase in methane production to 138.45 nmol/g/day (Figure 6.3). The methane production rate from molybdate incubations is what we are classifying as the molybdate control for this experiment, as it is the rate of methane production when sulfate reducing bacteria are inhibited. In incubation vials where molybdate and ^{13}C-labeled acetate were added, methane production rates were 109.16 nmol/g/d which was not statistically different from the molybdate control samples (Figure 6.3). When incubation vials were amended with molybdate and ^{13}C-labeled bicarbonate there was a significant increase in methane production to 305.27 nmol/g/day (Figure 6.3).

Isotopic analysis of evolved methane produced from GN Area 1 provides insight on substrate utilization by methanogens. Unamended sediment produced methane with a δ^{13}C value of –56.51‰ while sediments amended with only molybdate produced methane with a δ^{13}C value of –37.81‰ (Table 6.1; Figure 6.4). Just like with methane production rates, we will refer to the molybdate only treatment as the molybdate control. Sediments incubated with molybdate and 10µM ^{13}C-labeled acetate produced methane with a δ^{13}C value of –33.11‰, which is not statistically different from the molybdate control (Figure 6.4). Sediments incubated with molybdate and 10µM ^{13}C-labeled bicarbonate produced methane that was different from the molybdate control (P-value $\leq$ 0.05) with an average δ^{13}C value of –21.28‰ (Table 6.1; Figure 6.4).

October 2012. Sediments were collected in GN Area 1 in October 2012 and were analyzed to examine the extent to which bicarbonate is utilized as a substrate by methanogens for the production of methane when sulfate reducing bacteria are inhibited. This was accomplished through the analysis methane production rates and isotopic composition when various concentrations of ^{13}C-labeled bicarbonate was added to sediment amended with molybdate.

Methane production rates observed during the October 2012 sampling period were elevated in comparison to previous trips (Table 6.1; Chapter 5 Table 5.1). Unamended sediments produced methane with an average production rate of 22.48 nmol/g/day (Table 6.1; Figure 6.5). Sediments that were amended with only molybdate had a statistically significant increase in production rates to 823.28 nmol/g/day (Student T-test; P-value $\leq$ 0.001) (Figure 6.5). The rate of methane production for molybdate only incubations are what we are classifying as the molybdate control for this experiment, as it is the rate of methane production when SRB are inhibited.

Sediments which received the addition of 10µM, 100µM, and 1,000µM ^{13}C-labeled bicarbonate in addition to molybdate in GN Area 1 did not display a significant increase in methane production when compared to the molybdate control. Vials which received 10µM ^{13}C-labeled bicarbonate had an average methane production rate of 778.90 nmol/g/day (Figure 6.5). Vials which received the addition of 100µM ^{13}C-labeled bicarbonate had a production rate of 877.68 nmol/g/day (Figure 6.5). Vials which received the addition of 1,000µM ^{13}C-labeled bicarbonate had an average production rate of 973.28 nmol/g/day (Figure 6.5).

Isotopic analysis of the evolved methane from GN Area 1 incubations amended with ^{13}C-labeled bicarbonate and molybdate provides insight on the utilization of bicarbonate as a substrate for methane production. Unamended control sediment samples produced methane with an average δ^{13}C value of –46.7‰, while sediments amended with only molybdate produced

methane with an average $\delta^{13}C$ value of –35.4‰ (Figure 6.6). Just like with production rates, we will refer to the molybdate only incubations as molybdate controls. Incubations amended with molybdate and 10µM ^{13}C-labeled bicarbonate produced methane with average $\delta^{13}C$ value of –29.95‰ (Figure 6.6) which is not significantly different from the molybdate control. Incubations amended with molybdate and 100µM ^{13}C-labeled bicarbonate produced methane with an average $\delta^{13}C$-value of –28.94‰ (Figure 6.6) which is statistically different from the molybdate control (Student T-test; P-value ≤0.03). Incubations amended with molybdate and 1,000µM ^{13}C-labeled bicarbonate produced methane with an average $\delta^{13}C$-value of +29.93‰ (Figure 6.6), which is also statistically different than the molybdate control (P-value ≤0.001).

6.4 Discussion

In sulfate-rich sediments typical of marine environments, sulfate reduction is the dominant stage of carbon mineralization. While in sulfate-poor sediments typical of freshwater environments, methane production is the dominant stage of carbon mineralization (Reeburgh, 2007; Whiticar, 1999). In all of our hypersaline environments (both lower-salinity brine and higher-salinity extreme brine), sulfate levels in the sediment and porewater are relatively high (Bebout et al., 2004; Smith et al., 2008). Therefore there should be high activity of sulfate reducing bacteria (SRB) in our sites. In our study we did not measure sulfate reduction rates however we are analyzing the role SRB play in regards to availability of substrate for methanogens. We hypothesize that methane production rates will be lower in sediments with active sulfate reducing bacteria communities. We also hypothesize that in sediments where sulfate reducing bacteria are not active, methane production will proceed through the use of competitive substrates, acetate and bicarbonate, because competition is no longer a factor.

In order to determine if that was occurring, we performed incubations with molybdate, a specific inhibitor for sulfate reduction, and set out to first provide evidence of increased methane production when sulfate reducing bacteria are inhibited and secondly, to determine what competitive substrates are utilized by methanogens when sulfate reducing bacteria are inhibited.

6.4.1 Increased Methane Production When Sulfate Reducing Bacteria Are Inhibited

For the two different salinity sampling sites, brine (55 ppt to 126 ppt) and extreme brine (180 ppt to 320 ppt), we monitored the production of methane in incubations which received molybdate, an inhibitor of sulfate metabolism, and those that did not. We observed that in the presence of molybdate there was a statistically significant increase in methane production rates from the lower-salinity brine sites while at the higher-salinity extreme brine sites there was no significant change in methane production rates (Table 6.1; Figure 6.1). These differences in methane production in the two different salinity ranges are similar to what have been noted in other studies which looked at methane production when sulfate reducing bacteria are inhibited in the hypersaline ponds in Eilat, Israel (Oren et al., 2009; Sorensen et al., 2004).

Our findings suggest that there are two different communities of methanogenic Archaea present utilizing different substrates. In our lower-salinity brine sites, the increase in methane production is explained by the inhibiting effects to sulfate reducing bacteria from the addition of molybdate in the incubation vials. This inhibition allowed for the utilization of substrates already present in the sediments by methanogens, increasing the methane production rates in comparison to the control incubations because sulfate reducers were inhibited. This microbial community is presumably more adaptive to utilizing substrates for which they have to compete, acetate and/or

hydrogen/bicarbonate which are typically not available to methanogens in these environments because of competition with sulfate reducing bacteria.

While at our higher-salinity extreme brine sites the methanogenic community appears to be utilizing non-competitive substrates, which explains why no change in methane production were observed when sulfate reducing bacteria were inhibited. These substrates, such as methylated amines as well as dimethylsulfide are unable to be utilized by sulfate reducing bacteria and are known to be utilized by the most halophilic methanogens Archaea (Madigan and Martinko, 2006; Whiticar, 1999; Whitman et al., 2006). In fact, halophilic or halotolerant methanogens that use hydrogen or acetate as energy sources have not been found at salinity levels above around 100 ppt (Ollivier et al., 1994; Oren, 1999b; Oren, 2001; Oren et al., 2009).

Another explanation for the increase in methane production in our lower-salinity brine sites could be from the way in which molybdate inhibits SRB. The addition of molybdate allows for the production of hydrogen by SRB but prevents SRB from forming H_2S (Biswas et al., 2009; Fukui et al., 1997), creating an additional source of hydrogen for methanogens. Either of these explanations could be valid for what we observed in our brine site.

6.4.2 Isotopic Analysis of Methane Produced Under SRB Inhibition

When evaluating the isotopic signature from incubations amended with molybdate as an inhibitor of sulfate reduction and those that did not, there was an isotopic shifts in methane produced from the vials receiving the molybdate amendment. The differences observed varied between brine and extreme brine sites and will be discussed separately.

Brine sites. In the lower-salinity brine ponds, GN Area 1, GN Area 4, and CAL Pond 15, there was a significant enrichment in the $\delta^{13}C\text{-}CH_4$ from the molybdate treatment group in

comparison to the unamended controls (Figure 6.2). The enrichment in $\delta^{13}C\text{-}CH_4$ for the brine sites amended with molybdate could be related to the significant increase in methane production (Figure 6.1). Through the addition of molybdate, methanogens in those vials are no longer in competition with SRB for substrate as such they can produce methane so long as they have substrate available. We presume that this significant increase in methane production in the sample vials have caused less fractionation to occur by the methanogens resulting in methane that is enriched in ^{13}C when compared to control samples.

Extreme brine sites. In the higher-salinity extreme brine sites, GN Area 9 rubble, GN Area 9 crust, and CAL Pond A23, there was no enrichment in $\delta^{13}C\text{-}CH_4$ in comparison to the controls (Table 6.1; Figure 6.2). In GN Area 9 rubble and crust there was a depletion in $\delta^{13}C\text{-}CH_4$ becoming more negative for the molybdate control group while in CAL Pond A23 there was no significant change in the $\delta^{13}C\text{-}CH_4$ from the molybdate control group and the unamended controls.

A possible explanation for no isotopic shift from methane produced in CAL Pond A23 when molybdate was added could be that in the higher salinity extreme brine sites methanogens are not in competition with SRB for substrates, as such, no isotopic change would have been noted from the inhibition of SRB. Another explanation could be the activity of SRB are limited because of the extreme salinity and so the addition of molybdate to those locations does not result in an increase in methane production because methanogens are already free from competition in those sites.

In GN Area 9, an area with slightly lower salinity than in CAL Pond A23, we observed a depletion in $^{13}C\text{-}CH_4$ when sediments were amended with molybdate. One explanation for the ^{13}C depletion observed in these molybdate treatments could be from the release of substrates that

were not previously available to methanogens prior to the addition of molybdate. Molybdate as an inhibitor of sulfate reduction does not eliminate all processes performed by sulfate reducing bacteria, it only prevents the coupling of hydrogen produced to sulfur. This prevention causes there to be an abundant supply of hydrogen in the sediment which could now be utilized by methanogens as a substrate. The availability of this substrate would allow for biologic methanogenesis to occur subsequently producing methane that is depleted in $\delta^{13}C$ in comparison to the control.

6.4.3 Competitive Substrates Utilization In Sediments Experiencing SRB Inhibition

Analysis of sediments from Baja California in 2012, provide insight into the utilization of competitive substrates by methanogens when sulfate reducing bacteria are inhibited. Previous work done by Smith et al (2008), at GN Area 4 explored the effects inhibiting SRB with molybdate would have on methane production. They observed that from the addition of molybdate there was a short-term inhibition of sulfate reduction which resulted in increased methane production, suggesting that methanogenic activity is to some extent regulated by sulfate availability. One conclusion presented in their work, which was a building block for the work presented in this paper, is that although several lines of evidence support the hypotheses that microbial mats maintain a population of methanogens that compete for resources with SRB, none of their evidence provides the basis for inference about the resources for which they compete.

In March 2012, sediments were incubated from GN Area 1 with molybdate as an inhibitor of sulfate reduction in an effort to provide evidence for which resources methanogens in our microbial mats were competing. These incubations also received the addition of 10µM ^{13}C-labeled acetate or bicarbonate and the evolved methane was monitored and analyzed. From the

molybdate only controls, there was a statistically significant increase in methane production and an enrichment in $\delta^{13}C\text{-}CH_4$ (Figure 6.3 and 6.4) similar to what was previously measured (Table 6.1). Analysis of incubations with molybdate and 10µM ^{13}C-labeled acetate did not produce any additional methane in comparison to the molybdate control (Figure 6.3), nor did the methane produced show any enrichment in $\delta\ ^{13}C$ (Figure 6.4). Incubation vials which received molybdate and 10µM ^{13}C-labeled bicarbonate showed a statistically significant increase in methane production (Figure 6.3) as well as an enrichment in $^{13}C\text{-}CH_4$ in comparison to the molybdate control (Figure 6.4).

The increase in methane production as well as the isotopic enrichment in ^{13}C from the evolved methane in samples which received molybdate and 10µM ^{13}C-labeled bicarbonate provides evidence that methanogens in this site are being outcompeted by SRB for hydrogen and bicarbonate as substrates. The lack of increased methane production in the acetate/molybdate enriched samples provides evidence that in our sampling site methanogens are not in competition with SRB for acetate. One possible explanation for why methanogens would be in competition with SRB for bicarbonate and not acetate could be due to the amount of energy received from the reactions. Acetate fermentation is considerably slower than the formation of methane via CO_2-reduction (Formolo, 2010). The two processes, acetate fermentation and CO_2-reduction, yield free energy that are exogenic and the energy gain can be used to synthesize ATP. The formation of methane via acetate fermentation yields $\Delta Go'\sim = -31$ kJ mol^{-1} and CO_2-reduciton yields $\Delta Go'\sim = -135$ kJ mol^{-1} (more detail Introduction; Table 1.1). This significant difference in energy yield could explain why one substrate is utilized over another.

Another possibility could be that the methanogens present at GN Area 1 are not capable of using acetate as a substrate because of the salinity levels present in the pond (60 ppt). Previous

studies have analyzed methanogens tolerance in various salinity levels and have found that the utilization of $H_2 + CO_2$ does not occur in nature at salinity levels greater than around 100 ppt, while the maximum salinity levels for the utilization of acetate by methanogens is even lower at around 50 ppt (Ollivier et al., 1994; Oremland and King, 1989; Oren, 1999b; Oren, 2001).

Conclusions from the March 2012 incubation experiment revealed that methanogens can utilize hydrogen/bicarbonate as a substrate when SRB are inhibited and led to further questions about the use of bicarbonate as a substrate for methanogenesis. In October 2012 incubations were performed at GN Area 1, using molybdate and 3 concentrations of ^{13}C-labeled bicarbonate (10µM, 100µM, and 1,000µM). Analysis of methane production rates revealed a statistically significant increase in methane production between unamended control samples and the molybdate control, which are similar to what has previously been observed (Table 6.1; Figure 6.5). Analysis of methane production rates from incubations amended with molybdate and three concentrations of bicarbonate were not statistically different than what was observed from the molybdate control (Figure 6.5). The similarity in the production rates between the molybdate control and those which received molybdate and labeled bicarbonate show that we were successful in not stimulating additional methane production in our experiment. This allows us to draw conclusions that any incorporation of bicarbonate into methane production is directly related to methanogenic community preference for the substrate. This is very important because isotopic analysis of evolved methane from the molybdate and labeled bicarbonate additions reveal an enriched δ^{13}C-CH_4 in comparison to the molybdate control with only one exception. Sediments which received molybdate and 10 µM ^{13}C-labeled bicarbonate revealed an isotopic enrichment in ^{13}C; however the shift in ^{13}C it was not enough to be statistically significant.

In the higher additions of ^{13}C-labeled bicarbonate (100 µM and 1,000 µM) the enrichment in ^{13}C was statistically different than the molybdate control, however the enrichment was small in comparison to incubations with different substrates (Chapter 5). The small increase in ^{13}C enrichment as the ^{13}C-labeled bicarbonate concentration increased allows us to conclude that methanogens in GN Area 1 are capable of utilizing bicarbonate as a substrate when SRB are inhibited; however this substrate does not appear to be a dominate substrate for methane production. When comparing the relatively small isotopic enrichment (no more than 70‰ at times) from this experiment to the large isotopic changes (up to 10,000‰ at times) observed from previous experiments when ^{13}C-labeled non-competitive substrates were utilized (Chapter 5) one can conclude that either there is only a small population of methanogens present which can utilize bicarbonate as a substrate or that the methanogens are less efficient at methane production when utilizing bicarbonate as a substrate.

There is however one other possibility to explain why we observed such a big increase in methane production in the vials incubated with molybdate and ^{13}C labeled bicarbonate and a small ^{13}C enrichment. A study by Banat et al (1983) looking at the effects from the inhibition of sulfate reducing bacteria on methane production found that the initial addition of molybdate increased methane production in vials treated with molybdate and vials treated with molybdate and a H_2/CO_2 atmosphere, however they noted that after day 8 there was a significant increase in methane production and H_2 uptake in the sediment vials treated with the H_2/CO_2 atmosphere. They concluded that the 8 day lag before methane production increased presumably was the time required for the population of methanogens to respond to the enhanced concentration of H_2 + CO_2 available (Banat et al., 1983). In our experiments, we monitored methane production for 8 days and then concluded our production rate analysis and froze the samples until isotopic

analysis could be performed. Because of our relatively short incubation period, we could have not allowed for ample time for methanogens to respond to the ^{13}C-labeled bicarbonate in the incubation vials, hence the increase production rates but low ^{13}C enrichment values. In future work, we will consider having production rates monitored for a longer period of time in order to observe if a lag is present in our samples.

6.5 Conclusion

Obtaining a better understanding of the effects sulfate reducing bacteria have on methanogens in hypersaline environments are vital to having a complete understanding of methanogens in these environments. This work builds on previously published work and provides insights into which substrates methanogens compete with sulfate reducing bacteria for in our hypersaline environments. Analysis of methane production rates in our lower-salinity brine sites (55 ppt to 126 ppt) and our higher-salinity extreme brine sites (180 ppt to 320 ppt) reveal a significant difference in methane production when sulfate reducing bacteria are inhibited. We observed that in our brine sites methane production was significantly increased when sulfate reducing bacteria were inhibited. We also observed that in our extreme brine sites methane production rates were not increased when sulfate reducing bacteria were inhibited. We attribute these findings to effects on sulfate reducing bacteria population caused by salinity. Sulfate reducing bacteria have been shown to be limited in extreme salinity levels (Ollivier et al., 1994; Oren, 1999b; Oren, 2001) and this limitation can explain why we did not observe an increase in methane production when molybdate was added to sediments from extreme brine sites. Methane production rate analysis and isotopic analysis of incubations conducted with ^{13}C-labeled competitive substrates, acetate and bicarbonate, revealed that methanogens in our lower-

salinity brine site only utilize bicarbonate as a substrate for methane production when sulfate reducing bacteria are inhibited. Isotopic analysis of evolved methane revealed that in our brine sites there is either a small amount of methanogens capable of utilizing bicarbonate as a substrate or the methanogens present are unable to efficiently utilize bicarbonate as a substrate. From this research we can conclude that sulfate reducing bacteria only effect methane production in lower-salinity brine sites and that methanogens inhabiting these areas are able to utilize H_2/bicarbonate as a substrate only when sulfate reducing bacteria have ceased activity.

Table 6.1. Temperature, salinity, methane production rates in incubation samples, methane isotopic carbon values methane produced within incubation vials, and $\delta^{13}C\text{-}CO_2$ values for production within incubation vials. Values that were unable to be determined are depicted in the table as n.d.

Site	Date	Temp (°C)	Salinity (ppt)	Methane production in control incubation (nmol g-1 d-1)	Methane production in Molybdate addition (nmol g-1 d-1)	Control Incubations δ13C-CH4 (‰)	Molybdate Incubations δ13C-CH4 (‰)	Control Incubations δ13C-CO2 (‰)	Molybdate Incubations δ13C-CO2 (‰)
Don Edwards									
Pond 15	January 2010	12	126	0.71	16.05	-62.85	-39.91	n.d.	n.d.
	August 2010	14	115	0.06	2.68	-64.3	-43.4	n.d.	n.d.
Pond 23	January 2010	24	320	0.20	0.21	-41.51	-42.33	n.d.	n.d.
	August 2010	40	275	1.53	1.63	-44.5	-45.7	n.d.	n.d.
Guerrero Negro									
Area 1	October 2009	31	55	14.52	279.83	-48.07	-34.95	-14	-8.15
Area 4	October 2009	25	84	2.96	206.97	-47.61	-36.98	-17.89	-6.86
Area 9 rubble	October 2009	25	192	3.53	2.81	-33.08	-51.17	-19.28	-13.49
Area 9 crust	October 2009	25	192	18.80	17.40	-36.18	-54.4	-18.08	-15.7
Area 1	March 2012	20	62	4.30	138.45	-54.51	-37.81	-13.02	-11.47
Area 1	October 2012	n.d.	60	22.48	823.28	-46.70	-35.40	n.d.	-5.82

A.

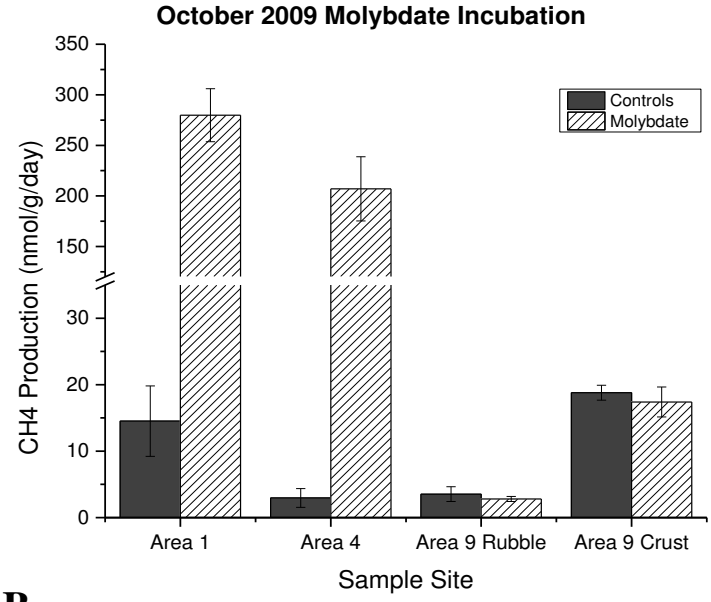

B.

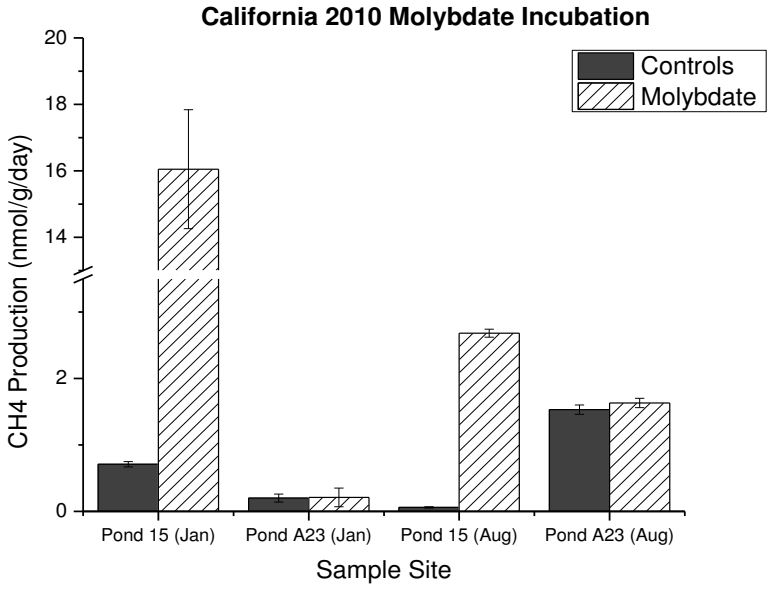

*Figure 6.1. Methane production rates from GN Area 1, GN Area 4, GN Area 9 rubble, and GN Area 9 crust sampled in October 2009 (**A**) and CAL Pond 15 and CAL Pond A23 sampled in January and August 2010 (**B**). Unamended control samples (solid fill) have lower methane production rates than molybdate amended samples (striped fill) in our brine locations, GN Area 1 and 4 and CAL Pond 15. Our extreme brine locations, GN Area 9 and CAL Pond A23, have no statistical difference between unamended sediment and molybdate amended sediment.*

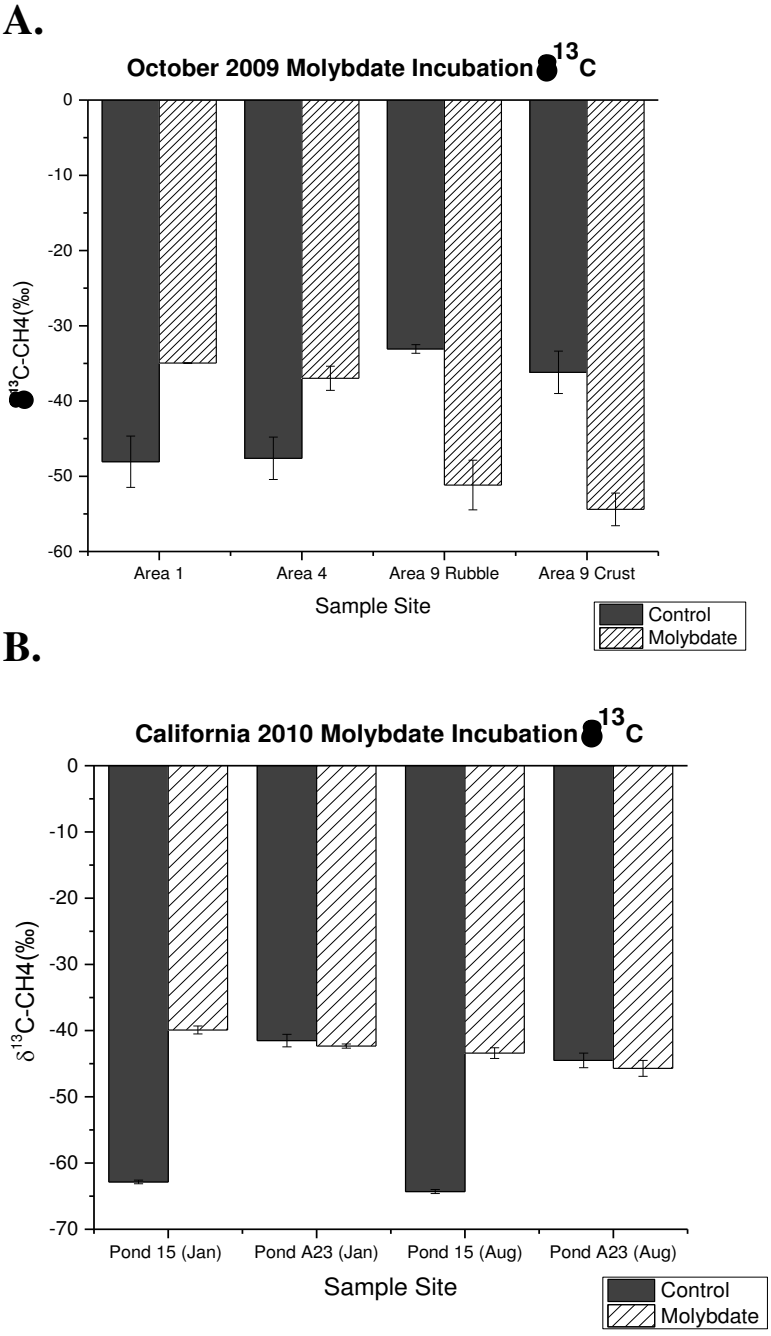

*Figure 6.2. Isotopic composition from GN Area 1, GN Area 4, GN Area 9 rubble, and GN Area 9 crust sampled in October 2009 (**A**) and CAL Pond 15 and CAL Pond A23 sampled in January and August 2010 (**B**). Unamended control samples (solid fill) are depleted in 13C-CH4 in comparison to molybdate amended samples (striped fill) in our brine locations, GN Area 1 and 4 and CAL Pond 15. Our extreme brine locations, CAL Pond A23, had no statistical difference between unamended sediment and molybdate amended sediment, however, GN Area 9 was more enriched in 13C-CH4 in the unamended control samples in comparison to the molybdate samples.*

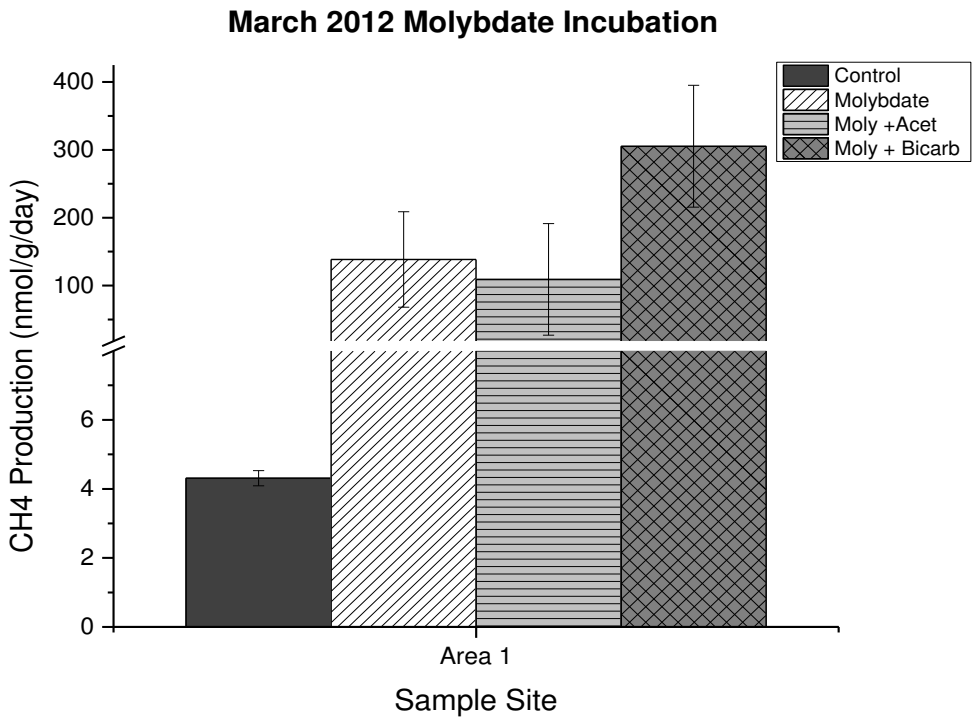

Figure 6.3. Methane production rates from GN Area 1 collected in March 2012. Unamended control sediment (solid fill) had the lowest production rates. Molybdate amended sediment (diagonally striped, no fill) had a significant increase in methane production. Molybdate and 10μM ^{13}C-labeled acetate amended sediment (striped, grey fill) was not different than the molybdate only control. Molybdate and 10μM ^{13}C-labeled bicarbonate (checkered, grey fill) was different than the molybdate only control.

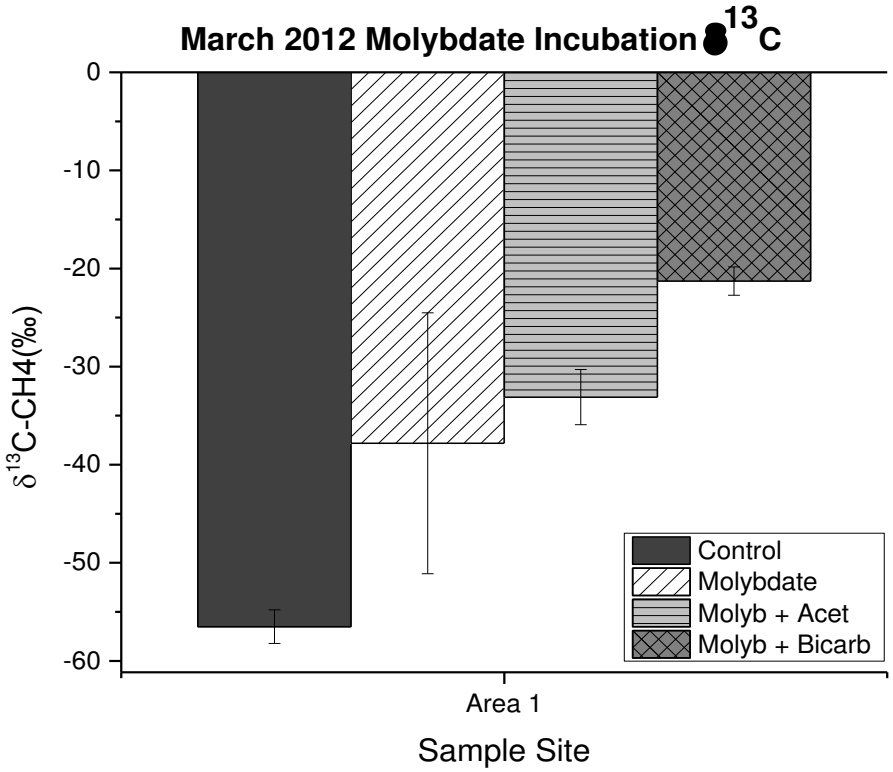

Figure 6.4. Methane isotopic composition from GN Area 1 collected in March 2012. Unamended control sediment (solid fill) was most depleted in $\delta^{13}C$-CH_4. Molybdate amended sediment (diagonally striped, no fill) had a significant enrichment in $\delta^{13}C$-CH_4. Molybdate and 10μM ^{13}C-labeled acetate amended sediment (striped, grey fill) was not different than the molybdate only control. Molybdate and 10μM ^{13}C-labeled bicarbonate (checkered, grey fill) was more enriched than the molybdate only control.

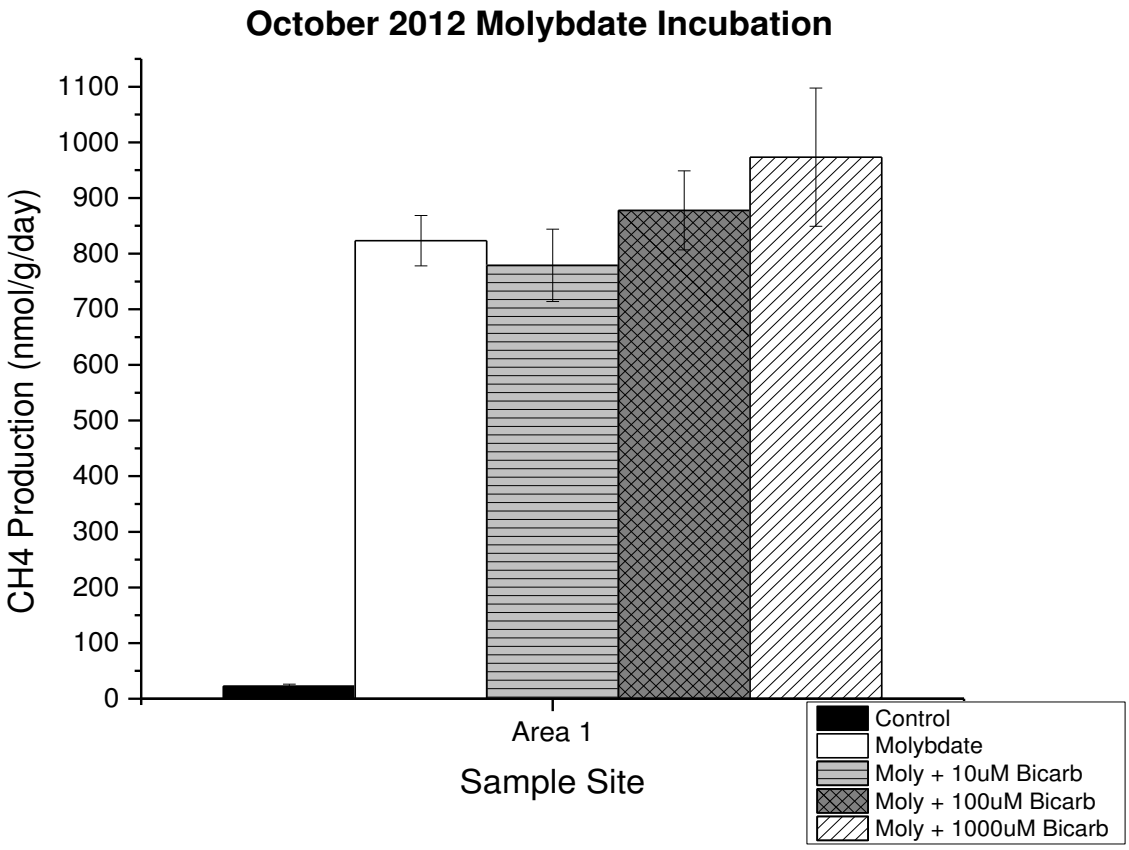

Figure 6.5. Methane production rates from GN Area 1 collected in October 2012. Unamended control sediment (solid fill) had the lowest production rates. Molybdate amended sediment (no fill) had a significant increase in methane production. Molybdate and 10μM ^{13}C-labeled bicarbonate amended sediment (striped, grey fill) was not different than the molybdate only control. Molybdate and 100μM ^{13}C-labeled bicarbonate (checkered, grey fill) was different than the molybdate only control. Molybdate and 1,000μM ^{13}C-labeled bicarbonate (diagonal striped, no fill) was different than the molybdate only control.

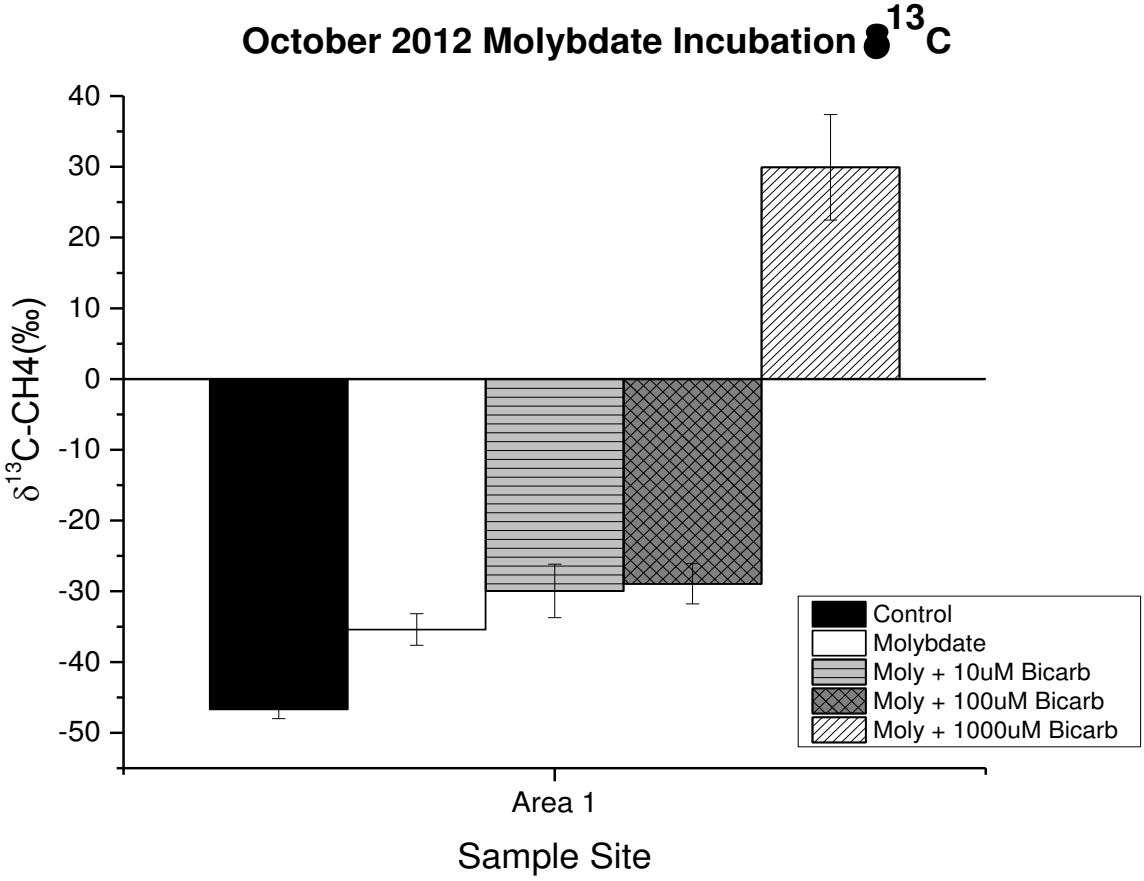

Figure 6.6. Methane isotopic composition from GN Area 1 collected in October 2012. Unamended control sediment (solid fill) was the most depleted in $\delta^{13}C\text{-}CH_4$. Molybdate amended sediment (no fill) had a significant enrichment in $\delta^{13}C\text{-}CH_4$. Molybdate and 10µM ^{13}C-labeled bicarbonate amended sediment (striped, grey fill) was not different than the molybdate only control. Molybdate and 100µM ^{13}C-labeled bicarbonate (checkered, grey fill) was more enriched in $\delta^{13}C\text{-}CH_4$ than the molybdate only control. Molybdate and 1,000µM ^{13}C-labeled bicarbonate (diagonal striped, no fill) was more enriched in $\delta^{13}C\text{-}CH_4$ than the molybdate only control.

CHAPTER SEVEN

FRACTIONATION FACTORS IN HYPERSALINE PONDS

7.1 Introduction

Methane (CH_4) is an end product from the degradation of organic matter under anoxic conditions when inorganic oxidants such as nitrate, ferric iron or sulfate are depleted (Conrad, 2005). Globally methane is formed by *Archaea* utilizing CO_2 + H_2 and acetate, however in some environments biogenic methane can also be produced from methylated compounds such as trimethylamine, methanol or dimethyl sulfide (Conrad, 2005; Oremland and King, 1989; Oremland and Polcin, 1982; Oremland et al., 1988; Whiticar, 1999).

The isotopic characteristic of methane has been used to differentiate between biogenic, thermogenic, and geologic methane. In the case of biogenic methane, isotopic data have been used to determine whether methanogenesis is primarily autotrophic (using H_2 and CO_2) or heterotrophic (Conrad, 2005; Londry et al., 2008; Whiticar et al., 1986). Heterotrophic methanogenesis occurs in only a subset of methanogens, predominantly the Methanosarcinaceae (Whitman et al., 2006). These methanogens are thought to use acetate and other small compounds like methanol, methylated amines, and methyl sulfide as the primary substrate during heterotrophic growth (Londry et al., 2008; Whitman et al., 2006).

In marine and hypersaline environments, these methylated substrates, like methanol, trimethylated amines, and dimethylsulfide, may be available in high enough abundance to serve as significant substrates for methanogens (King, 1984; Londry et al., 2008; Oremland and King, 1989; Oremland et al., 1982; Oremland and Polcin, 1982; Summons et al., 1998; Whiticar,

1999). Although the concentrations of theses substrates in hypersaline environments have not been measured due to analytical difficulty, their abundance is presumed in these environments because of the presence of precursor substrates such as glycine betaine an osmoregulate which can rapidly be transformed to trimethylamine, and the bacterial breakdown of pectin which leads to the production of methanol (King, 1984; King, 1988a; King et al., 1983; McGenity, 2010; Mitterer, 2010; Ollivier et al., 1994; Oremland and King, 1989; Oremland and Polcin, 1982; Summons et al., 1998; Visscher and Van Gemerden, 1991).

The use of carbon and hydrogen stable isotope ratios have been used to distinguish methane production pathways, which will be key in the determination of biogenic methane on Mars and/or other planets. Methane produced through biogenic processes are characterized by a $\delta^{13}C_{CH4}$ value < –50 ‰ and a $\delta^{2}H_{CH4}$ range from –275‰ to –100‰ (Whiticar, 1999). Through the use of stable isotopes we can further distinguish the substrate used for methane production. The reduction of CO_2 produces methane in the range of –100‰ to –55‰ and –250‰ to –150‰ for $\delta^{13}C_{CH4}$ and $\delta^{2}H_{CH4}$ values, respectively, and acetate assimilation produces methane in the range of –70‰ to –45‰ and –375‰ to –300‰ for $\delta^{13}C_{CH4}$ and $\delta^{2}H_{CH4}$ values, respectively (Whiticar, 1999). Less is known about the isotopic composition of methane produced from non-competitive substrates however culture work has suggested that there is a depletion in ^{13}C values for methane produced from both methylamines and methanol (Margulis et al., 1980; Summons et al., 1998; Zahnle et al., 2011).

During biologic methane production, the methane produced will have a lower isotopic ratio ($^{13}C/^{12}C$ or $^{2}H/^{1}H$) than the substrate used (Whiticar, 1999). Fractionation of isotopes generally results from kinetic processes; therefore is should be expected that for methane both the carbon isotopes and the hydrogen isotopes would be fractionated (Coleman et al., 1981). This

fractionation of carbon and hydrogen in methanogenesis results from the preferential use of the lighter isotope (^{12}C or ^{1}H) over the heavier isotope (^{13}C or ^{2}H) during methane production. The magnitude of fractionation depends on many factors including temperature, growth phase, hydrogen supply, species of methanogen, and isotope effects associated with the enzymes in its carbon acquisition pathway (Botz et al., 1996; Conrad, 2005; Londry et al., 2008; Valentine et al., 2004).

The isotopic composition of methane is also dependent on the isotopic composition of the starting material (the substrates) and the magnitude of the isotopic effect for methanogenesis can be described by its fractionation factor (α) (Burdige, 2006; Kelley et al., 2012; Sharp, 2007). Methane measurements obtained from environmental samples typically are produced from a combination of two or more substrates, in our sampling sites we did not obtain the isotopic composition of the substrates *in situ*, and so we report the apparent fractionation factors (Chanton et al., 2005; Chanton et al., 2006; Conrad, 2005) using $\delta^{13}C$ of dissolved inorganic carbon (DIC) and the δD of formation water (δD_{H2O}) as the proxy for all methanogenic substrates. Previously reported analysis of fractionation factors revealed that larger αC and smaller αD are typical of CO2 reduction, while smaller αC and larger αD are typical of acetate fermentation (Chanton et al., 2006).The goal of this study was to determine if apparent fractionation factors could be utilized to predict the substrates utilized by methanogens in our hypersaline environments.

7.2 Methods

7.2.1 Site Description

Sampling for this work was performed in two regions Northern California, USA and Baja California, Mexico, from 2008-2012. Northern California sampling sites (CAL) were within the Don Edwards National Wildlife Refuge, located in southern San Francisco Bay. CAL Pond 15 (~120 ppt) and CAL Pond A23 (~300 ppt) from the refuge were sampled in December 2008, January 2010, and August 2010. CAL Pond 15 consisted of soft microbial mat while CAL Pond A23 consisted of gypsum encrusted microbial mat (more details in Chapter 2). Baja California sampling was conducted in Guerrero Negro (GN), Laguna San Ignacio (LSI), and Laguna Figueroa. In Guerrero Negro the salterns GN Area 1 (~55 ppt), GN Area 4 (~84 ppt), GN Area 6 (~136), and GN Area 9 (~190 ppt) were sampled in March and October 2009. GN Area 1 and 4 consist of soft microbial mat, GN Area 6 consisted of a more gelatinous soft microbial mat, while GN Area 9, 10, and 11 consists of gypsum and halite encrusted microbial mat (more details in Chapter 2). In Laguna San Ignacio the salterns LSI Pond 1 (~360 ppt), LSI Pond 2 (~300 ppt) and LSI Pond 3 (~342 ppt) were sampled in March 2009 and consisted of gypsum and halite encrusted microbial mat (more details in Chapter 2). In Laguna Figuero (~54 to 200 ppt), the saltern was sampled in October 2009 and consisted of a transition between soft microbial mat and gypsum crustal material (more details in Chapter 2).

7.2.2 Sampling Methods

Overlying water. Overlying water was collected from each site in different quantities for multiple purposes. Salinity of the overlying water was determined with a hand-held

refractometer. In all locations 60 mls of site water was collected with no headspace in two 30 ml nalgene bottles for analysis of ^{18}O and ^{2}H.

Gas samples. Gas bubbles from GN Ponds 1, 9, 10, 11, 13 in Guerrero Negro, CAL Ponds 15 and A23 from Don Edwards, LSI Ponds 1, 2, 3 in Laguna San Ignacio and from multiple locations in Laguna Figueroa consisted of bubbles emitted during the perturbation of sediment and crustal material. In instances where evaporite crusts were thick, manual breaking of the crust was necessary to gain access to trapped gas. These samples were collected under water by means of an inverted capped funnel. Gas collected in the funnel was removed with a 10-ml syringe and then transferred to a previously evacuated 10-mL glass vial capped with a butyl rubber stopper. Bubbles collected from one area were pooled to obtain a total volume of 20-ml in each vial. At least triplicate, and in some cases up to 10 vials of gas samples, were collected from each site. Samples were then transported on ice to the laboratory, where subsamples were taken and analyzed for methane.

7.2.3 Analytical Methods

Dissolved Inorganic Carbon. Dissolved inorganic carbon (DIC) samples were obtained by taking a small section of microbial mat and/or sediment and centrifuging to separate pore water DIC from sediment particulate organic carbon (POC). All available pore water was injected into previously evacuated 2 mL glass serum vials and stored frozen upside down. Prior to analysis, 200 µL of 70% H_3PO_4 was injected into each vial along with enough helium to bring the vial pressure back to atmospheric pressure. Subsamples of headspace containing the evolved CO_2, was injected onto the GC connected to a continuous flow isotope ratio mass spectrometer (IRMS) for isotopic determination. DIC methods as described by Kelley et al. (2006) (Kelley et al., 2006). POC methods and analysis are described in Kelley et al (2012) (Kelley et al., 2012).

$\delta^{18}O$ and δD of water. In the laboratory, $\delta^{18}O$ and δD values were determined by sampling the headspace of a 500µL water sample in a borosilicate sample bottle. Samples for $\delta^{18}O$ were prepared by pipetting 500 µl of the overlying sample water using a 1 ml disposable pipette into an acid washed and dried Borosilicate sample bottle. The vials were then flushed with a mixture of 0.3% to 0.5% CO_2 in He using a Finnigan GasBench II as described by Hilkert and Avak (Hilkert and Avak). After flushing, samples were equilibrated for 24 hours in a temperature stabilized autosampler tray at 24°C. Once equilibrated, sampling proceeded. Samples for δD were prepared in a similar manner with the exception of the addition of a platinum catalyst to each sample. The samples were then flushed with a mixture of 2% H_2 in He using a Finningan GasBench II as described by Duhr and Hilkert (Duhr and Hilkert). After flushing, samples were equilibrated for approximately 40 minutes prior to the start of sequence acquisition.

7.2.4 Data Analysis and Calculations

The isotopic composition of the evolved methane was measured in the laboratory at Florida State University. The stable isotopic composition of the evolved methane from the incubations was determined by using a GC interfaced with a Finnegan Delta Plus Isotope Ratio Mass Spectrometer. When methane concentrations were not high enough for direct injection (<1000 ppm for ^{13}C and <4000 ppm for δ^2H_{CH4} values), cryofocusing was used to amplify the signal (more detail available in Chapter 3.2.6). Isotope data are reported in the "delta" notation (e.g., $\delta^{13}C$, δ^2H) :

$$\delta = 1000 \left[\left(\frac{R_{sample}}{R_{standard}}\right) - 1\right]$$

where R_{sample} is the isotopic ratio (e.g., $^{13}C/^{12}C$ and $^{2}H/^{1}H$) of the sample and $R_{standard}$ is the isotopic ratio of the referenced standard (Pee Dee belemnite (PDB) and standard mean ocean water (SMOW) for carbon and hydrogen, respectively). Delta values are reported in per mil, or parts per thousand, and the symbol for per mil is ‰. A positive δ value means that the ratio of the heavy to light isotope is higher in the sample than in the standard. A negative δ value means that the ratio of the heavy to light isotope is lower in the sample than in the standard.

Apparent fractionation factor (α) were calculated using $\delta^{13}C$ of dissolved inorganic carbon (DIC) and the δD of formation water (δD_{H2O}) as the proxy for all methanogenic substrates. In areas where no DIC was available or collected we used the $\delta^{13}C$ of the CO_2 from methane bubble samples. The apparent fractionation factors for $CO_2 \rightarrow CH_4$ (αC) and $H_2O \rightarrow CH_4$ (αH) are calculated:

$$\alpha_C = \frac{\delta^{13}C_{DIC} + 1{,}000}{\delta^{13}C_{CH_4} + 1{,}000}$$

and

$$\alpha_D = \frac{\delta D_{H_2O} + 1{,}000}{\delta D_{CH_4} + 1{,}000}$$

7.3 Results and Discussion

7.3.1 δD and $\delta^{18}O$ Water Analysis

The isotopic signatures of the overlying water (δD_{H2O} and $\delta^{18}O_{H2O}$) are reported in Table 7.1. Replicate analytical results are reported for all δD and $\delta^{18}O$ values presented. The δD_{H2O} ranged widely across the sites sampled from −28.7‰ at CAL Pond A23 to +33.7‰ at GN Area 9 (Table 7.1). Over the entire sampling system, there appears to be no pattern associated between

δD_{H2O} and the change in salinity, however, analysis of the overlying water from the Guerrero Negro pond system reveals a significant positive correlation between δD_{H2O} and salinity (Figure 7.1a, Table 7.2). Figure 7.1a is a plot of the overlying water δD versus the salinity in the Guerrero Negro pond systems, what can be noted is the positive correlation present representing increasing δD_{H2O} with increasing salinity within these ponds. The most depleted sample collected −28.7‰ at CAL Pond A23 we believe to be the result of some freshwater source input into the system. CAL Pond A23 is part of a restoration project in the San Francisco Bay area, and is subject to occasional freshwater input as part of the restoration process.

Analysis of the $\delta^{18}O_{H2O}$ revealed a variation across our sites, but not as widely as the δD_{H2O} (Table 7.1). One site in particular was the location for both our most enriched and our most depleted in regards to $\delta^{18}O_{H2O}$ collected. CAL Pond A23 sampled in December 2008 had a $\delta^{18}O_{H2O}$ value of −3.4‰, while in August 2010, the same location had a $\delta^{18}O_{H2O}$ value of +9.1‰. This wide range in $\delta^{18}O_{H2O}$ was observed only in that one site, as the remaining sites sampled had a $\delta^{18}O_{H2O}$ value ranging from +1.2‰ to +5.9‰ (Table 7.1). We believe that in December 2008 the area was subjected to freshwater input as part of its restoration process and so this data point does not accurately reflect conditions typically found at that site.

Analysis of $\delta^{18}O_{H2O}$ and salinity over the entire sampling system reveals no apparent pattern associated between $\delta^{18}O_{H2O}$ and the change in salinity, with the exception of our samples from the Guerrero Negro pond system (Table 7.2). Figure 7.1b is a plot of the overlying water $\delta^{18}O$ versus the salinity in the pond system, a positive correlation between $\delta^{18}O$ and salinity can be noted in these ponds.

The $\delta^{18}O$ and δD values for precipitation worldwide behave in a predictable manor falling along the global meteoric water line which expresses the relationship between ^{18}O and D in meteoric waters as follows (Craig, 1961):

$$\delta D = 8(\delta^{18}O) + 10$$

Analysis of the $\delta^{18}O$ and δD of the overlying water collected at our sampling sites in comparison to the global meteoric water line reveal that our samples fall to the right of the meteoric water line, in the closed basin evaporative zone (Figure 7.2). This zone depicts isotopically the location where evaporation dominates precipitation.

7.3.2 Porewater Analysis

Porewater samples were collected from a small subset of locations in our study. Sediments underlying the gypsum crust at CAL Pond A23 and GN Area 9, as well as, the soft microbial mats from CAL Pond 15 and GN Area 1, 4, and 6 provided porewater samples which were analyzed for $\delta^{13}C_{DIC}$. The $\delta^{13}C$ of the dissolved inorganic carbon (DIC) ranged from −12.2‰ at CAL Pond 15 to −4.2‰ at GN Area 6 (Table 7.1). There appears to be no consistent pattern in the DIC data.

7.3.2 α_C and α_D Analysis

Apparent fractionation factors (α_C and α_D) were determined utilizing the $\delta^{13}C$ of the DIC, when available, and the δD of the formation water (Table 7.1). In instances when DIC were not available for analysis the $\delta^{13}C_{CO2}$ from the methane bubble samples were utilized. A wide range of α_C values was observed, from 1.025 to 1.060. The α_D values ranged from 1.115 to 1.586.

Published carbon fractionation factors for methane production reveal in increase in values across the differing methanogenic substrates. The increase goes from acetate (1.01 to 1.03) to

dimethylsulfide (1.04 to 1.05) to CO_2 and trimethylamine having a common range of (1.05 to 1.07) to lastly methanol (1.07 to 1.09) utilization (Conrad, 2005; Whiticar, 1999). Analysis of the calculated apparent alphas from our study sites indicate acetate fermentation as the utilized substrate for methane production in a majority of our sampling sites, with the utilization of CO_2 and TMA limited to only CAL Pond 15 and GN Area 1.

For this study, we were interested in determining if the apparent fractionation factors (α) were able to be utilized as a predictive measure to determine the substrates utilized in our hypersaline environments. Samples collected revealed a calculated apparent alpha range indicating acetate fermentation as the substrate for all sites with the exception of CAL Pond 15 and GN Area 1 which showed utilization of CO_2 and TMA (Table 7.1). From our previous incubation experiments at CAL Pond 15 and GN Area 1 (Chapter 5) we have shown isotopically that methanogens at those sites are utilizing TMA as a substrate for methane production. For the samples collected from GN Area 9, our α calculations suggest the utilization of acetate as a substrate, however, incubation experiments in those locations reveal no utilization of acetate by the methanogens (Chapter 5). Calculations from our higher salinity sites in Guerrero Negro, Laguna San Ignacio and Laguna Figueroa suggest a utilization of acetate as well. We were unable to perform incubation experiments at that location, as such we cannot verify if that substrate is in fact utilized there. We suspect that acetate is not utilized in those locations due to salinity tolerance levels by methanogens who utilize acetate as a substrate (Oren, 1999a).

7.4 Conclusion

In conclusion analysis of $\delta^{18}O$ and δD did confirm that our sampling sites follow the typically expected isotopic shift expected for evaporative basins. The goal of this research was to

determine if the apparent fractionation factors (α) were able to be utilized as a predictive measure to determine the substrates utilized in our hypersaline environments. The use of apparent fractionation factors at our higher salinity gypsum sites did not prove to be predictive of the substrates utilized at those locations. More incubation work in higher salinity gypsum sites should be performed to confirm substrate utilization at those locations.

Table 7.1. Salinity, methane isotopic carbon values, carbon dioxide isotopic values, deuterium isotopic values oxygen isotopic values, and fractionation factors. Error estimates (standard deviations) presented in parentheses. Values that were unable to be determined are depicted in the table as n.d.

Site	Date	Temp	Salinity	Bubble δ13C-CH4	Bubble δ13C-CO2	Bubble δD-CH4	Porewater δ13C-DIC	Overlying water δD-H2O	Overlying water δ18O-H2O	Methane Incubations δ13C (‰)*	Incubation δ2H (‰)	αC from Bubbles*	αC from Incubations	αD from Bubbles	αD from Incubations
Don Edwards															
Pond 15	December 2008	n.d.	105	−62.6 (5.7)	−20.82 (0.35)	−100.8 (39.2)	−12.2 (0.4)	2.6 (0.3)	1.7 (0.02)	n.d.	n.d.	1.054	n.d.	1.115	n.d.
	January 2010	12	126	−65.1 (1.2)	n.d.	−108.0 (14.9)	n.d.	n.d.	n.d.	−62.9 (0.2)	n.d.	n.d.	n.d.	n.d.	n.d.
	August 2010	14	115	−66.0 (7.4)	n.d.	n.d.	n.d.	5.4 (0.3)	3.6 (0.1)	−64.3 (0.3)	n.d.	n.d.	n.d.	n.d.	n.d.
Pond 23	December 2008	n.d.	290	−35.1 (0.7)	−18.55(0.27)	−283.7 (41.8)	−6.4 (1.7)	−28.7 (0.2)	−3.4 (0.04)	n.d.	n.d.	1.030	n.d.	1.356	n.d.
	January 2010	24	320	−40.4 (0.1)	n.d.	−302.7 (2.9)	n.d.	n.d.	n.d.	−41.5 (0.7)	n.d.	n.d.	n.d.	n.d.	n.d.
	August 2010	40	275	−46.3 (1.3)	n.d.	n.d	n.d.	13.4 (0.3)	9.1 (0.1)	−44.5 (1.1)	n.d.	n.d.	n.d.	n.d.	n.d.
Guerrero Negro															
Area 1 site 1	March 2009	23	55	−61.8 (0.9)	−14.24(0.23)	−352.2 (2.9)	−5.6 (0.5)	15.5 (0.4)	2.8 (0.02)	−51.9 (1.6)	-307.63 (1.29)	1.060	1.049	1.568	1.467
Area 1 site 2	March 2009	23	55	−34.9 (0.8)	−13.62(0.07)	−341.6 (0.9)	−5.1 (0.1)	15.5 (0.4)	2.8 (0.02)	−45.6 (0.5)	-291.59 (13.65)	1.031	1.042	1.542	1.433
Area 1	October 2009	31	55	−60.6 (0.2)	−13.86(0.18)	−335.6 (6.2)	−4.9 (1.4)	16.9 (0.8)	3.6 (0.1)	−48.1 (3.4)	-344.06	1.059	1.045	1.531	1.550
Area 4	March 2009	19	93	n.d.	n.d.	n.d.	−3.1 (0.2)	22.8 (0.4)	4.0 (0.02)	−75.4 (7.4)	-397.20 (24.31)	n.d.	n.d.	n.d.	1.697
Area 6	March 2009	18	136	n.d.	n.d.	n.d.	−4.2 (0.1)	28.3 (0.5)	5.1 (0.04)	n.d.	n.d.	n.d.	n.d.	n.d.	n.d.
Area 9 crust	October 2009	25	192	−41.5 (1.4)	−17.65(0.12)	−327.1 (7.9)	n.d.	20.9 (0.4)	5.9 (0.1)	−36.2 (2.8)	-336.75	1.025	n.d.	1.517	1.539
Area 9 rubble	March 2009	22	184	−41.8 (0.3)	−17.24(0.17)	−317.8 (4.3)	n.d.	33.7 (0.8)	5.1 (0.03)	−33.5	-342.37 (10.93)	1.034	1.025	1.515	1.572
Area 9 rubble	October 2009	25	192	−41.5 (1.4)	−17.65(0.12)	−332.7 (5.2)	n.d.	20.9 (0.4)	5.9 (0.1)	−33.1 (0.6)	-345.88	1.025	n.d.	1.530	1.561
Area 9	September 2010	n.d.	190	−43.0 (0.5)	−17.39(0.14)	−344.0 (2.1)	n.d.	n.d.	n.d.	n.d.	n.d.	1.027	n.d.	n.d.	n.d.
Area 9 surface	March 2009	22	184	n.d.	n.d.	n.d.	−9.6 (0.2)	33.7 (0.8)	5.1 (0.03)	−40.9 (1.1)	-239.91 (51.78)	n.d.	n.d.	n.d.	1.360
Area 9 deep sediment	March 2009	22	184	n.d.	n.d.	n.d.	−9.0 (0.9)	33.7 (0.8)	5.1 (0.03)	n.d.	n.d.	n.d.	n.d.	n.d.	n.d.
Area 10-A	March 2009	n.d.	258	−37.0 (0.4)	−10.37(0.15)	−311.2 (1.0)	n.d.	23.2 (0.6)	4.5 (0.02)	n.d.	n.d.	1.028	n.d.	1.485	n.d.
Area 10-B	March 2009	n.d.	306	−34.3 (1.5)	−7.71(0.09)	−253.8 (7.2)	n.d.	4.2 (0.7)	1.2 (0.04)	n.d.	n.d.	1.028	n.d.	1.346	n.d.
Area 10-A	October 2009	28	270	−32.6 (0.9)	−7.19(0.20)	−298.4 (25.8)	n.d.	13.9 (0.5)	5.5 (0.1)	n.d.	n.d.	1.026	n.d.	1.445	n.d.
Area 10-B	October 2009	33	270	−33.8 (0.2)	−9.94(0.14)	−265.8 (8.7)	n.d.	13.9 (0.5)	5.5 (0.1)	n.d.	n.d.	1.025	n.d.	1.381	n.d.
Area 10-C	October 2009	33	298	−36.6 (1.7)	−5.72(0.15)	−266.3 (38.5)	n.d.	10.9 (0.3)	5.0 (0.1)	n.d.	n.d.	1.032	n.d.	1.378	n.d.
Area 11	March 2009	n.d.	300	−35.5 (0.8)	−8.63(0.21)	n.d.	n.d.	17.1 (0.5)	2.8 (0.03)	n.d.	n.d.	1.028	n.d.	n.d.	n.d.
Area 11	October 2009	n.d.	300	−38.6 (2.8)	−6.77(0.23)	−316.1 (1.7)	n.d.	7.1 (0.3)	4.6 (0.1)	n.d.	n.d.	1.033	n.d.	1.473	n.d.
Laguna Figueroa															
	October 2009	n.d.	54-200	−52.2 (14.3)	−14.09(0.08)	−369.0 (8.6)	n.d.	1.0 (8.9)	1.7 (0.9)	n.d.	n.d.	1.040	n.d.	1.586	n.d.
Laguna San Ignicio															
Pond 1	March 2009	n.d.	360	−38.5 (1.0)	−6.79(0.15)	−343.5 (21.1)	n.d.	22.6 (0.6)	5.2 (0.03)	n.d.	n.d.	1.033	n.d.	1.558	n.d.
Pond 2	March 2009	n.d.	300	−35.3 (0.4)	n.d.	−345.7 (7.4)	n.d.	18.9 (0.7)	5.5 (0.04)	n.d.	n.d.	n.d.	n.d.	1.557	n.d.
Pond 3	March 2009	n.d.	342	−39.9 (2.6)	−6.64(0.21)	−327.8 (2.4)	n.d.	17.2 (0.5)	4.0 (0.03)	n.d.	n.d.	1.035	n.d.	1.513	n.d.

Table 7.2. Salinity, methane isotopic carbon values, carbon dioxide isotopic values, deuterium isotopic values, and oxygen isotopic values. Values that were unable to be determined are depicted in the table as n.d.

Site	Date	Salinity	Bubble δ13C-CH4	Bubble δD-CH4	Bubble δ13C-CO2	Porewater δ13C-DIC	Methane Incubations δ13C (‰)*	Incubation δ2H (‰)	Overlying water δD-H2O	Overlying water δ18O-H2O
Guerrero Negro										
Area 1 site 1	March 2009	55	-61.8	-352.2	-14.24	-5.6	-51.9	-307.63	15.5	2.8
Area 1 site 2	March 2009	55	-34.9	-341.6	-13.62	-5.1	-45.6	-291.59	15.5	2.8
Area 1	October 2009	55	-60.6	-335.6	-13.86	-4.9	-48.1	-344.06	16.9	3.6
Area 4	March 2009	93	n.d.	n.d.	n.d.	-3.1	-75.4	-397.2	22.8	4
Area 6	March 2009	136	n.d.	n.d.	n.d.	-4.2	n.d.	n.d.	28.3	5.1
Area 9 crust	October 2009	192	-41.5	-327.1	-17.65	n.d.	-36.2	-336.75	20.9	5.9
Area 9 rubble	March 2009	184	-41.8	-317.8	-17.24	-9.3	-33.5	-342.37	33.7	5.1
Area 9 rubble	October 2009	192	-41.5	-332.7	-17.65	n.d.	-33.1	-345.88	20.9	5.9
Area 9	September 2010	190	-43	-344	-17.39	n.d.	n.d.	n.d.	n.d.	n.d.
Area 9 surface	March 2009	184	n.d.	n.d.	n.d.	n.d.	-40.9	-239.91	33.7	5.1
Area 9 deep sed.	March 2009	184	n.d.	n.d.	n.d.	n.d.	n.d.	n.d.	33.7	5.1

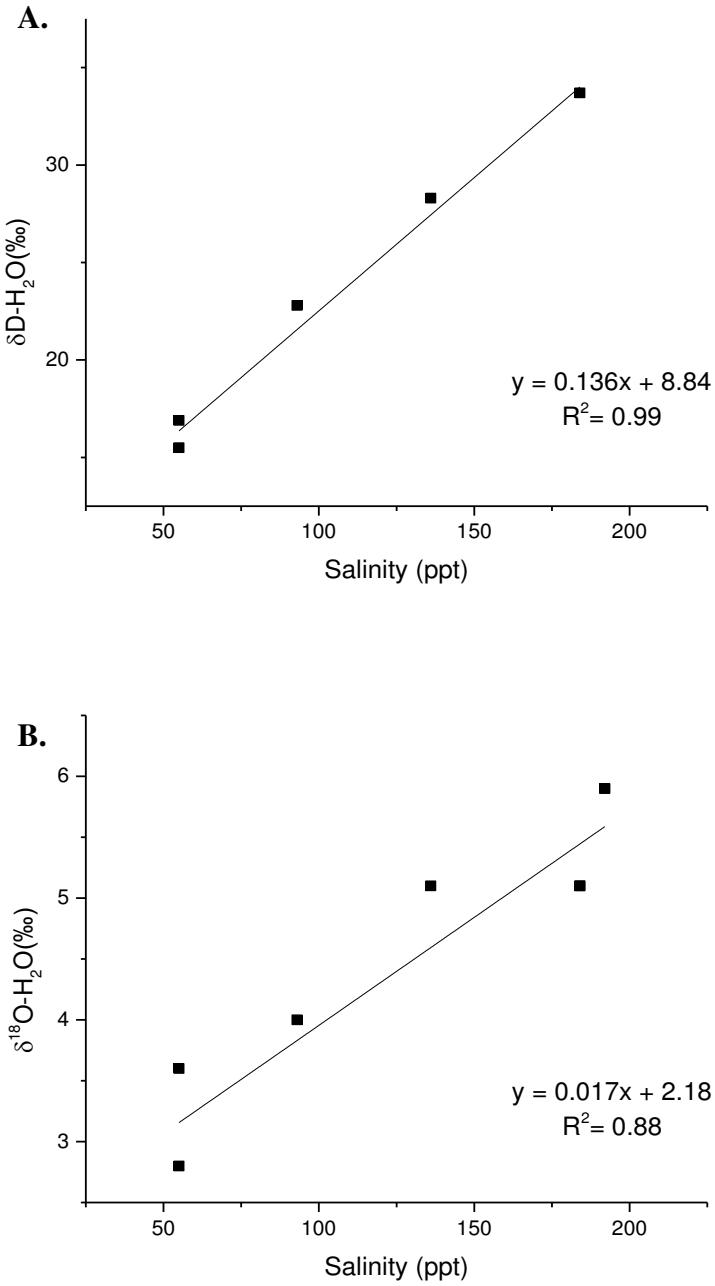

Figure 7.1. δD and $\delta^{18}O$ analysis of overlying water from GN Ponds 1-9. ***(A.)****δD-H_2O vs Salinity of samples collected in Guerrero Negro. (****B).*** *$\delta^{18}O$-H_2O vs Salinity of samples collected in Guerrero Negro.*

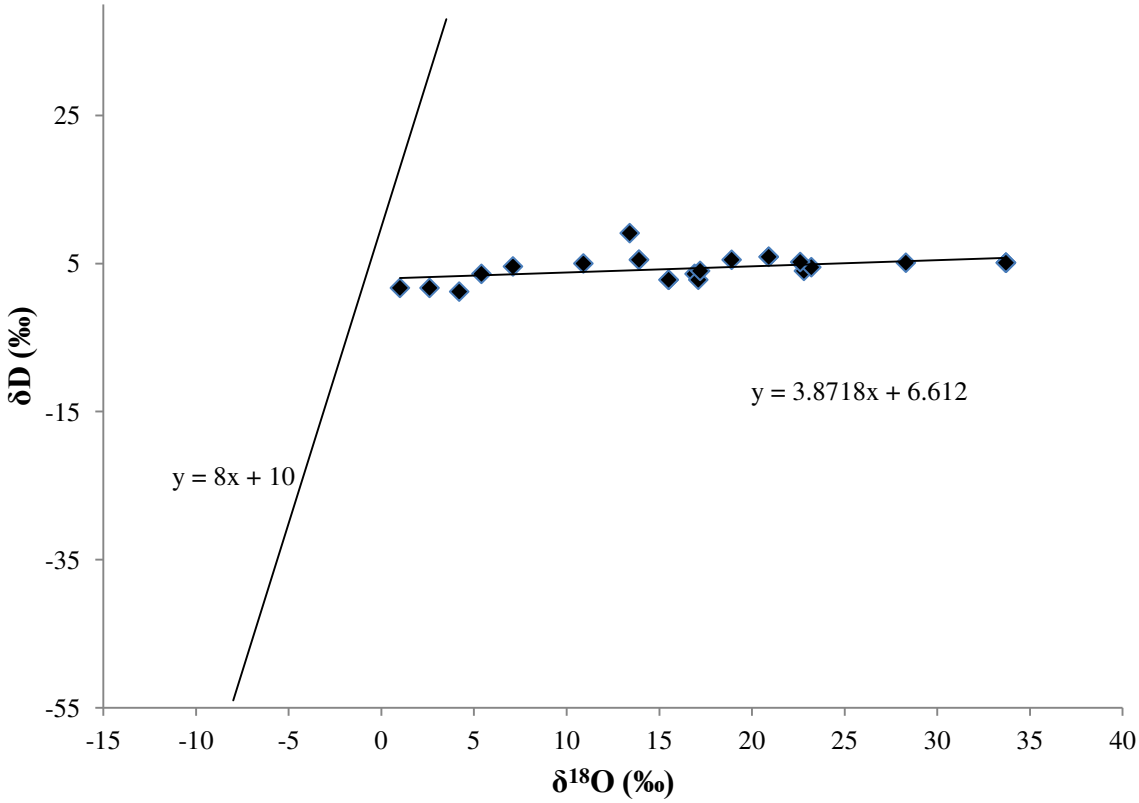

Figure 7.2. δD versus the $\delta^{18}O$ of the overlying water in the pond systems sampled in comparison to the global meteoric water line $\delta D = 8(\delta^{18}O) + 10$.

CHAPTER EIGHT

CONCLUSIONS

The search for life on planets both within and outside of our solar system has increased over the last 75 years. One planet which has received attention and consideration for the potential location of life is Mars. With the recent landing of the Curiosity Rover on the surface of Mars, more information will be available for analyses to determine the extent to which methane, if any, is present in the atmosphere or sediments of Mars. One way to assist in the understanding of data obtained from the Mars Science Laboratory, onboard the Curiosity Rover, is by studying and analyzing information from Mars-like analogue sites. Hypersaline environments have long been considered an analogue site because they exhibit compositional traits such as aridity and brines that are similar to what have been discovered or proposed to exist on Mars.

On Earth, biogenic production of methane accounts for approximately 85% of the total methane production. It has long been wondered the extent to which methane in hypersaline environments originated from biogenic processes. This research reveals that methane production in hypersaline environments are in fact primarily from biogenic production. This discovery led to questions about substrate utilization because biogenic methane production is typically thought to occur primarily from the use of $CO_2 + H_2$ and acetate. However, at the hypersaline environments studied in this research we found that the primary substrate utilized were methylated substrates. The use of these types of substrates had previously been thought of as less of an importance; however, we have shown that in these environments they are the primary source for methane production.

We were able to also conclude that the use of methylated substrates as a primary substrate is a factor of both competition for substrates between methanogens and sulfate reducing bacteria, as well as, the impact salinity has on the microbial population. Comparative analysis between two levels of hyper-salinity reveals that in our lower-salinity brine sites revealed that in competition exists between methanogens and sulfate reducing bacteria for the commonly shared CO_2 and acetate. However, in our higher-salinity extreme brine sites, we observed no competition between the two communities and concluded that the utilization of CO_2 and acetate must not be occurring due to the extreme salinity levels present.

Past research utilizing data on substrate utilization and methanogens community type have played a major role in forming the classification scheme used to differentiate methane production isotopically. This research reveals the importance of isotopic evaluation of methane in hypersaline environments. Previously, methane sources could be characterized by using a combination of $\delta^{13}C_{CH4}$, $\delta^{2}H_{CH4}$, and C_1/C_2 data from the environment. However, the data used to create the classification scheme for methane were derived from various environments, including marine, marsh, wetlands, and lake settings, but little if any of the data had come from hypersaline environments. The isotopic characterization of methane from this research has delineated a region for biogenic methane production from hypersaline environments. These revised boundaries will lessen the possibility that samples obtained from regions similar to those examined in this research will be misinterpreted as having thermoginc, geologic or mixed origin.

Since the conclusion of this research, there has been data returned from the Sample Analysis at Mars (SAM) onboard the NASA Curiosity rover indicating a lack of methane present in the Martian environment (Webster et al., 2013). Curiosity rover analyzed samples of the Martian atmosphere for methane six times from October 2012 through June 2013 and was unable

to detect methane. The conclusions of this report, reduced the upper limit of methane on Mars by approximately 6 times that what was previously expected. Data analysis currently being performed by SAM, as well as MAVEN (the recent departure on November 18th, 2013 of the Mars Atmosphere and Volatile EvolutioN orbiter), should be continued in order to determine if in fact there is no presence of methane in the atmosphere of Mars.

APPENDIX A

BUBBLE SAMPLE DATA

Table A.1. Methane bubble concentration, ethane concentration, methane isotopic carbon values, carbon dioxide isotopic values, deuterium isotopic values from California pond samples collected in December 2008.

California December 2008 Bubble samples													
Sample ID	**CH4 ppm**	**Ethylene ppm**	**Ethane ppm**	**Meth/Eth ratio**	**Avg CH4**	**Std Dev**	**Avg CO2**	**Std Dev**	**Avg H2**	**Std Dev**	**tot avg CH4**	**tot avg CO2**	**alpha C**
Pond 15 +KOH	n.d.	n.d.	n.d.	n.d.	-68.36	0.83	n.d.	n.d.	-134.06	0.12	-62.57	-20.82	1.04
Pond 15 bubble 2	10198.22	0.26	2.39	4275.63	-58.06	0.57	-19.65	0.29	-50.88	0.45			
Pond 15 bubble 3	295739.32	0.07	15.68	18863.26	-66.58	0.33	-20.70	0.26	-130.15	1.49			
Pond 15 bubble 4	30750.11	0.09	9.41	3267.04	-57.27	0.87	-22.10	0.52	-87.91	0.76			
A23 bubble 1	3438.66	2.66	1.09	3148.91	-35.37	0.37	-21.42	0.21	-245.36	43.02	-35.10	-18.55	1.02
A23 bubble 2	6624.05	4.37	3.44	1924.46	-34.40	0.35	-18.81	0.13	-299.70	10.86			
A23 bubble 3	7037.83	2.24	2.76	2553.51	-35.57	0.29	-18.38	0.61	-331.28	16.99			
A23 bubble 4	3459.97	2.36	1.33	2598.18	-35.87	0.39	-18.59	0.29	n.d.	n.d.			
A23 bubble 5	1908.94	2.32	0.82	2332.02	-35.50	0.11	-16.96	0.04	-253.55	3.34			
A23 bubble 6	1973.01	1.05	1.05	1874.21	-35.06	0.29	-18.11	0.09	-242.40	58.08			
A23 bubble 7	2466.02	1.01	1.15	2150.02	-33.90	0.02	-17.56	0.51	-329.97	22.60			

Table A.2. Methane bubble concentration, ethane concentration, methane isotopic carbon values, carbon dioxide isotopic values, deuterium isotopic values from Baja pond samples collected in March 2009.Values that were not determined are depicted in the table as n.d.

March 2009 Bubble Samples													
Sample ID	CH4 ppm's	Ethylene ppm	Ethane ppm	Meth/Eth ratio	Avg CH4	Std Dev	Avg CO2	Std Dev	Avg H2	Std Dev	tot avg CH4	tot avg CO2	alpha C
Pond 9-1	313050.34	n.d.	n.d.	n.d.	-42.38	0.06	-18.17	0.18	-322.70	1.76	-41.80	-17.24	1.03
Pond 9-2	316505.03	n.d.	n.d.	n.d.	-41.86	0.33	-17.71	0.13	-318.09	1.85			
Pond 9-3	332907.72	n.d.	n.d.	n.d.	-41.68	0.08	-17.39	0.02	-320.05	2.12			
Pond 9-4	306560.40	n.d.	n.d.	n.d.	-41.65	0.43	-16.92	0.23	-321.93	1.43			
Pond 9-5	348255.03	n.d.	n.d.	n.d.	-41.79	0.01	-16.34	0.45	-320.64	6.91			
Pond 9-6	316305.37	n.d.	n.d.	n.d.	-41.80	0.00	-17.28	0.15	-315.41	3.40			
Pond 9-7	286077.18	n.d.	n.d.	n.d.	-41.50	0.00	-16.92	0.13	-310.26	2.70			
Pond 9-8	331607.38	n.d.	n.d.	n.d.	-41.71	0.06	-17.21	0.12	-313.69	4.66			
LSI 1A	5160.15	n.d.	n.d.	n.d.	-38.52	0.12	-5.18	0.06	-328.63		-38.49	-6.79	1.03
LSI 1B	3065.50	n.d.	n.d.	n.d.	-39.43	0.26	-5.96	0.37	n.d.				
LSI 1C	7316.30	n.d.	n.d.	n.d.	-37.51	0.09	-9.22	0.01	-358.45				
LSI 2A	41863.71	n.d.	n.d.	n.d.	-35.51	0.04	n.d.	n.d.	-353.47	1.01	-35.26	n.d.	n.d.
LSI 2B	46059.90	n.d.	n.d.	n.d.	-35.45	0.00	n.d.	n.d.	-345.00	1.70			
LSI 2C	56376.20	n.d.	n.d.	n.d.	-34.82	0.02	n.d.	n.d.	-338.77	0.04			
LSI 3A	1108.42	n.d.	n.d.	n.d.	-42.21	0.34	-4.82	n.d.	-326.10		-39.92	-6.64	1.03
LSI 3B	356.50	n.d.	n.d.	n.d.	-40.55	0.00	-10.67	n.d.	n.d.				
LSI 3C	948.75	n.d.	n.d.	n.d.	-37.01	0.31	-4.43	0.21	-329.56				
pond 6-1	21.99	n.d.	n.d.	n.d.	n.d.	n.d.	n.d.	n.d.	n.d.		n.d.	n.d.	n.d.
pond 6-2	22.44	n.d.	n.d.	n.d.	n.d.	n.d.	n.d.	n.d.					
pond 6-3	21.23	n.d.	n.d.	n.d.	n.d.	n.d.	n.d.	n.d.					

Table A.2.continued

March 2009 Bubble Samples													
Sample ID	CH4 ppm's	Ethylene ppm	Ethane ppm	Meth/Eth ratio	Avg CH4	Std Dev	Avg CO2	Std Dev	Avg H2	Std Dev	tot avg CH4	tot avg CO2	alpha C
ESSA A1	464.85	n.d.	n.d.	n.d.	-34.64		-9.20						
ESSA A2	961.12	n.d.	n.d.	n.d.	-35.68	0.23	-8.01	0.00	n.d.		-35.52	-8.63	1.03
ESSA A3	1021.12	n.d.	n.d.	n.d.	-36.23	0.56	-8.68	0.21					
ESSA B1	32.27	n.d.	n.d.	n.d.	-33.56		-5.86						
ESSA B2	36.64	n.d.	n.d.	n.d.	0.00	0.00	n.d.	n.d.	n.d.		-33.56	-5.86	1.03
ESSA B3	42.01	n.d.	n.d.	n.d.	0.00	0.00	n.d.	n.d.					
ESSA C1	9174.28	n.d.	n.d.	n.d.	-37.15	0.06	-10.94	0.17	n.d.				
ESSA C2	7066.83	n.d.	n.d.	n.d.	-37.41	0.09	-9.68	0.09	-310.52		-37.04	-10.37	1.03
ESSA C3	5468.60	n.d.	n.d.	n.d.	-36.54	0.09	-10.48	0.18	-311.93				
ESSA D1	2104.08	n.d.	n.d.	n.d.	-32.53	0.18	-6.24	0.05	-248.67				
ESSA D2	7692.01	n.d.	n.d.	n.d.	-34.88	0.03	-8.79	0.11	n.d.		-34.26	-7.71	1.03
ESSA D3	2574.65	n.d.	n.d.	n.d.	-35.37	0.01	-8.09	0.12	-258.90				
pond1 site1-1	36761.89	n.d.	n.d.	n.d.	-61.80	0.04	-14.16	0.02	-348.65	8.95			
pond1 site1-2	38597.61	n.d.	n.d.	n.d.	-62.25	0.13	-14.50	0.40	-353.61	3.09			
pond1 site1-3	38591.05	n.d.	n.d.	n.d.	-62.36	0.12	-14.98	0.19	-355.74	0.45			
pond1 site1-4	40161.00	n.d.	n.d.	n.d.	-62.14	0.43	-14.77	0.53	-355.17	0.52			
pond1 site1-5	36999.77	n.d.	n.d.	n.d.	-61.49	0.07	-14.73	0.05	-353.33	0.79	-61.80	-14.24	1.05
pond1 site1-6	30278.65	n.d.	n.d.	n.d.	-63.03	0.00	-13.91	0.60	-354.57	3.36			
pond1 site1-7	36341.93	n.d.	n.d.	n.d.	-60.02	0.11	-13.39	0.08	-348.71	2.46			
pond1 site1-8	36643.78	n.d.	n.d.	n.d.	-61.16	0.12	-14.16	0.07	-348.50	2.22			
pond1 site1-9	37546.05	n.d.	n.d.	n.d.	-61.96	0.02	-13.61	0.15	-351.75	0.64			
pond1 site2-1	158908.37	n.d.	n.d.	n.d.	-34.65	0.08	-13.84	0.04	-340.89	4.39			
pond1 site2-2	142511.60	n.d.	n.d.	n.d.	-33.75	0.12	-13.37	0.01	-341.03	0.87			
pond1 site2-3	169353.41	n.d.	n.d.	n.d.	-34.93	0.08	-13.61	0.16	-341.20	2.69	-34.89	-13.62	1.02
pond1 site2-4	141507.62	n.d.	n.d.	n.d.	-35.78	0.08	-13.71	0.03	-343.26	3.25			
pond1 site2-5	151444.11	n.d.	n.d.	n.d.	-35.33	0.09	-13.58	0.11	-341.64	0.84			

Table A.3. Methane bubble concentration, ethane concentration, methane isotopic carbon values, carbon dioxide isotopic values, deuterium isotopic values from Baja pond samples collected in October 2009. Values that were not determined are depicted in the table as n.d.

Baja October 2009 Bubble Samples													
Sample ID	CH4 ppm	Ethylene ppm	Ethane ppm	Meth/Eth ratio	Avg CH4	Std Dev	Avg CO2	Std Dev	Avg H2	Std Dev	tot avg CH4	tot avg CO2	alpha C
Pond 1-1	41621.86	n.d.	34.77	1312.12	-60.55	0.16	-13.12	0.07	-337.23	1.76	-60.65	-13.86	1.05
Pond 1-2	41330.11	n.d.	36.72	1218.22	-60.41	0.13	-14.14	0.73	-332.99	1.41			
Pond 1-3	40263.23	n.d.	33.02	1311.02	-61.01	0.05	-13.93	0.00	-335.67	0.26			
Pond 1-4	34404.66	n.d.	31.10	1207.28	-60.83	0.01	-13.90	0.07	-346.10	1.62			
Pond 1-5	30935.93	n.d.	37.86	1225.72	-60.60	0.28	-14.09	0.05	-327.29	2.64			
Pond 1-6	36781.22	n.d.	35.37	1213.02	-60.49	0.12	-14.00	0.16	-334.12	0.26			
Pond 9-1	355823.40	1.34	24.80	19827.27	-40.42	0.05	-17.06	0.00	-330.25	0.56	-40.90	-17.23	1.02
Pond 9-2	359317.44	n.d.	22.40	18283.03	-37.89	0.35	-16.27	0.12	-318.26	1.46			
Pond 9-3	165827.23	n.d.	10.16	17023.61	-39.99	0.20	-16.90	0.24	-315.80	0.96			
Pond 9-4	177962.24	1.32	12.02	15317.86	-42.21	0.32	-17.60	0.07	-320.67	0.37			
Pond 9-5	308452.69	3.55	26.96	14305.06	-42.14	0.28	-16.50	0.17	-333.97	0.59			
Pond 9-6	381129.93	1.23	8.31	19037.05	-40.46	0.50	-17.54	0.03	-337.10	0.57			
Pond 9-7	306062.55	28.67	21.60	17731.10	-41.60	0.67	-17.74	0.02	-332.36	1.76			
Pond 9-8	200963.85	n.d.	14.26	16477.81	-42.47	0.21	-18.21	0.00	-328.64	0.56			
Pond 9B-1	375668.96	0.79	30.45	12137.28	-42.74	0.22	-17.70	0.34	-327.46	3.23	-41.90	-17.99	1.02
Pond 9B-2	473490.13	1.63	24.36	19029.52	-40.00	0.01	-16.72	0.09	-329.70	1.37			
Pond 9B-3	487095.63	0.78	28.33	16964.19	-40.53	0.02	-16.96	0.00	-333.85	1.61			
Pond 9B-4	379156.87	0.95	30.09	12321.88	-42.65	0.16	-18.06	0.13	-325.77	0.93			
Pond 9B-5	307335.26	1.21	18.54	16833.28	-42.99	0.08	-17.78	0.16	-326.73	2.27			
Pond 9B-6	484526.29	1.07	27.08	17778.34	-40.75	0.26	-17.37	0.30	-337.22	1.82			
Pond 9B-7	442698.03	1.68	28.18	15701.36	-42.36	0.09	-18.62	0.07	-331.84	1.09			
Pond 9B-8	480279.57	0.59	30.79	15526.47	-42.05	0.27	-18.43	0.13	-334.81	0.77			
Pond 9B-9	511431.11	2.19	24.75	20768.43	-42.36	0.18	-18.85	0.09	-338.48	0.51			
Pond 9B-10	507836.70	2.15	25.64	19992.59	-42.55	0.07	-19.38	0.20	-340.78	0.58			

Table A.3.continued

Baja October 2009 Bubble Samples													
Sample ID	**CH4 ppm**	**Ethylene ppm**	**Ethane ppm**	**Meth/Eth ratio**	**Avg CH4**	**Std Dev**	**Avg CO2**	**Std Dev**	**Avg H2**	**Std Dev**	**tot avg CH4**	**tot avg CO2**	**alpha C**
Pond 10-1	12236.55	4.98	105.81	119.60	-33.36	0.11	-6.54	0.22	-318.19				
Pond 10-2	13669.69	3.97	101.79	139.61	-32.95	0.02	-7.65	0.18	-307.95				
Pond 10-3	21913.84	3.23	189.98	116.07	-32.95	0.02	-7.56	0.27	-269.22				
Pond 10-4	2585.86	1.86	25.20	102.02	-31.12	0.05	-6.36	0.28	n.d.				
Pond 10-5	19075.37	3.21	163.79	113.94	-32.66	0.06	-7.84	0.06	n.d.		-33.13	-8.41	1.03
Pond 10-6	75166.21	n.d.	772.85	98.45	-33.99	0.02	-9.27	0.16	-253.15	0.33			
Pond 10-7	81441.67	n.d.	629.24	128.79	-33.87	0.06	-10.47	0.16	-270.71	0.81			
Pond 10-8	80035.03	n.d.	584.96	137.40	-33.65	0.14	-9.99	0.10	-272.08	0.39			
Pond 10-9	80516.74	n.d.	653.36	122.95	-33.60	0.12	-10.03	0.15	-267.30	0.64			
Pond 10C-1	515.00	1.65	1.83	161.25	-37.82	0.13	-7.44	0.27	n.d.				
Pond 10C-2	1288.71	3.07	4.29	185.14	-35.84	0.23	-5.07	0.11	-242.79				
Pond 10C-3	527.82	2.43	2.43	182.84	-37.39	3.54	-6.40	0.16	-310.83		-36.58	-5.72	1.03
Pond 10C-4	1731.36	0.67	1.91	88.53	-36.87	0.86	-5.47	0.12	n.d.				
Pond 10C-5	819.63	2.65	6.27	124.78	-38.00	0.57	-5.08	0.12	-245.41				
Pond 10C-6	1401.73	1.28	3.94	140.80	-33.59	0.29	-4.84	0.09	n.d.				
Pond 11-1	5736.11	2.96	119.42	48.88	-40.60	0.05	-6.71	0.13	n.d.				
Pond 11-2	11133.32	1.97	247.52	42.98	-38.66	0.16	-8.22	0.03	-314.14				
Pond 11-3	7672.36	1.82	122.35	59.51	-37.40	0.48	-7.12	0.40	-316.89				
Pond 11-4	4443.91	4.02	98.08	46.00	-39.94	0.09	-5.84	0.35	-317.38				
Pond 11-5	3372.03	3.15	78.05	43.92	-38.97	0.16	-4.31	0.20	n.d.		-38.61	-6.77	1.03
Pond 11-6	4921.62	4.31	165.00	24.17	-37.72	0.09	-6.56	0.35	n.d.				
Pond 11-7	12220.54	0.35	470.24	22.28	-32.12	0.41	-10.29	0.27	n.d.				
Pond 11-8	411.14	0.58	9.25	44.23	-40.03	0.03	-5.24	0.13	n.d.				
Pond 11-9	679.61	0.48	22.99	29.79	-42.08	1.15	-6.67	0.20	n.d.				
SQ-1	511.88	2.35	1.51	357.19	-75.06	0.20	-13.43	0.01	-358.73				
SQ-2	10201.25	n.d.	10.12	1070.78	-36.47	0.12	-15.22	0.25	n.d.				
SQ-3	1082.86	0.24	2.35	445.25	-62.12	0.24	-14.90	0.02	-373.57				
SQ-4	577.90	0.08	1.64	366.11	-68.03	0.20	-13.51	0.01	-361.02		-52.19	-14.09	1.04
SQ-5	1768.20	0.79	4.58	406.62	-46.61	0.03	-12.33	0.07	-372.96				
SQ-6	1950.50	n.d.	2.84	706.68	-46.16	0.37	-13.45	0.02	-360.66				
SQ-7	4388.02	n.d.	12.49	367.25	-38.03	0.64	-13.82	0.18	-379.42				
SQ-8	3675.09	n.d.	7.38	523.57	-45.07	0.36	-16.07	0.06	-376.65				

Table A.4. Methane bubble concentration, ethane concentration, methane isotopic carbon values, carbon dioxide isotopic values, deuterium isotopic values from California pond samples collected in January 2010. Values that were not determined are depicted in the table as n.d.

California January 2010 Bubble samples													
Sample ID	**CH4 ppm**	**Ethylene ppm**	**Ethane ppm**	**Meth/Eth ratio**	**Avg CH4**	**Std Dev**	**Avg CO2**	**Std Dev**	**Avg H2**	**Std Dev**	**tot avg CH4**	**tot avg CO2**	**alpha C**
Pond A23-1	461565.90	2.92	102.52	4502.21	-40.51	n.d.	n.d.	n.d.	-303.44	1.76			
Pond A23-2	457331.10	2.76	102.38	4467.11	-40.48	n.d.	n.d.	n.d.	-305.74	3.14	-40.43	n.d.	n.d.
Pond A23-3	463300.80	3.16	104.97	4413.60	-40.39	n.d.	n.d.	n.d.	-297.95	2.69			
Pond A23-4	470677.55	8.25	104.92	4485.90	-40.42	n.d.	n.d.	n.d.	-303.14	0.34			
Pond A23-5	466661.32	5.77	103.15	4524.00	-40.37	n.d.	n.d.	n.d.	-303.38	0.68			
Pond 15-1	693947.14	n.d.	56.94	12188.39	-64.53	n.d.	n.d.	n.d.	-99.88	2.06			
Pond 15-2	655027.96	n.d.	52.14	12561.91	-64.84	n.d.	n.d.	n.d.	-98.81	0.38			
Pond 15-3	778451.89	n.d.	29.98	25969.62	-67.24	n.d.	n.d.	n.d.	-134.40	2.56	-65.07	n.d.	n.d.
Pond 15-4	523038.80	n.d.	30.70	17037.64	-64.37	n.d.	n.d.	n.d.	-103.45	1.68			
Pond 15-5	516918.83	2.11	37.51	13779.20	-64.38	n.d.	n.d.	n.d.	-103.84	1.24			

Table A.5. Methane bubble concentration, ethane concentration, methane isotopic carbon values, carbon dioxide isotopic values, deuterium isotopic values from Baja pond samples collected in September 2010. Values that were not determined are depicted in the table as n.d.

Baja September 2010 Bubble Samples													
Sample ID	CH4 ppm	Ethylene ppm	Ethane ppm	Meth/Eth ratio	Avg CH4	Std Dev	Avg CO2	Std Dev	Avg H2	Std Dev	tot avg CH4	tot avg CO2	alpha C
Pond 9-1	234473.13	0.40	16.67	14066.51	-42.96	0.10	-17.27	0.03	-340.03	3.93			
Pond 9-2	16.73	0.32	n.d.	n.d.	n.d.	n.d.	n.d.	n.d.	n.d.	n.d.			
Pond 9-3	444770.13	0.88	27.60	16112.63	-42.22	0.12	-17.69	0.02	-345.01	1.19			
Pond 9-4	423385.49	2.02	31.31	13523.48	-43.88	0.39	-17.24	0.44	-344.16	0.93	-42.97	-17.39	1.03
Pond 9-6	449822.61	0.88	28.79	15622.34	-42.98	0.42	-17.23	0.06	-346.32	0.84			
Pond 9-7	414227.86	0.88	28.21	14682.48	-43.18	0.01	-17.70	0.15	-345.15	1.24			
Pond 9-8	429966.35	0.28	27.47	15654.84	-42.52	0.16	-16.79	0.16	-344.95	1.96			
Pond 9-9	431027.37	4.08	27.90	15448.22	-43.04	0.01	-17.79	0.10	-342.66	1.50			

APPENDIX B

METHANE RATE PRODCUTION DATA

Table B.1. Methane incubation rate production data from Baja pond incubation samples collected in March 2009.

Guerrero Negro March 2009									
	Substrate	**nmol CH4/g: day 1**	**stdev: day 1**	**nmol CH4/g: day 3**	**stdev: day 3**	**nmol CH4/g: day 4**	**stdev: day 4**	**nmol CH4/g: day 7**	**stdev: day 7**
Area 1 Site 1 - March 2009	Control	7.57	1.28	35.35	2.30	58.91	4.15	87.94	10.44
	500uM TMA	14.20	0.43	661.85	8.90	952.52	66.29	1035.54	70.06
	500uM DMS	8.21	0.56	49.21	3.77	62.79	11.26	102.69	18.96
	10uM MMA	7.45	0.74	49.15	1.23	74.51	4.22	100.55	10.78
	10uM Acetate	7.87	1.28	49.47	4.94	70.11	4.44	89.29	6.38
	10uM MeOH	11.02	0.67	56.26	17.36	75.87	19.56	95.84	22.47
	10uM Bicarbonate	8.85	0.26	45.32	7.25	68.10	7.18	89.71	11.23
		nmol CH4/g: day 1	**stdev: day 1**	**nmol CH4/g: day 3**	**stdev: day 3**	**nmol CH4/g: day 4**	**stdev: day 4**	**nmol CH4/g: day 7**	**stdev: day 7**
	Control	39.31	6.72	70.31	8.38	103.45	10.13	130.15	16.07
	500uM TMA	411.76	61.27	1428.02	94.92	1626.53	178.43	1602.93	123.27
	500uM DMS	47.80	11.49	154.70	24.93	247.04	35.23	275.53	40.54
	0.1uM MMA	41.85	2.45	74.41	14.03	102.08	12.45	113.28	13.94
Area 1 Site 2- March 2009	1uM MMA	43.10	4.88	86.59	11.57	110.72	13.83	119.43	15.08
	10uM MMA	52.87	0.66	99.52	9.74	123.80	13.66	128.72	7.59
	0.1uM Acetate	41.34	14.23	86.19	8.14	111.77	8.21	131.24	6.26
	1uM Acetate	45.42	7.58	83.23	9.24	105.73	8.33	125.85	10.90
	10uM Acetate	47.94	3.93	89.67	13.39	120.37	22.94	142.89	31.61
	0.1uM MeOH	39.54	2.30	77.79	4.71	103.67	9.68	123.74	14.50
	1uM MeOH	43.94	5.62	83.85	3.19	109.35	9.28	136.08	8.58
	10uM MeOH	61.78	6.55	108.83	10.02	137.86	14.22	156.56	17.43
	10uM Bicarbonate	46.68	7.80	85.89	10.59	109.42	12.45	133.61	16.44

Table B.1. continued

Guerrero Negro March 2009																	
		nmol CH4/g: day 1	**stdev: day 1**	**nmol CH4/g: day 4**	**stdev: day 4**	**nmol CH4/g: day 5**	**stdev: day 5**	**nmol CH4/g: day 10**	**stdev: day 10**	**nmol CH4/g: day 17**	**stdev: day 17**						
Area 4- March 2009	Control	1.06	0.14	6.30	0.62	12.30	0.83	26.18	2.36	54.72	5.84						
	500uM TMA	1.52	0.26	8.52	1.33	15.22	1.91	35.76	3.50	87.48	10.15						
	500uM DMS	3.16	1.96	7.40	0.76	13.32	1.17	29.47	1.43	52.03	3.00						
	0.1uM MMA	1.24	0.32	7.04	0.52	13.10	0.44	27.14	0.80	53.06	1.53						
	1uM MMA	1.29	0.25	7.38	1.03	14.45	1.93	32.92	4.44	57.64	6.95						
	10uM MMA	1.55	0.05	8.47	0.40	15.88	0.37	32.29	1.31	61.33	4.30						
	0.1uM Acetate	1.71	0.14	7.95	0.93	14.28	1.19	29.25	2.85	57.34	6.42						
	1uM Acetate	1.43	0.17	7.43	0.84	13.49	1.30	28.05	2.99	54.73	6.35						
	10uM Acetate	1.46	0.23	6.06	0.43	11.15	1.31	25.34	1.58	55.21	10.83						
	0.1uM MeOH	1.36	0.79	5.08	2.66	9.68	4.88	20.97	9.85	51.53	26.99						
	1uM MeOH	1.65	0.22	6.36	0.74	11.65	0.54	25.06	1.53	54.87	4.57						
	10uM MeOH	1.45	0.06	5.59	0.42	11.01	0.96	22.76	1.53	47.51	3.53						
	10uM Bicarbonate	1.32	0.15	5.74	0.64	10.84	0.85	23.26	2.30	50.96	6.62						
		nmol CH4/g: day 1	**stdev: day 1**	**nmol CH4/g: day 3**	**stdev: day 3**	**nmol CH4/g: day 9**	**stdev: day 9**	**nmol CH4/g: day 16**	**stdev: day 16**	**nmol CH4/g: day 23**	**stdev: day 23**	**nmol CH4/g: day 30**	**stdev: day 30**				
Area 9 Black Sediment- March 2009	Control	3.00	1.54	2.95	1.04	2.90	1.14	2.80	1.06	2.78	1.14	4.27	1.17				
	500uM TMA	6.55	0.41	6.86	0.42	8.49	2.04	7.16	1.20	14.50	12.24	88.26	118.84				
	500uM DMS	8.84	3.14	9.05	3.20	9.48	3.32	9.24	3.15	8.83	2.96	8.52	2.68				
	0.1uM MMA	3.94	0.97	3.80	0.57	5.97	0.73	3.33	0.39	4.10	0.56	6.08	0.82				
	1uM MMA	2.73	1.63	2.50	1.35	3.25	1.62	2.25	0.82	2.78	1.08	5.19	0.93				
	10uM MMA	2.16	0.31	2.73	0.66	3.36	1.11	2.53	0.51	3.34	1.08	6.57	3.60				
	0.1uM Acetate	2.01	0.50	1.76	0.65	2.63	0.99	1.68	0.58	2.58	0.80	4.88	1.09				
	1uM Acetate	2.66	0.88	1.50	0.58	1.95	0.65	1.49	0.47	2.36	0.46	4.74	1.35				
	10uM Acetate	3.12	0.95	1.42	0.45	2.82	1.18	1.26	0.14	2.30	0.39	5.43	1.04				
	0.1uM MeOH	2.48	1.13	1.32	0.54	1.98	0.71	1.22	0.28	2.83	0.97	5.50	0.43				
	1uM MeOH	1.89	0.90	1.06	0.29	2.48	0.68	1.83	1.02	3.28	1.76	4.95	0.86				
	10uM MeOH	2.54	0.55	1.35	0.72	2.27	1.76	1.50	0.53	3.92	2.48	6.73	3.96				
	10uM Bicarbonate	2.76	1.44	1.24	0.74	2.21	1.12	1.53	0.71	2.87	0.91	4.30	2.03				

Table B.1. continued

Guerrero Negro March 2009																	
		nmol CH4/g: day 1	stdev: day 1	nmol CH4/g: day 3	stdev: day 3	nmol CH4/g: day 9	stdev: day 9	nmol CH4/g: day 16	stdev: day 16	nmol CH4/g: day 23	stdev: day 23	nmol CH4/g: day 30	stdev: day 30				
Area 9 Top Mud-March 2009	Control	12.30	2.76	11.87	2.28	11.55	2.24	13.99	2.55	16.76	1.71	16.81	1.73				
	500uM TMA	10.02	4.84	11.31	1.45	13.06	2.36	36.07	17.38	290.33	77.38	0.00	0.00				
	500uM DMS	11.14	3.80	10.70	2.90	10.71	2.35	12.99	2.81	15.16	2.15	15.60	2.35				
	0.1uM MMA	12.79	2.18	12.35	2.05	11.65	0.33	15.37	1.92	16.77	1.67	17.47	1.95				
	1uM MMA	11.72	1.34	10.87	2.21	10.47	0.71	14.43	0.62	16.46	1.26	16.57	1.15				
	10uM MMA	11.92	2.56	10.40	1.44	10.74	1.59	17.70	3.29	25.54	4.91	26.01	5.86				
	0.1uM Acetate	12.76	2.14	11.27	1.65	12.22	1.56	15.59	1.88	18.22	2.64	17.87	2.21				
	1uM Acetate	12.23	2.84	9.77	1.35	11.14	1.53	14.58	0.95	16.77	0.82	16.88	0.37				
	10uM Acetate	12.34	1.14	9.01	0.82	11.27	2.17	15.32	0.82	16.82	0.52	17.49	0.66				
	0.1uM MeOH	10.32	1.76	9.26	0.80	9.64	0.98	13.03	0.85	15.07	1.09	15.48	0.82				
	1uM MeOH	10.90	2.57	8.84	1.96	9.25	1.65	12.69	2.08	16.93	1.65	17.37	1.36				
	10uM MeOH	12.97	4.13	9.53	0.91	10.75	1.68	18.44	4.80	22.50	2.93	22.54	3.13				
	10uM Bicarbonate	11.72	2.61	9.15	2.39	10.19	2.52	15.07	2.72	17.68	3.29	18.10	2.47				
		nmol CH4/g: day 1	stdev: day 1	nmol CH4/g: day 3	stdev: day 3	nmol CH4/g: day 4	stdev: day 4	nmol CH4/g: day 9	stdev: day 9	nmol CH4/g: day 16	stdev: day 16	nmol CH4/g: day 20	stdev: day 20	nmol CH4/g: day 23	stdev: day 23	nmol CH4/g: day 30	stdev: day 30
Area 9 Crust-March 2009	Control	2.40	1.10	3.01	1.15	3.78	1.14	16.49	6.26	59.51	0.11	69.97	6.17	81.14	7.51		
	500uM TMA	2.44	0.74	4.72	2.56	6.89	3.54	23.33	11.44	155.95	31.88	595.25	43.70				
	500uM DMS	3.77	0.78	4.11	0.90	4.50	0.54	4.67	0.38	5.75	0.83	6.67	0.50	6.24	1.40	7.56	3.05
	1uM MMA	6.67	1.68	2.72	0.09	3.70	0.53	15.68	4.22	60.02	3.08	54.39	4.40				
	10uM Bicarbonate	6.95	0.94	2.61	0.59	4.03	0.17	12.72	2.64	43.92	3.11	48.26	2.02				
	1uM MeOH	7.02	0.33	2.99	0.68	4.89	1.33	21.10	9.40	51.24	6.25	50.84	6.92				
	1uM Acetate	5.08	0.50	3.26	1.12	4.87	0.92	16.48	0.56	58.03	27.15	61.03	32.02				

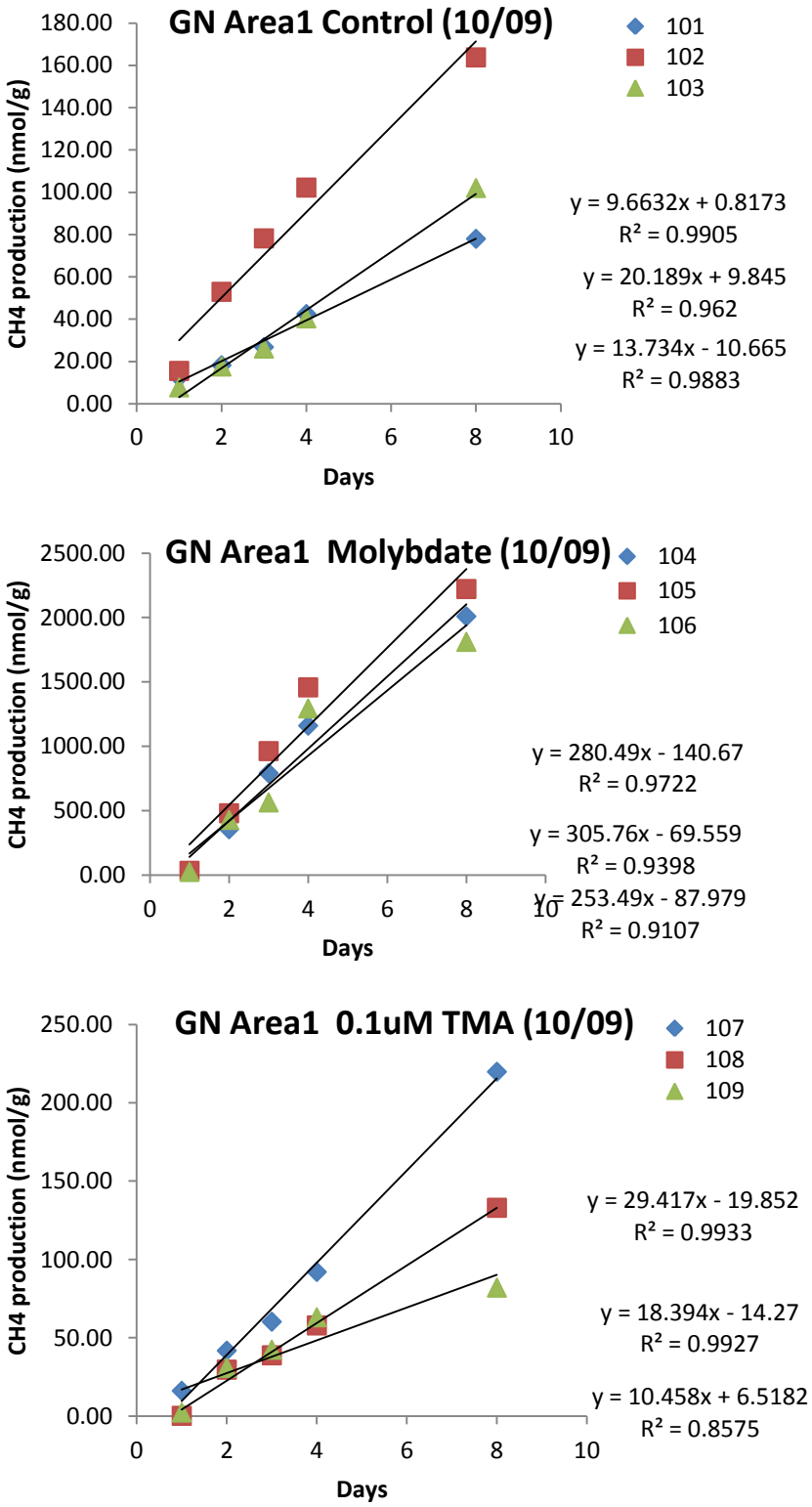

Figure B.1. Methane rate production values for Guerrero Negro Area 1 sampled in October 2009. This chart was conducted for all incubation samples performed in order to calculate rate production values.

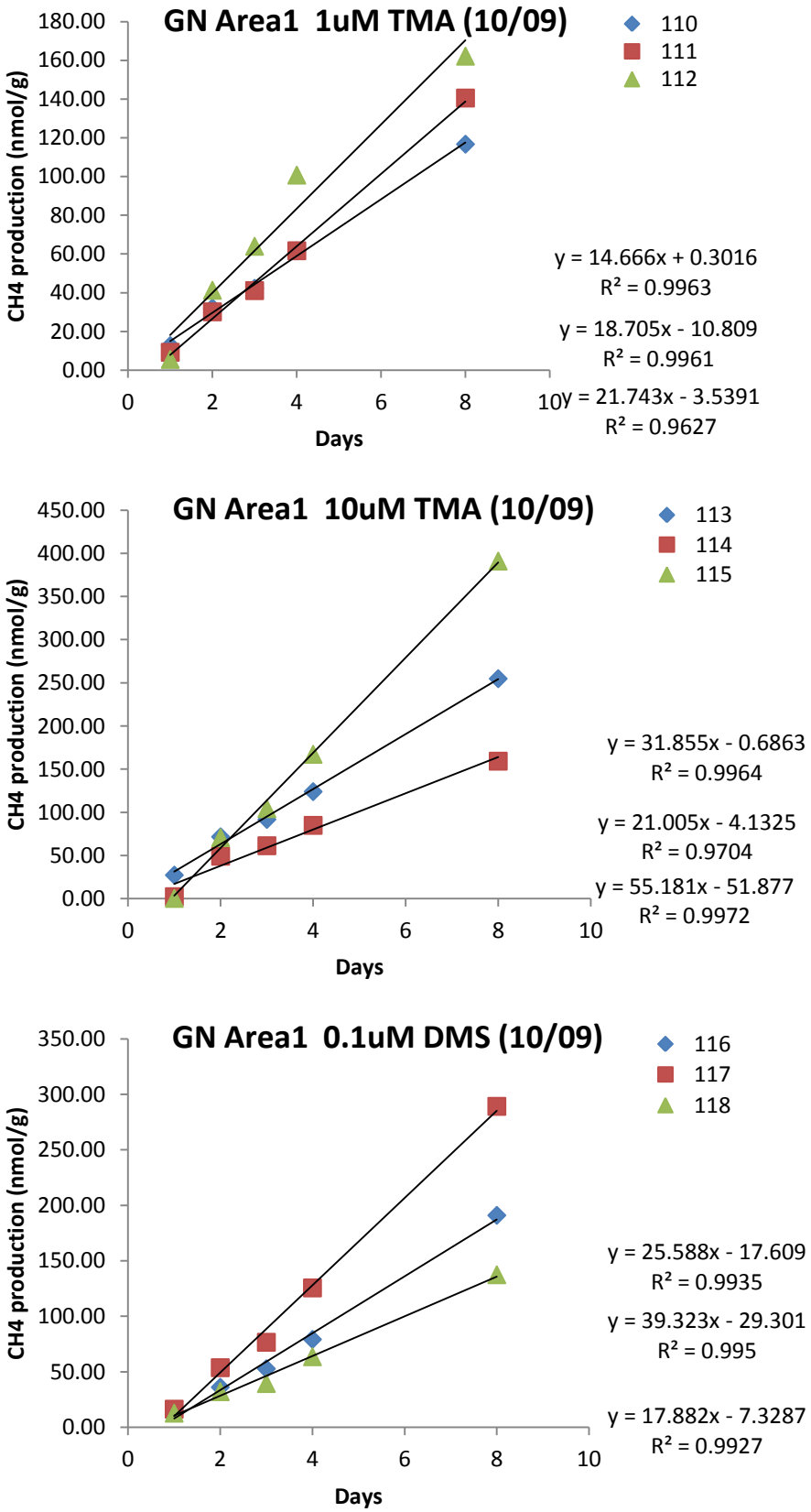

Figure B.1. continued

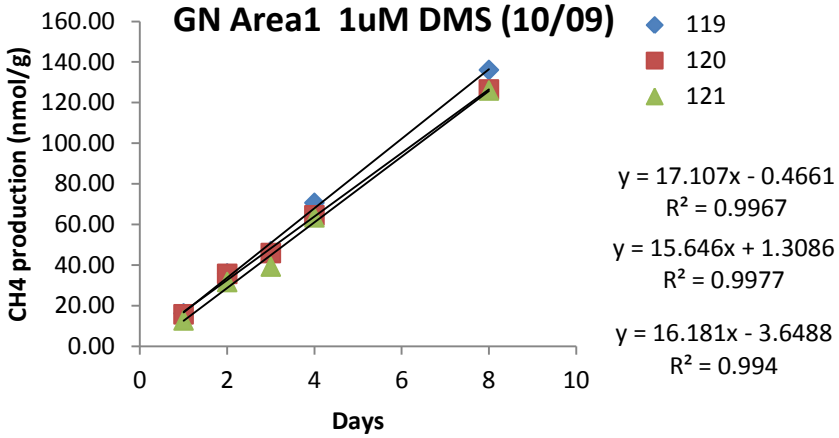

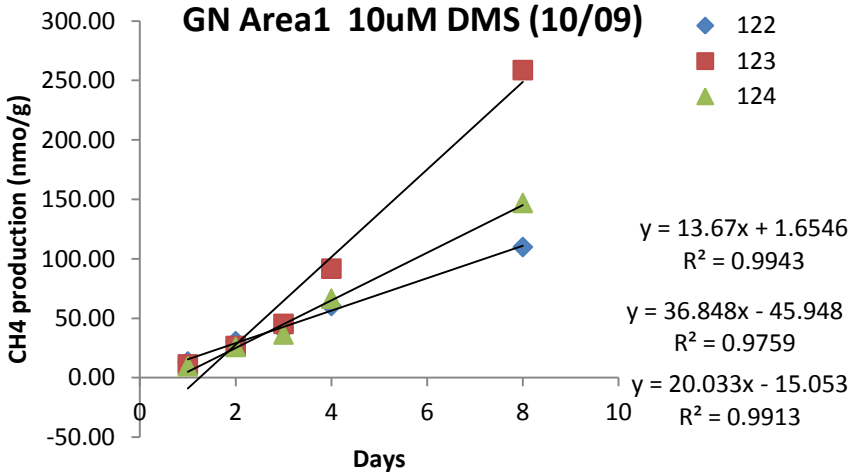

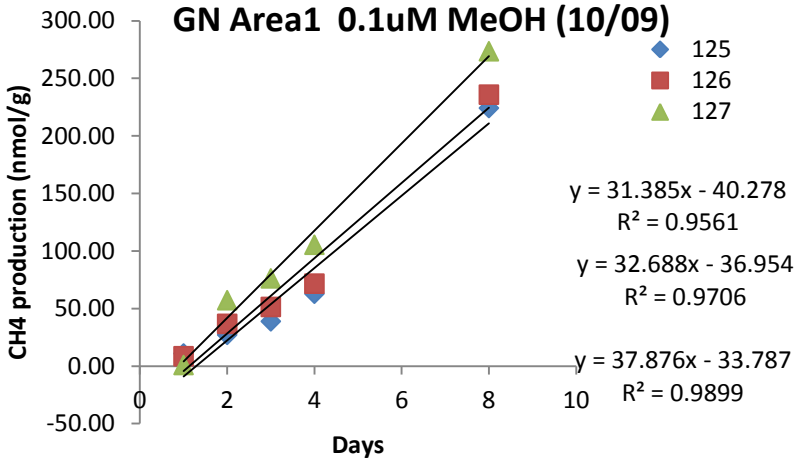

Figure B.1. continued

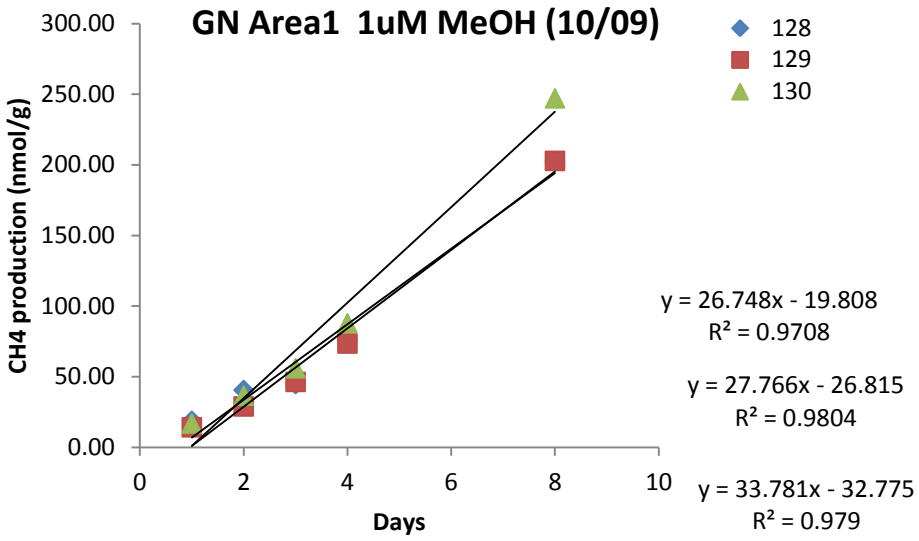

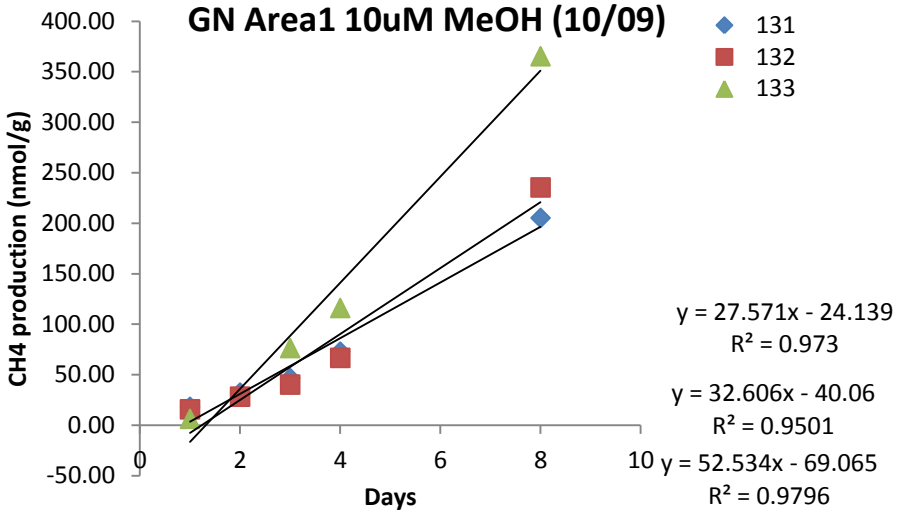

Figure B.1. continued

Table B.2. Methane incubation rate production data from Baja pond incubation samples collected in October 2009.

Guerrero Negro October 2009																	
	Substrate	**nmol CH4/g: day 1**	**stdev: day 1**	**nmol CH4/g: day 2**	**stdev: day 2**	**nmol CH4/g: day 3**	**stdev: day 3**	**nmol CH4/g: day 4**	**stdev: day 4**	**nmol CH4/g: day 8**	**stdev: day 8**						
Area 1 -October 2009	Control	11.96	3.92	29.59	20.21	43.69	29.87	61.68	35.13	114.59	44.25						
	Molybdate	28.41	4.48	421.34	62.51	772.94	199.96	1304.33	148.89	2014.46	205.24						
	0.1uM TMA	6.26	8.67	34.12	6.70	47.20	11.48	71.05	18.39	144.98	69.67						
	1uM TMA	9.16	3.59	34.51	5.94	49.13	12.88	74.68	22.56	139.79	22.73						
	10uM TMA	10.05	15.04	63.90	12.69	85.87	22.09	125.46	41.17	268.48	116.49						
	0.1uM DMS	14.20	1.89	40.62	11.49	56.24	18.82	89.45	32.24	205.85	76.94						
	1uM DMS	14.86	1.89	34.37	2.38	43.99	4.13	66.20	3.88	129.51	5.71						
	10uM DMS	11.50	2.04	27.77	2.59	40.44	4.48	72.84	16.63	171.85	77.45						
	0.1uM MeOH	6.72	5.23	40.25	15.37	55.40	19.00	79.87	22.47	244.42	25.79						
	1uM MeOH	16.58	2.30	35.33	5.88	49.02	6.04	79.05	7.67	217.46	25.64						
	10uM MeOH	13.48	6.30	30.34	2.84	54.50	19.29	85.25	26.91	268.70	85.05						
		nmol CH4/g: day 1	**stdev: day 1**	**nmol CH4/g: day 3**	**stdev: day 3**	**nmol CH4/g: day 5**	**stdev: day 5**	**nmol CH4/g: day 10**	**stdev: day 10**	**nmol CH4/g: day 12**	**stdev: day 12**	**nmol CH4/g: day 18**	**stdev: day 18**	**nmol CH4/g: day 25**	**stdev: day 25**		
	Control	2.26	0.14	3.85	0.32	7.34	2.00			20.66	12.68	39.75	22.73	75.36	31.90		
	Molybdate	3.55	0.46	10.81	0.69	63.55	19.38	1767.46	271.26	0.00	0.00	0.00	0.00	0.00	0.00		
	0.1uM TMA	2.36	0.11	3.81	0.15	6.46	0.24			17.74	2.47	27.91	10.96	60.91	6.52		
	1uM TMA	2.86	0.05	4.46	0.05	7.69	1.74			18.53	7.33	32.82	7.97	64.66	5.75		
	10uM TMA	3.50	0.23	10.00	1.09	16.10	0.64			28.81	8.23	47.92	12.94	81.17	13.81		
Area 4- October 2009	0.1uM DMS	2.74	0.09	4.79	1.14	6.84	0.82			11.18	1.31	19.97	1.64	48.11	0.98		
	1uM DMS	2.42	0.23	5.41	0.44	5.72	0.64			9.93	0.79	15.98	0.92	36.58	3.14		
	10uM DMS	2.63	0.31	4.42	0.87	6.32	1.52			9.34	0.50	18.66	2.09	43.01	8.34		
	0.1uM MeOH	2.40	0.19	3.72	0.19	5.94	0.30			13.57	3.67	23.86	7.05	47.89	10.93		
	1uM MeOH	2.54	0.06	3.82	0.03	5.87	0.33			13.19	2.93	24.23	4.64	46.37	8.21		
	10uM MeOH	3.11	0.11	4.58	0.17	7.22	0.75			9.22	5.68	26.93	3.88	50.80	3.21		
	0.1uM Acetate	2.35	0.04	3.67	0.08	6.76	1.16			11.13	0.60	33.92	2.46	46.03	17.70		
	1uM Acetate	2.38	0.05	3.57	0.10	5.56	0.20			10.95	0.68	21.08	2.06	40.74	6.29		
	10uM Acetate	2.43	0.09	3.58	0.02	5.85	0.70			11.70	2.47	20.88	2.13	37.92	1.67		
	10uM Bicarbonate	2.15	0.13	3.37	0.06	5.10	0.27			10.55	0.98	18.71	1.74	34.69	3.09		

Table B.2 continued

Guerrero Negro October 2009																	
		nmol CH4/g: day 1	stdev: day 1	nmol CH4/g: day 3	stdev: day 3	nmol CH4/g: day 4	stdev: day 4	nmol CH4/g: day 8	stdev: day 8	nmol CH4/g: day 11	stdev: day 11	nmol CH4/g: day 19	stdev: day 19	nmol CH4/g: day 26	stdev: day 26		
Area 9 Rubble-October 2009	Control	0.24	0.02	1.66	0.16	3.84	0.40	15.94	2.27	35.58	12.08						
	Molybdate	0.38	0.09	1.65	0.17	3.13	0.41	10.16	1.36	29.83	3.88						
	0.1uM TMA	0.41	0.11	2.20	0.54	5.45	1.57	20.94	4.13	39.64	5.39						
	1uM TMA	0.44	0.14	2.33	0.58	5.27	1.11	22.44	4.18	44.96	9.39						
	10uM TMA	0.27	0.08	2.04	0.59	4.82	1.29	20.72	5.13	38.35	7.06						
	0.1uM DMS	0.35	0.07	0.68	0.13	0.86	0.17	2.56	0.51	6.59	1.46	13.42	5.10	15.28	6.65		
	1uM DMS	0.42	0.06	0.86	0.13	1.21	0.18	2.95	0.41	6.99	0.74	12.99	1.69	15.62	2.59		
	10uM DMS	0.43	0.15	0.87	0.24	1.19	0.31	3.27	0.49	7.32	0.32	13.04	0.92	14.98	0.66		
	0.1uM MeOH	0.34	0.21	2.20	0.68	5.13	1.48	21.72	5.63	38.89	11.08						
	1uM MeOH	0.26	0.07	2.09	0.38	5.45	0.88	22.86	3.33	39.76	8.91						
	10uM MeOH	0.35	0.14	2.15	0.55	5.55	1.44	22.22	5.84	45.26	10.10						
	0.1uM Acetate	0.52	0.19	2.09	0.44	4.78	1.30	17.94	5.04	27.27	7.17						
	1uM Acetate	0.34	0.15	1.90	0.47	4.84	1.04	19.60	2.92	35.63	3.64						
	10uM Acetate	0.36	0.11	1.99	0.18	4.95	0.58	21.43	3.28	44.94	12.93						
	10uM Bicarbonate	0.26	0.14	1.28	0.40	3.28	1.11	12.99	3.62	21.69	4.80						
	Killed Control	0.19	0.10	0.47	0.16	0.60	0.16	1.04	0.39	1.21	0.32	2.02	0.62	2.01	0.39		
		nmol CH4/g: day 0.5	stdev: day 0.5	nmol CH4/g: day 2	stdev: day 2	nmol CH4/g: day 3	stdev: day 3	nmol CH4/g: day 8	stdev: day 8								
Area 9 crust-October 2009	Control	1.48	0.14	10.80	0.43	23.67	1.82	128.23	7.42								
	Molybdate	1.38	0.36	10.25	1.81	20.96	3.52	118.67	15.77								
	0.1uM TMA	2.07	0.89	12.81	2.91	27.71	5.61	23.73	2.31								
	1uM TMA	1.29	0.10	9.16	1.16	19.54	2.30	23.23	3.19								
	10uM TMA	1.55	0.35	11.37	1.69	24.52	3.28	19.89	7.60								
	0.1uM DMS	1.66	0.65	6.85	1.89	9.81	2.16	35.86	4.26								
	1uM DMS	1.26	0.29	6.00	0.94	8.49	1.63	34.06	5.18								
	10uM DMS	1.76	0.30	7.58	0.70	11.50	1.21	42.43	5.22								
	0.1uM MeOH	1.44	0.20	10.54	1.11	21.48	2.33	106.86	12.36								
	1uM MeOH	2.51	2.26	19.70	16.92	40.45	33.62	191.82	165.74								
	10uM MeOH	1.39	0.08	9.43	0.95	20.29	2.00	100.27	9.16								
	0.1uM Acetate	1.74	0.34	11.62	1.17	23.93	2.05	122.12	12.51								
	1uM Acetate	1.45	0.13	9.66	0.97	20.85	2.79	107.04	3.15								
	10uM Acetate	1.27	0.12	8.96	0.92	18.84	2.05	107.10	11.85								
	10uM Bicarbonate	1.71	0.26	11.69	1.70	24.50	3.28	130.72	17.50								

Table B.3. Methane incubation rate production data from California pond incubation samples collected in January 2010.

California January 2010																	
	Substrate	**nmol CH4/g: day 0.25**	**stdev: day 0.25**	**nmol CH4/g: day 2**	**stdev: day 2**	**nmol CH4/g: day 3**	**stdev: day 3**	**nmol CH4/g: day 4**	**stdev: day 4**	**nmol CH4/g: day 6**	**stdev: day 6**						
Pond 15-January 2010	control	5.77	1.36	7.31	1.65			8.77	1.36	9.83	1.49						
	molybdate	7.55	0.79	25.28	2.89			55.99	6.46	99.88	10.81						
	0.1 µM TMA	4.19	0.27	5.85	0.54			6.73	0.67	7.44	0.75						
	1 µM TMA	5.64	0.60	8.24	0.99			9.47	1.10	10.55	1.21						
	10 µM TMA	6.61	2.17	25.37	7.11			26.72	5.18	28.07	5.36						
	0.1 µM MeOH	4.77	0.25	6.80	0.67			7.74	0.87	8.63	0.81						
	1 µM MeOH	4.24	0.13	5.41	0.67			7.20	1.34	8.41	1.75						
	10 µM MeOH	5.17	0.40	9.66	1.81			11.51	0.81	12.70	1.03						
	0.1 µM acetate	4.26	0.53	5.67	1.02			7.37	1.21	9.32	2.51						
	1 µM acetate	3.66	0.45	4.97	0.34			6.09	0.40	6.95	0.23						
	10 µM acetate	3.50	0.20	4.65	0.21			5.59	0.08	6.35	0.20						
	10 µM bicarbonate	4.36	0.29	6.02	0.85			7.33	0.82	8.39	1.06						
	killed control *	2.60	0.61	2.69	0.67			2.63	0.61	2.60	0.62						
	10 µM TMA (no label)	7.86	0.62	17.70	0.94			18.89	1.28	20.54	1.85						
	100 µM TMA (no label)	7.11	1.25	78.61	15.83	110.67	33.12										
	1000 µM TMA (no label)	7.88	0.64	90.92	2.30	185.82	2.32										
	10 µM DMS (no label)	6.19	0.35	8.79	0.43	0.00	0.00	11.53	1.54	12.03	0.73						
	100 µM DMS (no label)	10.83	0.75	16.44	3.14	19.23	4.17	20.88	3.73	19.64	1.02						
	1000 µM DMS (no label)	13.68	0.94	177.39	14.31	274.74	21.16										
		nmol CH4/g: day 1	**stdev: day 1**	**nmol CH4/g: day 3**	**stdev: day 3**	**nmol CH4/g: day 5**	**stdev: day 5**	**nmol CH4/g: day 7**	**stdev: day 7**								
Pond A23-January 2010	control	0.35	0.29	0.65	0.39	1.04	0.48	1.56	0.67								
	molybdate	0.17	0.05	0.47	0.14	0.80	0.19	1.45	0.39								
	0.1 µM TMA	0.18	0.08	0.46	0.20	1.03	0.27	1.28	0.53								
	1 µM TMA	0.26	0.08	0.57	0.11	1.02	0.17	1.69	0.25								
	10 µM TMA	0.24	0.04	0.63	0.11	1.24	0.20	1.95	0.26								
	0.1 µM MeOH	0.24	0.06	0.53	0.09	0.87	0.17	1.34	0.21								
	1 µM MeOH	0.27	0.06	0.59	0.23	1.09	0.18	1.61	0.25								
	10 µM MeOH	0.43	0.24	0.74	0.25	1.12	0.16	1.60	0.29								
	0.1 µM acetate	0.55	0.19	1.01	0.31	1.60	0.83	1.88	0.54								
	1 µM acetate	0.39	0.09	0.75	0.18	1.21	0.30	1.47	0.36								
	10 µM acetate	0.41	0.17	0.75	0.33	1.22	0.57	1.48	0.74								
	10 µM bicarbonate	0.45	0.14	0.94	0.25	1.46	0.37	1.82	0.43								
	killed control *	0.43	0.14	0.57	0.04	0.59	0.04	0.74	0.13								
	10 µM TMA (no label)	0.33	0.04	0.76	0.10	1.51	0.19	2.13	0.24								
	100 µM TMA (no label)	0.23	0.14	0.50	0.30	0.93	0.54	1.28	0.77								
	1000 µM TMA (no label)	0.25	0.11	0.50	0.20	0.95	0.36	1.38	0.50								
	10 µM DMS (no label)	0.99	0.14	1.44	0.47	1.47	0.34	1.80	0.36								
	100 µM DMS (no label)	1.01	0.21	1.11	0.23	1.23	0.21	1.36	0.19								
	1000 µM DMS (no label)	0.83	0.02	0.79	0.21	1.06	0.06	1.12	0.07								

Table B.4. Methane incubation rate production data from California pond incubation samples collected in August 2010.

California August 2010													
	Substrate	**nmol CH4/g: day 1**	**stdev: day 1**	**nmol CH4/g: day 3**	**stdev: day 3**	**nmol CH4/g: day 5**	**stdev: day 5**	**nmol CH4/g: day 11**	**stdev: day 11**	**nmol CH4/g: day 34**	**stdev: day 34**	**nmol CH4/g: day 36**	**stdev: day 36**
Pond 15-August2010	control	4.41	0.32	4.84	0.30	4.98	0.38	5.47	0.44			6.59	0.55
	molybdate	5.12	0.40	9.98	1.20	12.82	0.82	24.67	2.81	90.53	4.08	102.96	
	0.1 µM TMA	4.26	0.07	4.69	0.21	6.34	0.91	5.75	0.81	6.52	0.85		
	1 µM TMA	5.29	0.64	6.02	0.64	7.16	1.85	7.12	1.64	7.57	0.72		
	10 µM TMA	5.62	0.50	15.50	1.10	17.79	2.63	17.50	1.93	18.57	2.21		
	0.1 µM MeOH	4.22	0.32	4.88	0.56	6.41	0.96	4.93	0.62	8.35	3.77		
	1 µM MeOH	4.44	0.51	5.19	1.11	6.48	0.57	5.19	1.61	6.51	2.18		
	10 µM MeOH	4.59	0.51	6.61	1.11	7.65	0.57	7.55	1.61	8.95	2.18		
	0.1 µM acetate	4.24	0.41	4.63	0.47	5.71	1.35	5.05	0.49	5.92	0.52		
	1 µM acetate	4.44	0.10	4.85	0.14	6.75	0.24	4.89	0.44	6.23	0.19		
	10 µM acetate	4.08	0.38	4.49	0.30	5.87	0.29	5.05	0.56	7.65	3.58		
	10 µM bicarbonate	4.06	0.17	4.77	0.12	6.60	1.22	5.23	0.05	6.49	0.13		
	10 µM TMA	4.98	0.29	15.84	0.37	18.55	1.01	18.26	0.96	21.40	5.25		
	100 µM TMA	5.06	0.52	21.02	0.78	69.74	1.11						
	1000 µM TMA	5.15	0.53	19.44	0.98	56.65	4.36						
	10 µM DMS	4.06	0.38	4.63	0.36	5.08	0.47	5.09	0.30	8.10	3.96		
	100 µM DMS	5.35	0.12	6.86	0.37	7.53	0.21	7.51	0.36	8.60	0.37		
	1000 µM DMS	0.00	0.00	22.45	1.66	23.98	2.58	25.35	3.16	26.91	2.56		
		nmol CH4/g: day 1	**stdev: day 1**	**nmol CH4/g: day 3**	**stdev: day 3**	**nmol CH4/g: day 5**	**stdev: day 5**	**nmol CH4/g: day 11**	**stdev: day 11**	**nmol CH4/g: day 13**	**stdev: day 13**	**nmol CH4/g: day 34**	**stdev: day 34**
Pond A23-August2010	control	6.17	0.812827	8.83	1.132784	11.99	1.591008	20.78	2.667885			56.36	3.358705
	molybdate	3.82	0.506075	6.31	0.825841	9.52	1.305977	15.59	2.333492			57.36	2.93232
	0.1 µM TMA	5.24	0.63795	7.75	0.888886	10.76	1.245219	20.12	2.420494			51.37	6.653632
	1 µM TMA	3.53	0.329369	5.21	0.492424	7.51	0.638529	13.06	1.165421				
	10 µM TMA	2.59	0.534072	3.83	0.764393	5.49	1.057421	9.46	2.045603				
	0.1 µM MeOH	2.00	1.451713	2.99	2.133336	4.22	2.953277	8.80	6.633086	5.75			
	1 µM MeOH	1.46	2.053854	2.12	2.99611	2.87	4.195685	5.25	7.343298				
	10 µM MeOH	4.57	0.925106	6.47	1.262736	8.98	1.77749	16.46	3.407698			46.86	3.245284
	0.1 µM acetate	3.44	0.201216	5.28	0.3135	7.49	0.350547	14.03	0.580364			42.88	2.122346
	1 µM acetate	3.48	0.385768	5.32	0.5789	7.57	0.868322	12.40	1.352715			40.33	8.682001
	10 µM acetate	3.07	0.480873	4.65	0.780468	6.59	0.963502	11.95	1.461911			39.30	
	10 µM bicarbonate	3.85	0.638965	5.86	0.875191	8.29	1.190325	15.38	2.305079			44.63	
	10 µM TMA	2.93	0.659996	4.42	1.119564	6.27	1.649652	11.69	3.324235				
	100 µM TMA	2.11	1.855952	3.20	2.799982	4.46	3.925392	8.29	7.390163			20.88	36.16016
	1000 µM TMA	2.40	1.319809	3.58	1.976644	4.98	2.70307	8.95	4.773515				
	10 µM DMS	3.97	0.608967	5.91	0.882734	7.98	1.226478	14.63	2.082835				
	100 µM DMS	4.07	0.885696	6.33	1.283104	8.66	1.72753	16.42	3.413838			34.60	30.00665
	1000 µM DMS	2.78	0.462131	4.37	0.605533	6.19	0.87225	11.72	1.360093				
	killed control	2.70	1.062447	3.37	1.513247	3.58	1.490776	3.74	1.597588			3.17	1.251001
	1000 DMS unflushed	1.88	1.056852	2.18	1.144631	2.65	1.366832	3.45	1.523078			10.74	4.91607

APPENDIX C

INCUBATION ISOTOPE DATA

Table C.1. Methane incubation rate production data, methane isotopic data from Baja pond incubation samples collected in March 2009. Values that were not determined are depicted in the table as n.d.

Guerrero Negro										
Date	**Site**	**Substrate**	**CH4 production (nmol g-1 d-1)**	**CH4 production std dev**	**δ13C-CH4 (‰)**	**stdev**	**δ13C-CO2 (‰)**	**stdev**	**δ2H-CH4 (‰)**	**stdev**
March 2009	Area 1 site 1	Control	13.50	2.14	-51.89	1.57	-15.31	1.08	-307.63	1.29
		500uM TMA	163.60	12.91	-48.95	0.27	-15.80	0.85	-374.20	25.72
		500uM DMS	15.46	3.45	-56.75	0.75	-13.43	0.05	-294.87	11.31
		10uM MMA	15.36	2.03	4179.56	450.24	-10.43	1.25	-322.05	21.49
		10uM Acetate	13.28	1.37	-46.77	0.65	-6.54	1.26	-262.16	38.54
		10uM MeOH	13.75	3.43	3190.70	1093.46	-10.14	2.25	-173.93	88.82
		10uM Bicarbonate	13.34	1.84	-48.07	n.d.	-8.44		-300.78	53.05
March 2009	Area 1 site 2	Control	15.36	3.50	-45.56	0.48	-16.50	2.61	-291.59	13.65
		500uM TMA	182.00	17.30	-46.64	0.06	-17.83	0.19	-399.07	12.75
		500uM DMS	37.85	5.07	-63.51	0.40	-15.08	0.25	-307.35	25.94
		0.1uM MMA	11.88	2.12	-19.45	0.35	-17.61	0.81	-290.72	7.55
		1uM MMA	12.39	2.21	381.87	42.94	-17.30	2.09	-305.71	7.27
		10uM MMA	12.23	1.08	5761.23	627.94	-7.62	2.09	-334.28	14.27
		0.1uM Acetate	14.72	1.25	-44.69	0.76	-17.72	0.81	-308.65	15.98
		1uM Acetate	13.23	2.29	-44.16	0.60	-16.61	1.71	-293.38	24.56
		10uM Acetate	15.75	5.21	-44.66	2.12	-2.82	2.62	-318.83	1.41
		0.1uM MeOH	13.92	2.34	-24.44	17.89	-16.09	1.61	-311.62	21.26
		1uM MeOH	11.24	6.49	254.12	82.36	-13.88	1.33	-277.28	26.42
		10uM MeOH	15.56	2.25	2828.74	2499.47	-4.81	0.10	-92.15	108.04
		10uM Bicarbonate	14.33	1.83	-44.52	5.78	-1.81	0.72	-304.14	0.91

Table C.1 continued

Guerrero Negro										
Date	**Site**	**Substrate**	**CH4 production (nmol g-1 d-1)**	**CH4 production std dev**	**δ13C-CH4 (‰)**	**stdev**	**δ13C-CO2 (‰)**	**stdev**	**δ2H-CH4 (‰)**	**stdev**
March 2009	Area 4	Control	3.41	0.38	-75.37	7.45	n.d.	n.d.	-397.20	24.31
		500uM TMA	5.46	0.63	-77.59	0.11	n.d.	n.d.	-399.03	11.25
		500uM DMS	3.17	0.20	-70.25	0.43	n.d.	n.d.	-417.89	38.31
		0.1uM MMA	3.29	0.08	-71.97	1.43	n.d.	n.d.	-432.56	52.08
		1uM MMA	3.63	0.36	-68.25	0.93	n.d.	n.d.	-428.78	3.46
		10uM MMA	3.79	0.27	-46.33	4.91	n.d.	n.d.	-410.57	37.12
		0.1uM Acetate	3.53	0.39	-70.85	1.66	n.d.	n.d.	-381.71	5.16
		1uM Acetate	3.38	0.40	-70.83	0.35	n.d.	n.d.	-406.79	30.10
		10uM Acetate	3.43	0.68	-67.56	2.17	n.d.	n.d.	-413.87	24.40
		0.1uM MeOH	3.18	1.67	-67.82	4.36	n.d.	n.d.	-401.50	8.18
		1uM MeOH	3.38	0.29	-70.21	1.54	n.d.	n.d.	-407.58	9.26
		10uM MeOH	2.93	0.22	-62.37	0.79	n.d.	n.d.	-434.26	10.90
		10uM Bicarbonate	3.15	0.41	-69.07	1.26	n.d.	n.d.	-412.14	0.76
March 2009	Area 9 Blk Sed	Control	0.03	0.01	-49.45	1.64	n.d.	n.d.	n.d.	n.d.
		500uM TMA	2.13	3.13	-70.11	9.33	n.d.	n.d.	n.d.	n.d.
		500uM DMS	0.00	0.01	-43.00	0.60	n.d.	n.d.	n.d.	n.d.
		0.1uM MMA	0.04	0.04	-28.33	n.d.	n.d.	n.d.	n.d.	n.d.
		1uM MMA	0.06	0.03	2136.06	n.d.	n.d.	n.d.	n.d.	n.d.
		10uM MMA	0.11	0.09	n.d.	n.d.	n.d.	n.d.	n.d.	n.d.
		0.1uM Acetate	0.08	0.03	-52.47	0.92	n.d.	n.d.	n.d.	n.d.
		1uM Acetate	0.07	0.04	-52.84	7.28	n.d.	n.d.	n.d.	n.d.
		10uM Acetate	0.07	0.06	-47.32	3.31	n.d.	n.d.	n.d.	n.d.
		0.1uM MeOH	0.10	0.03	243.59	4.37	n.d.	n.d.	n.d.	n.d.
		1uM MeOH	0.10	0.05	2282.25	18.89	n.d.	n.d.	n.d.	n.d.
		10uM MeOH	0.14	0.10	23829.30	n.d.	n.d.	n.d.	n.d.	n.d.
		10uM Bicarbonate	0.06	0.03	-41.43	12.45	n.d.	n.d.	n.d.	n.d.

Table C.1 continued

Guerrero Negro										
Date	**Site**	**Substrate**	**CH4 production (nmol g-1 d-1)**	**CH4 production std dev**	**δ13C-CH4 (‰)**	**stdev**	**δ13C-CO2 (‰)**	**stdev**	**δ2H-CH4 (‰)**	**stdev**
March 2009	Area 9 Top Mud	Control	0.19	0.06	-40.88	1.59	n.d.	n.d.	-239.92	51.78
		500uM TMA	10.93	3.13	-67.92	0.97	n.d.	n.d.	n.d.	n.d.
		500uM DMS	0.18	0.04	-41.21	0.82	n.d.	n.d.	-280.13	2.80
		0.1uM MMA	0.20	0.02	103.47	4.84	n.d.	n.d.	-284.63	11.26
		1uM MMA	0.22	0.05	2825.50	42.35	n.d.	n.d.	3.52	427.40
		10uM MMA	0.60	0.19	34563.32		n.d.	n.d.	-366.79	102.01
		0.1uM Acetate	0.24	0.07	-33.37	1.18	n.d.	n.d.	27.81	507.47
		1uM Acetate	0.24	0.07	-39.35	0.70	n.d.	n.d.	-59.92	351.77
		10uM Acetate	0.26	0.04	-33.53	1.95	n.d.	n.d.	n.d.	n.d.
		0.1uM MeOH	0.23	0.08	238.29	23.51	n.d.	n.d.	-320.71	237.88
		1uM MeOH	0.30	0.08	2397.87	66.58	n.d.	n.d.	n.d.	n.d.
		10uM MeOH	0.47	0.08	27171.89	n.d.	n.d.	n.d.	n.d.	n.d.
		10uM Bicarbonate	0.31	0.05	-37.85	2.25	n.d.	n.d.	n.d.	n.d.
March 2009	Area 9 Crust	Control	3.91	0.40	-33.51	n.d.	n.d.	n.d.	-342.35	10.93
		500uM TMA	26.08	2.31	-56.69	n.d.	n.d.	n.d.	-444.96	51.17
		500uM DMS	0.12	0.06	-46.76	n.d.	n.d.	n.d.	-246.80	n.d.
		1uM MMA	3.24	0.05	10305.97	n.d.	n.d.	n.d.	-328.25	n.d.
		10uM Bicarbonate	2.60	0.12	6.39	n.d.	n.d.	n.d.	-303.22	n.d.
		1uM MeOH	2.86	0.38	9354.09	n.d.	n.d.	n.d.	232.29	n.d.
		1uM Acetate	3.45	1.92	309.28	n.d.	n.d.	n.d.	-318.44	n.d.

Table C.2. Methane incubation rate production data, methane isotopic data from Baja pond incubation samples collected in October 2009. Values that were not determined are depicted in the table as n.d.

Guerrero Negro										
Date	**Site**	**Substrate**	**CH4 production (nmol g-1 d-1)**	**CH4 production std dev**	**δ13C-CH4 (‰)**	**stdev**	**δ13C-CO2 (‰)**	**stdev**	**δ2H-CH4 (‰)**	**stdev**
October 2009	Area 1	Control	14.52	5.30	-48.07	3.41	-14.54	1.00	-344.06	0.00
		Molybdate	279.83	26.15	-34.95	0.05	-8.15	0.23	-392.76	15.40
		0.1uM TMA	19.42	9.52	8.90	15.49	-18.35	5.77	-361.95	n.d.
		1uM TMA	18.37	3.55	600.94	209.05	-13.22	0.47	-397.99	n.d.
		10uM TMA	36.01	17.47	5601.88	2846.77	-18.62	21.40	-327.52	n.d.
		0.1uM DMS	27.59	10.86	-52.05	5.15	-17.86	5.89	n.d.	n.d.
		1uM DMS	16.31	0.74	-52.86	1.34	-25.02	14.80	-269.56	n.d.
		10uM DMS	23.51	11.97	-50.36	6.94	-24.01	17.13	n.d.	n.d.
		0.1uM MeOH	33.95	3.39	-38.86	0.89	-13.58	1.75	-346.84	n.d.
		1uM MeOH	29.43	3.80	86.48	17.59	-13.36	0.59	-392.36	n.d.
		10uM MeOH	37.57	13.20	1659.84	348.69	-9.87	0.53	-206.62	n.d.
October 2009	Area 4	Control	2.96	1.41	-47.61	2.82	-17.89	0.55	-388.62	12.18
		Molybdate	206.97	31.74	-36.98	1.61	-6.86	0.14	n.d.	n.d.
		0.1uM TMA	2.27	0.40	-25.79	3.24	n.d.	n.d.	-409.91	n.d.
		1uM TMA	2.44	0.30	394.12	42.16	-16.66	1.77	-389.49	n.d.
		10uM TMA	3.03	0.66	5998.62	428.99	n.d.	n.d.	-362.32	n.d.
		0.1uM DMS	1.68	0.08	-53.47	1.37	n.d.	n.d.	-391.11	n.d.
		1uM DMS	1.25	0.09	-59.13	6.81	n.d.	n.d.	-384.32	n.d.
		10uM DMS	1.51	0.31	-55.80	4.95	n.d.	n.d.	117.06	n.d.
		0.1uM MeOH	1.78	0.48	-58.95	6.99	n.d.	n.d.	-376.32	n.d.
		1uM MeOH	1.74	0.33	35.15	36.80	n.d.	n.d.	n.d.	n.d.
		10uM MeOH	1.87	0.16	816.96	145.25	n.d.	n.d.	-395.22	n.d.
		0.1uM Acetate	1.87	0.54	-53.00	0.12	-16.36	0.61	-329.51	n.d.
		1uM Acetate	1.51	0.23	-57.28	5.84	-15.36	1.23	-386.70	n.d.
		10uM Acetate	1.41	0.07	-52.46	2.27	n.d.	n.d.	-382.94	n.d.
		10uM Bicarbonate	1.29	0.13	-58.04	3.49	n.d.	n.d.	-385.07	n.d.

Table C.2 continued

Guerrero Negro										
Date	**Site**	**Substrate**	**CH4 production (nmol g-1 d-1)**	**CH4 production std dev**	**δ13C-CH4 (‰)**	**stdev**	**δ13C-CO2 (‰)**	**stdev**	**δ2H-CH4 (‰)**	**stdev**
October 2009	Area 9 Rubble	Control	3.53	1.11	-33.08	0.58	-19.28	0.34	-345.88	n.d.
		Molybdate	2.81	0.38	-51.17	3.30	-13.49	0.71	-83.05	n.d.
		0.1uM TMA	4.01	0.50	90.21	4.92	-17.38	0.45	-349.64	n.d.
		1uM TMA	4.53	0.92	1312.23	48.78	-13.17	0.64	-344.03	n.d.
		10uM TMA	3.92	0.75	14672.15	299.51	42.04	3.60	-290.49	n.d.
		0.1uM DMS	0.67	0.29	-37.76	2.70	n.d.	n.d.	147.03	n.d.
		1uM DMS	0.67	0.11	-39.17	1.81	n.d.	n.d.	3176.71	n.d.
		10uM DMS	0.65	0.03	-39.91	0.31	n.d.	n.d.	30271.63	n.d.
		0.1uM MeOH	3.99	1.11	-5.94	5.36	-19.42	1.30	-346.71	n.d.
		1uM MeOH	4.11	0.85	276.50	14.75	-15.66	0.35	-350.13	n.d.
		10uM MeOH	4.55	1.04	3626.18	147.63	5.51	0.77	-131.73	33.30
		0.1uM Acetate	2.84	0.77	-33.68	0.39	-20.08	0.07	-352.09	n.d.
		1uM Acetate	3.65	0.24	-32.76	1.15	-17.74	0.23	-352.80	n.d.
		10uM Acetate	4.51	1.22	-31.85	0.49	-0.04	1.87	-349.32	n.d.
		10uM Bicarbonate	2.25	0.52	-31.78	1.01	17.18	0.84	-372.98	n.d.
		Killed Control	0.08	0.02	-61.01	0.00	n.d.	n.d.	0.00	n.d.

Table C.2 continued

Guerrero Negro										
Date	**Site**	**Substrate**	**CH4 production (nmol g-1 d-1)**	**CH4 production std dev**	**δ13C-CH4 (‰)**	**stdev**	**δ13C-CO2 (‰)**	**stdev**	**δ2H-CH4 (‰)**	**stdev**
October 2009	Area 9 Crust	Control	18.80	1.13	-36.18	2.82	-18.08	0.18	-336.75	n.d.
		Molybdate	17.40	2.26	-54.40	2.17	-15.70	0.14	-300.79	n.d.
		0.1uM TMA	2.36	0.64	15.06	3.83	-18.20	0.40	-342.19	n.d.
		1uM TMA	2.68	0.41	526.29	1.92	-13.11	2.57	-347.31	n.d.
		10uM TMA	1.94	1.02	6201.43	1136.67	57.14	6.43	-322.03	n.d.
		0.1uM DMS	4.90	0.51	-42.23	1.06	-19.21	0.59	-218.81	n.d.
		1uM DMS	4.72	0.70	-44.77	4.20	-18.98	1.02	-151.24	n.d.
		10uM DMS	5.84	0.74	-42.40	0.66	-19.08	0.79	483.11	n.d.
		0.1uM MeOH	15.54	1.98	-18.03	6.80	-17.74	0.33	-341.73	n.d.
		1uM MeOH	27.83	24.07	99.44	1.76	-16.42	0.44	-330.54	n.d.
		10uM MeOH	14.60	1.34	1351.04	214.30	2.85	1.71	-232.33	2.67
		0.1uM Acetate	17.78	1.82	-30.39	1.67	-16.60	0.01	-369.51	n.d.
		1uM Acetate	15.62	0.48	-32.64	3.31	-15.75	0.61	-336.79	n.d.
		10uM Acetate	15.72	1.82	-36.54	6.53	-9.15	2.41	-363.26	n.d.
		10uM Bicarbonate	19.10	2.55	-29.94	0.52	36.67	7.29	-335.51	n.d.
		Killed Control	1.07	1.07	-50.54	1.20	n.d.	n.d.	0.00	n.d.

Table C.3. Methane incubation rate production data, methane isotopic data from California pond incubation samples collected in January 2010. Values that were not determined are depicted in the table as n.d.

Don Edwards										
Date	**Site**	**Substrate**	**CH4 production (nmol g-1 d-1)**	**CH4 production std dev**	**δ13C-CH4 (‰)**	**stdev**	**δ13C-CO2 (‰)**	**stdev**	**δ2H-CH4 (‰)**	**stdev**
January 2010	Pond 15	control	0.71	0.04	-62.85	0.28	n.d.	n.d.	n.d.	n.d.
		molybdate	16.05	1.79	-39.91	0.60	n.d.	n.d.	n.d.	n.d.
		0.1 µM TMA	0.55	0.15	375.86	100.92	n.d.	n.d.	n.d.	n.d.
		1 µM TMA	0.82	0.23	5532.64	1151.39	n.d.	n.d.	n.d.	n.d.
		10 µM TMA	3.34	0.89	55760.02	4352.48	n.d.	n.d.	n.d.	n.d.
		0.1 µM MeOH	0.65	0.17	57.86	56.97	n.d.	n.d.	n.d.	n.d.
		1 µM MeOH	0.87	0.53	694.18	49.33	n.d.	n.d.	n.d.	n.d.
		10 µM MeOH	1.26	0.05	13000.03	1746.67	n.d.	n.d.	n.d.	n.d.
		0.1 µM acetate	0.88	0.32	-61.49	0.91	n.d.	n.d.	n.d.	n.d.
		1 µM acetate	0.57	0.04	-61.00	0.51	n.d.	n.d.	n.d.	n.d.
		10 µM acetate	0.49	0.01	-54.15	0.35	n.d.	n.d.	n.d.	n.d.
		10 µM bicarbonate	0.69	0.13	-56.68	1.15	n.d.	n.d.	n.d.	n.d.
		killed control	0.00	0.01	n.d.	n.d.	n.d.	n.d.	n.d.	n.d.
January 2010	Pond 23	control	0.20	0.06	-41.51	0.95	n.d.	n.d.	n.d.	n.d.
		molybdate	0.21	0.06	-42.33	0.32	n.d.	n.d.	n.d.	n.d.
		0.1 µM TMA	0.19	0.08	506.20	14.15	n.d.	n.d.	n.d.	n.d.
		1 µM TMA	0.24	0.03	6384.25	85.02	n.d.	n.d.	n.d.	n.d.
		10 µM TMA	0.29	0.04	61115.43	3488.45	n.d.	n.d.	n.d.	n.d.
		0.1 µM MeOH	0.18	0.03	139.39	2.42	n.d.	n.d.	n.d.	n.d.
		1 µM MeOH	0.23	0.02	1849.32	47.92	n.d.	n.d.	n.d.	n.d.
		10 µM MeOH	0.19	0.02	17047.06	1530.12	n.d.	n.d.	n.d.	n.d.
		0.1 µM acetate	0.23	0.07	-38.84	3.02	n.d.	n.d.	n.d.	n.d.
		1 µM acetate	0.18	0.05	-37.03	4.32	n.d.	n.d.	n.d.	n.d.
		10 µM acetate	0.18	0.10	-35.76	0.85	n.d.	n.d.	n.d.	n.d.
		10 µM bicarbonate	0.23	0.05	-37.88	0.17	n.d.	n.d.	n.d.	n.d.
		killed control	0.05	0.03	n.d.	n.d.	n.d.	n.d.	n.d.	n.d.

Table C.4. Methane incubation rate production data, methane isotopic data from California pond incubation samples collected in August 2010. Values that were not determined are depicted in the table as n.d.

Don Edwards										
Date	**Site**	**Substrate**	**CH4 production (nmol g-1 d-1)**	**CH4 production std dev**	**δ13C-CH4 (‰)**	**stdev**	**δ13C-CO2 (‰)**	**stdev**	**δ2H-CH4 (‰)**	**stdev**
August 2010	Pond 15	control	0.06	0.01	n.d.	n.d.	n.d.	n.d.	n.d.	n.d.
		molybdate	2.68	0.14	n.d.	n.d.	n.d.	n.d.	n.d.	n.d.
		0.1 µM TMA	0.05	0.02	n.d.	n.d.	n.d.	n.d.	n.d.	n.d.
		1 µM TMA	0.05	0.01	n.d.	n.d.	n.d.	n.d.	n.d.	n.d.
		10 µM TMA	0.21	0.05	n.d.	n.d.	n.d.	n.d.	n.d.	n.d.
		0.1 µM MeOH	0.11	0.12	n.d.	n.d.	n.d.	n.d.	n.d.	n.d.
		1 µM MeOH	0.04	0.01	n.d.	n.d.	n.d.	n.d.	n.d.	n.d.
		10 µM MeOH	0.09	0.05	n.d.	n.d.	n.d.	n.d.	n.d.	n.d.
		0.1 µM acetate	0.04	0.00	n.d.	n.d.	n.d.	n.d.	n.d.	n.d.
		1 µM acetate	0.03	0.00	n.d.	n.d.	n.d.	n.d.	n.d.	n.d.
		10 µM acetate	0.10	0.11	n.d.	n.d.	n.d.	n.d.	n.d.	n.d.
		10 µM bicarbonate	0.05	0.01	n.d.	n.d.	n.d.	n.d.	n.d.	n.d.
August 2010	Pond 23	control	1.53	0.07	-44.53	1.09	n.d.	n.d.	n.d.	n.d.
		molybdate	1.63	0.07	-45.75	1.18	n.d.	n.d.	n.d.	n.d.
		0.1 µM TMA	1.40	0.18	46.38	14.61	n.d.	n.d.	n.d.	n.d.
		1 µM TMA	0.96	0.08	1167.02	25.15	n.d.	n.d.	n.d.	n.d.
		10 µM TMA	0.69	0.15	9809.47	119.20	n.d.	n.d.	n.d.	n.d.
		0.1 µM MeOH	0.56	0.38	-1.35	6.93	n.d.	n.d.	n.d.	n.d.
		1 µM MeOH	0.68	0.15	443.69	60.08	n.d.	n.d.	n.d.	n.d.
		10 µM MeOH	1.15	0.22	3870.15	1496.12	n.d.	n.d.	n.d.	n.d.
		0.1 µM acetate	1.21	0.06	-45.74	0.39	n.d.	n.d.	n.d.	n.d.
		1 µM acetate	1.10	0.18	-47.55	3.40	n.d.	n.d.	n.d.	n.d.
		10 µM acetate	0.97	0.16	-50.22	2.29	n.d.	n.d.	n.d.	n.d.
		10 µM bicarbonate	1.11	0.09	-48.49	3.93	n.d.	n.d.	n.d.	n.d.
		Killed Control	0.00	0.00	n.d.	n.d.	n.d.	n.d.	n.d.	n.d.

REFERENCES

Allen, M., et al., 2006. Is Mars Alive? Eos Trans. AGU. 87**,** 433-448.

Atreya, S. K., Mahaffy, P. R., Wong, A.-S., 2007. Methane and related trace species on Mars: Origin, loss, implications for life, and habitability. Planetary and Space Science. 55**,** 358-369.

Banat, I. M., Nedwell, D. B., Balba, M. T., 1983. Stimulation of Methanogenesis by Slurries of Saltmarsh Sediment after the Addition of Molybdate to Inhibit Sulphate-reducing Bacteria. Journal of General Microbiology. 129**,** 123-129.

Bebout, B. M., et al., 2002. Long-term manipulations of intact microbial mat communities in a greenhouse collaboratory: simulating earth's present and past field environments. Astrobiology. 2**,** 383-402.

Bebout, B. M., et al., 2004. Methane production by microbial mats under low sulphate concentrations. Geobiology. 2**,** 87-96.

Bernard, B. B., Brooks, J. M., Sackett, W. M., 1976. Natural gas seepage in the Gulf of Mexico. Earth and Planetary Science Letters. 31**,** 48-54.

Bernard, B. B., Brooks, J. M., Sackett, W. M., 1978. Light Hydrocarbons in Recent Texas Continental Shelf and Slope Sediments. Journal of Geophysical Research. 83**,** 4053-4061.

Biswas, K., Woodards, N., Xu, H., Barton, L., 2009. Reduction of molybdate by sulfate-reducing bacteria. BioMetals. 22**,** 131-139.

Botz, R., Pokojski, H.-D., Schmitt, M., Thomm, M., 1996. Carbon isotope fractionation during bacterial methanogenesis by CO2 reduction. Organic Geochemistry. 25**,** 255-262.

Brady, A. L., Slater, G., Laval, B., Lim, D. S., 2009. Constraining carbon sources and growth rates of freshwater microbialites in Pavilion Lake using 14C analysis. Geobiology. 7**,** 544-555.

Burdige, D. J., 2006. Geochemistry of marine sediments. Princeton University Press, Princeton, NJ.

Canfield, D. E., Kristensen, E., Thamdrup, B., 2005. Aquatic geomicrobiology. Elsevier Academic Press, Amsterdam [etc.].

Chanton, J., Chaser, L., Glasser, P., Siegel, D., 2005 Carbon and Hydrogen Isotopic Effects in Microbial, Methane from Terrestrial Environments. Stable Isotopes and Biosphere Atmosphere Interactions. Academic Press, San Diego, pp. 85-105.

Chanton, J. P., Fields, D., Hines, M. E., 2006. Controls on the hydrogen isotopic composition of biogenic methane from high-latitude terrestrial wetlands. J. Geophys. Res. 111**,** G04004.

Chanton, J. P., et al., 2008. Radiocarbon evidence for the importance of surface vegetation on fermentation and methanogenesis in contrasting types of boreal peatlands. Global Biogeochem. Cycles. 22**,** GB4022.

Chassefière, E., Leblanc, F., 2011a. Constraining methane release due to serpentinization by the observed D/H ratio on Mars. Earth and Planetary Science Letters. 310**,** 262-271.

Chassefière, E., Leblanc, F., 2011b. Methane release and the carbon cycle on Mars. Planetary and Space Science. 59**,** 207-217.

Coleman, D. D., Risatti, J. B., Schoell, M., 1981. Fractionation of carbon and hydrogen isotopes by methane-oxidizing bacteria. Geochimica et Cosmochimica Acta. 45**,** 1033-1037.

Conrad, R., 2005. Quantification of methanogenic pathways using stable carbon isotopic signatures: a review and a proposal. Organic Geochemistry. 36**,** 739-752.

Conrad, R., Frenzel, P., Cohen, Y., 1995. Methane emission from hypersaline microbial mats: Lack of aerobic methane oxidation activity. FEMS Microbiology Ecology. 16**,** 297-305.

Craig, H., 1961. Isotopic Variations in Meteoric Waters. Science. 133**,** 1702-1703.

Davis, J. B., Squires, R. M., 1954. Detection of Microbially Produced Gaseous Hydrocarbons Other than Methane. Science. 119**,** 381-382.

Des Marais, D. J., 1990. Microbial mats and the early evolution of life. Trends in ecology & evolution. 5**,** 140-144.

Des Marais, D. J., 2003. Biogeochemistry of Hypersaline Microbial Mats Illustrates the Dynamics of Modern Microbial Ecosystems and the Early Evolution of the Biosphere. The Biological Bulletin. 204**,** 160-167.

Des Marais, D. J., 2010 Marine Hypersaline *Microcoleus*-Dominated Cyanobacterial Mats in the Saltern at Guerrero Negro, Baja California Sur, Mexico: A System-Level Perspective. In: J. Seckbach, A. Oren, (Eds.), Microbial Mats. Springer Netherlands, pp. 401-420.

Didyk, B. M., Simoneit, B. R. T., 1989. Hydrothermal oil of Guaymas Basin and implications for petroleum formation mechanisms. Nature. 342**,** 65-69.

Duhr, A., Hilkert, A., Finnigan GasBench II: Automated H2/H2O Equilibration for δD Determination on Aqueous Samples. T. E. Corporation, (Ed.), Finnigan MAT Application Flash Report, Vol. 30049, Bremen, Germany, pp. 4.

Dupraz, C., Visscher, P. T., 2005. Microbial lithification in marine stromatolites and hypersaline mats. Trends in Microbiology. 13**,** 429-438.

Emmanuel, S., Ague, J. J., 2007. Implications of present-day abiogenic methane fluxes for the early Archean atmosphere. Geophys. Res. Lett. 34**,** L15810.

Ettwig, K. F., van Alen, T., van de Pas-Schoonen, K. T., Jetten, M. S. M., Strous, M., 2009. Enrichment and Molecular Detection of Denitrifying Methanotrophic Bacteria of the NC10 Phylum. Applied and Environmental Microbiology. 75**,** 3656-3662.

Formisano, V., Atreya, S., Encrenaz, T., Ignatiev, N., Giuranna, M., 2004. Detection of Methane in the Atmosphere of Mars. Science. 306**,** 1758-1761.

Formolo, M., 2010 The Microbial Production of Methane and Other Volatile Hydrocarbons. In: K. N. Timmis, (Ed.), Handbook of Hydrocarbon and Lipid Microbiology. Springer Berlin Heidelberg, pp. 113-126.

Foster, J. S., Green, S. J., 2011 Microbial diversity in modern stromatolites. Stromatolites: interaction of microbes with sediments. Springer, pp. 383-405.

Foster, J. S., Mobberley, J. M., 2010 Past, Present, and Future: Microbial Mats as Models for Astrobiological Research

Microbial Mats. In: J. Seckbach, A. Oren, (Eds.). Springer Netherlands, pp. 563-582.

Franks, J., Stolz, J. F., 2009. Flat laminated microbial mat communities. Earth-Science Reviews. 96**,** 163-172.

Fukui, M., Suh, J., Yonezawa, Y., Urushigawa, Y., 1997. Major substrates for microbial sulfate reduction in the sediments of Ise Bay, Japan. Ecological Research. 12**,** 201-209.

Fulghum, R. S., Worthington, J. M., 1977. Butyl Rubber Stoppers Increase the Shelf Life of Prereduced, Anaerobically Sterilized Media. Applied and Environmental Microbiology. 33**,** 1220-1221.

Giovannoni, S. J., DeLong, E. F., Olsen, G. J., Pace, N. R., 1988. Phylogenetic group-specific oligodeoxynucleotide probes for identification of single microbial cells. J. Bacteriol. 170**,** 720-726.

Green, S. J., Blackford, C., Bucki, P., Jahnke, L. L., Prufert-Bebout, L., 2008. A salinity and sulfate manipulation of hypersaline microbial mats reveals stasis in the cyanobacterial community structure. ISME J. 2**,** 457-470.

Hilkert, A., Avak, H., Finnigan GasBench II: 18O-Equilibration on water, Fruit Juice, and Wine., T. E. Corporation, (Ed.), Finnigan MAT Application Flash Report, Vol. 30048, Bremen, Germany, pp. 4.

Hoehler, T. M., Bebout, B. M., Des Marais, D. J., 2001. The role of microbial mats in the production of reduced gases on the early Earth. Nature. 412, 324-327.

Horita, J., 2005. Some perspectives on isotope biosignatures for early life. Chemical Geology. 218, 171-186.

Horita, J., Berndt, M. E., 1999. Abiogenic Methane Formation and Isotopic Fractionation Under Hydrothermal Conditions. Science. 285, 1055-1057.

Horodyski, R. J., 1977. Lyngbya mats at Laguna Mormona, Baja California, Mexico; comparison with Proterozoic stromatolites. Journal of Sedimentary Research. 47, 1305-1320.

Horodyski, R. J., Bloeser, B., 1977. Laminated algal mats from a coastal lagoon, Laguna Mormona, Baja California, Mexico. Journal of Sedimentary Research. 47, 680-696.

Horodyski, R. J., Vonder Haar, S. P., 1975. Recent calcareous stromatolites from Laguna Mormona (Baja California), Mexico. Journal of Sedimentary Research. 45, 894-906.

Huerta-Diaz, M., et al., 2011. Iron and Trace Metals in Microbial Mats and Underlying Sediments: Results From Guerrero Negro Saltern, Baja California Sur, Mexico. Aquatic Geochemistry. 17, 603-628.

Javor, B. J., 1983. Planktonic Standing Crop and Nutrients in a Saltern Ecosystem. Limnology and Oceanography. 28, 153-159.

Javor, B. J., 2002. Industrial microbiology of solar salt production. Journal of Industrial Microbiology and Biotechnology. 28, 42-47.

Jones, B. E., Grant, W. D., Duckworth, A. W., Owenson, G. G., 1998. Microbial diversity of soda lakes. Extremophiles. 2, 191-200.

Jonkers, H. M., Koopmans, G. F., Gemerden, H. v., 1998. Dynamics of Dimethyl Sulfide in a Marine Microbial Mat. Microbial Ecology. 36, 93-100.

Jorgensen, B. B., Des Marais, D. J., 1986. A Simple Fiberoptic Microprobe for High-Resolution Light Measurements-Application in Marine Sediment. Limnology and Oceanography. 31, 1376-1383.

Jorgensen, B. B., Revsbech, N. P., Blackburn, T. H., Cohen, Y., 1979. Diurnal cycle of oxygen and sulfide microgradients and microbial photosynthesis in a cyanobacterial mat sediment. Appl. Environ. Microbiol. 38, 46-58.

Kelley, C. A., Poole, J. A., Tazaz, A. M., Chanton, J. P., Bebout, B. M., 2012. Substrate Limitation for Methanogenesis in Hypersaline Environments. Astrobiology. 12, 89-97.

Kelley, C. A., Prufert-Bebout, L. E., Bebout, B. M., 2006. Changes in carbon cycling ascertained by stable isotopic analyses in a hypersaline microbial mat. J. Geophys. Res. 111**,** G04012.

Kiene, R. P., 1991. Production and consumption of methane in aquatic systems. Microbial production and consumption of greenhouse gases: Methane, nitrogen oxides and halomethanes. American Society for Microbiology. 111-146.

Kiene, R. P., Oremland, R. S., Catena, A., Miller, L. G., Capone, D. G., 1986. Metabolism of Reduced Methylated Sulfur Compounds in Anaerobic Sediments and by a Pure Culture of an Estuarine Methanogen. Applied and Environmental Microbiology. 52**,** 1037-1045.

King, G. M., 1984. Metabolism of Trimethylamine, Choline, and Glycine Betaine by Sulfate-Reducing and Methanogenic Bacteria in Marine Sediments. Applied and Environmental Microbiology. 48**,** 719-725.

King, G. M., 1988a. Methanogenesis from Methylated Amines in a Hypersaline Algal Mat. Applied and Environmental Microbiology. 54**,** 130-136.

King, G. M., 1988b. Methanogenesis from Methylated Amines in a Hypersaline Algal Mat. Appl. Environ. Microbiol. 54**,** 130-136.

King, G. M., Klug, M. J., Lovley, D. R., 1983. Metabolism of Acetate, Methanol, and Methylated Amines in Intertidal Sediments of Lowes Cove, Maine. Applied and Environmental Microbiology. 45**,** 1848-1853.

Kirk Harris, J., et al., 2013. Phylogenetic stratigraphy in the Guerrero Negro hypersaline microbial mat. ISME J. 7**,** 50-60.

Kotelnikova, S., 2002. Microbial production and oxidation of methane in deep subsurface. Earth-Science Reviews. 58**,** 367-395.

Krasnopolsky, V. A., Maillard, J. P., Owen, T. C., 2004. Detection of methane in the martian atmosphere: evidence for life? Icarus. 172**,** 537-547.

Kristjansson, J. K., Schönheit, P., 1983. Why do sulfate-reducing bacteria outcompete methanogenic bacteria for substrates? Oecologia. 60**,** 264-266.

Krzycki, J. A., Kenealy, W. R., DeNiro, M. J., Zeikus, J. G., 1987. Stable Carbon Isotope Fractionation by Methanosarcina barkeri during Methanogenesis from Acetate, Methanol, or Carbon Dioxide-Hydrogen. Applied and Environmental Microbiology. 53**,** 2597-2599.

Kunin, V., et al., 2008. Millimeter-scale genetic gradients and community-level molecular convergence in a hypersaline microbial mat. Mol Syst Biol. 4.

Lelieveld, J. O. S., Crutzen, P. J., Dentener, F. J., 1998. Changing concentration, lifetime and climate forcing of atmospheric methane. Tellus B. 50**,** 128-150.

Ley, R. E., et al., 2006. Unexpected Diversity and Complexity of the Guerrero Negro Hypersaline Microbial Mat. Appl. Environ. Microbiol. 72**,** 3685-3695.

Londry, K. L., Dawson, K. G., Grover, H. D., Summons, R. E., Bradley, A. S., 2008. Stable carbon isotope fractionation between substrates and products of Methanosarcina barkeri. Organic Geochemistry. 39**,** 608-621.

Lopez-Castro, M. C., Koch, V., Mariscal-Loza, A., Nichols, W. J., 2010. Long-term monitoring of black turtles Chelonia mydas at coastal foraging areas off the Baja California Peninsula. Endangered Species Research. 11**,** 35-45.

Lovley, D. R., Dwyer, D. F., Klug, M. J., 1982. Kinetic-analysis of competition between sulfate reducers and methanogens for hydrogen in sediments. Applied and Environmental Microbiology. 43**,** 1373-1379.

Lovley, D. R., Goodwin, S., 1988. Hydrogen concentrations as an indicator of the predominant terminal electron-accepting reactions in aquatic sediments. Geochimica et Cosmochimica Acta. 52**,** 2993-3003.

Lozupone, C. A., Knight, R., 2007. Global patterns in bacterial diversity. Proceedings of the National Academy of Sciences. 104**,** 11436-11440.

Lyons, J. R., Manning, C., Nimmo, F., 2005. Formation of methane on Mars by fluid-rock interaction in the crust. Geophys. Res. Lett. 32**,** L13201.

Madigan, M. T., Martinko, J. M., 2006. Brock biology of microorganisms. Prentice Hall/Pearson Education, Upper Saddle River, NJ [etc.].

Margulis, L., et al., 1980. The microbial community in the layered sediments at Laguna Figueroa, Baja California, Mexico: Does it have Precambrian analogues? Precambrian Research. 11**,** 93-123.

Marlow, J. J., Martins, Z., Sephton, M. A., 2011. Organic host analogues and the search for life on Mars. International Journal of Astrobiology. 10**,** 31-44.

Martens, C. S., Chanton, J. P., Paull, C. K., 1991. Biogenic methane from abyssal brine seeps at the base of the Florida escarpment. Geology. 19**,** 851-854.

McEwen, A. S., et al., 2011. Seasonal Flows on Warm Martian Slopes. Science. 333**,** 740-743.

McGenity, T. J., 2010 Methanogens and Methanogenesis in Hypersaline Environments. In: K. N. Timmis, (Ed.), Handbook of Hydrocarbon and Lipid Microbiology. Springer Berlin Heidelberg, pp. 665-680.

Mischna, M. A., Allen, M., Richardson, M. I., Newman, C. E., Toigo, A. D., 2011. Atmospheric modeling of Mars methane surface releases. Planetary and Space Science. 59**,** 227-237.

Mitterer, R. M., 2010. Methanogenesis and sulfate reduction in marine sediments: A new model. Earth and Planetary Science Letters. 295**,** 358-366.

Mumma, M. J., et al., 2009. Strong Release of Methane on Mars in Northern Summer 2003. Science. 323**,** 1041-1045.

Muyzer, G., Stams, A. J. M., 2008. The ecology and biotechnology of sulphate-reducing bacteria. Nat Rev Micro. 6**,** 441-454.

Nair, H., Summers, M. E., Miller, C. E., Yung, Y. L., 2005. Isotopic fractionation of methane in the martian atmosphere. Icarus. 175**,** 32-35.

Ollivier, B., Caumette, P., Garcia, J. L., Mah, R. A., 1994. Anaerobic bacteria from hypersaline environments. Microbiol. Mol. Biol. Rev. 58**,** 27-38.

Oremland, R. S., 1981. Microbial Formation of Ethane in Anoxic Estuarine Sediments. Appl. Environ. Microbiol. 42**,** 122-129.

Oremland, R. S., King, G. M., 1989 Methanogenesis in Hypersaline Environments. In: Y. Cohen, E. Rosenberg, (Eds.), Microbial mats: physiological ecology of benthic microbial communities. American Society for Microbiology, Washington, DC, pp. 180-190.

Oremland, R. S., Marsh, L. M., Polcin, S., 1982. Methane production and simultaneous sulphate reduction in anoxic, salt marsh sediments. Nature. 296**,** 143-145.

Oremland, R. S., Miller, L. G., Whiticar, M. J., 1987. Sources and flux of natural gases from Mono Lake, California. Geochimica et Cosmochimica Acta. 51**,** 2915-2929.

Oremland, R. S., Polcin, S., 1982. Methanogenesis and Sulfate Reduction: Competitive and Noncompetitive Substrates in Estuarine Sediments. Applied and Environmental Microbiology. 44**,** 1270-1276.

Oremland, R. S., Taylor, B. F., 1978. Sulfate reduction and methanogenesis in marine sediments. Geochimica et Cosmochimica Acta. 42**,** 209-214.

Oremland, R. S., Whiticar, M. J., Strohmaier, F. E., Kiene, R. P., 1988. Bacterial ethane formation from reduced, ethylated sulfur compounds in anoxic sediments. Geochimica et Cosmochimica Acta. 52**,** 1895-1904.

Oren, A., 1999a. Bioenergetic Aspects of Halophilism. Microbiol. Mol. Biol. Rev. 63**,** 334-348.

Oren, A., 1999b. Bioenergetic Aspects of Halophilism. Microbiology and Molecular Biology Reviews. 63**,** 334-348.

Oren, A., 2001. The bioenergetic basis for the decrease in metabolic diversity at increasing salt concentrations: implications for the functioning of salt lake ecosystems. Hydrobiologia. 466**,** 61-72.

Oren, A., et al., 2009. Microbial communities and processes within a hypersaline gypsum crust in a saltern evaporation pond (Eilat, Israel). Hydrobiologia. 626**,** 15-26.

Orphan, V. J., et al., 2008. Characterization and spatial distribution of methanogens and methanogenic biosignatures in hypersaline microbial mats of Baja California. Geobiology. 6**,** 376-393.

Ortega-Rubio, A., Lluch-Cota, D., Castellanos-Vera, A., 2001. Salt production at San Ignacio Lagoon: a Sustainable Development Project? International Journal of Sustainable Development & World Ecology. 8**,** 155-165.

Osterloo, M. M., et al., 2008. Chloride-Bearing Materials in the Southern Highlands of Mars. Science. 319**,** 1651-1654.

Peck, H. D., 1959. The ATP-dependent reduction of sulfate with hydrogen in extracts of *desulfovibrio desulfuricans*. Proceedings of the National Academy of Sciences. 45**,** 701-708.

Petit, J. R., et al., 1999. Climate and atmospheric history of the past 420,000 years from the Vostok ice core, Antarctica. Nature. 399**,** 429-436.

Phleger, F. B., Ewing, G. C., 1962. Sedimentology and Oceanography of Coastal Lagoons in Baja California, Mexico. Geological Society of America Bulletin. 73**,** 145-182.

Poole, J., 2010. Dominant substrates used by methanogens in hypersaline environments. Department of Geological Sciences, Vol. Master of Science. University of Missouri-Columbia, Columbia.

Potter, E. G., Bebout, B. M., Kelley, C. A., 2009. Isotopic Composition of Methane and Inferred Methanogenic Substrates Along a Salinity Gradient in a Hypersaline Microbial Mat System. Astrobiology. 9**,** 383-390.

Reeburgh, W. S., 2007. Oceanic Methane Biogeochemistry. Chemical Reviews. 107**,** 486-513.

Rennó, N. O., Stan-Lotter, H., Szathmáry, E., Möhlmann, D. T. F., 2010. To Search for Life on Mars: Follow the Brines. Astrobiology Science Conference 2010: Evolution and Life: Surviving Catastrophes and Extremes on Earth and Beyond, League City, Texas, pp. p.5182.

Rice, A. L., Gotoh, A. A., Ajie, H. O., Tyler, S. C., 2001. High-Precision Continuous-Flow Measurement of δ13C and δD of Atmospheric CH4. Analytical Chemistry. 73**,** 4104-4110.

Rothschild, L. J., Giver, L. J., White, M. R., Mancinelli, R. L., 1994. METABOLIC ACTIVITY OF MICROORGANISMS IN EVAPORITES1. Journal of Phycology. 30**,** 431-438.

Sahl, J. W., Pace, N. R., Spear, J. R., 2008. Comparative Molecular Analysis of Endoevaporitic Microbial Communities. Appl. Environ. Microbiol. 74**,** 6444-6446.

Seager, S., 2010. Exoplanet atmospheres: A theoretical outlook. Proceedings of the International Astronomical Union. 6**,** 198-207.

Senko, J., Koch, V., Megill, W. M., Carthy, R. R., Templeton, R. P., Nichols, W. J., 2010a. Fine scale daily movements and habitat use of East Pacific green turtles at a shallow coastal lagoon in Baja California Sur, Mexico. Journal of Experimental Marine Biology and Ecology. 391**,** 92-100.

Senko, J., López-Castro, M. C., Koch, V., Nichols, W. J., 2010b. Immature East Pacific Green Turtles (Chelonia mydas) Use Multiple Foraging Areas off the Pacific Coast of Baja California Sur, Mexico: First Evidence from Mark-Recapture Data1. Pacific Science. 64**,** 125-130.

Sharp, Z., 2007. Principles of stable isotope geochemistry. Pearson Education.

Sherwood Lollar, B., Lacrampe-Couloume, G., Voglesonger, K., Onstott, T. C., Pratt, L. M., Slater, G. F., 2008. Isotopic signatures of CH4 and higher hydrocarbon gases from Precambrian Shield sites: A model for abiogenic polymerization of hydrocarbons. Geochimica et Cosmochimica Acta. 72**,** 4778-4795.

Sherwood Lollar, B., Westgate, T. D., Ward, J. A., Slater, G. F., Lacrampe-Couloume, G., 2002. Abiogenic formation of alkanes in the Earth's crust as a minor source for global hydrocarbon reservoirs. Nature. 416**,** 522-524.

Shumilin, E., Grajeda-Muñoz, M., Silverberg, N., Sapozhnikov, D., 2002. Observations on trace element hypersaline geochemistry in surficial deposits of evaporation ponds of Exportadora de Sal, Guerrero Negro, Baja California Sur, Mexico. Marine Chemistry. 79**,** 133-153.

Smith, J. M., Green, S. J., Kelley, C. A., Prufert-Bebout, L., Bebout, B. M., 2008. Shifts in methanogen community structure and function associated with long-term manipulation of sulfate and salinity in a hypersaline microbial mat. Environmental Microbiology. 10**,** 386-394.

Smith, P. H., et al., 2009. H2O at the Phoenix Landing Site. Science. 325**,** 58-61.

Smith, R. L., Klug, M. J., 1981. Electron Donors Utilized by Sulfate-Reducing Bacteria in Eutrophic Lake Sediments. Applied and Environmental Microbiology. 42**,** 116-121.

Sørensen, J., Christensen, D., Jørgensen, B. B., 1981. Volatile Fatty Acids and Hydrogen as Substrates for Sulfate-Reducing Bacteria in Anaerobic Marine Sediment. Applied and Environmental Microbiology. 42**,** 5-11.

Sorensen, K. B., Canfield, D. E., Oren, A., 2004. Salinity Responses of Benthic Microbial Communities in a Solar Saltern (Eilat, Israel). Appl. Environ. Microbiol. 70**,** 1608-1616.

Sorensen, K. B., Canfield, D. E., Teske, A. P., Oren, A., 2005. Community Composition of a Hypersaline Endoevaporitic Microbial Mat. Appl. Environ. Microbiol. 71**,** 7352-7365.

Spear, J. R., Ley, R. E., Berger, A. B., Pace, N. R., 2003. Complexity in Natural Microbial Ecosystems: The Guerrero Negro Experience. Biol Bull. 204**,** 168-173.

Stal, L. J., 1995. Tansley Review No. 84. Physiological Ecology of Cyanobacteria in Microbial Mats and Other Communities. New Phytologist. 131**,** 1-32.

Stal, L. J., van Gemerden, H., Krumbein, W. E., 1985. Structure and development of a benthic marine microbial mat. FEMS Microbiology Letters. 31**,** 111-125.

Summons, R. E., Franzmann, P. D., Nichols, P. D., 1998. Carbon isotopic fractionation associated with methylotrophic methanogenesis. Organic Geochemistry. 28**,** 465-475.

Thauer, R. K., Kaster, A.-K., Seedorf, H., Buckel, W., Hedderich, R., 2008. Methanogenic archaea: ecologically relevant differences in energy conservation. Nat Rev Micro. 6**,** 579-591.

Turnbull, J. C., Lehman, S. J., Miller, J. B., Sparks, R. J., Southon, J. R., Tans, P. P., 2007. A new high precision 14CO2 time series for North American continental air. J. Geophys. Res. 112**,** D11310.

Valentine, D. L., Chidthaisong, A., Rice, A., Reeburgh, W. S., Tyler, S. C., 2004. Carbon and hydrogen isotope fractionation by moderately thermophilic methanogens. Geochimica et Cosmochimica Acta. 68**,** 1571-1590.

Visscher, P. T., Van Gemerden, H., 1991. Production and Consumption of Dimethylsulfoniopropionate in Marine Microbial Mats. Appl. Environ. Microbiol. 57**,** 3237-3242.

Vogel, T. M., Oremland, R. S., Kvenvolden, K. A., 1982. Low-temperature formation of hydrocarbon gases in San Francisco Bay sediment (California, U.S.A.). Chemical Geology. 37**,** 289-298.

Webster, C. R., Mahaffy, P. R., Atreya, S. K., Flesch, G. J., Farley, K. A., Team, M. S., 2013. Low Upper Limit to Methane Abundance on Mars. Science. 342**,** 355-357.

Whiticar, M. J., 1999. Carbon and hydrogen isotope systematics of bacterial formation and oxidation of methane. Chemical Geology. 161**,** 291-314.

Whiticar, M. J., Faber, E., 1986. Methane oxidation in sediment and water column environments - Isotope evidence. Organic Geochemistry. 10**,** 759-768.

Whiticar, M. J., Faber, E., Schoell, M., 1986. Biogenic methane formation in marine and freshwater environments: CO_2 reduction vs. acetate fermentation--Isotope evidence. Geochimica et Cosmochimica Acta. 50**,** 693-709.

Whitman, W., Bowen, T., Boone, D., 2006 The Methanogenic Bacteria. The Prokaryotes, pp. 165-207.

Zahnle, K., Freedman, R. S., Catling, D. C., 2011. Is there methane on Mars? Icarus. 212**,** 493-503.

Zharkov, M. A., Yànshin, A. L., 1981. History of Paleozoic salt accumulation. Springer

Zinder, S. H., Anguish, T., 1992. Carbon Monoxide, Hydrogen, and Formate Metabolism during Methanogenesis from Acetate by Thermophilic Cultures of Methanosarcina and Methanothrix Strains. Applied and Environmental Microbiology. 58**,** 3323-3329.

BIOGRAPHICAL SKETCH

Amanda Tazaz

Education:

January 2008-Present
PhD Candidate in Oceanography, Florida State University, Tallahassee, Fl
Concentrations: Biogeochemical Oceanography
*Anticipated Graduation Fall 2013
August 2008, Economics (BSc), Florida State University, Tallahassee, Fl
December 2006, Marine Biology (BSc), Florida International University, Miami, Fl

Experience:

Assistant in Research, 2013 - Present
Learning Systems Institute
Florida State University
Project Director – *Replicating the CGI Experiment*

Graduate Research Assistant, 2008 - 2013
Earth, Ocean and Atmospheric Science
Florida State University
Research: Biogeochemical Oceanography, Isotopic characterization of hypersaline methane production

Graduate Research Assistant, 2011 - 2013
Learning Systems Institute
Florida State University
Research: Integrating STEM in the classroom

Teaching Assistant, 2008
Florida State University
Course: Marine Mammals

Laboratory Instructor, 2006 - 2007
Florida International University
Course: Human Biology, General Chemistry, Chemistry and Society

Laboratory Research Assistant, 2006 - 2007
Florida International University
Research: Behavioral response of predation on turtles.

Research Skills:
Ion Chromatograph
Gas Chromatograph
Isotope Ratio Mass Spectrometer
Knowledge of Statistix statistical program
Proficient in ecological sampling techniques

Fellowships and Awards:
- Florida Education Fund Carl Crawford Award 2012
- Florida State University Leadership Award Nominee 2012
- Florida State University Seminole Torchbearer 2011
- Student Poster Award, American Geophysical Union Fall meeting 2009
- Florida State University Fellows Society
- McKnight Doctoral Fellowship recipient 2008
- Dean's List, Florida State University 2007-2008
- Florida Bright Futures recipient 2002

Participation in Research Projects:

2013-Present	Replicating the CGI Experiment
2011- Present	Integrating STEM into secondary school teaching, partnership with Helios and FSU Learning System Institute
2008 - Present	Microbial Mats at Guerrero Negro, Mexico, partnership with NASA
2008	Gulf of Mexico Gas Hydrate Research Consortium
2006 - 2007	Behavioral response of predation in Sea Turtles

University Service:

2009 – 2013	17^{th}, 18^{th}, 19^{th},20^{th} and 21^{st} Congress of Graduate Students Deputy Speaker for Finance – 19^{th} thru 21^{st} Congress Florida State University
2012	Member, Florida State University Vice-President for Research Search Committee
2011 and 2012	Capital Regional Science and Engineering Fair Judge

Department Service:

2008 – Present	Thalassic Society Organization Treasurer 2009-2011 Salmonole 5k Run event organizer 2009 - 2012
2010 –2011	College of Arts and Science Leadership Council Earth, Ocean and Atmospheric Science Graduate Student Representative

Community Service:

2012	Florida Education Fund Brain Bowl Mathematics Judge
2011 and 2012	Capital Regional Science and Engineering Fair Judge

Posters and Presentations:

Tazaz A.M., R. M. Wilson , R. Schoen, S. Blumsack, L. King, M. Dyehouse (2013). Utilizing Model Eliciting Activities (MEA's) to engage middle school teachers and students in storm water management practices to mitigate human impacts of land development. Oral presentation. American Geophysical Union Fall Meeting, December 2013.

Schoen R., **Tazaz A**., Brooks L. (2013) Studying the Effects of CGI Professional Development on Teachers and Students. Oral Presentation. Cognitively Guided Instruction 7th Biennial National Mathematics Conference, Des Moines, IA, July 2013.

Tazaz A.M., Detweiler A.M., Bebout, B.M., Nicholson B.E., Mauney M.T., Kelley C.A., Chanton J.P.(2013). Methane production and isotopic analysis from hypersaline microbial mat incubations when sulfate reduction is inhibited. Oral Presentation. ASLO Aquatic Sciences Meeting, New Orleans, LA, February 2013.

Mauney M.T., **Tazaz A.M.**, Bebout, B.M., Chanton J.P., Kelley C.A., Nicholson B.E., Detweiler A.M., Davila A.F. (2013). Isotopic analysis of methane bubbles obtained from Mars analogue hypersaline environments. Oral Presentation. ASLO Aquatic Sciences Meeting, New Orleans, LA, February 2013.

Nicholson B.E., Kelley C.A., Detweiler A.M., Bebout, B.M., Mauney M.T., **Tazaz A.M.**, Chanton J.P., Davila A.F. (2013). Stable carbon isotopes and rates of methane produced in the hypersaline environments of the Atacama desert, Chile and Baja California Sur, Mexico. Poster Presentation. ASLO Aquatic Sciences Meeting, New Orleans, LA, February 2013.

Dyehouse M., **Tazaz A**., King L., Martone R. (2012). The Integrated STEM Project: Utilizing Model Eliciting Activities to Merge Science, Engineering, Mathematics, and English Language Arts. Oral Presentation. 2012 FCR-STEM Conference, St. Petersburg, Fl, December 2012.

Schoen R., Blumsack S., **Tazaz A**., King L., Wilson R. (2012) Integrating Math and Science through Unit Conversions. Oral Presentation. 2012 FCR-STEM Conference, St. Petersburg, Fl, December 2012.

Bebout, B., Bramall N.E., Kelley C.A., Chanton J.P., **Tazaz A.M.**, J. Poole, Nicholson B., Detweiler A., Gupta M., Ricco A.J.(2012). Methane as an Indicator of Life on Mars: Necessary Measurements and Some Possible Measurement Strategies. Oral presentation. Lunar and Planetary Institute: Concepts and Approaches for Mars Exploration meeting, June 2012.

Tazaz, A. M.; Chanton, J. P.; Kelley, C. A.; Poole, J.; Bebout, B. M. (2012). Redefining isotopic boundaries for biogenic methane: How hypersaline environments provide insight on Mars research. Oral presentation. McKnight Research Conference, Tampa, FL, February 2012.

Kelley, C. A., J.A. Poole, **A.M. Tazaz,** J.P. Chanton, B. Bebout (2011). ^{13}C-enriched methane produced biologically at hypersaline Mars analog sites. Oral presentation. 2011 Geological Society of America Annual Meeting, Minneapolis, MN, October, 2011.

Tazaz, A. M.; Bebout, B. M.; Chanton, J. P.; Kelley, C. A.; Poole, J.; (2011). Isotopic expansion of traditional biogenic methane boundaries obtained from data collected from Mars analogue hypersaline ponds. Oral presentation. 242nd ACS National Meeting, Denver, CO, August 2011.

Bebout, B., **A.M. Tazaz** , C. A. Kelley, J. Poole, A. Davila, J.P. Chanton (2011). The Stable Isotopic Composition of Biogenic Methane in Mars Analogue Hypersaline Environment.

Oral presentation. Lunar and Planetary Institute: Analogue Sites for Mars Missions: MSL and Beyond meeting, March 2011.

Tazaz, A. M.; Chanton, J. P.; Kelley, C. A.; Poole, J.; Bebout, B. M.;(2011). Isotopic methane data from hypersaline ponds extends the traditional biogenic methane boundaries. Oral presentation. ASLO Aquatic Sciences Meeting, February 2011.

Bebout, B., **A.M. Tazaz** , C. A. Kelley, J. Poole, A. Davila, J.P. Chanton (2010). Methane as a biomarker in the search for extraterrestrial life: Lessons learned from Mars analog hypersaline environments. Oral presentation. American Geophysical Union Fall Meeting, December 2010.

Kelley, C. A., J. Poole, **A.M. Tazaz,** J.P. Chanton, B. Bebout (2010). Unusually high stable carbon isotopic values of methane from low organic carbon Mars analog hypersaline environments. Poster presentation. American Geophysical Union Fall Meeting, December 2010.

Tazaz, A.M., J.P. Chanton, C. A. Kelley, J. Poole, B. Bebout (2010). Traditional biogenic methane boundaries extended in hypersaline ponds. Oral presentation. 5th Annual Thalassic Society Oceanography Symposium Tallahassee, Fl, November 12, 2010.

Bebout, B., J.P. Chanton, C. A. Kelley, **A.M. Tazaz**, J. Poole, A.L.Cortés, J.G.Maldonado (2010). Methanogenesis in hypersaline environments – Analogs for Ancient Mars? Oral presentation. 38th COSPAR Scientific assembly, July 2010.

Kelley, C. A., J. Poole, J.P. Chanton, **A.M. Tazaz**, B. Bebout, (2010). Methanogenesis in Hypersaline Environments. Oral presentation. ASLO Summer Meeting, June 2010.

Tazaz, A.M., J.P. Chanton, C. A. Kelley, J. Poole, B. Bebout (2009). Methane Production in Extreme Environments. Poster presentation at American Geophysical Union meeting, December 2009.

Poole, J.A., C. A. Kelley, J. Chanton, **A.M. Tazaz**, B. Bebout (2009). Methanogens in hypersaline environments and their substrates for methane production. Poster presentation at American Geophysical Union meeting, December 2009.

Tazaz, A.M., J.P. Chanton, C. A. Kelley, J. Poole, B. Bebout (2009). Methane Production in Extreme Environments. Poster presentation at 4th Annual Thalassic Society Oceanography Symposium Tallahassee, Fl, November 6, 2009.

Tazaz, A.M., L.L. Lapham, J.P. Chanton (2008). Biological Processes at Mississippi Canyon 118. Poster presentation at 3rd Annual Thalassic Society Oceanography Symposium Tallahassee, Fl, November 13, 2008.

Tazaz, A.M., L.L. Lapham, J.P. Chanton (2008). Sulfate distribution across MC118. The Gulf of Mexico Hydrate Research Consortium annual meeting. Oral presentation. University of Mississippi. Oxford, MS October 14-15, 2008.

Publications:

Tazaz, A. M.; Bebout, B. M.; Chanton, J. P.; Kelley, C. A.; Poole, J.; (2013). Redefining the isotopic boundaries of biogenic methane: Methane from endoevaporites. ICARUS. doi:10.1016/j.icarus.2012.06.008.

Kelley, C. A., J.A. Poole, **A.M. Tazaz,** J.P. Chanton, B. Bebout (2012). Substrate limitation for methanogenesis in hypersaline environments. Astrobiology. doi:10.1089/ast.2011.0703.

Organizational Affiliations:

- American Geophysical Union (AGU)

- Association for the Sciences of Limnology and Oceanography (ASLO)
- American Chemical Society (ACS)
- Florida Council of Teachers of Mathematics (FCTM)
- National Black Graduate Student Association (NBGSA)
- National Association of Graduate-Professional Students (NAGPS)
- Society for Research on Educational Effectiveness (SREE)